UNIVERSIDAD DE LAS PALMAS DE GRAN CANARIA

DOCTORADO EN INGENIERÍAS QUÍMICA, MECÁNICA Y FABRICACIÓN

INVESTIGACIÓN DE NUEVAS ALEACIONES DE TITANIO CREADAS EXPERIMENTALMENTE PARA USOS BIOMÉDICOS

TESIS DOCTORAL

Las Palmas de Gran Canaria, abril de 2025

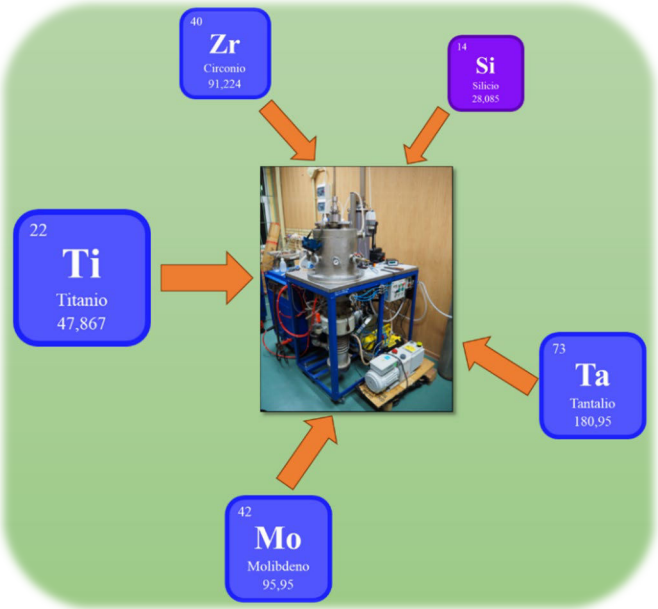

Autora: Cristina Jiménez Marcos

Directora: Julia Claudia Mirza Rosca

Codirector: Petrica Vizureanu

SHEng SMART HEALTHCARE ENGINEERING
Erasmus+ Programme – Cooperation partnerships
Project No.: 2023-1-RO01-KA220-HED-000159985

Co-funded by the European Union

UNIVERSIDAD DE LAS PALMAS DE GRAN CANARIA

DOCTORADO EN INGENIERÍAS QUÍMICA, MECÁNICA Y FABRICACIÓN

INVESTIGACIÓN DE NUEVAS ALEACIONES DE TITANIO CREADAS EXPERIMENTALMENTE PARA USOS BIOMÉDICOS

TESIS DOCTORAL

Doctoranda	Directora	Codirector
JIMENEZ MARCOS CRISTINA - 45398413R Firmado digitalmente por JIMENEZ MARCOS CRISTINA - 45398413R Fecha: 2025.03.29 18:04:57 Z	MIRZA ROSCA JULIANA CLAUDIA - 45360672A Firmado digitalmente por MIRZA ROSCA JULIANA CLAUDIA - 45360672A Fecha: 2025.03.30 19:10:21 +01'00'	VIZUREANU PETRICA Digitally signed by VIZUREANU PETRICA DN: cn=VIZUREANU PETRICA, o, ou, email=peviz2002@yahoo.com, c=RO Date: 2025.03.31 16:13:35 +03'00'
Cristina Jiménez Marcos	Julia Claudia Mirza Rosca	Petrica Vizureanu

Las Palmas de Gran Canaria, a 27 de marzo de 2025

AGRADECIMIENTOS

En primer lugar, quiero expresar mi gratitud a los directores de mi tesis, doña Julia Claudia Mirza Rosca y don Petrica Vizureanu, por depositar su confianza en mí para llevar a cabo este proyecto de tesis doctoral. Su contribución ha sido inestimable, ya que no solo han proporcionado el material de ensayo y el equipamiento necesarios, sino que también han compartido sus conocimientos sobre caracterización de materiales. Además, han demostrado una motivación, dedicación, profesionalidad y cercanía ejemplares, guiándome en todo momento durante su desarrollo. Gracias a su orientación, he podido descubrir mi lugar en el mundo de la investigación. Asimismo, es preciso expresar un reconocimiento a don Pedro Pablo Socorro Perdomo y a don Santiago José Brito García, quienes contribuyeron significativamente en las labores técnicas de preparación de ensayos y muestras desde mi primera visita al laboratorio para realizar el Trabajo de Fin de Grado. Sin su ayuda, no habría sido posible alcanzar los resultados obtenidos.

También, quiero mostrar mi agradecimiento a Madalina Simona Baltatu por participar y contribuir como coautora de todos los artículos que conforman mi proyecto de tesis.

Finalmente, quiero expresar mi más sincero agradecimiento a mis amigos, a mi padre, a mi hermana y a mi pareja por apoyarme en todo momento y quererme de forma incondicional. En especial, dedico este trabajo a mi madre, que, aunque no ha podido ver este documento tan importante para mí finalizado, sé que me apoya desde el cielo y que está muy orgullosa de mí.

RESUMEN

Los avances en medicina y desarrollo de materiales han permitido el estudio, diseño y aplicación de numerosos biomateriales en diversos campos como la ortodoncia, la administración de fármacos, la odontología, la ingeniería dental y los sistemas cardiovasculares. Estos biomateriales pueden mejorar la calidad de vida y la longevidad de las personas, pero también aumentar la esperanza de vida de la población de edad avanzada, más susceptible de padecer enfermedades musculoesqueléticas crónicas como la artritis.

Dichos biomateriales deben cumplir ciertos criterios, como alta biocompatibilidad, ductilidad, resistencia a la corrosión, resistencia a la fatiga, resistencia al desgaste, ausencia de toxicidad, osteointegración y una combinación de alta resistencia y bajo módulo de Young equivalente al hueso cortical humano. Los biomateriales de base metálica, como el acero inoxidable 316L o las aleaciones de CoCrMo, son populares para aplicaciones médicas debido a su alta biocompatibilidad, ductilidad y resistencia a la corrosión, a la fatiga y al desgaste, no obstante, el titanio (Ti) y sus aleaciones tienen la capacidad de mejorar dichas propiedades y convertirlas en excepcionales., por lo que su estudio ha ido incrementándose con el paso de los años.

La aleación Ti-6Al-4V es la más utilizada para aplicaciones ortopédicas debido a sus buenas propiedades y bajo coste. Sin embargo, en contacto con el cuerpo humano se liberan iones de vanadio, considerado tóxico y cancerígeno, y de aluminio, que puede causar enfermedades neurodegenerativas como demencia o Alzheimer. Los investigadores han intentado mejorar las prestaciones del titanio añadiendo elementos no tóxicos como hierro (Fe), circonio (Zr), niobio (Nb), cromo (Cr), cobre (Cu), Oro (Au), molibdeno (Mo), silicio (Si) o tantalio (Ta) para mejorar las características superficiales, las propiedades mecánicas, la resistencia a la corrosión y la biocompatibilidad.

La **finalidad** del presente proyecto de tesis es la caracterización de propiedades mecánicas y químicas de nuevas aleaciones de titanio para conocer su grado de biocompatibilidad para sus posibles aplicaciones en dispositivos médicos relacionados con el cuerpo humano.

Para ello, se han tenido en cuenta los siguientes **objetivos específicos**:

1. Se han sintetizado dos nuevas aleaciones **Ti20MoZrxSi (x = 0, 0.5 %)** utilizando un horno de refundición de arco al vacío (VAR), y en este estudio se examinaron su microestructura, comportamiento frente a la corrosión en solución Ringer a temperatura ambiente, a 40ºC y en solución salina de 3.5 NaCl%, microanálisis cuantitativo, módulo de elasticidad y dureza Vickers. Estos métodos incluyeron metalografía, electroquímica, microscopía electrónica de barrido, flexión en tres puntos y ensayos de microdureza.
2. Examinar el efecto de la adición del silicio en las nuevas aleaciones titanio de **Ti15MoZrxSi (siendo x = 0, 0.5, 0.75, 1 %)**, fabricadas en un horno de refundición por arco al vacío en la microestructura, las propiedades mecánicas (microdureza y flexión en tres puntos) y la resistencia a la corrosión en solución Ringer a temperatura ambiente, en un esfuerzo por desarrollar nuevas aleaciones para aplicaciones biomédicas.
3. Fabricación de dos nuevas aleaciones **Ti20Mo7ZrxSi (x = 0.75, 1 %)** mediante un horno de refundición por arco al vacío y examinación de su microestructura, comportamiento frente a la corrosión, microanálisis cuantitativo, módulo de Young y dureza. La metalografía, la microscopía electrónica de barrido, la electroquímica, la flexión en tres puntos y el ensayo de microdureza fueron algunas de las técnicas utilizadas para este estudio.
4. Evaluación del comportamiento frente a la corrosión y las propiedades mecánicas de las aleaciones **TixMoTaZr (x = 15, 20 %)** en solución Ringer a temperatura ambiente, comparándolas con materiales de referencia como el titanio puto comercial (Cp-Ti) y la aleación comercial Ti-6Al-4V. Dichas aleaciones presentan una superior resistencia a la corrosión, mayor biocompatibilidad y capacidad para eludir reacciones adversas, como las asociadas al uso de aluminio (Al) o vanadio (V). Estas composiciones no sólo mejoran las propiedades conocidas del titanio, sino que amplían las posibilidades de diseño de implantes biomédicos más duraderos, seguros y funcionales.

5. Análisis del efecto de la adición de silicio sobre la microestructura y la resistencia a la corrosión de las aleaciones de titanio liberadas de tensiones y tratadas térmicamente. Las muestras analizadas fueron aleaciones de **Ti15MoxSi (x = 0, 0.5, 0.75 y 1 %)**. Se investigó el comportamiento frente a la corrosión para evaluar su comportamiento en fluido corporal simulado (solución Ringer a temperatura ambiente). Además de las pruebas de corrosión, este estudio pretende investigar la microestructura y el comportamiento de microdureza de estas aleaciones, con el fin de evaluar el potencial de estos materiales para su uso en el cuerpo humano, con especial atención a los dispositivos médicos en los que la durabilidad, la dureza y la resistencia a la corrosión son factores críticos.

El tema del proyecto de tesis propuesto se encuentra relacionado con la línea de investigación del programa de doctorado en Ingenierías Química, Mecánica y de Fabricación (QUIMEFA) "**Corrosión de los metales**".

Dicho proyecto se basa en la realización de estudios relacionados con la caracterización de propiedades mecánicas y químicas de novedosas aleaciones de titanio fabricadas mediante el proceso de **refundición por arco al vacío** (VAR), principalmente de **Titanio-Molibdeno**, para conocer su grado de biocompatibilidad y descubrir sus posibles aplicaciones en dispositivos médicos relacionados con el cuerpo humano. A través de estos estudios y los resultados obtenidos, se ha podido escribir una serie de publicaciones científicas que conforman la presentación de la denominada "**tesis por compendio**".

En el artículo *"**Experimental Research on New Developed Titanium Alloys for Biomedical Applications**"* de la revista **Bioengineering** se han analizado las propiedades mecánicas y el comportamiento electroquímico de dos nuevas aleaciones de titanio, Ti20Mo7ZrxSi (x = 0, 0.5 %). Se han realizado observaciones metalográficas utilizando el reactivo de ataque Kroll y microanálisis cuantitativos por microscopía electrónica de barrido (SEM) y espectroscopia de energía dispersiva (EDX) con el objetivo de conocer la microestructura de las muestras. Asimismo, se ha podido determinar los valores de módulo de elasticidad y de Dureza Vickers a través de los ensayos de flexión en tres

puntos y de microdureza. Finalmente, para conocer el comportamiento frente a la corrosión de las dos muestras, estas fueron sometidas a tres ambientes diferentes: Solución Ringer a temperatura ambiente, solución Ringer a 40ºC simulando condiciones de fiebre y solución de cloruro sódico (NaCl) al 3.5%.

En el artículo *"**Effect of Si Contents on the Properties of Ti15Mo7ZrxSi Alloys**"* de la revista **Materials,** se ha podido evaluar las características mecánicas y la biocompatibilidad de cuatro nuevas aleaciones de titanio, Ti15Mo7ZrxSi (x = 0, 0,5, 0,75, 1 %). Para ello, se realizaron estudios electroquímicos, metalográficos, de flexión en tres puntos y de microdureza en los materiales estudiados para determinar su comportamiento frente a la corrosión en disolución Ringer a temperatura ambiente, microestructura atacada con el reactivo Kroll, módulo de Young y dureza Vickers.

En el artículo *"**Evaluation of New Titanium Alloys as Potential Materials for Medical Devices**"* de la revista **Microscopy and Microanalysis**, se ha caracterizado las propiedades mecánicas, así como el comportamiento frente a la corrosión, la microestructura y ciertas propiedades mecánicas de las aleaciones Ti20Mo7ZrxSi (x = 0.75, 1 %) a través de la realización de ensayos de metalografía utilizando el reactivo Kroll y observaciones de SEM y de EDS, electroquímicos, de flexión en tres puntos y de microdureza.

En el artículo *"**Two novel Ti-Mo-Ta-Zr alloys for medical devices: their microstructure, corrosion resistance and microhardness characteristics**"* de la revista **Materials Chemistry and Physics**, se ha presentado el estudio de dos aleaciones de titanio, TixMo15Ta7Zr (x = 15, 20 %), a través de la caracterización microestructural proporcionada por los ensayos de metalografía, SEM y difracción de rayos-X (XRD), de los ensayos de dureza realizados a diferentes cargas y de la comparación del comportamiento frente a la corrosión de estas dos aleaciones con respecto a cp-Ti y a Ti-6Al-4V en solución Ringer a temperatura ambiente.

En el artículo *"**Preliminary studies of new heat-treated titanium alloys for use in medical equipment**"* de la revista **Results in Engineering**, se han analizado las características de cuatro aleaciones de titanio tratadas térmicamente, Ti15MoxSi (x = 0, 0.5, 0.75, 1 %), mediante la realización de ensayos preliminares de metalografía, SEM y XRD con el fin de conocer su microestructura, además de los ensayos de dureza Vickers

aplicando cargas diferentes y los diferentes ensayos electroquímicos en solución Ringer a temperatura ambiente para ver su comportamiento frente a la corrosión.

Mediante la caracterización preliminar de la microestructura, el comportamiento frente a la corrosión en distintos ambientes y de ciertas propiedades mecánicas como la dureza y el módulo de elasticidad de diferentes aleaciones de base Ti-Mo, se ha observado que todas las muestras ensayadas, en mayor o menor medida, han presentado unas características óptimas, para un futuro diseño y fabricación de material médico, y superiores a las de aleaciones comerciales como CoCrMo o Ti-6Al-4V, destacando el uso de distintos porcentajes de silicio y de molibdeno para este fin.

La investigación futura debería concentrarse en una homogeneización de los ensayos realizados en todas las aleaciones para obtener un mejor análisis de sus características. Además, sería recomendable evaluar su comportamiento electroquímico en una disolución acidulada que simule las condiciones del fenómeno de "agujetas" en el cuerpo humano, lo que permitiría comprender mejor su durabilidad en escenarios clínicos exigentes. También, el estudio puede enfocarse en la fabricación de nuevas aleaciones de titanio modificando el porcentaje de Molibdeno o de Silicio que tan buenos resultados han aportado.

ÍNDICE DE CONTENIDOS

1.1. ANTECEDENTES

Los avances en ciencia y tecnología de materiales han permitido el desarrollo de una amplia variedad de biomateriales con propiedades adecuadas para una variedad de aplicaciones médicas, entre las que se incluyen la ortopedia, la odontología, la administración de medicamentos, la ingeniería de tejidos de la piel y de dispositivos cardiovasculares [1], resolviendo muchos de los problemas médicos actuales y mejorando así la calidad de vida y la longevidad de las personas.

Sin embargo, a medida que la esperanza de vida aumenta en los países en desarrollo, también lo hace el número de procedimientos de reparación con implantes quirúrgicos. Asimismo, ha aumentado tanto la población anciana como la población obesa, esta última producida por la adquisición de un estilo de vida más sedentario, por lo que presentan un mayor riesgo de desarrollar enfermedades musculoesqueléticas crónicas como la osteoartritis, principalmente en caderas y rodillas [2].

En el ámbito de la cirugía ortopédica, se realizan anualmente aproximadamente 1,5 millones de reemplazos articulares en Europa y 7 millones en Estados Unidos [3]. Sin embargo, la durabilidad a largo plazo del biomaterial implantado no está garantizada, ya que todavía no se ha logrado una combinación óptima de propiedades mecánicas, químicas, tribológicas y de biocompatibilidad. Por tanto, la vida útil de un implante es de aproximadamente veinte años, lo que genera la necesidad de realizar nuevas intervenciones quirúrgicas de sustitución de dispositivos protésicos, aumentando los riesgos y los costes de las cirugías de reemplazo asociadas [4].

Para superar estas limitaciones, diversos grupos de investigación han diseñado y creado nuevos biomateriales con superficies modificadas con el fin de mejorar su comportamiento al entrar en contacto con el cuerpo humano. Estos biomateriales son esenciales para diversas funciones corporales y deben cumplir ciertos criterios, como alta biocompatibilidad, ductilidad, corrosión, fatiga, resistencia al desgaste, ausencia de toxicidad, osteointegración y una combinación de alta resistencia y bajo módulo de Young equivalente al hueso cortical humano [5,6].

Aunque los biomateriales se clasifican en metales, polímeros, cerámicas y materiales compuestos, los metálicos, como el acero inoxidable 316L, las aleaciones de CoCrMo y el titanio y NiTi, representan aproximadamente el 95 % de los dispositivos ortopédicos y el

80% de los implantes, debido a su alta biocompatibilidad, ductilidad y resistencia a la corrosión, a la fatiga y al desgaste [7,8]. En particular, las aleaciones de titanio destacan por su excepcional biocompatibilidad, elevada resistencia a la corrosión, alto rendimiento mecánico, bajo módulo de elasticidad en comparación a otras aleaciones comerciales y gran estabilidad térmica [9].

El titanio (Ti) puro está presente en dos formas alotrópicas: la fase α, caracterizada por una estructura hexagonal compacta a temperaturas inferiores a 882 °C, y la fase β, caracterizada por una estructura cúbica centrada en el cuerpo a temperaturas superiores a 882 °C, además de una fase intermedia, α+β [10].

Dentro de las aleaciones de titanio, Ti-6Al-4V es la más utilizada para aplicaciones ortopédicas debido a sus muy buenas propiedades y bajo coste. No obstante, en contacto con el cuerpo humano, se produce la liberación de iones del vanadio, que se considera un material tóxico y cancerígeno y del aluminio, el cual, en grandes dosis, puede causar enfermedades neurodegenerativas como la demencia o el Alzheimer [11]. Para disminuir estos efectos, se han desarrollado nuevas aleaciones de titanio introduciendo elementos no tóxicos como hierro (Fe), circonio (Zr), niobio (Nb), cromo (Cr), cobre (Cu), Oro (Au), molibdeno (Mo), silicio (Si) o tantalio (Ta) con el fin de mejorar el rendimiento del titanio, además de mejorar las características superficiales, las propiedades mecánicas, la resistencia a la corrosión y la biocompatibilidad.

1.2. OBJETIVOS DE LA TESIS

La **finalidad** del presente proyecto de tesis es la caracterización de propiedades mecánicas y químicas de nuevas aleaciones de titanio para conocer su grado de biocompatibilidad para sus posibles aplicaciones en dispositivos médicos relacionados con el cuerpo humano.

Para ello, se han tenido en cuenta los siguientes **objetivos específicos**:

1. Se han sintetizado dos nuevas aleaciones **Ti20MoZrxSi (x = 0, 0.5 %)** utilizando un horno de refundición de arco al vacío (VAR), y en este estudio se examinaron su microestructura, comportamiento frente a la corrosión en solución Ringer a temperatura ambiente, a 40ºC y en solución salina de 3.5

NaCl%, microanálisis cuantitativo, módulo de elasticidad y dureza Vickers. Estos métodos incluyeron metalografía, electroquímica, microscopía electrónica de barrido, flexión en tres puntos y ensayos de microdureza.

2. Examinar el efecto de la adición del silicio en las nuevas aleaciones titanio de **Ti15MoZrxSi (siendo x = 0, 0.5, 0.75, 1 %)**, fabricadas en un horno de refundición por arco al vacío en la microestructura, las propiedades mecánicas (microdureza y flexión en tres puntos) y la resistencia a la corrosión en solución Ringer a temperatura ambiente, en un esfuerzo por desarrollar nuevas aleaciones para aplicaciones biomédicas.
3. Fabricación de dos nuevas aleaciones **Ti20Mo7ZrxSi (x = 0.75, 1 %)** mediante un horno de refundición por arco al vacío y examinación de su microestructura, comportamiento frente a la corrosión, microanálisis cuantitativo, módulo de Young y dureza. La metalografía, la microscopía electrónica de barrido, la electroquímica, la flexión en tres puntos y el ensayo de microdureza fueron algunas de las técnicas utilizadas para este estudio.
4. Evaluación del comportamiento frente a la corrosión y las propiedades mecánicas de las aleaciones **TixMoTaZr (x = 15, 20 %)** en solución Ringer a temperatura ambiente, comparándolas con materiales de referencia como el Cp-Ti y el Ti-6Al-4V. Dichas aleaciones presentan una superior resistencia a la corrosión, mayor biocompatibilidad y capacidad para eludir reacciones adversas, como las asociadas al uso de aluminio (Al) o vanadio (V). Estas composiciones no sólo mejoran las propiedades conocidas del titanio, sino que amplían las posibilidades de diseño de implantes biomédicos más duraderos, seguros y funcionales.
5. Análisis del efecto de la adición de silicio sobre la microestructura y la resistencia a la corrosión de las aleaciones de titanio liberadas de tensiones y tratadas térmicamente. Las muestras analizadas fueron aleaciones de **Ti15MoxSi (x = 0, 0.5, 0.75 y 1 %)**. Se investigó el comportamiento frente a la corrosión para evaluar su comportamiento en fluido corporal simulado (solución Ringer a temperatura ambiente). Además de las pruebas de corrosión, este estudio pretende investigar la microestructura y el comportamiento de microdureza de estas aleaciones, con el fin de evaluar el potencial de estos materiales para su uso en el cuerpo humano, con especial

atención a los dispositivos médicos en los que la durabilidad, la dureza y la resistencia a la corrosión son factores críticos.

El tema del proyecto de tesis propuesto se encuentra relacionado con la línea de investigación del programa de doctorado en Ingenierías Química, Mecánica y de Fabricación (QUIMEFA) "**Corrosión de los metales**".

Dicho proyecto se basa en la realización de estudios relacionados con la caracterización de propiedades mecánicas y químicas de novedosas aleaciones de titanio fabricadas mediante el proceso de **refundición por arco al vacío** (VAR), principalmente de **Titanio-Molibdeno**, para conocer su grado de biocompatibilidad y descubrir sus posibles aplicaciones en dispositivos médicos relacionados con el cuerpo humano. A través de estos estudios y los resultados obtenidos, se ha podido escribir una serie de publicaciones científicas que conforman la presentación de la denominada "**tesis por compendio**".

1.3. JUSTIFICACIÓN DE LA UNIDAD TEMÁTICA DE LA TESIS

El presente proyecto de tesis doctoral se compone de cinco artículos pertenecientes a cinco revistas diferentes e indexadas (Bioengineering, Materials, Microscopy and Microanalysis, Materials Chemistry and Physics y Results in Engineering). El objetivo común de dichos artículos es la caracterización preliminar de la microestructura, de la resistencia a la corrosión y de propiedades mecánicas de aleaciones de titanio fabricadas a través del proceso de fundición por arco al vacío con elementos como el molibdeno, el silicio, el circonio y el tantalio.

La elección de estos elementos con composiciones específicas se debe tanto a hallazgos anteriores como a la necesidad de combinar biocompatibilidad, durabilidad y propiedades mecánicas superiores. El molibdeno es un elemento β-estabilizador de baja toxicidad que, al combinarse con el titanio, produce una película de óxido estable (MoO_3) que lo protege de la corrosión y el deterioro en entornos agresivos [12]. El tantalio es también un β-estabilizador que, en concentraciones superiores al 15 %, mejora la biocompatibilidad y facilita la formación de tejido óseo alrededor de los implantes [13]. El circonio es un estabilizador neutro y cada vez es más deseable para aplicaciones médicas debido a su

biocompatibilidad, bajo módulo de elasticidad y resistencia a la corrosión [14,15]. Finalmente, el silicio puede mejorar la biocompatibilidad y ayudar a controlar las características mecánicas de un material [16].

A continuación, se muestran los datos identificativos y un resumen del contenido de cada artículo. Se puede observar que los artículos se encuentran publicados en revistas indexadas de alto impacto y visibilidad ya que se encuentran entre los cuartiles Q1 y Q2 (ver Tablas 1, 2, 3, 4 y 5).

1. **Experimental Research on New Developed Titanium Alloys for Biomedical Applications**

Este artículo muestra el análisis de las propiedades mecánicas y el comportamiento electroquímico de dos nuevas aleaciones de titanio, Ti20Mo7ZrxSi (x = 0, 0.5 %). Se han realizado observaciones metalográficas utilizando el reactivo de ataque Kroll y microanálisis cuantitativos por microscopía electrónica de barrido (SEM) y espectroscopia de rayos X de energía dispersiva (EDX) con el objetivo de conocer la microestructura de las muestras. Asimismo, se ha podido determinar los valores de módulo de elasticidad y de Dureza Vickers a través de los ensayos de flexión en tres puntos y de microdureza. Finalmente, para conocer el comportamiento frente a la corrosión de las dos muestras, estas fueron sometidas a tres ambientes diferentes: Solución Ringer a temperatura ambiente para obtener los valores del potencial y de la velocidad de corrosión además de los valores de impedancia a distintos potenciales, mientras que la solución Ringer a 40ºC simulando condiciones de fiebre y solución NaCl al 3.5% se utilizaron para la obtención de valores de impedancia a distintos potenciales. Las muestras presentaron una estructura bifásica y dendrítica, con una mayor resistencia a la corrosión para las que contenían un menor contenido de silicio. El análisis cuantitativo por EDX reveló la presencia de una capa de óxido de titanio en las superficies. Se observó que la presencia de silicio disminuía el módulo de elasticidad, lo que daba lugar a la formación de fases blandas y duras en las pruebas de microdureza. Las mediciones de espectroscopia de impedancia electroquímica (EIS) indicaron un sistema de dos constantes temporales, lo que sugiere la presencia de una película pasiva de doble capa en las muestras.

Tabla 1. Datos identificativos del artículo "Experimental Research on New Developed Titanium Alloys for Biomedical Applications".

Autores	Cristina Jiménez-Marcos, Julia Claudia Mirza-Rosca, Madalina Simona Baltatu, Patrica Vizureanu
Revista	Bioengineering
Año	2022
Volumen	9
Páginas	21
DOI	10.3390/bioengineering9110686
ISSN	2306-5354
Editorial	Multidisciplinary Digital Publishing Institute
Índice de impacto	3.8
Cuartil	Q2

2. Effect of Si Contents on the Properties of Ti15Mo7ZrxSi Alloys

En este artículo se han podido evaluar las características mecánicas y la biocompatibilidad de cuatro nuevas aleaciones de titanio, Ti15Mo7ZrxSi (x = 0, 0,5, 0,75, 1 %). Para ello, se realizaron estudios metalográficos, electroquímicos, de flexión en tres puntos y de microdureza en los materiales estudiados para determinar su comportamiento frente a la corrosión en disolución Ringer a temperatura ambiente, obteniendo a su vez los valores del potencial y de velocidad de corrosión además de hallar los valores de impedancia a distintos potenciales, su microestructura atacada con el reactivo Kroll, los valores del módulo de Young y de dureza Vickers. El estudio reveló que todas las muestras revelan estructuras bifásicas y dendríticas y sugiere que presentan un comportamiento favorable en contacto con fluidos fisiológicos a temperatura ambiente, una elevada biocompatibilidad, resultados más bajos del módulo de Young comparables a los del hueso humano y valores de dureza más elevados en comparación con el titanio comercialmente puro.

Tabla 2. Datos identificativos del artículo "Effect of Si Contents on the Properties of Ti15Mo7ZrxSi Alloys".

Autores	Cristina Jiménez-Marcos, Julia Claudia Mirza-Rosca, Madalina Simona Baltatu, Patrica Vizureanu
Revista	Materials
Año	2023
Volumen	16
Páginas	15
DOI	10.3390/ma16144906
ISSN	1996-1944
Editorial	Multidisciplinary Digital Publishing Institute
Índice de impacto	3.1
Cuartil	Q1

3. Evaluation of New Titanium Alloys as Potential Materials for Medical Devices

El presente artículo expone la caracterización de las propiedades mecánicas, así como el comportamiento frente a la corrosión de las aleaciones Ti20Mo7ZrxSi (x = 0.75, 1 %). Dicha caracterización se ha llevado a cabo mediante la realización de ensayos de metalografía utilizando el reactivo Kroll, así como mediante observaciones de SEM y EDX. Asimismo, se han realizado ensayos electroquímicos sumergiendo las muestras en solución Ringer a temperatura ambiente, obteniendo los valores del potencial y de la velocidad de corrosión y de impedancia a distintos potenciales. Finalmente, se han realizado ensayos de flexión en tres puntos y de microdureza. Se confirma la estructura bifásica y dendrítica para ambas muestras con una zona rica en titanio y otra de Mo, Zr y Si. Asimismo, se comprobó que la superficie de cada muestra formaba una capa de óxido pasiva (TiO_2). En las pruebas electroquímicas, el potencial de la muestra TiMoZrSi0.75 tendía a corroerse y mostraba una menor resistencia a la corrosión. Por último, el módulo de elasticidad fue inferior al de muchas aleaciones comerciales y los valores de dureza Vickers aumentaron al aumentar el contenido de silicio. Según los resultados obtenidos, la adición de un mayor porcentaje de silicio conduce a una ligera mejora de las propiedades mecánicas.

Tabla 3. Datos identificativos del artículo "Evaluation of New Titanium Alloys as Potential Materials for Medical Devices".

Autores	Cristina Jiménez-Marcos, Julia Claudia Mirza-Rosca, Madalina Simona Baltatu, Patrica Vizureanu
Revista	Microscopy and Microanalysis
Año	2023
Volumen	29
Número	Suppl 1
Páginas	6
DOI	10.1093/micmic/ozad067.088
ISSN	1435-8115
Editorial	Oxford University Press
Índice de impacto	2.9
Cuartil	Q1

4. Two novel Ti-Mo-Ta-Zr alloys for medical devices: their microstructure, corrosion resistance and microhardness characteristics

En este artículo se ha presentado el estudio de dos aleaciones de titanio, TixMo15Ta7Zr (x = 15, 20 %), a través de la caracterización microestructural proporcionada por los ensayos de metalografía, SEM y difracción de rayos-X (XRD), de los ensayos de dureza realizados a diferentes cargas y de la comparación del comportamiento frente a la corrosión de estas dos aleaciones con respecto al titanio puro y a Ti-6Al-4V en solución Ringer a temperatura ambiente, obteniendo los valores de potencial y velocidad de corrosión y de la impedancia aplicando distintos potenciales. La metalografía avanzada, la microscopía electrónica de barrido, la difracción de rayos X, las mediciones de microdureza y los ensayos electroquímicos han demostrado que un alto contenido en molibdeno mejora la resistencia a la corrosión al favorecer una capa pasiva flexible. Estas aleaciones conservan propiedades mecánicas comparables a las de los biomateriales de titanio convencionales, con valores de dureza Vickers en torno a 350 HV. Estos resultados sugieren que estas aleaciones ofrecen una solución revolucionaria para implantes biomédicos más seguros y duraderos.

Tabla 4. Datos identificativos del artículo "Two novel Ti-Mo-Ta-Zr alloys for medical devices: their microstructure, corrosion resistance and microhardness characteristics".

Autores	Cristina Jiménez-Marcos, Julia Claudia Mirza-Rosca, Madalina Simona Baltatu, Patrica Vizureanu
Revista	Materials Chemistry and Physics
Año	2025
Volumen	334
Páginas	6
DOI	10.1016/j.matchemphys.2025.130511
ISSN	1879-3312
Editorial	Elsevier
Índice de impacto	4.3
Cuartil	Q2

5. Preliminary studies of new heat-treated titanium alloys for use in medical equipment

En este último artículo se han analizado las características de cuatro aleaciones de titanio tratadas térmicamente, Ti15MoxSi (x = 0, 0.5, 0.75, 1.0), mediante la realización de ensayos preliminares de metalografía, SEM y XRD con el fin de conocer su microestructura, además de los ensayos de dureza Vickers aplicando cargas diferentes y los diferentes ensayos electroquímicos en solución Ringer a temperatura ambiente para ver su comportamiento frente a la corrosión (potencial y velocidad de corrosión e impedancia). La adición de molibdeno a los estabilizadores de β-fase mejoró la microestructura laminar de α + β-fase para el rendimiento mecánico. Un mayor contenido de silicio dio lugar a una capa pasiva protectora más gruesa, reduciendo la velocidad de corrosión en fluido corporal simulado. Las aleaciones enriquecidas con silicio demostraron una microdureza superior en condiciones de tensión en comparación con el titanio puro, lo que indica su potencial para aplicaciones biomédicas.

Tabla 5. Datos identificativos del artículo "Preliminary studies of new heat-treated titanium alloys for use in medical equipment".

Autores	Cristina Jiménez-Marcos, Julia Claudia Mirza-Rosca, Madalina Simona Baltatu, Patrica Vizureanu
Revista	Results in Engineering
Año	2025
Volumen	25
Páginas	13
DOI	10.1016/j.rineng.2025.104477
ISSN	2590-1230
Editorial	Elsevier
Índice de impacto	6.0
Cuartil	Q1

1.4. REFERENCIAS

[1] Kaur, M., and Singh, K. (2019). Review on titanium and titanium based alloys as biomaterials for orthopaedic applications. *Materials Science and Engineering: C*, *102*, 844–862. https://doi.org/10.1016/j.msec.2019.04.064

[2] Quinn, J., McFadden, R., Chan, C. W., and Carson, L. (2020). Titanium for Orthopedic Applications: An Overview of Surface Modification to Improve Biocompatibility and Prevent Bacterial Biofilm Formation. *IScience*, *23*(11), 101745. https://doi.org/10.1016/J.ISCI.2020.101745

[3] Romanò, C. L., Tsuchiya, H., Morelli, I., Battaglia, A. G., and Drago, L. (2019). Antibacterial coating of implants: Are we missing something? *Bone and Joint Research*, *8*(5), 199–206. https://doi.org/10.1302/2046-3758.85.BJR-2018-0316/ASSET/IMAGES/LARGE/2046-3758.85.BJR-2018-0316-FIG1.JPEG

[4] Tranquillo, E., and Bollino, F. (2020). Surface Modifications for Implants Lifetime extension: An Overview of Sol-Gel Coatings. *Coatings 2020, Vol. 10, Page 589*, *10*(6), 589. https://doi.org/10.3390/COATINGS10060589

[5] Niinomi, M., Nakai, M., and Hieda, J. (2012). Development of new metallic alloys for biomedical applications. *Acta Biomaterialia*, *8*(11), 3888–3903. https://doi.org/10.1016/J.ACTBIO.2012.06.037

[6] Băltatu, I., Vizureanu, P., Ciolacu, F., Achiţei, D. C., Băltatu, M. S., and Vlad, D. (2019). In Vitro study for new Ti-Mo-Zr-Ta alloys for medical use. *IOP Conference Series: Materials Science and Engineering*, *572*(1), 012030. https://doi.org/10.1088/1757-899X/572/1/012030

[7] Aggarwal, D., Kumar, V., and Sharma, S. (2022). Drug-loaded biomaterials for orthopedic applications: A review. *Journal of Controlled Release*, *344*, 113–133. https://doi.org/10.1016/j.jconrel.2022.02.029

[8] Hanawa, T. (2021). Metals and Medicine. *MATERIALS TRANSACTIONS*, *62*(2), 139–148. https://doi.org/10.2320/matertrans.MT-M2020268

[9] Kolli, R. P., and Devaraj, A. (2018). A Review of Metastable Beta Titanium Alloys. *Metals*, *8*(7), 506. https://doi.org/10.3390/met8070506

[10] Oliveira, N. T. C., Aleixo, G., Caram, R., and Guastaldi, A. C. (2007). Development of Ti–Mo alloys for biomedical applications: Microstructure and electrochemical characterization. *Materials Science and Engineering: A*, *452–453*, 727–731. https://doi.org/10.1016/J.MSEA.2006.11.061

[11] Khadija, G., Saleem, A., Akhtar, Z., Naqvi, Z., Gull, M., Masood, M., Mukhtar, S., Batool, M., Saleem, N., Rasheed, T., Nizam, N., Ibrahim, A., and Iqbal, F. (2018). Short term exposure to titanium, aluminum and vanadium (Ti 6Al 4V) alloy powder drastically affects behavior and antioxidant metabolites in vital organs of male albino mice. *Toxicology Reports*, *5*, 765–770. https://doi.org/10.1016/j.toxrep.2018.06.006

[12] Xu, W., Chen, M., Lu, X., Zhang, D. wei, Singh, H. preet, Jian-shu, Y., Pan, Y., Qu, X. hui, and Liu, C. zong. (2020). Effects of Mo content on corrosion and tribocorrosion behaviours of Ti-Mo orthopaedic alloys fabricated by powder metallurgy. *Corrosion Science*, *168*, 108557. https://doi.org/10.1016/J.CORSCI.2020.108557

[13] Bălţatu, S., Vizureanu, P., Mareci, D., Burtan, L. C., Chiruţă, C., and Trincă, L. C. (2016). Effect of Ta on the electrochemical behavior of new TiMoZrTa alloys in artificial physiological solution simulating in vitro inflammatory conditions. *Materials and Corrosion*, *67*(12), 1314–1320. https://doi.org/10.1002/maco.201609041

[14] Sharma, A., Waddell, J. N., Li, K. C., A Sharma, L., Prior, D. J., and Duncan, W. J. (2021). Is titanium–zirconium alloy a better alternative to pure titanium for oral implant? Composition, mechanical properties, and microstructure analysis. *The Saudi Dental Journal*, *33*(7), 546–553. https://doi.org/10.1016/J.SDENTJ.2020.08.009

[15] Sandu, A. V., Baltatu, M. S., Nabialek, M., Savin, A., and Vizureanu, P. (2019). Characterization and Mechanical Proprieties of New TiMo Alloys Used for Medical Applications. *Materials*, *12*(18), 2973. https://doi.org/10.3390/ma12182973

[16] Verestiuc, L., Spataru, M.-C. C., Baltatu, M. S., Butnaru, M., Solcan, C., Sandu, A. V., Voiculescu, I., Geanta, V., and Vizureanu, P. (2021). New Ti–Mo–Si materials for bone prosthesis applications. *Journal of the Mechanical Behavior of Biomedical Materials*, *113*, 104198. https://linkinghub.elsevier.com/retrieve/pii/S1751616120307402

1 INTRODUCCIÓN

2 PUBLICACIONES

3 DOCUMENTOS DE AUTORÍA

4 PARTICIPACIONES EN CONGRESOS

5 OTRAS PUBLICACIONES

6 CONCLUSIONES FINALES

Artículo 1. Experimental Research on New Developed Titanium Alloys for Biomedical Applications

bioengineering

MDPI

Article

Experimental Research on New Developed Titanium Alloys for Biomedical Applications

Cristina Jimenez-Marcos [1], Julia Claudia Mirza-Rosca [1,*], Madalina Simona Baltatu [2,*] and Petrica Vizureanu [2,*]

[1] Mechanical Engineering Department, Las Palmas de Gran Canaria University, 35017 Tafira, Spain
[2] Department of Technologies and Equipment for Materials Processing, Faculty of Materials Science and Engineering, Gheorghe Asachi Technical University of Iaşi, 700050 Iasi, Romania
* Correspondence: julia.mirza@ulpgc.es (J.C.M.-R.); cercel.msimona@yahoo.com (M.S.B.); peviz@tuiasi.ro (P.V.)

Abstract: The mechanical properties and electrochemical behavior of two new titanium alloys, Ti20Mo7Zr and Ti20Mo7Zr0.5Si, are investigated in this paper. The alloys have been manufactured by vacuum arc remelting (VAR) technique and studied to determine their microstructure, corrosion behavior, and mechanical properties. Metallographic observations and quantitative microanalysis by optical microscopy, scanning electron microscopy SEM, and energy dispersive X-rays spectroscopy EDX were performed. Data about the three-point bending test and microhardness are presented. For electrochemical properties, three different environments were used: Ringer solution at 25 °C, Ringer solution at 40 °C simulating fever condition, and 3.5% NaCl solution. Metallographic investigation revealed the biphasic and dendritic structure of both samples when the procedures were performed. Electrochemical testing in body simulation fluid, fever conditions, and saline medium showed that the lower the proportion of silicon in the samples, the higher the corrosion resistance. The formation of a titanium oxide layer on the surface of both samples was noticed using quantitative EDX analysis. The three-point bending test for the two samples revealed that the presence of silicon decreases the modulus of elasticity; the surface of the samples displayed soft and hard phases in the microhardness test. Electrochemical impedance spectroscopy (EIS) measurements were carried out at different potentials, and the obtained spectra exhibit a two-time constant system, attesting double-layer passive film on the samples.

Keywords: titanium alloys; Ti20Mo7Zr; Ti20Mo7Zr0.5Si; microstructure; corrosion behavior; mechanical properties

Citation: Jimenez-Marcos, C.; Mirza-Rosca, J.C.; Baltatu, M.S.; Vizureanu, P. Experimental Research on New Developed Titanium Alloys for Biomedical Applications. *Bioengineering* **2022**, *9*, 686. https://doi.org/10.3390/bioengineering9110686

Academic Editors: Bingbing Li, Himansu Sekhar Nanda, Geetha Manivasagam and Sushma Kumari

Received: 26 October 2022
Accepted: 10 November 2022
Published: 12 November 2022

1. Introduction

Nowadays, progress in medicine and materials development has made possible the study, design, and application of numerous biomaterials covering a wide range of medical fields covering orthopedics, drug administration, dentistry, skin tissue engineering, and cardiovascular systems, among many others, for the benefit of the human being [1,2]. In this way, people's quality of life and longevity can be improved. However, as human life expectancy rises, so does the elderly population, which is more prone to chronic musculoskeletal diseases such as osteoarthritis. It is believed that up to 15% of the population is affected by osteoarthritis [3].

For this reason, any biomaterial has to meet a number of requirements, the main one being biocompatibility with the human body, which is the ability of a material to fulfill its function in medical treatment by generating the most appropriate beneficial cellular or tissue response in that specific situation and optimizing the clinically relevant performance of that treatment [4,5]. In order to prevent implant loosening and to obtain a longer duration of service, which would save revision surgery, these biomaterials must have the following properties: high ductility, high fatigue and wear resistance, absence of cytotoxicity, and

a combination of high strength and low Young's modulus that is equivalent to human cortical bone and ranges from 10 to 30 GPa. Furthermore, the implant must integrate well with the nearby bone [2,5–8].

Biomedical implants based on polymers and ceramics show low mechanical strength and brittleness, which limits their applications for harsh working conditions [9]. Therefore, currently, within orthopedic surgery, it is necessary to develop prostheses made mainly of metallic materials.

Around 70–80% of implants are made of metallic biomaterials [7]. The most commonly used metals for medical applications are 316L stainless steel, CoCrMo alloys, and Ti and its alloys, such as Ti6Al4V and NiTi alloys [5,10]. The modulus of elasticity of metals is generally much higher than that of bone and prevents load transfer to the bone. The stress shielding effect can cause osteoporosis due to the excessive difference between the elastic modulus of metal and bone. In addition, there are few adequate metal candidates recommended for their use as long-term implants due to the toxic effect of the ions that they release in the adjacent tissues, their poor resistance to wear and corrosion, and, therefore, their low biocompatibility. Nevertheless, these issues can be solved by mixing the base metal with alloying components that do not exhibit any harmful impact on the body [2,5,9,11].

One of the most significant risks that can be caused by a metallic implant is corrosion, which is the deterioration of a material due to an electrochemical attack in its environment. Losses resulting from corrosion are estimated at hundreds of billions of dollars each year. This is in the order of 2–4% of the Gross National Product [12]. In order to prevent this phenomenon; a film is usually produced on the surface of the material, which makes it impermeable and protects it from the environment.

In general, titanium and its alloys have triumphed with respect to more traditional and are today widely used in aerospace, industrial, and biomedical applications, especially as tissue substitutes, such as dental implants, femoral heart valves, and fracture plates, due to the possibility of modifying their properties by changing the composition of the alloying elements, their biocompatibility with biological materials, their high corrosion resistance, high mechanical performance, low modulus and high thermal stability [2,3,8,12–17]. Due to titanium's poor electrical conductivity, which aids in the material's electrochemical oxidation by forming a highly stable passive oxide coating on its surface naturally, this material is biocompatible. The material is hence very resistant to corrosion [1,6,16,18].

There are three different kinds of titanium-based alloys: α, α + β, and β titanium. When heated above 882 °C, pure titanium changes from its alpha structure, known as the compact hexagonal structure (HCP), to its beta structure, body-centered cubic (BCC), as a result of an allotropic transition. Yet, the beta phase may often be kept at ambient temperature in this element's alloys, resulting in a material that has both phases. Additionally, changes in alloy characteristics such as ductility, plasticity, or formability result from differences in the relative quantities of different phases. These metallographic transformations and the properties of titanium alloys can be improved by the addition of α-stabilizers (C, N, O, Al), which increase the allotropic transformation temperature, β-stabilizers (V, Nb, Mo, Ta, Fe, Mn, Cr, Co, W, Ni, Cu, Si), which decrease the allotropic transformation temperature and the α / β ratio is affected, leading to an increase in the amount of β phase and finally neutral stabilizers (Zr, Sn, Hf, Ge, Th) [2,19–25].

Ti6Al4V alloy is the most widely used of all titanium alloys for orthopedic applications, as it has excellent mechanical properties, corrosion resistance in biofluids due to the stable passive oxide layer formed on its surface, biocompatibility and its properties can be modified by heat treatment. However, it does not have good wear resistance, even with soft tissue friction. Furthermore, it is highly toxic, as it causes harmful tissue reactions caused by the release of vanadium ions, which is a toxic and carcinogenic element and can even lead to aseptic loosening of the prosthesis, and of aluminum ions which, in high concentrations, can cause certain long-term health disorders such as peripheral neuropathy,

dementia, apathy or severe tremors, Alzheimer's and Parkinson's diseases and adverse tissue effects [15,26–32].

Taking all of this into account, four elements, Ti, Mo, Zr, and Si, were chosen for the construction of these new alloys because there is an important demand to develop new Ti alloys that have good mechanical properties and contain no toxic elements.

Ti-Mo alloys were investigated because molybdenum is a less poisonous element than common metals such as cobalt, nickel, and chromium, it is a β-stabilizing element, and some research suggests that adding molybdenum results in mechanical qualities resembling those of human bone. It also has low cost, high melting temperature, thermal stability, and corrosion resistance, being able to form a highly adherent stable oxide film (MoO_3) that stops titanium corrosion [11,12,19,33–36].

Ti-Mo-Zr alloys were developed because zirconium is becoming a desirable alternative for the majority of medical applications. It is highly biocompatible with human tissues, has a low modulus of elasticity, and is very resistant to corrosion [19,25,37,38].

New Ti-Mo-Zr-Si alloys were recently fabricated when small quantities of Si were added to Ti-Mo-Zr because silicon is an element present in human bone and is deemed biocompatible due to its effects on corrosion resistance, creep resistance, ductility, and titanium strength at high temperatures. Similar to molybdenum, it is a β-stabilizing element that affects the decline in the elastic modulus [19,32,37,39].

Thus, two new TiMoZrxSi alloys have been synthesized using a vacuum arc remelting furnace (VAR), and their microstructure, corrosion behavior, quantitative microanalysis, modulus of elasticity, and hardness were all examined in this study. These methods included metallography, electrochemical, scanning electron microscopy, three-point bending, and microhardness tests.

2. Materials and Methods

2.1. Material Preparation

We have carried out the analysis of two different compositional alternatives of new alloys with Titanium, Molybdenum, Zirconium, and Silicon, with the purpose of performing different experiments in order to determine the effect produced by the addition of silicon in one of the samples and in this way, to obtain their properties. The chemical composition of the studied alloys is TiMoZr (73% Ti, 20% Mo, 7% Zr) and TiMoZr0.5Si (72.5% Ti, 20% Mo, 7% Zr, 0.5% Si). The raw materials used were high-purity elements such as Ti (99% purity), Mo (99% purity), and Zr (99% purity) supplied by Alfa Aesar by Thermo Fisher Scientific. The production of these alloys was carried out at the Faculty of Materials Science and Engineering from Ghe, Asachi Technical University of Iasi, Romania, using a vacuum arc remelting furnace (VAR) where a consumable electrode was fused in a vacuum at a monitored rate using the heat produced by an electric arc between the electrode and the ingot. To achieve an adequate uniformity of the alloys, these were centrifuged and remelted six times (three times in each part) in an inert atmosphere of argon and ultimately solidified in an ingot. Arc melting was chosen for developing the new TiMoZrxSi alloys because the method produces ingots of the highest purity. Part of the ingots was sent to Las Palmas de Gran Canaria University for their preparation and testing.

First of all, the surfaces of the two samples were prepared by embedding them by adding a 4:1 ratio of epoxy resin in molds. It is to say, for every 4 drops of resin, a drop of catalyst was added. The samples were then cut longitudinally with a thickness of 1 to 1.5 mm using the Buehler IsoMet 4000 precision saw (Buehler, Lake Bluff, IL, USA). Furthermore, vertical cuts of about 0.5 mm thickness were performed employing the cutting device. Then, grinding and polishing were performed in two stages using the Struers TegraPol-11 polishing machine (Struers ApS, Ballerup, Denmark): using progressive grit silicon carbide papers from 280 to 1200 and the final polishing by applying 0.1 microns of alpha alumina suspension to polish the surfaces to a mirror finish. The experimental steps were in accordance with ASTM E3-11(2017) for the preparation of metallography samples.

Finally, the samples were immersed in a heated "Ultrasons-HD" ultrasonic apparatus from J.P. Selecta (JPS, Barcelona, Spain) for 10 minutes to remove all traces of dirt and impurities (see Figure 1).

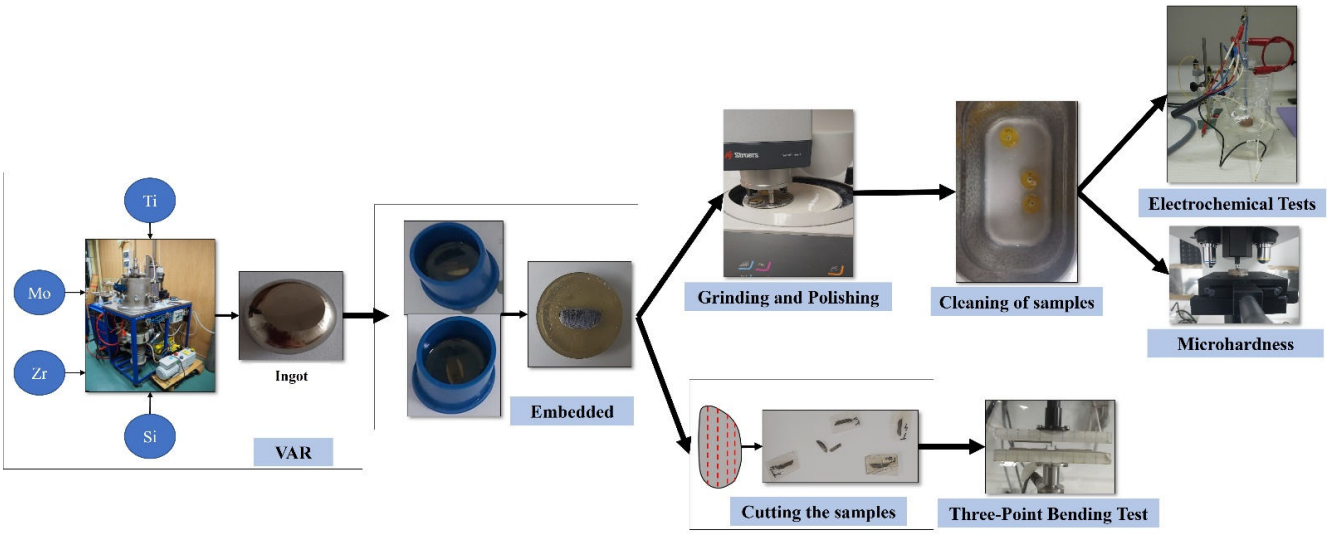

Figure 1. Schematic representation of the material preparation.

The titanium alloys under study, as mentioned above, have a passive titanium oxide layer that protects them from the medium, and this layer has different properties from those of the base metal. Thus, to obtain a correct hardness measurement, first, a lower load is applied to make the indenter penetrate to a certain depth, and then progressively higher loads are applied to obtain the hardness values of the base metal.

2.2. Metallography

For this test, images of the sample surfaces were taken using the Axio Vert.A1 MAT ZEISS (Zeiss, Jena, Germany) metallographic optical microscope, magnifying 10 and 20 times their actual size. Each sample was immersed in a Kroll etching reagent composed of H_2O, HNO_3, and HF for 15 seconds, and images of the etched surface were taken.

2.3. Electrochemical Tests

In order to carry out these tests, a sample (working electrode) in Ringer's solution is introduced in the electrochemical cell together with two electrodes: the saturated calomel electrode (SCE) is used as the reference electrode, and the platinum electrode acts as the counter electrode. The Ringer Grifols solution (from Grifols Laboratories, Barcelona, Spain) had the following contents in mmol/L: Na+ 129.9; K+ 5.4; Ca2+ 1.8; Cl− 111.7; and $C_3H_5O_3$ 27.2.

Five techniques were applied using the BioLogic Essential SP-150 potentiostat (Bio-Logic Science Instruments SAS, Seyssinet-Pariset, France): Corrosion Potential, Electrochemical Impedance Spectroscopy in Ringer's solution, in saline medium, and in fever state, Corrosion Rate, Corrosimetry, and Pitting Potential.

2.3.1. Corrosion Potential

In order to measure the corrosion potential, the "Ecorr vs. time" technique was applied for 24 h, with potential values of ±10 V and with a potential recording every 300 s or every time varying by 200 mV. The data obtained were plotted as a graph of potential vs. time, which may remain constant with respect to time or show a trend toward passivation or corrosion.

2.3.2. Electrochemical Impedance Spectroscopy (EIS)

For the impedance measurement, "Potential Electrochemical Impedance Spectroscopy" was selected, and the surface value and the measurement duration of 5 minutes were entered. This measurement was performed 7 times for each sample, at ± 300 mV vs. Ecorr in Ringer's solution, with maximum and minimum potential values of ±10 V. These data were represented by Bode and Nyquist diagrams and equivalent circuits.

This same technique, with the same data, was applied in the simulation of saline and fever-state media. In the saline medium, however, the saline solution was first created using 35 g of NaCl in 1 L of solution, and the sample was immersed for 24 h. On the other hand, in the case of fever states, the electrochemical cell was immersed in a Grant Instruments Y14 thermostatic bath (Grant Instruments, Cambridgeshire, England), applying heat (40 °C) for 24 h. After the measurements were taken, they were plotted on bode diagrams.

2.3.3. Corrosion Rate

In order to perform these measurements, the "Linear Polarization" technique was selected, and the sample surface area value and the test duration of 20 minutes were entered to stabilize its potential. The maximum and minimum potential values were ±10 V, with the potential scanning presenting a 0.167 mV/s time-variation relationship from −0.025 to 0.025 V versus open circuit potential (Eoc), with data recording every 0.5 s and intensity throughout the potential scanning at 100%. These linear polarization curves were then plotted, and EC-Lab's "Tafel Fit" analysis was applied to find the corrosion rate values for each sample.

2.3.4. Corrosimetry

The measurement of the Rp was performed by applying the "Corrosimetry" technique within the software and filling in the configuration window the parameters such as surface area, equivalent weight, and density of the samples with the duration time of each cycle to be performed being a total of 10 cycles for each sample, in addition to parameters previously obtained by means of linear polarization (βa and βc). The maximum and minimum potential values were ±10 V, and the potential scan showed a time-varying ratio of 0.167 mV/s from −0.025 to 0.025 V versus Eoc, with data recorded every 1 s and intensity throughout the potential scan at 100%. Next, polarization resistance data were plotted versus time.

2.3.5. Pitting Potential

In order to carry out the test, the "Cyclic Potentiodynamic Polarization" technique was selected where the applied potential scan was −0.7 V and 2 V with respect to the reference electrode and with a reverse scan of up to −0.5 V with a data recording every 0.5 s and of the intensity every time 200 mA or every 1 s varies. The maximum and minimum values of the potential were ±10 V. After performing the test for each sample, the graphs obtained were curves as a function of current intensity (mA) and potential (V).

2.4. Scanning Electron Microscopy (SEM)

In order to realize this test, the samples were prepared and placed inside the Zeiss Sigma 300 VP (Zeiss, Jena, Germany) microscope using a sample holder, and a vacuum was applied. Then, using SmartSEM, an image of the surface of the sample was taken at 1000× magnification and for 20kV, and, using SmartEDX, the quantitative microanalysis of the sample was carried out, obtaining the percentages of the elements and the spectrum.

2.5. Three-Point Bending Test

The three-point bending method was carried out using the Bose ElectroForce® 3100 machine (Bose Corporation, Framingham, MA, USA), which complies with ISO 7438:2020 and can withstand up to 20 N of applied force. In this case, each specimen of rectangular cross-section, with a length varying from approximately 13 to 12 mm, was placed at the

extremities of the bottom shank of the testing device, allowing enough space between the supports, which ranged from 7.80 to 10.63 mm, depending on the length of the specimens. Then, a vertical load with a linear velocity of 3 mm/s was applied at the center point of the specimen until the specimen exceeded its yield strength or split. In order to determine the modulus of elasticity, the obtained values of the applied load versus the displacement of the specimens were plotted, and their slope was obtained.

2.6. Microhardness

According to ISO 14577-1:2015, 10 indentations were made for each applied load of each sample, in this case, 5 gf, 25 gf, and 50 gf using the Affri DM8 B hardness tester. When very small loads are applied, there is a good chance that the mark will be found in only one phase so that the hardness of that phase can be evaluated; as the load increases, the mark may cover parts of several phases, giving an idea of the total hardness of the material. Then, using the Aries software, the lengths of the diagonals were measured, and the Vickers microhardness values were automatically calculated. These hardness values were plotted against the number of indentations performed.

3. Results and Discussion

3.1. Metallography

Metallography is the study of the structural or constitutive characteristics of metals or alloys in order to relate them to their physical and mechanical properties. In this way, the spatial structure of the phases and compounds that make up a metallic material may be demonstrated in this method, and the impurities, fiber orientation, and potential mechanical flaws in the samples can also be determined [40].

After the electrochemical etching representative, metallographic images of the analyzed alloys are presented in Figure 2.

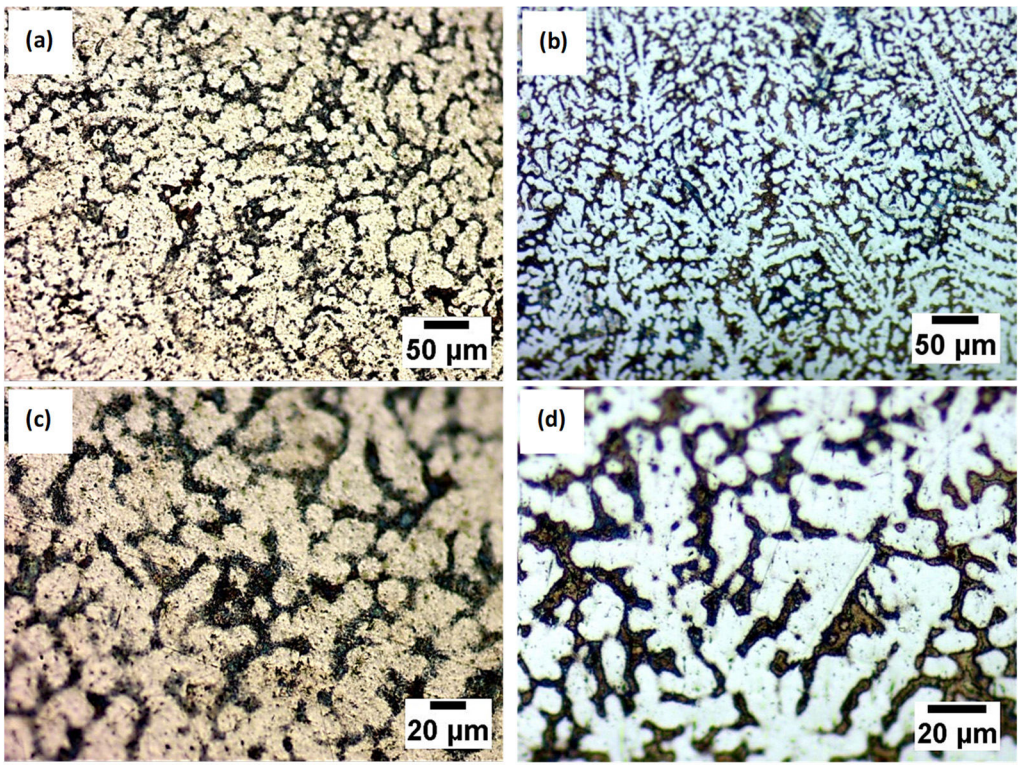

Figure 2. Microstructure by optical microscopy after chemical etching for different magnifications of the Ti20Mo7Zr (**a**,**c**) and Ti20Mo7Zr0.5Si (**b**,**d**) sample.

While cpTi has an HCP structure, or an α-phase, at ambient temperature, there is a BCC structure, called β-phase, at temperatures over 883 °C. With the inclusion of β-stabilizers such as Mo and Si, the β-phase is stable at temperatures below 883 °C; in contrast, Zr is regarded as a neutral element since it almost has no impact on the α/β phases [2].

It can be observed that both analyzed samples, after being attacked, contain a biphasic and dendritic structure, distinguishable for both magnifications. Furthermore, the size of dendrites decreased by almost 25% with the Si addition while the interdendritic zone increased.

3.2. Electrochemical Tests

3.2.1. Corrosion Potential

The corrosion potential is the point at which the cathodic current density becomes anodic when a metal is introduced into the solution, although, according to the Mixed Potential Theory developed by Wagner and Traud [41], the oxidation and reduction reactions in corrosion occur at the same rate at the surface of the metal.

The evolution of corrosion potential with time is used as a quantitative criterion for corrosion behavior but remains insufficient for a complete analysis.

We noted that the corrosion potential of both samples increased during the immersion time, indicating the passivation of the samples in the Ringer solution. The curves did not exhibit potential drops associated with surface activation during the exposure, suggesting that the passive film is thermodynamically resistant in these conditions (see Figure 3).

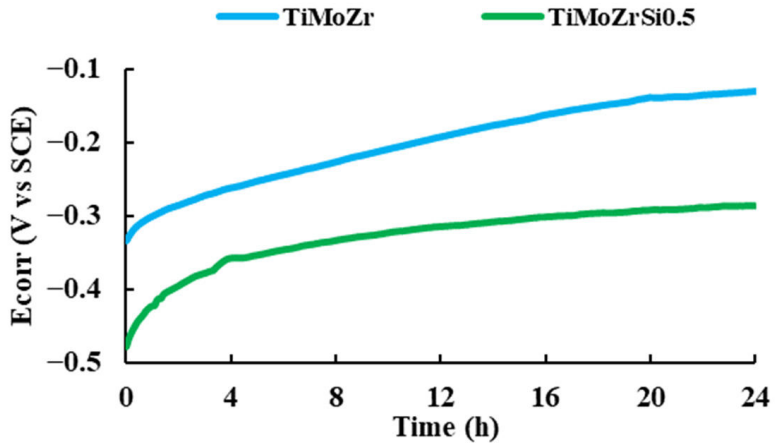

Figure 3. Corrosion potential vs. time for 24 h of immersion in Ringer solution.

The corrosion potential of Ti20Mo7Zr0.5Si (−0.286 V) is more negative than that of Ti20Mo7Zr (−0.150 V) and of cpTi (between −0.1 V and −0.15 V), suggesting that the characteristics of passive film changed with Si addition [42].

3.2.2. Electrochemical Impedance Spectroscopy (EIS)

Electrochemical Impedance Spectroscopy (EIS) allows the characterization of material properties and electrochemical systems by applying a variable frequency sine electric potential perturbation to the study and recording the current response within the electrochemical cell. Electrochemical impedance spectroscopy (EIS) is a high-performance technique used for the examination of interfacial characteristics associated with processes that occur on the surface of metallic alloys. With respect to other electrochemical techniques, EIS provides various benefits as it is a stationary state technique, which involves the measurement of small signals and is capable of probing, in our case, from 100 mHz to 100 KHz.

Bode and Nyquist diagrams in Ringer's solution

The electrochemical impedance spectroscopy results are presented in Bode plots (see Figure 4) for both alloys recorded at three different potentials in the Ringer solution. The

maximum impedance value and the maximum phase angle for each case are presented in Table 1.

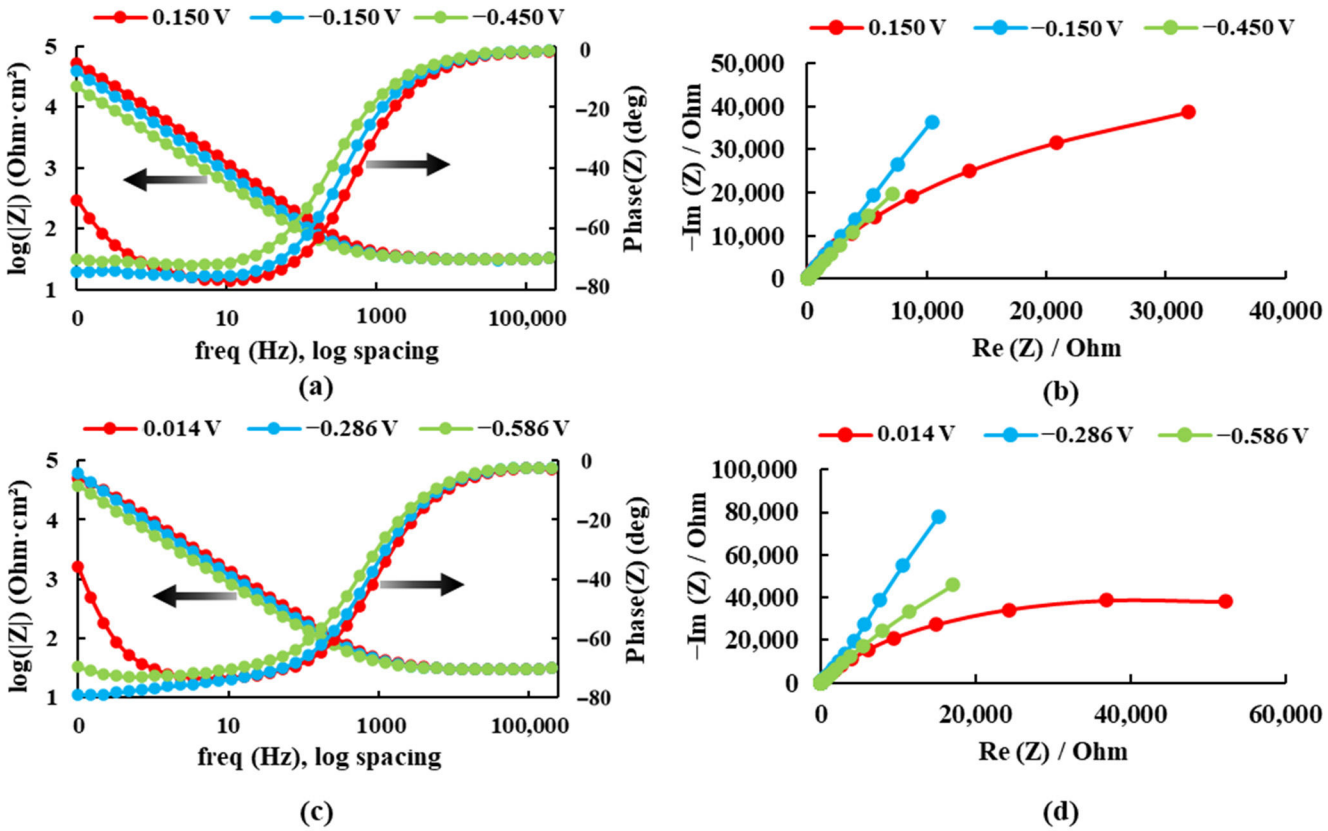

Figure 4. Bode and Nyquist diagrams for: (**a**,**b**) Ti20Mo7Zr and (**c**,**d**) Ti20Mo7Zr0.5Si in Ringer's solution.

Table 1. Results obtained in the Bode diagrams for the Ti20Mo7Zr and Ti20Mo7Zr0.5Si samples.

Alloys	Ti20Mo7Zr			Ti20Mo7Zr0.5Si		
Potential [V]	−0.450	−0.150	0.150	−0.586	−0.286	0.014
Max. Impedance [Ω]	21,380	38,905	51,286	38,019	60,256	50,119
Max. phase angle [°]	72	76	77	73	79	74

For the sample Ti20Mo7Zr, when analyzing Figure 4a and Table 1, the impedance and phase angle values tend to increase as the applied potential becomes more positive. The process occurs in a single stage (time constant) as the curve tends to decrease. Whereas, for the Ti20MoZr sample, both Figure 4b and Table 1 show an increase in the impedance and phase angle values as the applied potential value increases, apart from the 0.014 V potential curves, where the values decrease, and it is observed that, at 0.1 Hz, the Bode Phase curve presents two-time constants. Therefore, the maximum corrosion resistance value was obtained by the Ti20Mo7Zr0.5Si sample.

Equivalent Circuits

For all the EIS spectra of cpTi, a capacitive behavior can be observed that was fitted by the compact passive film model [42] in Figure 5, the circuit that has been adapted to the results obtained by means of the Bode diagrams in Ringer's solution is R(QR)(QR). This

circuit indicates that the samples present a resistance to dissolution and two passive layers (porous and compact) until the alloy is reached.

$$Z(f) = R_1 + \frac{R_2}{R_2Q_2(j2\pi f)^{n_2} + 1} + \frac{R_3}{R_3Q_3(j2\pi f)^{n_3} + 1} \quad (1)$$

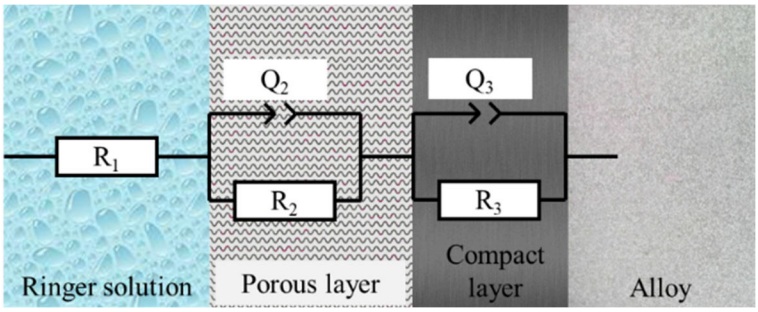

Figure 5. Equivalent circuit R(QR)(QR).

Equation (1) indicates the impedance value for the equivalent circuit R(QR)(QR). According to Equation (1), the value of the impedance depends on the following parameters:

- R_1: Resistance of the dissolution.
- R_2: Resistance of the porous layer.
- R_3: Resistance of the compact layer.
- Q_2 and Q_3: Constant phase element.
- f: Frequency.
- n_2 and n_3: Parameter indicating whether the constant phase element simulates a capacitor (n = 1), a semi-infinite Warburg impedance (n = 0.5), or a resistor (n = 0).

Sample Ti20Mo7Zr

After the selection of the equivalent circuit, the values of the circuit resistances and the constant phase elements (Table 2) were obtained, and the values of the impedance and phase angle measured and calculated by this circuit were plotted for the most negative and the most positive potential (Figure 6), thus obtaining the value of the corrosion resistance of the passive layers higher for the most positive potential.

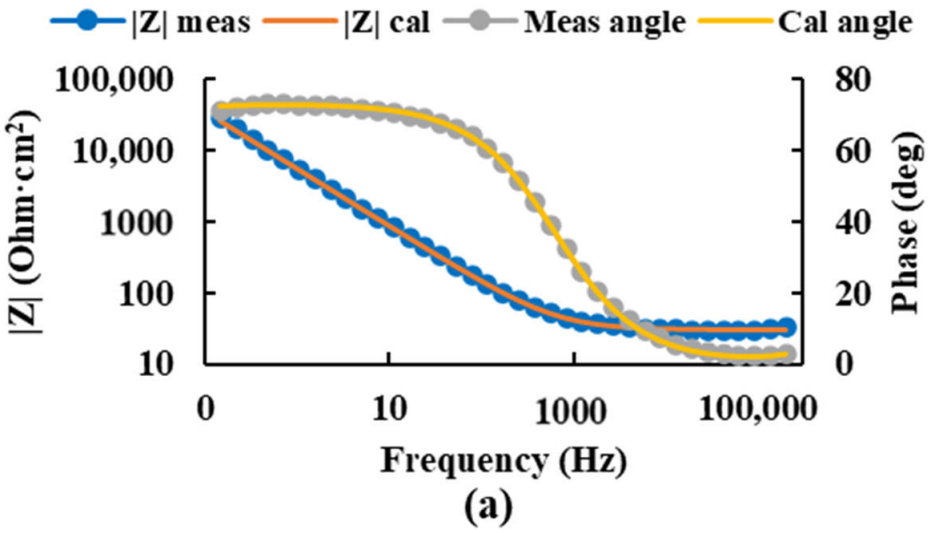

Figure 6. *Cont.*

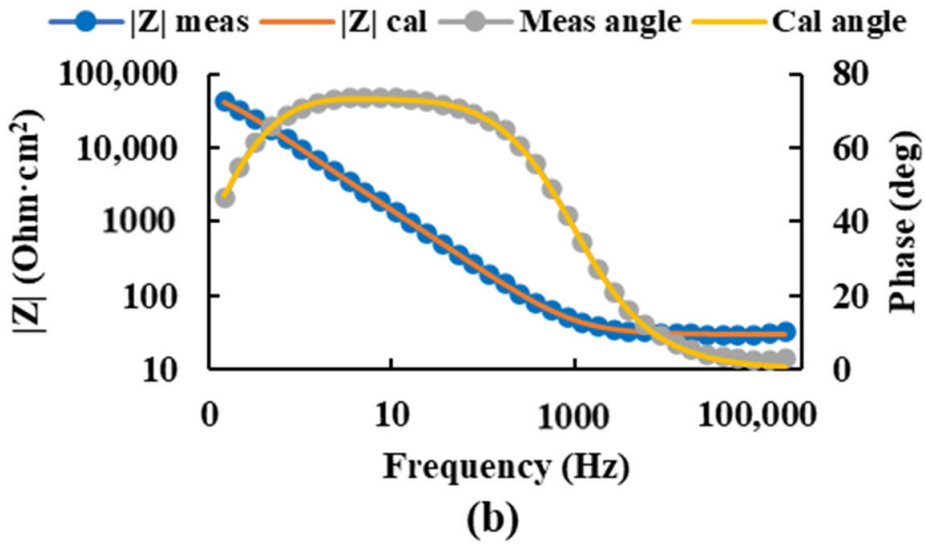

Figure 6. Bode diagram of the measured and calculated impedance and angle of the Ti20Mo7Zr sample at potentials −0.450 V (**a**) and 0.150 V (**b**) using the equivalent circuit R(QR)(QR).

Table 2. Equivalent circuit R(QR)(QR) of sample Ti20Mo7Zr.

Potential	R_1 (Ω)	Y_{01} (S × Sec^n)	n_1	R_2 (Ω)	Y_{02} (S × Sec^n)	n_2	R_3 (Ω)	χ^2
−0.450 V	31.55	1.48×10^{-4}	0.76	3.41×10^{3}	7.25×10^{-5}	0.95	1.18×10^{5}	4.73×10^{-4}
0.150 V	31.47	2.78×10^{-5}	0.98	8.00×10^{4}	5.53×10^{-5}	0.82	7.72×10^{3}	4.45×10^{-4}

Sample Ti20Mo7Zr0.5Si

For the Ti20Mo7Zr0.5Si sample, the measured impedance and phase angle values were plotted as calculated by the circuit using Figure 7, and the values of the circuit resistances and constant phase elements were obtained (Table 3). In this case, the values of the corrosion resistance of the porous layers were higher for the more positive potential.

In this case, higher corrosion resistance was obtained in the compact layer for the most negative potential. However, in the porous layer, it was higher for the most positive potential.

Table 3. Equivalent circuit R(QR)(QR) of sample Ti20Mo7Zr0.5Si.

Potential	R_1 (Ω)	Y_{01} (S × Sec^n)	n_1	R_2 (Ω)	Y_{02} (S × Sec^n)	n_2	R_3 (Ω)	χ^2
−0.586 V	18.2	6.87×10^{-9}	0.99	1.16×10^{1}	3.98×10^{-5}	0.81	2.01×10^{6}	5.19×10^{-4}
0.014 V	29.6	1.97×10^{-5}	0.89	7.36×10^{4}	1.52×10^{-4}	0.75	4.78×10^{2}	5.49×10^{-4}

Simulation of Saline Environments

In view of the Bode diagram curves in Figure 8 and the results in Table 4, it is observed that the values of the logarithm of the impedance and phase angle tend to increase with the application of a more positive potential and, therefore, the corrosion resistance increases, which is maximum for the Ti20Mo7Zr0. 5Si sample. The dissolution process of the Ti20Mo7Zr sample occurs in two stages, while that of the Ti20Mo7Zr0.5Si sample occurs in three stages, as the phase angle curve grows, decreases, grows, decreases, and grows again.

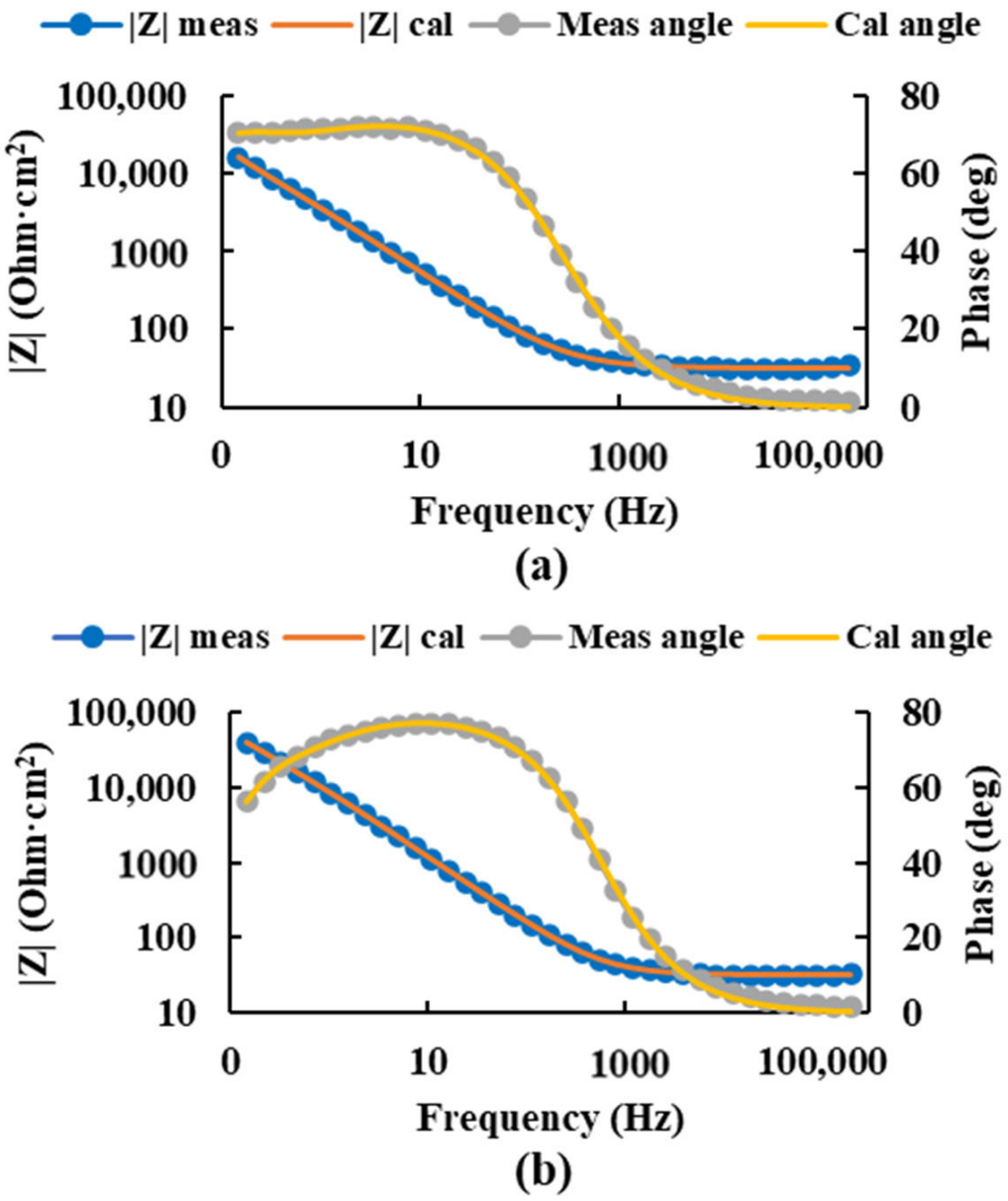

Figure 7. Bode diagram of the measured and calculated impedance and angle of the Ti20Mo7Zr0.5Si sample at potentials −0.586 V (**a**) and 0.014 V (**b**) using the equivalent circuit R(QR)(QR).

Table 4. Results obtained in Bode diagrams for Ti20Mo7Zr and Ti20Mo7Zr0.5Si in saline environments.

Alloys	**Ti20Mo7Zr**			**Ti20Mo7Zr0.5Si**		
Potential [V]	−0.450	−0.150	0.150	−0.586	−0.286	0.014
Max. Impedance [Ω]	29,512	43,652	45,709	3981	4786	5129
Max. phase angle [°]	72	74	73	60	63	66

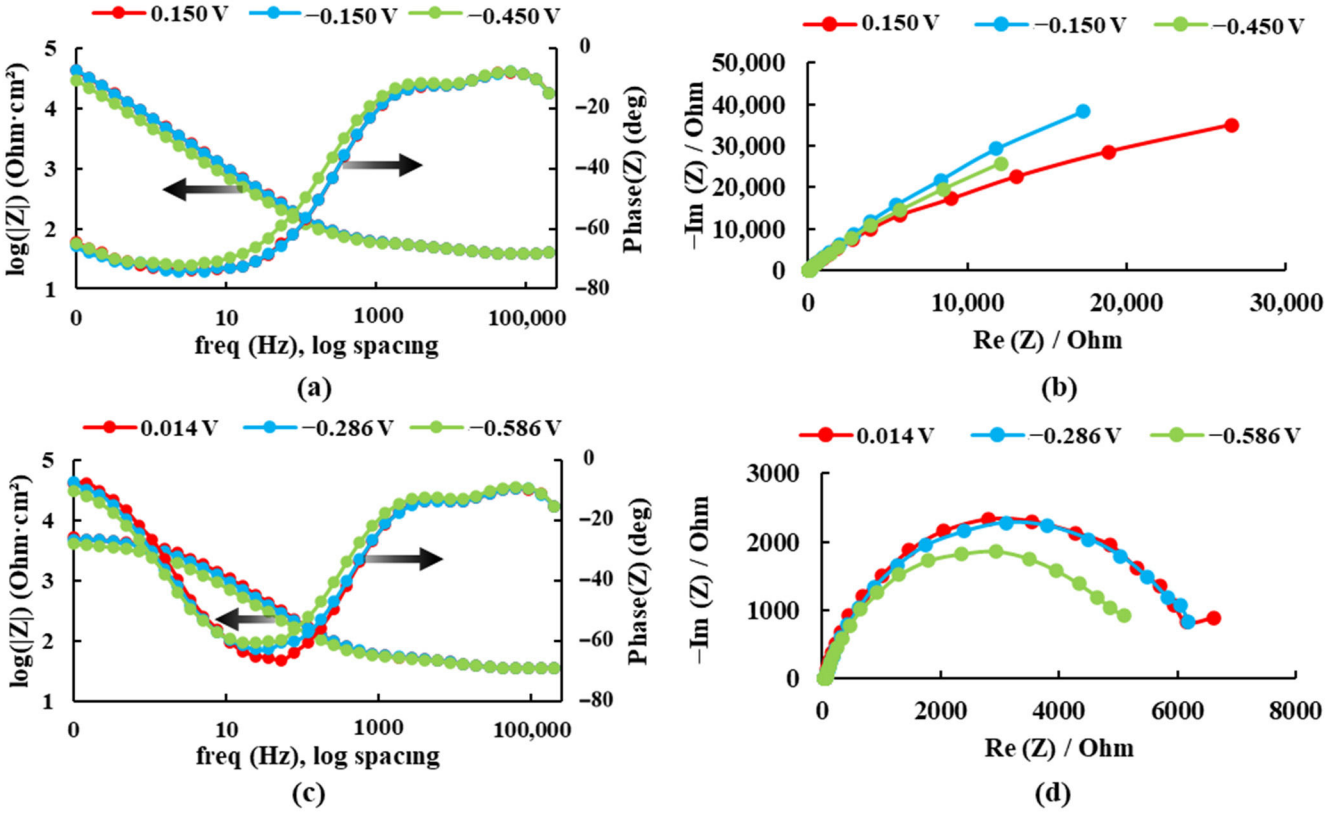

Figure 8. Bode and Nyquist diagrams for: (**a**,**b**) Ti20Mo7Zr and (**c**,**d**) Ti20Mo7Zr0.5Si in saline environments.

Simulation of Fever States (40 °C)

As in the salt medium simulation, it can be seen in Figure 9 and Table 5 that the impedance and phase angle values tend to increase as the applied potential becomes more positive. The dissolution process of the Ti20Mo7Zr sample occurs in three stages as the phase angle curve grows, decreases, grows, and decreases again. However, in the Ti20Mo7Zr0.5Si sample, only two-time constants are observed. In this case, the highest corrosion resistance value was presented by Ti20Mo7Zr.

Table 5. Results obtained in Bode diagrams for Ti20Mo7Zr and Ti20Mo7Zr0.5Si a 40 °C.

Alloys	Ti20Mo7Zr			Ti20Mo7Zr0.5Si		
Potential [V]	−0.450	−0.150	0.150	−0.586	−0.286	0.014
Max. Impedance [Ω]	40,738	56,234	61,660	22,387	42,658	47,863
Max. phase angle [°]	48	50	50	71	78	76

3.2.3. Corrosion Rate

The corrosion rate provides information about the impact of an environment on material and can be found by means of linear polarization curves, which are represented by potential and intensity.

The linear polarization test carried out to determine the corrosion rate of the alloys, plotted on a semi-logarithmic scale of current values, is presented in Figure 10.

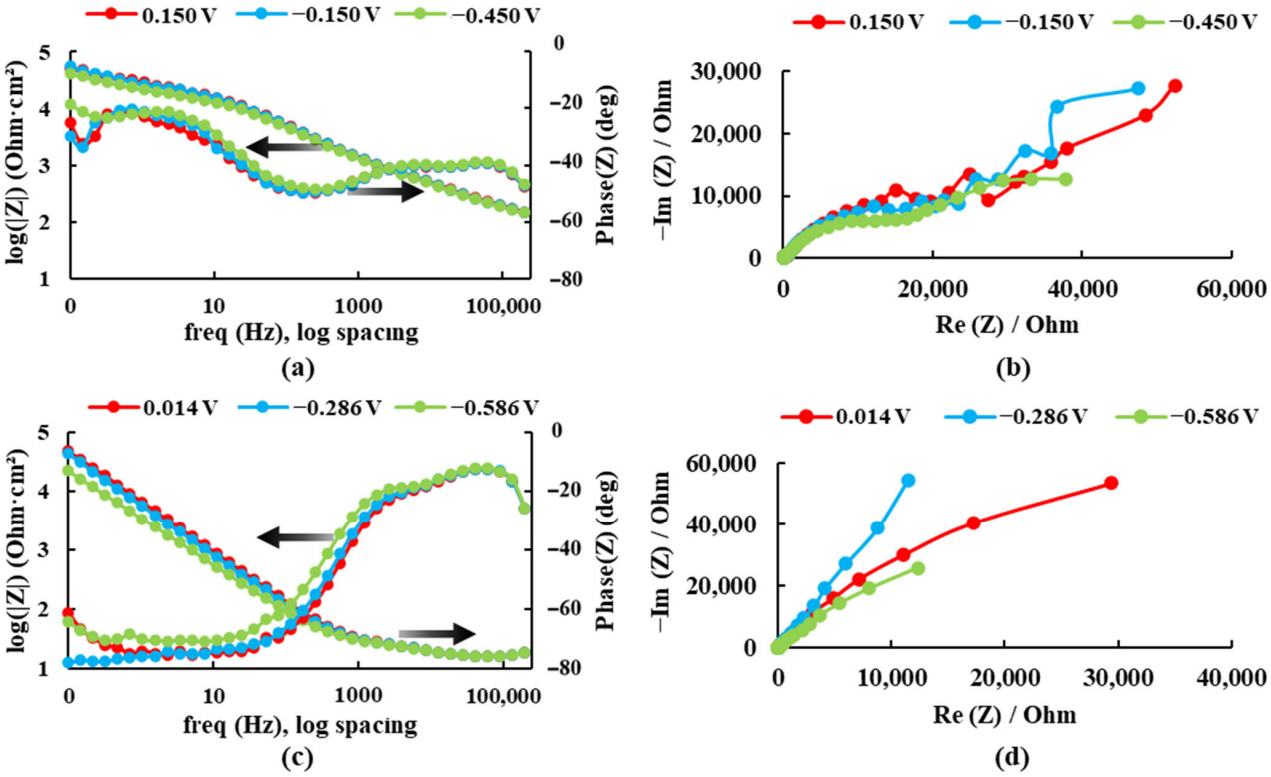

Figure 9. Bode and Nyquist diagrams for: (**a**,**b**) Ti20Mo7Zr and (**c**,**d**) Ti20Mo7Zr0.5Si in Ringer's solution at 40 °C.

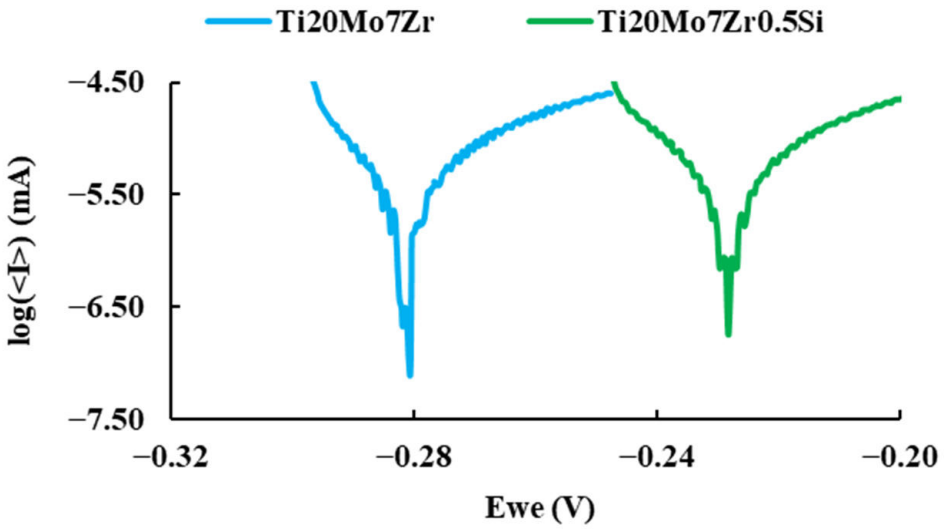

Figure 10. Comparison of the polarization curves of the samples.

It can be observed more anodic corrosion potential values for Ti20Mo7Zr0.5Si than those of Ti20Mo7Zr. The corrosion current (i_{corr}) is indicative of the degree of oxidation of the alloy, and it can be observed that it is bigger for the alloy with Si addition. The Tafel slopes (β_a and β_c) were determined by analyzing the curve plotted in a range of ±250 mV vs. open circuit potential (OCP). An alloy with a tendency to passivate will have a value of βa greater than βc, whereas an alloy that tends to corrode will have an anodic slope smaller than the cathodic slope. In our case (see Table 6), both alloys tend to passivate.

Table 6. Corrosion parameters entered and obtained for all samples tested.

Parameters	Ti20Mo7Zr	Ti20Mo7Zr0.5Si
E_{corr} (mV vs. Ref)	−228.76	−282.06
I_{corr} (nA/cm^2)	1.94	2.58
β_c (mV/dec)	12.8	12.9
β_a (mV/dec)	19.2	17.3
Equivalent weight (g/eq)	60.52	60.42
Density (g/cm^3)	5.75	5.77
Surface (cm^2)	1.03	0.78
Corrosion rate (mpy)	2.63×10^{-3}	3.50×10^{-3}

Table 6 shows the parameters of the Tafel line and the corrosion rate (CR) of the tested samples, which is expressed in thousandths of an inch of annual penetration (mpy) according to the following equation:

$$CR = \frac{I_{corr} \times K \times EW}{d \times A}$$

where:

I_{corr} is corrosion current (in A).

K is the constant that defines the units of the corrosion rate (1.288×10^5 miliinches/A-cm-year).

EW is the equivalent weight (in g/cm^3).

A is the sample area (in cm^2).

In this case, a maximum corrosion rate of 3.50×10^{-3} mpy (Ti20Mo7Zr0.5Si) and a minimum corrosion rate of 2.63×10^{-3} mpy (Ti20Mo7Zr) were obtained, while cpTi in the same conditions has a higher corrosion rate of 4.8×10^{-3} mpy [42].

3.2.4. Corrosimetry

Corrosimetry is designed to follow the evolution of standard corrosion values (R_p, E_{corr}, I_{corr}) as a function of time. The polarization resistance (R_p) is defined as the slope of the potential-current density curve at the free corrosion potential and is inversely proportional to the uniform corrosion rate.

After obtaining the corrosion rate, Figure 11 shows the variation of the polarization resistance with respect to the 3 hours' time for the two study samples.

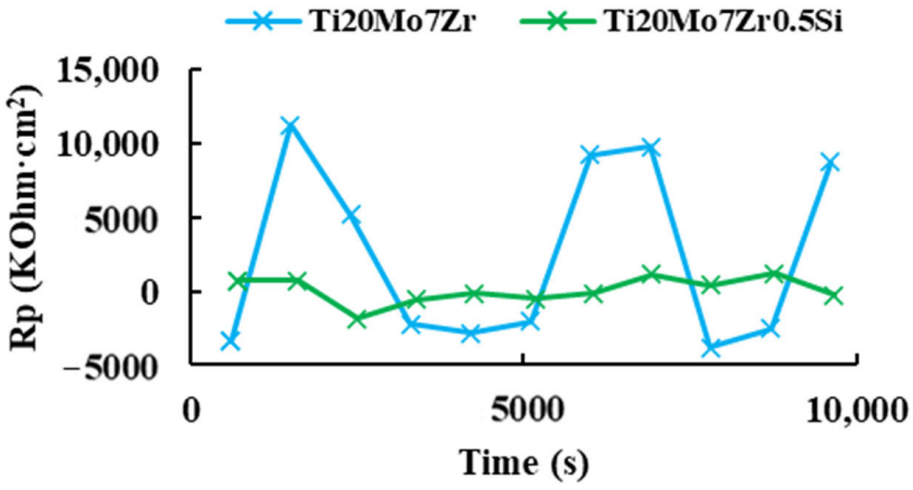

Figure 11. Polarization resistance versus time of Ti20Mo7Zr and Ti20Mo7Zr0.5Si.

For both samples, it was not possible to appreciate a behavior of decrease or increase in the polarization resistance with respect to the time, being in the case of Ti20Mo7Zr0.5Si,

the obtained values of the polarization resistance were very dispersed during the duration of the test. Then, it could be verified in the EC-Lab software manual that this is a technique that requires application over long periods of time (months). Therefore, it was decided to apply the "R_p Fit" analysis of the EC-Lab software to the linear polarization plots of the corrosion rate, where the X-axis shows the potential Vs. the reference electrode, while the Y-axis shows the current intensity.

The data obtained for the polarization resistance are shown in Table 7. As the value of the polarization resistance (R_p) is bigger, the alloy is more resistant to corrosion. For highly corrosion-resistant materials, the R_p may even reach 10^6 Ω·cm^2, so both alloys are very resistant to corrosion.

Table 7. Polarization resistance of Ti20Mo7Zr and Ti20Mo7Zr0.5Si applying "R_p Fit."

Parameters	Ti20Mo7Zr	Ti20Mo7Zr0.5Si
Rp (Ohm·cm^2)	836,389	1,080,000
E_{corr} (mV)	−226.32	−233.88
I_{corr} (μA/cm^2)	3.99×10^{-3}	2.97×10^{-3}

3.2.5. Pitting Potential

Pitting is one of the most insidious forms of localized corrosion in which small holes appear on the surface of the material since the passive layer on the surfaces of many metals breaks down in the presence of ionic concentrations such as chlorides and bromides. The pitting corrosion behavior of titanium alloy samples in Ringer's solution was examined by cyclic potentiodynamic polarization at room temperature, and the plots of intensity versus time were plotted in Figure 12.

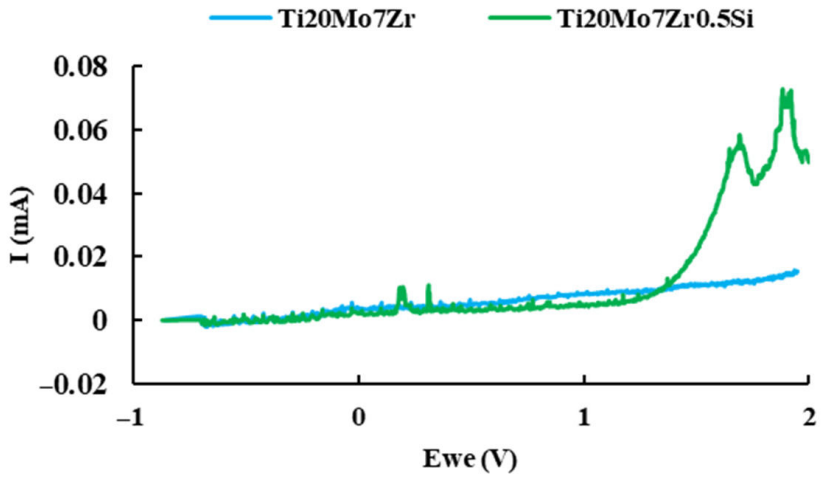

Figure 12. Current versus potential curve of Ti20Mo7Zr and Ti20Mo7Zr0.5Si samples.

The Ti20Mo7Zr sample reaches the maximum 2 V set in the test parameters without corroding. The same happens with Ti20Mo7Zr0.5Si, although, in this case, when the sample reaches 2 V, the intensity values are higher.

3.3. Scanning Electron Microscopy (SEM)

Scanning electron microscopy is a topographical, structural, and compositional analysis technique widely used in the study of semiconductors or nanoparticles, among others.

Energy dispersive X-rays spectroscopy EDX results for the investigated area of each sample after the corrosion process are presented in Figure 13.

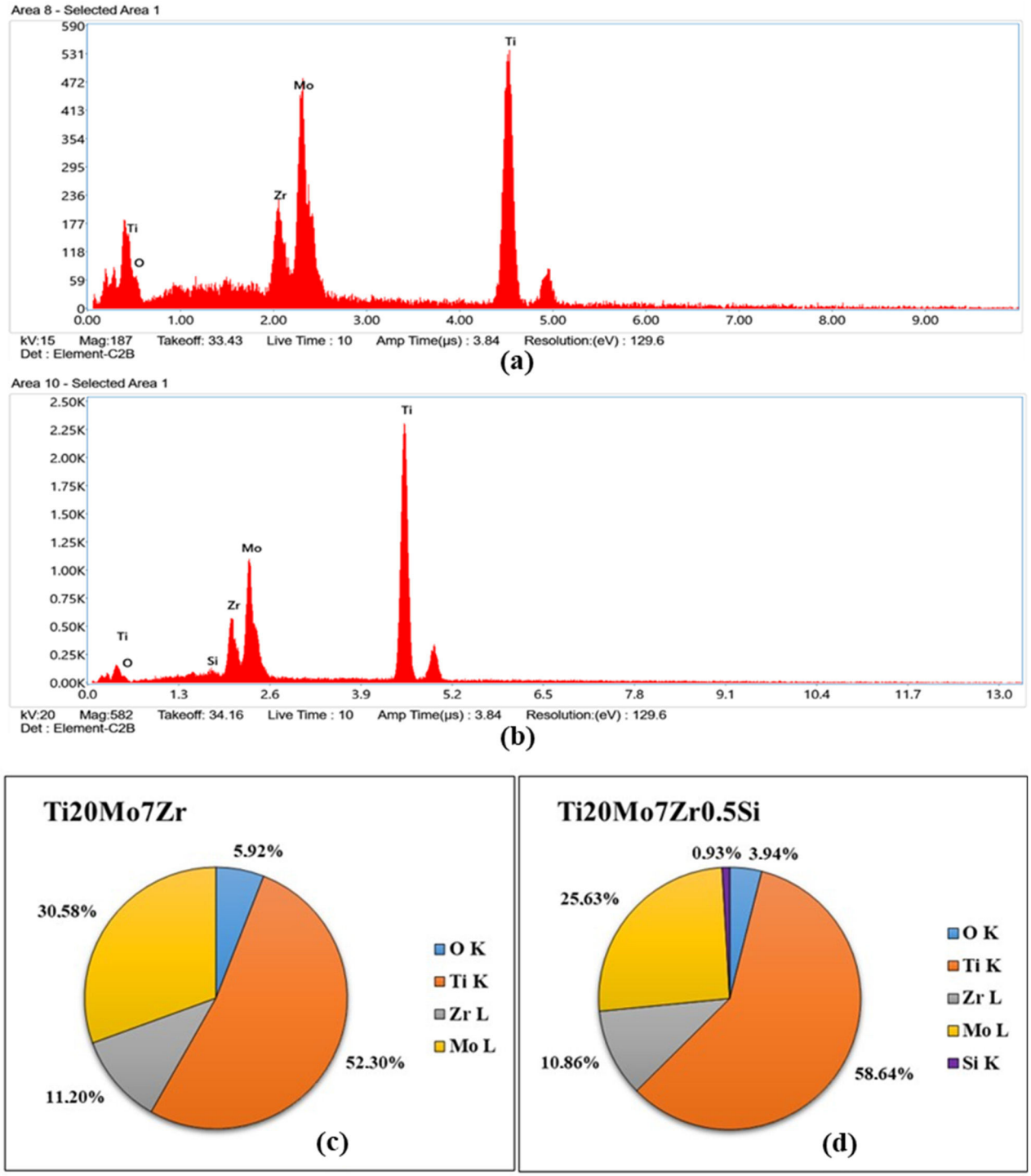

Figure 13. EDX spectra for Ti20Mo7Zr (**a**) and Ti20Mo7Zr0.5Si (**b**) samples and quantification (**c**,**d**).

EDX spectra show the energy dispersive obtained for both samples, which indicate the presence of the constituent elements in addition to oxygen (see Figure 13c,d), probably due to the formation of the titanium oxide layer and the corrosion processes carried out previously. On the other hand, with respect to the quantitative values provided, by selecting only a small area of the part of the sample surface at 1000 magnification by SEM, the percentages differ with respect to those produced by the manufacturer due to the fact that on the alloy's surface there are dendrites and interdendritic areas and the area selected for the microanalysis could have been found in one of the different phases presented by the

sample. It can be observed that there is one area rich in Mo, Zr, and Si and another area rich in Titanium.

3.4. Three-Point Bending Test

After determining the values of the modulus of elasticity for each specimen, it was decided to calculate the mean of the samples tested, taking into account their mean deviation, which corresponds to the arithmetic mean of the absolute values of the deviations from the mean.

In Table 8, the average value of the modulus of elasticity of the tested specimens of the Ti20Mo7Zr sample was 86.85 ± 10 GPa, while, in the case of sample Ti20Mo7Zr0.5Si, it was obtained at 49.33 ± 12 GPa, which is lower than the other specimen and close to Young's modulus of human bone.

Table 8. Modulus of elasticity values obtained from the tested specimen of Ti20Mo7Zr and Ti20Mo7Zr0.5Si.

Sample	E Average (GPa)
Ti20Mo7Zr	86.85 ± 10.16
Ti20Mo7Zr0.5Si	49.33 ± 12.00

In turn, these results obtained are in similar ranges to those found in previous research for the TiMoZrTa alloy (52–69 GPa). However, if zirconium is eliminated in the alloy of this study (TiMoSi), lower values of the modulus of elasticity (20–43 GPa) close to that of human bone (7–30 GPa) are obtained [19]. On the other hand, when compared to more common dental and commercially used alloys such as CoCrMo (210–253 GPa), stainless steel (190–210 GPa), Ti6Al4V (119 GPa), C. P. Ti (105 GPa), it can be stated that the new alloy, TiMoZrSi, has a much lower modulus of elasticity.

3.5. Microhardness

Generically, this test consists of applying a vertical load on the surface of the samples using the pyramidal tetrahedral indenter of the hardness tester, which has an angle between edges of 136°, until the indentation is created and, following the Vickers method, the load applied, and the area left in the indentation are related.

For the analysis of the results obtained in this technique, according to the equivalent circuit obtained in the electrochemical tests, it must be taken into account that these alloys have different layers: the porous passive layer, the compact passive layer, and the base metal. Therefore, if a very small load is applied, the indenter will only reach the porous layer, but with increasing loads, the hardness of the base metal can be reached.

For both samples, the graphs in Figure 14 show widely dispersed Vickers hardness values of each indentation for each sample at each applied load (5, 25, and 50 gf), attributed to the different hardness values of the α and β phases, as well as the crystalline orientation within the material. Therefore, the surface of the samples had soft and hard zones, as shown in Table 9.

Table 9. Microhardness values of applied loads of soft and hard phase Ti20Mo7Zr and Ti20Mo7Zr0.5Si.

Load (g)	Ti20Mo7Zr		Ti20Mo7Zr0.5Si	
	Microhardness (HV)		Microhardness (HV)	
	Soft Phase	Hard Phase	Soft Phase	Hard Phase
5	174	343	275	357
25	192	386	323	371
50	318	374	323	366

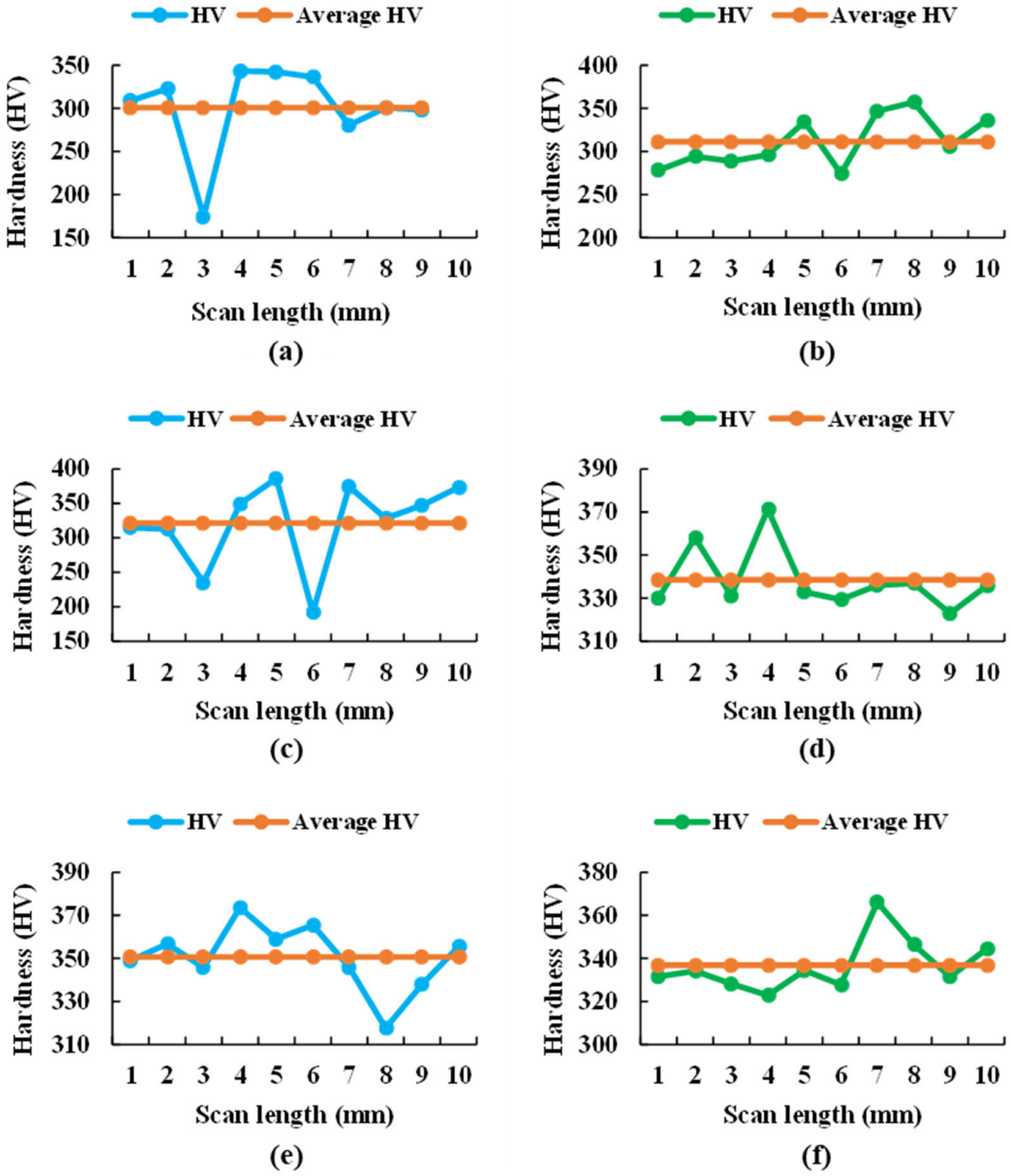

Figure 14. Microhardness values of each indentation for the 5 (**a**), 25 (**c**), and 50 g (**e**) loading of the Ti20Mo7Zr sample and for the 5 (**b**), 25 (**d**), and 50 g (**f**) loading of the Ti20Mo7Zr0.5Si sample.

Thus, the maximum values of the hard phase obtained during this test with respect to the Vickers microhardness occurred in the Ti20Mo7Zr0.5Si sample, while in the soft zone of Ti20Mo7Zr0.5Si, they are slightly higher. This phenomenon is due to the previous forming of the alloy. Moreover, the maximum hardness values obtained in this study were lower than those of common alloys such as Ti6Al4V (541 HV) and CoCrMo (155-601 HV) [19] but higher than for cpTitanium [43].

4. Conclusions

This research evaluated and compared the corrosion behavior and mechanical properties of two titanium alloys. By means of microstructural analysis, corrosion potential curves, EIS, corrosion rate, pitting potential, corrosimetry, SEM, three-point bending test, and microhardness, the following conclusions have been reached:

- The surfaces of the attacked samples have similar dendritic biphasic structures. The size of the dendrites decreases with the addition of silicon. On the surface of the alloys, there is one area rich in Mo, Zr, and Si and another area rich in Titanium. The presence of a passive oxide layer on the surface of each sample was detected by EDX results, with a porous aspect in contact with the electrolyte and a compact structure in contact with the alloy.
- The potential of both samples increased during the immersion time with no drops in potential values, which demonstrated that the passive film formed on the surface is thermodynamically resistant in these conditions. The polarization resistance (Rp) is very big, so both alloys are very resistant to corrosion.
- The low corrosion rates and low corrosion currents testify to the good performance of the studied samples in the analyzed environment, Ringer solution, saline solution, and fever simulation.
- The modulus of elasticity and hardness values obtained for both new alloys were lower than those of many commercial alloys. Moreover, the addition of silicon decreases the modulus of elasticity by almost 45% compared to the alloy without silicon, thus approaching the modulus of elasticity of bone.

In view of the results obtained, the new alloys showed good mechanical properties (hardness and modulus of elasticity) and high corrosion resistance in comparison with commercial alloys.

Author Contributions: Conceptualization, J.C.M.-R.; Funding acquisition, M.S.B.; Investigation, C.J.-M., M.S.B., and P.V.; Methodology, P.V.; Project administration, P.V.; Validation, J.C.M.-R.; Writing—original draft, C.J.-M.; Writing—review & editing, M.S.B. All authors have read and agreed to the published version of the manuscript.

Funding: This paper was financially supported by the Project "Network of excellence in applied research and innovation for doctoral and postdoctoral programs / InoHubDoc", project co-funded by the European Social Fund financing agreement no. POCU/993/6/13/153437. This paper was also supported by "Gheorghe Asachi" Technical University from Iaşi (TUIASI), through the Project "Performance and excellence in postdoctoral research 2022".

Institutional Review Board Statement: Not applicable.

Informed Consent Statement: Not applicable.

Data Availability Statement: All data provided in the present manuscript are available to whom it may concern.

Conflicts of Interest: The authors declare no conflict of interest.

References

1. Baltatu, M.S.; Tugui, C.A.; Perju, M.C.; Benchea, M.; Spataru, M.C.; Sandu, A.V.; Vizureanu, P. Biocompatible Titanium Alloys used in Medical Applications. *Rev. Chim.* **2019**, *70*, 1302–1306. [CrossRef]
2. Kaur, M.; Singh, K. Review on titanium and titanium based alloys as biomaterials for orthopaedic applications. *Mater. Sci. Eng. C* **2019**, *102*, 844–862. [CrossRef]
3. Quinn, J.; McFadden, R.; Chan, C.W.; Carson, L. Titanium for Orthopedic Applications: An Overview of Surface Modification to Improve Biocompatibility and Prevent Bacterial Biofilm Formation. *iScience* **2020**, *23*, 101745. [CrossRef] [PubMed]
4. Ratner, B.D. The biocompatibility manifesto: Biocompatibility for the twenty-first century. *J. Cardiovasc. Transl. Res.* **2011**, *4*, 523–527. [CrossRef] [PubMed]
5. Aggarwal, D.; Kumar, V.; Sharma, S. Drug-loaded biomaterials for orthopedic applications: A review. *J. Control. Release* **2022**, *344*, 113–133. [CrossRef]

6. Băltatu, I.; Vizureanu, P.; Ciolacu, F.; Achiţei, D.C.; Băltatu, M.S.; Vlad, D. In Vitro study for new Ti-Mo-Zr-Ta alloys for medical use. *IOP Conf. Ser. Mater. Sci. Eng.* **2019**, *572*, 012030. [CrossRef]
7. Niinomi, M.; Nakai, M.; Hieda, J. Development of new metallic alloys for biomedical applications. *Acta Biomater.* **2012**, *8*, 3888–3903. [CrossRef]
8. Bai, Y.; Deng, Y.; Zheng, Y.; Li, Y.; Zhang, R.; Lv, Y.; Zhao, Q.; Wei, S. Characterization, corrosion behavior, cellular response and in vivo bone tissue compatibility of titanium–niobium alloy with low Young's modulus. *Mater. Sci. Eng. C* **2016**, *59*, 565–576. [CrossRef]
9. Wen, C.E.; Yamada, Y.; Shimojima, K.; Chino, Y.; Asahina, T.; Mabuchi, M. Processing and mechanical properties of autogenous titanium implant materials. *J. Mater. Sci. Mater. Med.* **2002**, *13*, 397–401. [CrossRef]
10. Yadav, V.S.; Sankar, M.R.; Pandey, L.M. Coating of bioactive glass on magnesium alloys to improve its degradation behavior: Interfacial aspects. *J. Magnes. Alloy.* **2020**, *8*, 999–1015. [CrossRef]
11. Verestiuc, L.; Spataru, M.C.; Baltatu, M.S.; Butnaru, M.; Solcan, C.; Sandu, A.V.; Voiculescu, I.; Geanta, V.; Vizureanu, P. New Ti–Mo–Si materials for bone prosthesis applications. *J. Mech. Behav. Biomed. Mater.* **2021**, *113*, 104198. [CrossRef] [PubMed]
12. Meenakshi, K.S.; Kumar, S.A. Corrosion resistant behaviour of titanium—Molybdenum alloy in sulphuric acid environment. *Mater. Today Proc.* **2022**, *65*, 3282–3287. [CrossRef]
13. Spataru, M.C.; Cojocaru, F.D.; Sandu, A.V.; Solcan, C.; Duceac, I.A.; Baltatu, M.S.; Voiculescu, I.; Geanta, V.; Vizureanu, P. Assessment of the Effects of Si Addition to a New TiMoZrTa System. *Materials* **2021**, *14*, 7610. [CrossRef]
14. Seemann, A.; Akbaba, S.; Buchholz, J.; Tü, S.; En Tezcaner, A.; Woche, S.K.; Guggenberger, G.; Kirschning, A.; Dräger, G. RGD-Modified Titanium as an Improved Osteoinductive Biomaterial for Use in Dental and Orthopedic Implants. *ACS Publ.* **2022**, *33*, 294. [CrossRef]
15. Krzakała, A.; Służalska, K.; Dercz, G.; Maciej, A.; Kazek, A.; Szade, J.; Winiarski, A.; Dudek, M.; Michalska, J.; Tylko, G.; et al. Characterisation of bioactive films on Ti–6Al–4V alloy. *Electrochim. Acta* **2013**, *104*, 425–438. [CrossRef]
16. Correa, D.R.N.; Kuroda, P.A.B.; Grandini, C.R.; Rocha, L.A.; Oliveira, F.G.M.; Alves, A.C.; Toptan, F. Tribocorrosion behavior of β-type Ti-15Zr-based alloys. *Mater. Lett.* **2016**, *179*, 118–121. [CrossRef]
17. Liang, S.X.; Feng, X.J.; Yin, L.X.; Liu, X.Y.; Ma, M.Z.; Liu, R.P. Development of a new β Ti alloy with low modulus and favorable plasticity for implant material. *Mater. Sci. Eng. C* **2016**, *61*, 338–343. [CrossRef]
18. Civantos, A.; Martínez-Campos, E.; Ramos, V.; Elvira, C.; Gallardo, A.; Abarrategi, A. Titanium Coatings and Surface Modifications: Toward Clinically Useful Bioactive Implants. *ACS Biomater. Sci. Eng.* **2017**, *3*, 1245–1261. [CrossRef]
19. Sandu, A.V.; Baltatu, M.S.; Nabialek, M.; Savin, A.; Vizureanu, P. Characterization and Mechanical Proprieties of New TiMo Alloys Used for Medical Applications. *Materials* **2019**, *12*, 2973. [CrossRef]
20. Spataru, M.C.; Butnaru, M.; Sandu, A.V.; Vulpe, V.; Vlad, M.D.; Baltatu, M.S.; Geanta, V.; Voiculescu, I.; Vizureanu, P.; Solcan, C. In-depth assessment of new Ti-based biocompatible materials. *Mater. Chem. Phys.* **2021**, *258*, 123959. [CrossRef]
21. Oliveira, N.T.C.; Aleixo, G.; Caram, R.; Guastaldi, A.C. Development of Ti–Mo alloys for biomedical applications: Microstructure and electrochemical characterization. *Mater. Sci. Eng. A* **2007**, *452–453*, 727–731. [CrossRef]
22. González, J.E.G.; Mirza-Rosca, J.C. Study of the corrosion behavior of titanium and some of its alloys for biomedical and dental implant applications. *J. Electroanal. Chem.* **1999**, *471*, 109–115. [CrossRef]
23. Raabe, D.; Sander, B.; Friák, M.; Ma, D.; Neugebauer, J. Theory-guided bottom-up design of β-titanium alloys as biomaterials based on first principles calculations: Theory and experiments. *Acta Mater.* **2007**, *55*, 4475–4487. [CrossRef]
24. Pitchi, C.S.; Priyadarshini, A.; Sana, G.; Narala, S.K.R. A review on alloy composition and synthesis of β-Titanium alloys for biomedical applications. *Mater. Today Proc.* **2020**, *26*, 3297–3304. [CrossRef]
25. Sharma, A.; Waddell, J.N.; Li, K.C.; Sharma, L.A.; Prior, D.J.; Duncan, W.J. Is titanium–zirconium alloy a better alternative to pure titanium for oral implant? Composition, mechanical properties, and microstructure analysis. *Saudi Dent. J.* **2021**, *33*, 546–553. [CrossRef]
26. Socorro-Perdomo, P.P.; Florido-Suárez, N.R.; Mirza-Rosca, J.C.; Saceleanu, M.V. EIS Characterization of Ti Alloys in Relation to Alloying Additions of Ta. *Materials* **2022**, *15*, 476. [CrossRef]
27. Tudoran, S.; Voiculescu, I.; Geantă, V.; Vizureanu, P.; Marza Roşca, I.; Pătraşcu, I.; Gălbinaşu, B.M.; Ciocoiu, R. Effects of the chemical composition on the microstructural characteristics of Ti-Nb-Ta-Zr alloys. *IOP Conf. Ser. Mater. Sci. Eng.* **2019**, *572*, 012022. [CrossRef]
28. Verma, R.P. Titanium based biomaterial for bone implants: A mini review. *Mater. Today Proc.* **2020**, *26*, 3148–3151. [CrossRef]
29. Ahmadi, R.; Asadpourchallou, N.; Kaleji, B.K. In vitro study: Evaluation of mechanical behavior, corrosion resistance, antibacterial properties and biocompatibility of HAp/TiO_2/Ag coating on Ti6Al4V/TiO_2 substrate. *Surf. Interfaces* **2021**, *24*, 101072. [CrossRef]
30. Zhang, Y.; Xiu, P.; Jia, Z.; Zhang, T.; Yin, C.; Cheng, Y.; Cai, H.; Zhang, K.; Song, C.; Leng, H.; et al. Effect of vanadium released from micro-arc oxidized porous Ti6Al4V on biocompatibility in orthopedic applications. *Colloids Surf. B Biointerfaces* **2018**, *169*, 366–374. [CrossRef]
31. Vasilescu, E.; Drob, P.; Raducanu, D.; Cinca, I.; Mareci, D.; Calderon Moreno, J.M.; Popa, M.; Vasilescu, C.; Mirza Rosca, J.C. Effect of thermo-mechanical processing on the corrosion resistance of Ti6Al4V alloys in biofluids. *Corros. Sci.* **2009**, *51*, 2885–2896. [CrossRef]
32. Kopova, I.; Stráský, J.; Harcuba, P.; Landa, M.; Janeček, M.; Bačákova, L. Newly developed Ti–Nb–Zr–Ta–Si–Fe biomedical beta titanium alloys with increased strength and enhanced biocompatibility. *Mater. Sci. Eng. C* **2016**, *60*, 230–238. [CrossRef] [PubMed]

33. Oliveira, N.T.C.; Guastaldi, A.C. Electrochemical behavior of Ti–Mo alloys applied as biomaterial. *Corros. Sci.* **2008**, *50*, 938–945. [CrossRef]
34. Eisenbarth, E.; Velten, D.; Müller, M.; Thull, R.; Breme, J. Biocompatibility of β-stabilizing elements of titanium alloys. *Biomaterials* **2004**, *25*, 5705–5713. [CrossRef] [PubMed]
35. Mareci, D.; Fernández-Pérez, B.M.; Trinca, L.C.; Fotea, L.; Souto, R.M. Electrochemical Investigation of the Corrosion Resistance of Ti20Mo Alloys in Simulated Physiological Solution with Added Proteins for Biomaterial Application. *Int. J. Electrochem. Sci.* **2016**, *11*, 6922–6932. [CrossRef]
36. Baltatu, M.S.; Vizureanu, P.; Sandu, A.V.; Florido-Suarez, N.; Saceleanu, M.V.; Mirza-Rosca, J.C. New Titanium Alloys, Promising Materials for Medical Devices. *Materials* **2021**, *14*, 5934. [CrossRef] [PubMed]
37. Baltatu, M.S.; Spataru, M.C.; Verestiuc, L.; Balan, V.; Solcan, C.; Sandu, A.V.; Geanta, V.; Voiculescu, I.; Vizureanu, P. Design, Synthesis, and Preliminary Evaluation for Ti-Mo-Zr-Ta-Si Alloys for Potential Implant Applications. *Materials* **2021**, *14*, 6806. [CrossRef]
38. Popa, M.V.; Vasilescu, E.; Drob, P.; Vasilescu, C.; Drob, S.I.; Mareci, D.; Mirza Rosca, J.C. Corrosion Resistance Improvement of Titanium Base Alloys. *Química Nova* **2010**, *33*, 1892–1896. [CrossRef]
39. Jiang, Z.; Dai, X.; Middleton, H. Effect of silicon on corrosion resistance of Ti–Si alloys. *Mater. Sci. Eng. B* **2011**, *176*, 79–86. [CrossRef]
40. Hanawa, T. Overview of metals and applications. In *Metals for Biomedical Devices*; Woodhead Publishing: Cambridge, UK, 2010; pp. 3–24. [CrossRef]
41. Wagner, C.; Traud, W. "On the Interpretation of Corrosion Processes through the Superposition of Electrochemical Partial Processes and on the Potential of Mixed Electrodes," with a Perspective by F. Mansfeld. *Corrosion* **2006**, *62*, 843–855. [CrossRef]
42. Popa, M.V.; Demetrescu, I.; Vasilescu, E.; Drob, P.; Lopez, A.S.; Mirza-Rosca, J.; Vasilescu, C.; Ionita, D. Corrosion susceptibility of implant materials Ti–5Al–4V and Ti–6Al–4Fe in artificial extra-cellular fluids. *Electrochim. Acta* **2004**, *49*, 2113–2121. [CrossRef]
43. Da Rocha, S.S.; Adabo, G.L.; Henriques, G.E.P.; Nóbilo, M.A.D.A. Vickers hardness of cast commercially pure titanium and Ti-6Al-4V alloy submitted to heat treatments. *Braz. Dent. J.* **2006**, *17*, 126–129. [CrossRef] [PubMed]

Artículo 2. Effect of Si Contents on the Properties of Ti15Mo7ZrxSi Alloys

materials

MDPI

Article

Effect of Si Contents on the Properties of Ti15Mo7ZrxSi Alloys

Cristina Jimenez-Marcos [1], Julia Claudia Mirza-Rosca [1,2,*], Madalina Simona Baltatu [3,*] and Petrica Vizureanu [3,4]

[1] Mechanical Engineering Department, Las Palmas de Gran Canaria University, 35017 Tafira, Spain; cristina.jimenez112@alu.ulpgc.es
[2] Materials Engineering and Welding Department, Transilvania University of Brasov, 500036 Brasov, Romania
[3] Department of Technologies and Equipments for Materials Processing, Faculty of Materials Science and Engineering, Gheorghe Asachi Technical University of Iaşi, Blvd. Mangeron, No. 51, 700050 Iasi, Romania; peviz@tuiasi.ro
[4] Technical Sciences Academy of Romania, Dacia Blvd 26, 030167 Bucharest, Romania
* Correspondence: julia.mirza@ulpgc.es (J.C.M.-R.); cercel.msimona@yahoo.com (M.S.B.)

Abstract: The main purpose of this research is to evaluate the mechanical characteristics and biocompatibility of two novel titanium alloys, Ti15Mo7ZrxSi (x = 0, 0.5, 0.75, 1). These samples had already undergone grinding, polishing, cutting, and chipping. Electrochemical, metallographic, three-point bending, and microhardness studies were conducted on the studied materials to determine their corrosion behavior, microstructure, Young's modulus, and hardness. The first investigations revealed that both samples had biphasic and dendritic structures, elastic moduli that were between the highest and minimum values achieved by around 20 GPa, and favorable behavior when in contact with physiological fluids at ambient temperature. Ti15Mo7Zr0.5Si and Ti15Mo7Zr0.75Si, the research samples, had greater corrosion potentials, reduced corrosion rates, and therefore higher corrosion resistance, as well as modulus of elasticity values that were comparable to and closer to those of human bone. The results of this investigation indicate that both alloys exhibit favorable corrosion behavior, great biocompatibility, Young's modulus results lower than those of conventional alloys used in biomedical implants, and hardness values higher than commercially pure titanium.

Keywords: titanium-based alloys; microstructure; corrosion behavior; mechanical properties

Citation: Jimenez-Marcos, C.; Mirza-Rosca, J.C.; Baltatu, M.S.; Vizureanu, P. Effect of Si Contents on the Properties of Ti15Mo7ZrxSi Alloys. *Materials* **2023**, *16*, 4906. https://doi.org/10.3390/ma16144906

Academic Editor: Lili Tan

Received: 12 June 2023
Revised: 6 July 2023
Accepted: 7 July 2023
Published: 9 July 2023

1. Introduction

Nowadays, there is a growing interest in the development of biomaterials for various medical applications, such as orthopedics [1], drug administration [2,3], dentistry [4], tissue engineering [5], and cardiovascular systems [6]. These biomaterials aim to improve the quality of life and longevity of individuals, particularly in the context of chronic musculoskeletal diseases like osteoarthritis, which affects a significant portion of the population.

Biocompatibility is a crucial requirement for any biomaterial intended for medical use. Biocompatibility refers to the ability of a material to fulfill its function in medical treatment without causing adverse reactions in the body. To be successful, biomaterials must possess specific properties, including high ductility, fatigue and wear resistance, absence of cytotoxicity, a combination of high strength and low Young's modulus similar to human cortical bone (ranging from 10 to 30 GPa), and the ability to integrate well with the surrounding bone.

While polymers and ceramics are commonly used biomaterials [7], they often exhibit low mechanical strength and brittleness, limiting their applications in harsh conditions. Therefore, metallic materials, particularly titanium and its alloys [8], have gained prominence in orthopedic surgery. Approximately 70–80% of implants are made from metallic biomaterials, such as 316L stainless steel, CoCrMo alloys, Ti6Al4V, and NiTi alloys [9].

However, using metals as implants presents challenges as the higher elastic modulus of metals compared to bone can lead to stress shielding, causing osteoporosis due to the

mismatch in mechanical properties. Moreover, many metallic biomaterials release toxic ions into adjacent tissues, exhibit poor wear and corrosion resistance, and may have low biocompatibility [10]. To address these issues, the addition of alloying components that do not have harmful effects on the body has been explored [11,12].

Corrosion is a significant concern when using metallic implants, as it can lead to material deterioration and subsequent implant failure. To prevent corrosion, a protective film is usually formed on the material's surface to make it impermeable to the surrounding environment. Titanium and its alloys have emerged as suitable biomaterials for various applications due to their biocompatibility, corrosion resistance, mechanical properties, low modulus of elasticity, and thermal stability [13–16]. Titanium's ability to form a stable oxide coating on its surface contributes to its excellent corrosion resistance.

Different types of titanium-based alloys exist, including α, α + β, and β titanium alloys. The addition of alloying elements allows for the modification of alloy properties. α-stabilizers (C, N, O, Al) increase the allotropic transformation temperature, while β-stabilizers (V, Nb, Mo, Ta, Fe, Mn, Cr, Co, W, Ni, Cu, Si) decrease it [8,15,17].

Titanium–molybdenum (Ti-Mo) alloys have gained attention as potential biomaterials due to their favorable mechanical and corrosion resistance. Ti-Mo alloys can form a stable oxide layer on their surface, protecting them from corrosion and degradation in aggressive environments [18–20].

The design considerations for Ti-Mo-Zr alloys were based on several factors influenced by fabrication method [21] or another alloying element, such as chromium [22]. Titanium is considered to have extremely low toxicity for the human body and exhibits excellent interaction with bone due to its corrosion resistance and lack of rejection by the body. Molybdenum is a beta-stabilizing element with low toxicity and can help adjust the alloy's mechanical properties to be more similar to human bone by decreasing the modulus of elasticity. Zirconium, a neutral stabilizer, is becoming increasingly desirable for medical applications due to its biocompatibility, low modulus of elasticity, and corrosion resistance [23].

In recent years, Ti-Mo-Zr-Si alloys have been developed as potential biomaterials by incorporating small quantities of silicon into Ti-Mo-Zr alloys [24]. Silicon is a biocompatible element found in human bone, and its addition to the alloy improves corrosion resistance, creep resistance at high temperatures, ductility, and strength. It also contributes to reducing the elastic modulus, making it closer to that of human bone [25,26]. The specific effects of silicon content on titanium alloys can vary depending on the other alloying elements, processing conditions, and the intended application of the alloy. Therefore, comprehensive testing and characterization are necessary to determine the optimal silicon content for a particular titanium alloy to achieve the desired properties.

In the current study, a Ti-15Mo-7Zr base alloy is considered, and we analyze the effect of the addition of silicon (with 0%, 0.50%, 0.75%, and 1.00% Si) in the microstructure, and the corrosion resistance, microhardness, and elastic modulus of the alloys obtained in an effort to develop new alloys for biomedical applications.

2. Materials and Methods

2.1. Material Preparation

The examined alloys' chemical compositions (%wt) are shown in Table 1. The alloys were produced using the arc remelting method in an argon environment. The melting process takes place under high vacuum conditions, achieved by utilizing a pump system to evacuate the working chamber. When the samples are melted, the presence of oxygen leads to a significant decrease in vacuum within the working chamber. Once the high vacuum is restored, argon is introduced into the working chamber, where the samples are melted, under atmospheric conditions. This approach ensures the proper temperature and facilitates easy handling of the samples, resulting in a high level of uniformity in their chemical composition.

Table 1. Ti15Mo7ZrxSi experimental samples' chemical composition obtained by EDX (wt %).

Alloy	Ti (%)	Mo (%)	Zr (%)	Si (%)
Ti15Mo7Zr	77.87	15.03	7.10	-
Ti15Mo7Zr0.5Si	77.52	15.10	6.89	0.49
Ti15Mo7Zr0.75Si	78.15	14.59	6.53	0.73
Ti15Mo7Zr1Si	77.24	15.00	6.79	0.97

The Faculty of Materials Science and Engineering at Gheorghe Asachi Technical University in Iasi, Romania, carried out this technique. The alloys were melted, then remelted six times (three times in each face), and finally formed into an ingot in order to obtain the proper homogeneity. Moreover, for their preparation and testing, Las Palmas de Gran Canaria University (Las Palmas de Gran Canaria, Spain) received a portion of the ingots.

Several operations were carried out as a first step to analyze the electrochemical, metallographic, bending, and microhardness properties of the studied samples, such as embedding the samples by adding epoxy resin or catalyst in a 4:1 ratio into a mold, which was demolded after 24 h. The specimens were then cut into 1 to 1.5 mm thick plates using a grinding wheel and jaws on a Buehler IsoMet 4000 precision saw (Chicago, IL, USA). For the mechanical and electrochemical testing, the sliced specimens were reassembled. The specimens were then polished using the Struers TegraPol-11 polishing machine (Copenhagen, Denmark) at a force of 20 N and at a speed of 300 rpm. The progressive carbide grinding method was utilized. Carbide abrasive sheets of increasing grit were utilized, beginning with 400 grits, and ending with P2500 grit. Finally, mirror polishing cloths with 0.1 μm α alumina suspension were utilized. These procedures for sample preparation for metallographic testing followed ASTM E3-11(2017) [27]. In order to realize the mechanical tests, vertical slices with a thickness of about 2 mm were produced once more on the cutting machine.

2.2. Microstructure

The compounds and phases that make up a metallic substance are arranged spatially in metallography, together with any impurities or potential mechanical faults.

Images of the surfaces of every specimen were acquired using the Axio Vert.A1 MAT ZEISS optical metallographic microscope (Jena, Germany) to analyze the microstructure. At intervals of about 15 s, each sample was submerged in Kroll's reagent, which is made of 20 mL glycerin, 30 mL hydrochloric acid, and 10 mL nitric acid, and the attacked surface was photographed. The test was carried out three times.

2.3. Electrochemical Tests

A sample was placed in an electrochemical cell with three electrodes for the electrochemical tests: the samples acted as the working electrodes, a saturated calomel electrode served as the reference electrode, and a platinum electrode acted as the counter electrode. The area of each sample was determined to run the tests. The mmol/L values of the Grifols Laboratories' (Barcelona, Spain) Ringer solution were as follows: Na^+ 129.9, Cl^- 111.7, $C_3H_5O_3$ 27.2, K^+ 5.4, and Ca^{2+} 1.8.

Corrosion Potential, Corrosion Rate, and Electrochemical Impedance Spectroscopy were performed by applying the BioLogic Essential SP-150 potentiostat (Seyssinet-Pariset, France). The tests were performed at 25 °C in aerated Ringer solution.

2.3.1. Corrosion Potential (E_{corr})

Applying the "E_{corr} vs. Time" approach found in the Ec-Lab program, the 24 h corrosion potential of each sample was determined. Potential readings were taken every 300 s or every time there was a 100 mV change in potential. The collected data were analyzed, and a potential versus time graph was created.

2.3.2. Corrosion Rate (V_{corr})

The "Linear Polarization" approach was selected to carry out these experiments [28], and the sample surface area value and the 20 min test period were entered to verify its viability. With data taken every 0.50 s, the potential scanning revealed a 0.167 mV/s time-variation relationship from −0.025 to 0.025 V against open circuit potential (OCP) and intensity maintained at 100 % during the potential scanning [29]. Following the presentation of these linear polarization curves, EC-Lab's "Tafel Fit" approach was used to obtain the corrosion rate estimates for each sample.

2.3.3. Electrochemical Impedance Spectroscopy (EIS)

The AC impedance measurements were recorded with an AC potential amplitude of 20 mV and single sine wave measurements were conducted at frequencies between 10^{-1} and 2×10^{-5} Hz. To analyze the characteristics of the oxide film, the impedance spectra were recorded at 7 different DC potentials around corrosion potential, in the range $E_{corr} \pm 300$ mV, with a 100 mV step from E_{corr}, permitting the system to stabilize for 5 min at each potential. To represent these data, Nyquist and Bode diagrams were utilized, and for their simulation, equivalent circuits (EC) were employed [30].

2.4. Three-Point Bending Test

The Bose ElectroForce® 3100 machine (Framingham, MA, USA) was used to perform the three-point bending method; it complies with ISO 7438:2020 [31] and has a 20 N force resistance limit.

In order to realize this methodology, each rectangular cross-section specimen was positioned at the extremities of the bottom shank of the testing apparatus, with a distance between supports ranging from 7.80 to 10.63 mm depending on the specimen length. During the experiment, the specimen was loaded vertically while moving at a 3 mm/s linear speed at its center until it reached its yield stress or broke. The obtained values of the applied force against the displacement of the samples were plotted, and their slope was calculated to establish the modulus of elasticity.

2.5. Microhardness Test

Using the Future Tech FM-810 hardness tester (Kawasaki, Japan), for each sample's applied load, in this case 5, 25, and 50 gf, 10 measurements were taken, in accordance with ISO 14577-1:2015 [32]. The mark may contain fragments of many phases as the stress rises, providing an approximation of the material's total hardness. When relatively light weights are placed, it is likely that the mark will only be discovered in one phase, allowing the hardness of that phase to be assessed. The Vickers microhardness values were then computed automatically by the iVicky software (v2.0, Sinowon, Dongguan, China) using the observed diagonal lengths. The number of indents created was plotted against the scan length.

3. Results and Discussion

3.1. Microstructural Analysis

Figure 1 displays the surfaces of the four studied samples after they were etched with the reagent.

At room temperature, cpTi has a hexagonal closest-packed (HCP) structure with an α-phase, but beyond 883 °C, it has a body-centered cubic (BCC) structure with a β-phase [33].

In contrast to Zr, which is regarded as a neutral element because it virtually has no influence on the α/β-phases, the β-phase is stable at temperatures below 883 °C when Mo and Si are present [8].

After being chemically etched, it can be seen that all four of the tested samples had a biphasic and dendritic structure. Additionally, the addition of Si caused the interdendritic zone to expand while the size of the dendrites dropped by about 12% as the silicon concen-

tration increased with 0.25%. Fine grains hinder the propagation of cracks, enhancing the material's resistance to fatigue.

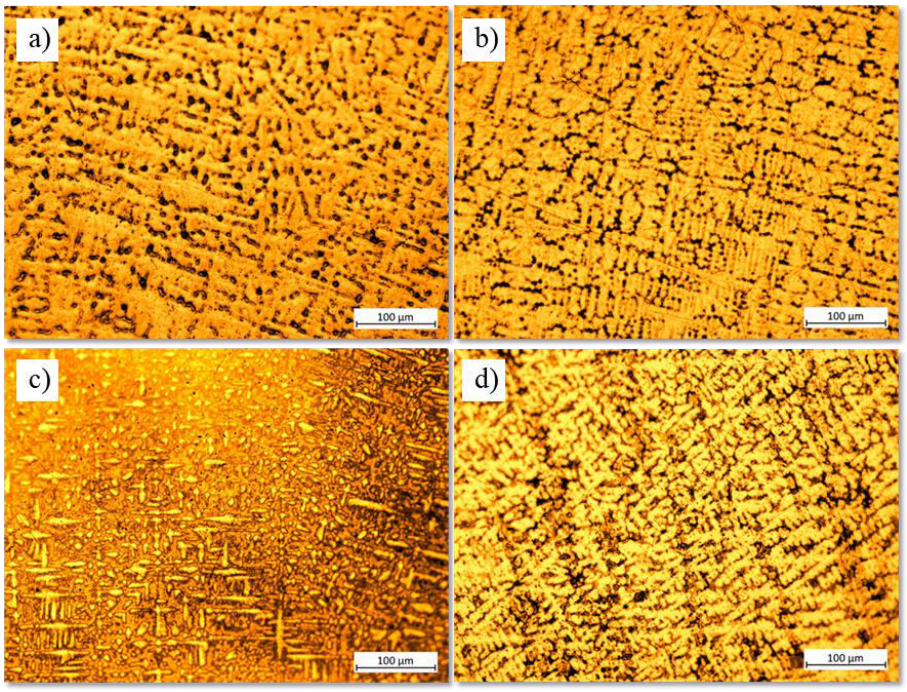

Figure 1. Optical microstructure after Kroll reagent etching for (**a**) Ti15Mo7Zr, (**b**) Ti15Mo7Zr0.5Si, (**c**) Ti15Mo7Zr0.75Si, and (**d**) Ti15Mo7Zr1Si samples.

3.2. Electrochemical Tests

3.2.1. Corrosion Potential (E_{corr})

A quantitative measure of corrosion behavior is corrosion potential evolution over time, although this information is still insufficient for a thorough examination.

Figure 2 and Table 2 show the curves of corrosion potential as a function of time after 24 h of immersion in Ringer's solution with their respective values of initial potential, after 1 hour and after 24 h of testing. The potential, known as open-circuit potential (OCP) in these circumstances, reveals the sample's tendency for corrosion. From the data obtained after one hour of immersion, the potential of the samples Ti15Mo7Zr, Ti15Mo7Zr0.75Si, and Ti15Mo7Zr1Si increases due to passivation of the surfaces, reaching values between −0.337 V and 0.328 V, while the potential of Ti15Mo7Zr0.5Si slightly decreases to −0.227 V.

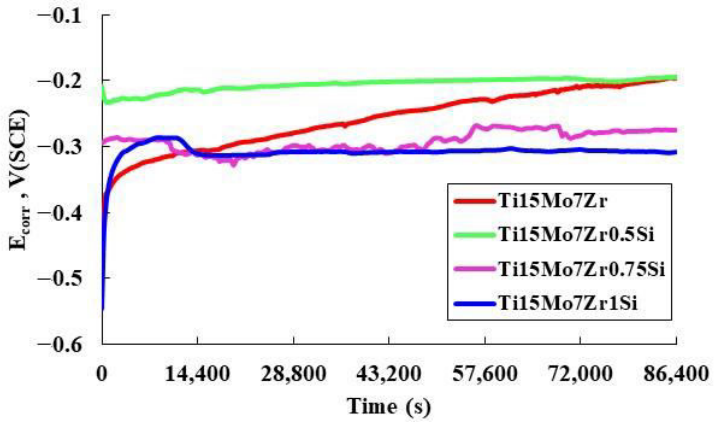

Figure 2. Corrosion potential curves for Ti15Mo7Zr, Ti15Mo7Zr0.5Si, Ti15Mo7Zr0.75Si, and Ti15Mo7Zr1Si alloys after 24 h' immersion.

Table 2. For the four samples dipped in Ringer Grifols solution, open-circuit potential (OCP) measurements were made initially, one hour later, and one day later.

Alloy	OCP, V vs. SCE		
	Initial	After 1 h	After 1 Day
TiMo15Zr7	−0.432	−0.337	−0.194
TiMo15Zr7Si0.5	−0.207	−0.227	−0.194
TiMo15Zr7Si0.75	−0.294	−0.284	−0.263
TiMo15Zr7Si1	−0.546	−0.307	−0.308

Overall, during the 24 h experiment, the potentials of every studied sample increased because of the passive layer thickening, reaching final values of −0.194 V, −0.194 V, −0.263 V, and −0.308 V, respectively. Therefore, the potential curves tended to increase progressively until signs of a possible stabilization of the potential could be observed, suggesting that the passive layer is thermodynamically resistant under Ringer's solution conditions, with the exception of Ti15Mo7Zr0.75Si, which presents a plot with many irregular peaks.

Since the corrosion potentials values of Ti15Mo7Zr and Ti15Mo7Zr0.5Si are equal and they are higher to those of the examined samples and cpTi (from −0.10 V to −0.15 V), this indicates that the inclusion of Si alters the passive layer's properties.

As the Si content in the titanium alloy increases, the corrosion potential becomes more negative. This shift towards more negative values suggests that the alloy becomes more susceptible to corrosion and indicates a decrease in the alloy's stability in the given environment. If the added silicon content exceeds 0.5%, the open circuit potential shifts to more negative values due to the formation of galvanic couples between the Si-containing regions and the rest of the titanium alloy, leading to localized electrochemical reactions and a negative shift in the OCP. The Si content may influence the composition, thickness, and stability of the passive oxide layer formed on the surface of the alloy. Changes in the passivation behavior can result in variations of the OCP.

3.2.2. Corrosion Rate (V_{corr})

Figure 3 shows the results of the linear polarization technique, which was performed to measure the alloys' rate of corrosion, displayed on a semi-logarithmic scale of the current results.

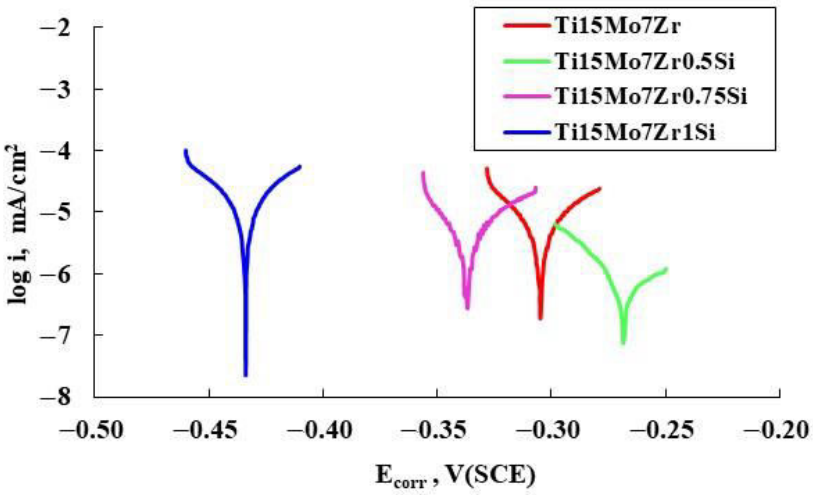

Figure 3. Polarization curves of the four test samples.

Ti15Mo7Zr1Si shows higher values of anodic corrosion potential and current (E_{corr} and I_{corr}, respectively), which is a measure of how much the alloy has been oxidized, than the other samples studied, as can be seen in Table 3. By examining the curve displayed

against open circuit potential (OCP) across a range of 0.25 V, Tafel slopes (β_c and β_a) were calculated. An alloy prone to passivation will have a value of a greater than c, while an alloy prone to corrosion will have a value of a less than c. In our case, all four samples have a tendency to passivate, i.e., to have a passive layer created on their surface.

Table 3. Corrosion parameters for all samples tested.

Parameters	Ti15Mo7Zr	Ti15Mo7Zr0.5Si	Ti15Mo7Zr0.75Si	Ti15Mo7Zr1Si
E_{corr} (mV vs. Ref)	−305.03	−264.59	−337.50	−445.46
I_{corr} (nA/cm^2)	2.00	2.40	2.00	4.00
β_c (mV/dec)	13.30	14.70	12.00	9.60
β_a (mV/dec)	15.30	16.70	15.80	10.00
Equivalent weight (g/eq)	58.12	58.02	57.97	57.92
Density (g/cm^3)	5.50	5.49	5.48	5.48
Surface (cm^2)	0.62	0.31	1.23	0.63
Corrosion rate (µm/year)	0.11	0.03	0.06	0.22
Rp (Ω·cm^2)	9.86×10^5	6.09×10^6	1.2×10^6	4.48×10^5

Moreover, using the corrosion current (I_{corr}), the constant (K) that establishes the corrosion rate units (1.288×10^5 miliinches/A-cm-year), the equivalent weight (EW) in g/eq, the density (d) in g/cm^3, and the area (A) of each sample (in cm^2), Table 3 displays the Tafel curve parameters and the corrosion rate (V_{corr}) of the tested samples.

$$V_{corr} = \frac{I_{corr} \cdot K \cdot EW}{d \cdot A} \quad (1)$$

In this case, a minimum V_{corr} of 0.03 µm/year (Ti15Mo7Zr0.5Si) and a maximum V_{corr} of 0.22 µm/year (Ti15Mo7Zr1Si) were achieved, whereas commercial pure titanium, under similar circumstances, had a greater V_{corr} of 0.12 µm/year.

As the polarization resistance (R_p) value rises, the alloy's corrosion resistance increases, according to the results of the "Rp Fit" study performed using the EC-Lab program on the linear polarization curves of the V_{corr}. Ti15Mo7Zr0.5Si and Ti15Mo7Zr0.75 alloys are extremely corrosion-resistant, with the R_p even reaching 10^6 Ω·cm^2 for highly corrosion-resistant materials, whereas Ti15Mo7Zr and Ti15Mo7Zr1Si had lower values of about 10^5 Ω·cm^2. Thus, the Ti15Mo7Zr1Si sample obtained the worst corrosion resistance [34].

3.2.3. Electrochemical Impedance Spectroscopy (EIS)

A high-throughput method for examining interfacial properties linked to processes occurring on the alloy surfaces is electrochemical impedance spectroscopy. EIS has a variety of benefits over other electrochemical techniques, since it is a steady-state methodology that can probe, in this case, from 0.1 Hz to 1×10^6 Hz and can quantify very small signals.

Each alloy's EIS data are shown in Nyquist and Bode plots for the seven distinct potentials that were recorded in Ringer solution. By measuring EIS at both cathodic and anodic potentials relative to the corrosion potential, it is possible to obtain a comprehensive understanding of the corrosion behavior of the alloy over a range of electrochemical conditions. This information helps to evaluate the overall corrosion resistance and stability of the alloy in the given environment and identify critical potentials or conditions that favor corrosion or passivation.

When using Nyquist graphs, the hypothetical impedance results were contrasted with the actual values. For each and every applied potential, a capacitive arc is shown in Figure 4. In general, in these Nyquist curves, a capacitive arc is shown and it can be seen that the impedance values increase as more positive potentials are applied.

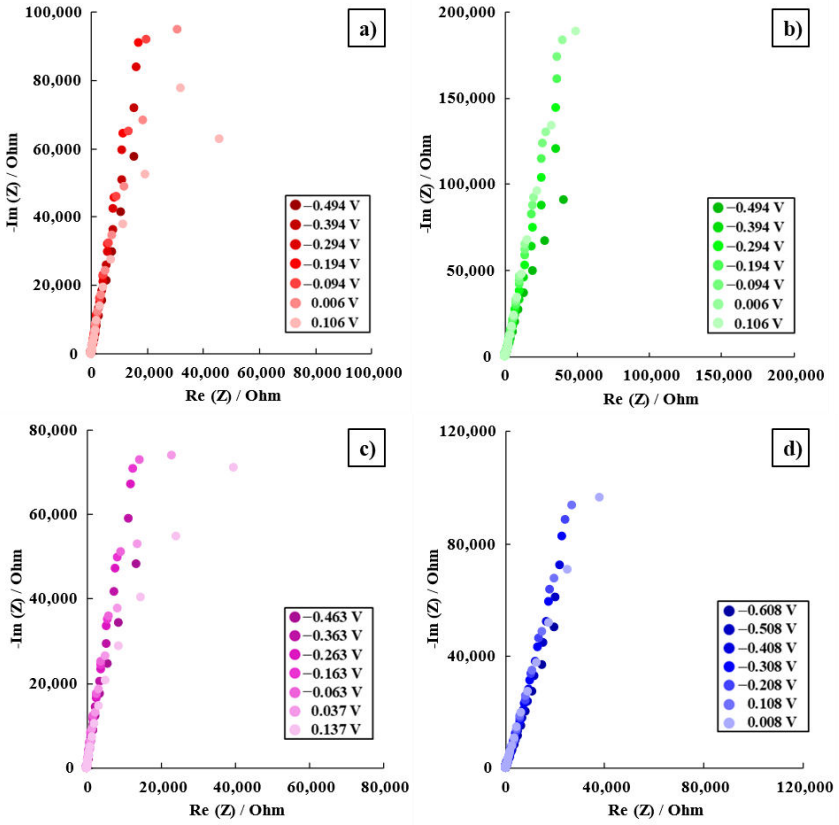

Figure 4. Nyquist diagrams for Ti15Mo7Zr (**a**), Ti15Mo7Zr0.5Si (**b**), Ti15Mo7Zr0.75Si (**c**), and Ti15Mo7Zr1Si (**d**) in Ringer's solution.

The logarithm curves of the impedance modulus and phase shift angle of the Ti15Mo7ZrxSi samples dissolved in Ringer's solution are displayed using Bode plots.

Figures 5 and 6 show the Bode impedance and Bode phase diagrams, respectively, while Table 4 shows the results obtained from E_{corr} and ±300 mV versus E_{corr}.

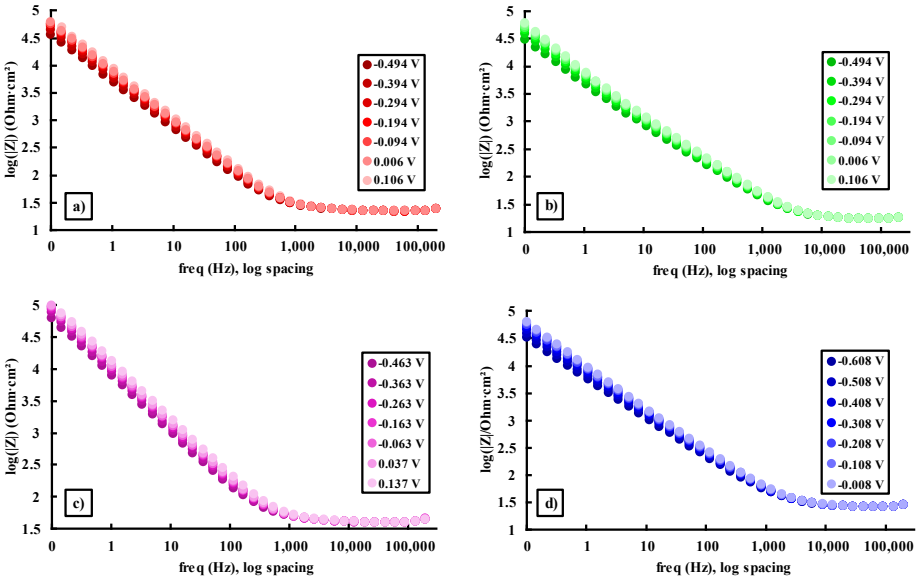

Figure 5. Bode impedance diagrams for Ti15Mo7Zr (**a**), Ti15Mo7Zr0.5Si (**b**), Ti15Mo7Zr0.75Si (**c**), and Ti15Mo7Zr1Si (**d**) in Ringer's solution.

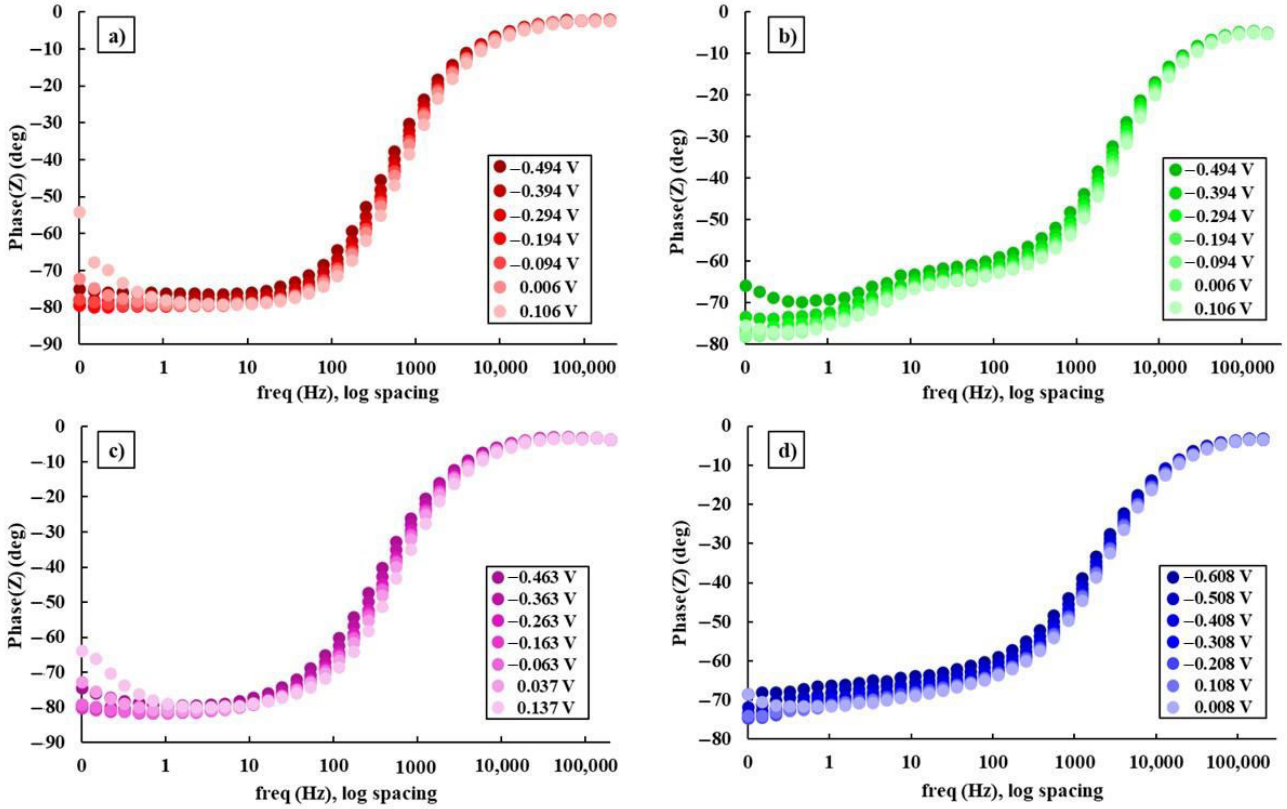

Figure 6. Bode phase graphs for: Ti15Mo7Zr (**a**), Ti15Mo7Zr0.5Si (**b**), Ti15Mo7Zr0.75Si (**c**), and Ti15Mo7Zr1Si (**d**) in Ringer's solution.

Table 4. Results from the samples' Bode diagrams under study at E_{corr} and at ±300 mV.

Samples	Potential (V)	Maximum Impedance (Ω)	Maximum Phase Angle (°)
Ti20Mo7Zr	−0.494	59,795.00	76
	−0.194	92,456.59	80
	−0.106	77,547.44	79
Ti20Mo7Zr0.5Si	−0.494	99,123.73	70
	−0.194	164,512.91	77
	−0.106	194,874.17	77
Ti20Mo7Zr0.75Si	−0.463	50,019.06	79
	−0.163	72,085.70	82
	−0.137	81,420.35	80
Ti20Mo7Zr1Si	−0.608	54,039.71	68
	−0.308	85,686.74	74
	−0.008	103,741.00	72

Figure 5 and Table 4 indicate greater impedance values for the four samples at the lowest frequency (0.1 Hz), with lower values for the Ti15Mo7Zr0.75Si sample and higher results for the Ti15Mo7Zr0.5Si sample, showing that the latter alloy's corrosion resistance has improved. In addition, the impedance values tended to increase the more positive the applied potentials were. In addition, a specific behavior of passive film growth was observed for each sample, which has a tendency to exhibit a capacitive behavior.

Figure 6 and Table 4 show the curves and maximum values obtained for the phase angles of the samples, which tend to increase the more positive the applied potentials are. As a result, after examining the studied samples, it was found that the Bode phase curves showed a single-phase process. Furthermore, with increasing potential value, the phase

angle tends to increase and the process takes place in a single step, i.e., in a time constant, when the curve starts to decline, although in the curves of the Ti15Mo7Zr, Ti15Mo7Zr0.5Si, and Ti15Mo7Zr0.75Si samples there is the possibility of the onset of a second time constant.

The equivalent circuit model R(QR)(QR), which best fits the experimental findings of the study for Ti15Mo7ZrxSi alloys, is shown in Figure 7. This circuit shows that, up until the alloy is achieved, the surface of the samples exhibits a resistance to dissolving, together with porous and compact passive films.

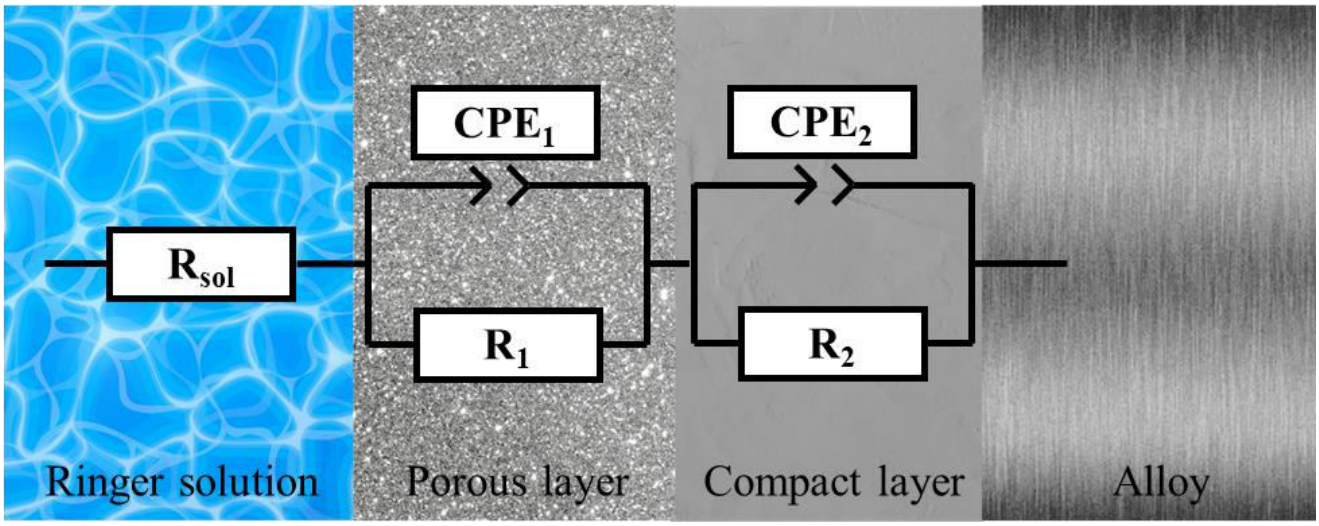

Figure 7. Equivalent circuit R(QR)(QR).

The resistance in ohms of the electrolyte was represented in the model and in Equation (1) as R_{sol}, the resistances of the porous and compact passive films as R_1 and R_2, respectively, and the capacitances of the passive film as CPE_1 and CPE_2, which are the constant phase elements. The constant phase element reproduces a capacitor (n = 1.0), a semi-infinite Warburg impedance (n = 0.5), or a resistor (n = 0.0) as a function of the values of the parameters n_1 and n_2, as well as the applied frequency, f.

$$Z(f) = R_{sol} + \frac{R_1}{R_1 CPE_1 (j2\pi f)^{n_1} + 1} + \frac{R_2}{R_2 CPE_2 (j2\pi f)^{n_2} + 1} \quad (2)$$

In Table 5, it is noted that the corrosion resistance ($R_p = R_1 + R_2$) increased with the addition of silicon, reaching values up to 10^6 Ω cm^2 for the Ti15Mo7Zr0.5Si and Ti15Mo7Zr1Si samples, indicating that the materials present high corrosion resistance, being higher for Ti15Mo7Zr0.5Si.

Table 5. Equivalent circuit R(QR)(QR) of samples Ti15Mo7Zr0.5Si and Ti15Mo7Zr1Si.

Sample	Potential (V)	R_{sol} (Ω·cm^2)	Y_{01} (S·s^n/cm^2)	n_1	R_1 (Ω·cm^2)	Y_{02} (S·s^n)	n_2	R_2 (Ω·cm^2)	χ^2
Ti15Mo7Zr	0.106	22.47	2.04×10^{-5}	1	1.19	2.07×10^{-5}	0.90	1.99×10^{5}	6.55×10^{-4}
Ti15Mo7Zr0.5Si	0.106	17.04	7.52×10^{-5}	0.73	401.20	2.55×10^{-5}	0.87	1.67×10^{6}	6.86×10^{-4}
Ti15Mo7Zr0.75Si	0.137	39.91	4.55×10^{-4}	0.65	620.30	1.35×10^{-5}	0.93	2.42×10^{5}	9.63×10^{-4}
TiMo15Zr71Si	−0.008	26.08	1.48×10^{-4}	0.75	100.80	2.27×10^{-5}	0.81	1.52×10^{6}	4.44×10^{-4}

3.3. Three-Point Bending Test

Table 6 shows the modulus of elasticity's average values (E) of the four specimens tested with their respective standard deviation, which were found by following Equation (3), consid-

ering the applied load (F), the distance between supports at which the equipment's lower shank is placed for placing samples (L), the moment of inertia (I), and the deformation (δ):

$$E = \frac{F \cdot L^3}{48 \cdot \delta \cdot I} \cdot 10^{-3} \quad (3)$$

Table 6. Young's modulus of the studied alloys.

Sample	E Average (GPa)
TiMo15Zr7	82.4 ± 9.2
TiMo15Zr7Si0.5	61.5 ± 8.4
TiMo15Zr7Si0.75	66.0 ± 8.0
TiMo15Zr7Si1	73.4 ± 8.2

Since the specimens have a rectangular cross-section, Equation (4) defines the moment of inertia where w is the specimen's width and h is its thickness.

$$I = \frac{w \cdot h^3}{12} \quad (4)$$

After calculating the average values of each specimen's elasticity modulus, it can be observed that the lower E value was obtained for the TiMo15Zr7Si0.5 sample (82.4 ± 9.2 GPa), while the upper E value was for TiMo15Zr7 (61.5 ± 8.4 GPa). This fact indicates that the small addition of silicon could help the samples to decrease their Young's modulus and to approach the E of human bone (7–30 GPa).

Nevertheless, the results obtained are higher than those of the TiMoSi alloy (20–43 GPa) and within ranges that are comparable to those discovered in earlier studies, such as those of the TiMoZrTa alloy (52–69 GPa). The research alloy, TiMoZrSi, has a substantially lower Young's modulus when compared to more widely used alloys in industry, medicine, and dentistry, such as stainless steel (190–210 GPa), cpTitanium (105 GPa), Ti6Al4V (110 GPa), and CoCrMo (210–253 GPa) [35,36].

3.4. Microhardness Test

The microhardness values in HV 0.005, HV 0.025, and HV 0.05, as well as the standard deviation and the minimum and maximum values for the 10 indentations made on each sample, are shown in Figure 8 and Table 7.

Table 7. Microhardness values of applied loads of the four samples for 5, 25, and 50 gf.

Load (gf)	Samples	Average (HV)	Min	Max
5	TiMo15Zr7	374 ± 16	349	408
	TiMo15Zr7Si0.5	357 ± 56	247	451
	TiMo15Zr7Si0.75	389 ± 32	350	437
	TiMo15Zr7Si1	396 ± 32	320	437
25	TiMo15Zr7	348 ± 21	317	392
	TiMo15Zr7Si0.5	365 ± 24	334	403
	TiMo15Zr7Si0.75	389 ± 13	366	409
	TiMo15Zr7Si1	382 ± 50	268	433
50	TiMo15Zr7	339 ± 32	258	372
	TiMo15Zr7Si0.5	362 ± 63	218	427
	TiMo15Zr7Si0.75	395 ± 14	379	419
	TiMo15Zr7Si1	382 ± 22	345	406

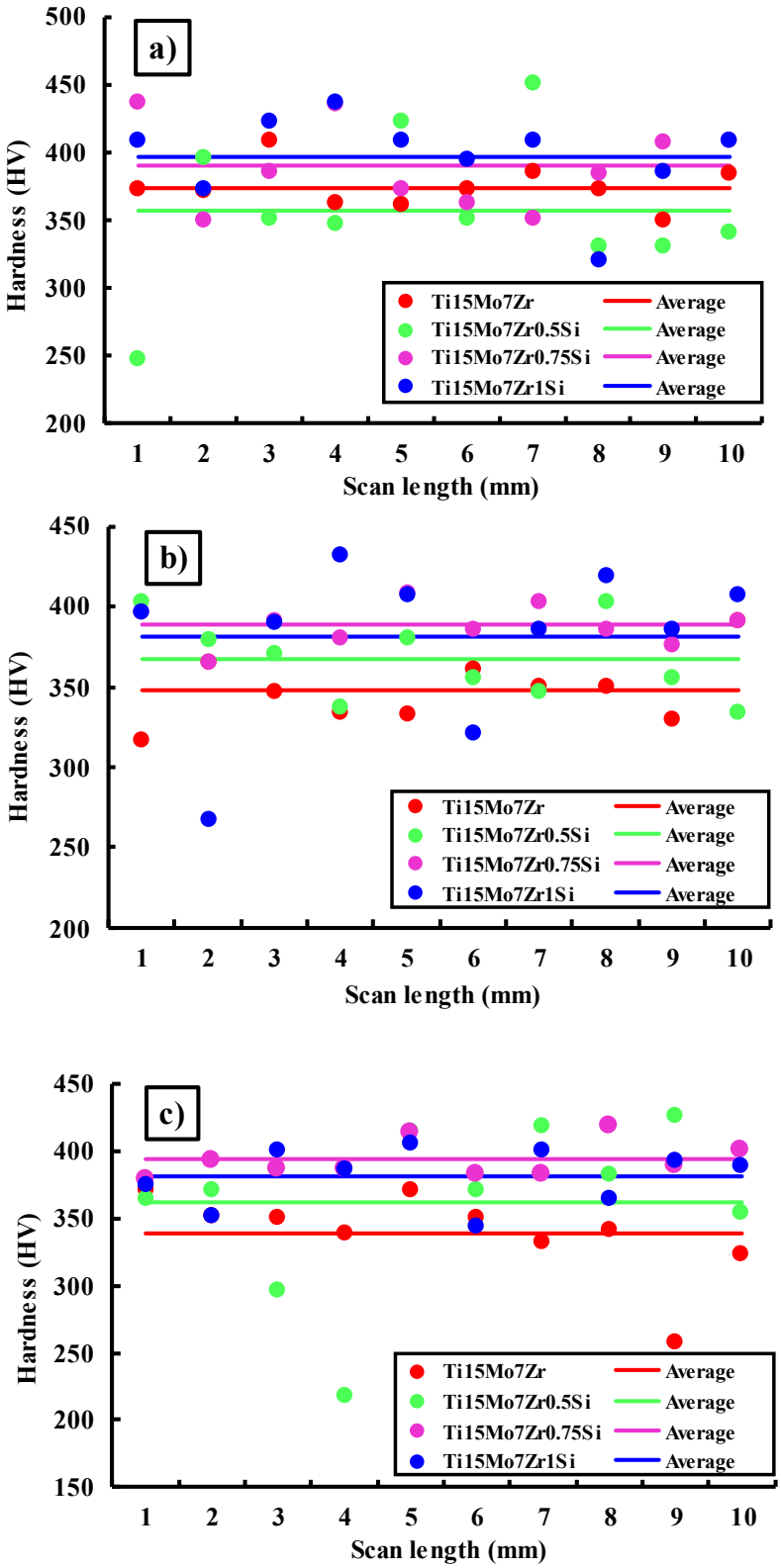

Figure 8. Microhardness values for each indentation for the four samples under study under loadings of 5 (**a**), 25 (**b**), and 50 (**c**) gf.

Figure 8 shows a comparison of the 10 indentations performed on the four specimens for each load applied and their calculated averages. In general, the values obtained range between 300 and 450 HV for the three applied loads, although some very high peaks can be observed against other very low ones, which would indicate the existence of harder

or softer areas on the surface of the samples and, therefore, a slight lack of homogeneity during the manufacturing process of the samples due to the varying hardness ratings of the alpha and beta phases and the orientation of the material's crystals. Additionally, for the three loads applied, the mean HV values of the studied samples were around 350 and 400 HV, approximately.

Table 7 shows more clearly the obtained averages, where for 5 gf applied, the TiMo15Zr7Si1 sample achieved a higher value (396 ± 32 HV), while for 25 and 50 gf, the sample that presented higher microhardness values was TiMo15Zr7Si0.75 (389 ± 13 HV; 395 ± 14). In turn, for the 5 gf load, the minimum and maximum values were 247 and 451 HV (TiMo15Zr7Si0.5), respectively. For the 25 gf loading, the minimum value was 268 HV, and a maximum of 433 HV was reached for the TiMo15Zr7Si1 sample. Finally, when applying the 50 gf load, TiMo15Zr7Si0.5 obtained the minimum and maximum values of 218 and 427 HV, respectively. Therefore, by adding silicon to the samples, a slight increase of the hardness values appears.

Moreover, the values found in this research were lower than those of conventional alloys like CoCrMo (155–601 HV) and Ti6Al4V (541 HV) [35], but higher than those of cpTi [37,38].

By measuring hardness at different loads, we can observe how the hardness of the material changes with increasing plastic deformation. This information is especially important for understanding the alloy's resistance to deformation, its ability to withstand applied loads, and its response to forming or shaping processes. In some cases, variations in hardness values with different loads may suggest the presence of localized variations in the microstructure, such as variations in grain size, phases, or the presence of inclusions. By examining the hardness through different loadings, the different phases of the material's microstructure can be identified.

4. Conclusions

Four new titanium alloys' mechanical properties and corrosion behavior have been compared and contrasted in this study. Microstructural, corrosion potential and corrosion rate curves, EIS, three-point bending, and microhardness results have produced the following findings:

- After the samples were exposed to Kroll reagent, biphasic dendritic patterns were seen on their surfaces. The dendrites became smaller when silicon was added because silicon is a strong grain refiner in titanium alloys. It promotes the formation of fine grains that hinder the propagation of cracks, enhancing the material's resistance to fatigue.
- Both samples' potential values grew during the immersion duration without diminishing, indicating that the passive layer, which was produced on the surface of each sample, is thermodynamically resilient under standard circumstances. Silicon oxide forms a protective oxide layer on the alloy surface, reducing the rate of oxidation and improving the alloys' resistance to body fluid degradation.
- Since the polarization resistance was fairly large, the low corrosion currents and rates showed the tested samples' exceptional performance in the evaluated environment, Ringer solution. R(QR)(QR) was the EC that most closely fit the measured EIS data, and as additional positive potentials were applied, the phase angle and the impedance results tended to rise. The sample 0.5%Si had the lowest corrosion rate because this is the solubility limit of silicon in the particular titanium alloy, and when exceeding this content, the presence of Si may create galvanic couples between the Si-containing regions and the rest of the titanium alloy, leading to localized electrochemical reactions.
- By examining the hardness through different loadings, two different phases, one hard and one soft, of the material's microstructure were identified. Microhardness and elastic modulus values for both instances were lower than those for several conventional biomedical alloys.

In general, all samples showed good chemical and biological qualities, with slightly better results for the Ti15Mo7Zr0.5Si sample.

Author Contributions: Conceptualization, J.C.M.-R.; methodology, P.V.; validation, J.C.M.-R.; investigation, C.J.-M., M.S.B., and P.V.; writing—original draft, C.J.-M.; funding acquisition, M.S.B.; project administration, P.V. All authors have read and agreed to the published version of the manuscript.

Funding: This paper was financially supported by the Project "Network of excellence in applied research and innovation for doctoral and postdoctoral programs/InoHubDoc", a project co-funded by the European Social Fund financing agreement no. POCU/993/6/13/153437. This paper was also supported by "Gheorghe Asachi" Technical University from Iaşi (TUIASI), through the Project "Performance and excellence in postdoctoral research 2022".

Institutional Review Board Statement: Not applicable.

Informed Consent Statement: Not applicable.

Data Availability Statement: Not applicable.

Conflicts of Interest: The authors declare no conflict of interest.

References

1. Zaokari, Y.; Persaud, A.; Ibrahim, A. Biomaterials for Adhesion in Orthopedic Applications: A Review. *Eng. Regen.* **2020**, *1*, 51–63. [CrossRef]
2. Aggarwal, D.; Kumar, V.; Sharma, S. Drug-Loaded Biomaterials for Orthopedic Applications: A Review. *J. Control. Release* **2022**, *344*, 113–133. [CrossRef]
3. Marcello, E.; Chiono, V. Biomaterials-Enhanced Intranasal Delivery of Drugs as a Direct Route for Brain Targeting. *Int. J. Mol. Sci.* **2023**, *24*, 3390. [CrossRef] [PubMed]
4. Lin, Y.; Fu, M.L.; Harb, I.; Ma, L.X.; Tran, S.D. Functional Biomaterials for Local Control of Orthodontic Tooth Movement. *J. Funct. Biomater.* **2023**, *14*, 294. [CrossRef] [PubMed]
5. Rafique, M.; Ali, O.; Shafiq, M.; Yao, M.; Wang, K.; Ijima, H.; Kong, D.; Ikeda, M. Insight on Oxygen-Supplying Biomaterials Used to Enhance Cell Survival, Retention, and Engraftment for Tissue Repair. *Biomedicines* **2023**, *11*, 1592. [CrossRef]
6. Morrison, E.; Suvarnapathaki, S.; Blake, L.; Camci-Unal, G. Unconventional Biomaterials for Cardiovascular Tissue Engineering. *Curr. Opin. Biomed. Eng.* **2021**, *17*, 100263. [CrossRef]
7. He, L.; Yin, J.; Gao, X. Additive Manufacturing of Bioactive Glass and Its Polymer Composites as Bone Tissue Engineering Scaffolds: A Review. *Bioengineering* **2023**, *10*, 672. [CrossRef] [PubMed]
8. Kaur, M.; Singh, K. Review on Titanium and Titanium Based Alloys as Biomaterials for Orthopaedic Applications. *Mater. Sci. Eng. C* **2019**, *102*, 844–862. [CrossRef]
9. Niinomi, M.; Nakai, M.; Hieda, J. Development of New Metallic Alloys for Biomedical Applications. *Acta Biomater.* **2012**, *8*, 3888–3903. [CrossRef] [PubMed]
10. Rao, S.; Ushida, T.; Tateishi, T.; Okazaki, Y.; Asao, S. Effect of Ti, Al, and V Ions on the Relative Growth Rate of Fibroblasts (L929) and Osteoblasts (MC3T3-E1) Cells. *Biomed. Mater. Eng.* **1996**, *6*, 79–86. [CrossRef]
11. Zhou, Y.L.; Niinomi, M.; Akahori, T. Changes in Mechanical Properties of Ti Alloys in Relation to Alloying Additions of Ta and Hf. *Mater. Sci. Eng. A* **2008**, *483–484*, 153–156. [CrossRef]
12. Zhou, Y.L.; Niinomi, M.; Akahori, T. Effects of Ta Content on Young's Modulus and Tensile Properties of Binary Ti-Ta Alloys for Biomedical Applications. *Mater. Sci. Eng. A* **2004**, *371*, 283–290. [CrossRef]
13. Zhang, L.C.; Chen, L.Y. A Review on Biomedical Titanium Alloys: Recent Progress and Prospect. *Adv. Eng. Mater.* **2019**, *21*, 1801215. [CrossRef]
14. Mareci, D.; Chelariu, R.; Dan, I.; Gordin, D.M.; Gloriant, T. Corrosion Behaviour of β-Ti20Mo Alloy in Artificial Saliva. *J. Mater. Sci. Mater. Med.* **2010**, *21*, 2907–2913. [CrossRef]
15. Kolli, R.P.; Devaraj, A. A Review of Metastable Beta Titanium Alloys. *Metals* **2018**, *8*, 506. [CrossRef]
16. Carobolante, J.P.A.; Pereira Júnior, A.; Bortolini Junior, C.; Barboza da Silva, K.; Sabino, R.M.; Popat, K.C.; Claro, A.P.R.A. Processing and Characterization of a New Quaternary Alloy Ti10Mo8Nb6Zr for Potential Biomedical Applications. *Materials* **2022**, *15*, 8636. [CrossRef]
17. Oliveira, N.T.C.; Aleixo, G.; Caram, R.; Guastaldi, A.C. Development of Ti-Mo Alloys for Biomedical Applications: Microstructure and Electrochemical Characterization. *Mater. Sci. Eng. A* **2007**, *452–453*, 727–731. [CrossRef]
18. Perdomo, P.P.S.; Suárez, N.R.F.; Verdú-Vázquez, A.; Rosca, J.C.M. Comparative EIS Study of Titanium-Based Materials in High Corrosive Environments. *Int. J. Surf. Sci. Eng.* **2021**, *15*, 152–164. [CrossRef]
19. Rosca, J.C.M.; Santana, E.D.H.; Castro, J.R.; Lopez, A.S.; Vasilescu, E.V.; Drob, P.; Vasilescu, C. Characterisation of Anodic Films Formed on Titanium and Its Alloys. *Mater. Corros.* **2005**, *56*, 692–696. [CrossRef]

20. Xu, W.; Chen, M.; Lu, X.; Zhang, D.-W.; Singh, H.-P.; Yu, J.-S.; Pan, Y.; Qu, X.-H.; Liu, C.-Z. Effects of Mo Content on Corrosion and Tribocorrosion Behaviours of Ti-Mo Orthopaedic Alloys Fabricated by Powder Metallurgy. *Corros. Sci.* **2020**, *168*, 108557. [CrossRef]
21. Zhang, J.; Wang, C.; Shareef, N. Microstructure and Properties of Ti-Zr-Mo Alloys Fabricated by Laser Directed Energy Deposition. *Materials* **2023**, *16*, 1054. [CrossRef] [PubMed]
22. Elshalakany, A.B.; Ali, S.; Amigó Mata, A.; Eessaa, A.K.; Mohan, P.; Osman, T.A.; Amigó Borrás, V. Microstructure and Mechanical Properties of Ti-Mo-Zr-Cr Biomedical Alloys by Powder Metallurgy. *J. Mater. Eng. Perform.* **2017**, *26*, 1262–1271. [CrossRef]
23. Florido-suarez, N.; Hulka, I.; Mirza-Rosca, J.; Saceleanu, A. Stability Range of Ti-Zr Alloy for Dental Implants. *Microsc. Microanal.* **2022**, *28*, 1034–1039. [CrossRef]
24. Jimenez-Marcos, C.; Mirza-Rosca, J.C.; Baltatu, M.S.; Vizureanu, P. Experimental Research on New Developed Titanium Alloys for Biomedical Applications. *Bioengineering* **2022**, *9*, 686. [CrossRef]
25. Verestiuc, L.; Spataru, M.-C.; Baltatu, M.S.; Butnaru, M.; Solcan, C.; Sandu, A.V.; Voiculescu, I.; Geanta, V.; Vizureanu, P. New Ti–Mo–Si Materials for Bone Prosthesis Applications. *J. Mech. Behav. Biomed. Mater.* **2021**, *113*, 104198. [CrossRef]
26. Jiang, Z.; Dai, X.; Middleton, H. Effect of Silicon on Corrosion Resistance of Ti–Si Alloys. *Mater. Sci. Eng. B* **2011**, *176*, 79–86. [CrossRef]
27. *ASTM E3-11(2017)*; Standard Guide for Preparation of Metallographic Specimens. ASTM International: West Conshohocken, PA, USA, 2017.
28. Material, C.; Databases, P. Standard Reference Test Method for Making Potentiostatic and Potentiodynamic Anodic. *Annu. B ASTM Stand.* **2004**, *94*, 1–12.
29. *ASTM G 102-89*; Standard Practice for Calculation of Corrosion Rates and Related Information from Electrochemical Measurements. ASTM International: West Conshohocken, PA, USA, 1999; Volume 89, pp. 1–7.
30. *ISO 16773-1-4:2016*; Electrochemical Impedance Spectroscopy (EIS) on Coated and Uncoated Metallic Specimens. ISO: Geneva, Switzerland, 2016.
31. *ISO 7438:2020*; International Organization for Standardization Metallic Materials—Bend Test. ISO: Geneva, Switzerland, 2020.
32. *ISO 14577-1:2015*; Metallic Materials—Instrumented Indentation Test for Hardness and Materials Parameters—Part 1: Test Method. ISO: Geneva, Switzerland, 2015. Available online: https://www.iso.org/standard/56626.html (accessed on 10 January 2023).
33. Peters, M.; Leyens, C. *Titanium and Titanium Alloys: Fundamentals and Applications*; Wiley-VCH: Weinheim, Germany, 2003; ISBN 3527305343.
34. Popa, M.V.; Vasilescu, E.; Drob, P.; Anghel, M.; Vasilescu, C.; Mirza-Rosca, I.; Lopez, A.S. Anodic Passivity of Some Titanium Base Alloys in Aggressive Environments. *Mater. Corros.* **2002**, *53*, 51–55. [CrossRef]
35. Sandu, A.V.; Baltatu, M.S.; Nabialek, M.; Savin, A.; Vizureanu, P. Characterization and Mechanical Proprieties of New TiMo Alloys Used for Medical Applications. *Materials* **2019**, *12*, 2973. [CrossRef]
36. Bocchetta, P.; Chen, L.Y.; Tardelli, J.D.C.; Dos Reis, A.C.; Almeraya-Calderón, F.; Leo, P. Passive Layers and Corrosion Resistance of Biomedical Ti-6al-4v and β-Ti Alloys. *Coatings* **2021**, *11*, 487. [CrossRef]
37. Da Rocha, S.S.; Adabo, G.L.; Henriques, G.E.P.; Nóbilo, M.A.D.A. Vickers Hardness of Cast Commercially Pure Titanium and Ti-6Al-4V Alloy Submitted to Heat Treatments. *Braz. Dent. J.* **2006**, *17*, 126–129. [CrossRef] [PubMed]
38. Baltatu, M.S.; Spataru, M.C.; Verestiuc, L.; Balan, V.; Solcan, C.; Sandu, A.V.; Geanta, V.; Voiculescu, I.; Vizureanu, P. Design, Synthesis, and Preliminary Evaluation for Ti-Mo-Zr-Ta-Si Alloys for Potential Implant Applications. *Materials* **2021**, *14*, 6806. [CrossRef] [PubMed]

Artículo 3. Evaluation of New Titanium Alloys as Potential Materials for Medical Devices

Microscopy and Microanalysis, **29** (Suppl 1), 2023, 196–201
https://doi.org/10.1093/micmic/ozad067.088

Microscopy AND Microanalysis

Meeting-report

Evaluation of New Titanium Alloys as Potential Materials for Medical Devices

Cristina Jiménez-Marcos[1], Julia Claudia Mirza-Rosca[1,*], Madalina Simona Baltatu[2], and Petrica Vizureanu[2]

[1]*Department of Mechanical Engineering, University of Las Palmas de Gran Canaria, Las Palmas de Gran Canaria, Spain*
[2]*Department of Technologies and Equipment for Materials Processing, "Gheorghe Asachi" Technical University of Iasi, Iasi, Romania*
*Corresponding author: julia.mirza@ulpgc.es

Introduction

The continuing relevance of research in medicine, biology, chemistry and engineering has led biomaterials science to develop new materials that can resolve many of today's medical problems and improve the quality and longevity of human life [1]. However, as life expectancy has increased in developed countries, the elderly population has increased, as has the obese population, the latter due to the adoption of a more sedentary lifestyle, putting them at greater risk of suffering chronic musculoskeletal diseases such as osteoarthritis, particularly in the hips and knees, and requiring a greater number of surgical implant repairs.

Metal biomaterials, such as CoCrMo alloys, 316L stainless steel, and titanium and its alloys, are often the most frequently employed for medical applications [2–4]. The very superior biocompatibility, great corrosion resistance, high mechanical performance, low modulus, and high thermal stability of titanium alloys make them stand out above the others [5].

Two novel Ti20Mo7ZrxSi (x = 0.75, 1) alloys were produced by vacuum arc remelting (VAR) furnace, and this study examined their microstructure, corrosion behaviour, quantitative microanalysis, Young's modulus and hardness. Metallography, scanning electron microscopy, electrochemistry, three-point bending, and microhardness testing were some of the used techniques for this study.

Experimental

The Ti20Mo7Zr0.75Si and Ti20Mo7Zr1Si samples obtained in a vacuum arc remelting furnace were prepared for the subsequent analysis (see Figure 1). Electrochemical testing, Vickers hardness measurements and SEM observations on the embedded samples were performed (see Figure 2). A part of the samples have been cut and the Young's modulus of each specimen was calculated by a three-point bending test (see Figure 3).

Results and discussion

In the metallographic examination, in Figure 4, both samples have biphasic and dendritic structures and the size of dendrites are reduced with the addition of Si, whereas the interdendritic zone grew.

EIS measurements were performed on each sample at different potentials to obtain impedance plots (see Figure 5) where the corrosion resistance increases as the applied potential became more positive and the impedance and phase angle values increase. Thus, the sample with the highest corrosion resistance was Ti20Mo7Zr1Si.

The impedance experimental data were fitted with an electrical equivalent circuit with one-time constant for Ti20Mo7Zr0.75Si and with two-time constant for Ti20Mo7Zr1Si (see Figure 6).

The dispersive energy obtained from the EDS spectra of the samples studied revealed the existence of the alloy's elements together with oxygen (see Figures 7c and Figures 7d), most likely as a result of the past corrosion processes and the creation of the titanium oxide layer. On the other hand, it is evident from the quantitative results that there are two zones, one rich in titanium and the other in Mo, Zr, and Si.

In the three-point bending method, in Table 1, the Young's modulus achieved for both samples were similar to that normally found in human bone, lower than that of commercial alloys and lower for the TiMoZrSi0.5 sample. In addition, the Vickers hardness versus scan length plots for both samples show widely scattered maxima and minima, as the surfaces of the samples have hard and soft areas, and it is confirmed that hardness increases with higher silicon content (see Table 2).

Conclusions

This research investigated the effect of silicon concentration on microstructure, biocompatibility, modulus of elasticity, microhardness and corrosion resistance of the TiMoZrSi alloy in a simulated body fluid, confirming the two-phase and dendritic structure for both samples in metallographic tests. Two zones, one rich in titanium and the other in Mo, Zr, and Si, may be found on the surface of the alloys. Each sample's surface was found to form a passive oxide layer (TiO_2), which was verified. In electrochemical tests, the potential of the TiMoZrSi0.75 sample tended to corrode and showed lower corrosion resistance. The modulus of elasticity was less than that of many commercial alloys. Finally, the Vickers hardness values increased as the silicon content increased. According to the results obtained, the addition of a higher percentage of silicon leads to slightly improved mechanical properties but both alloys can be used for medical devices.

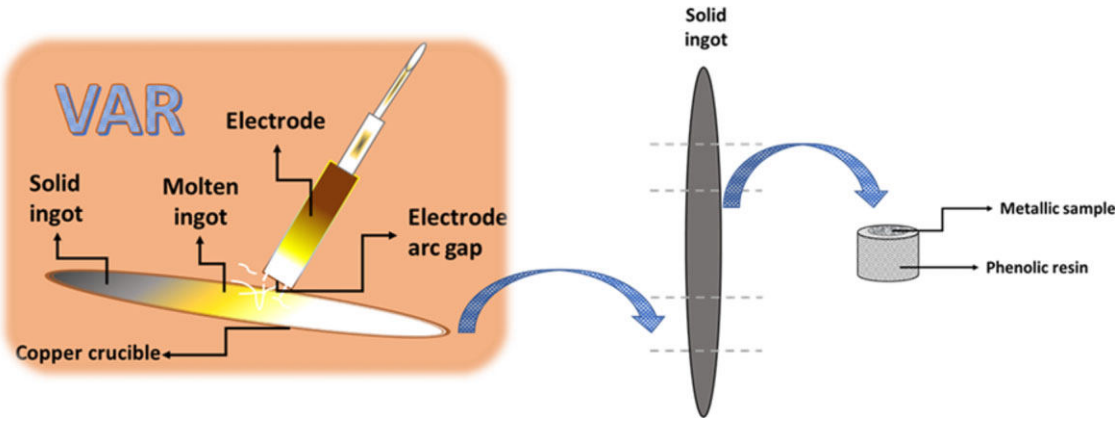

Fig. 1. Fabrication and posterior preparation of the studied samples.

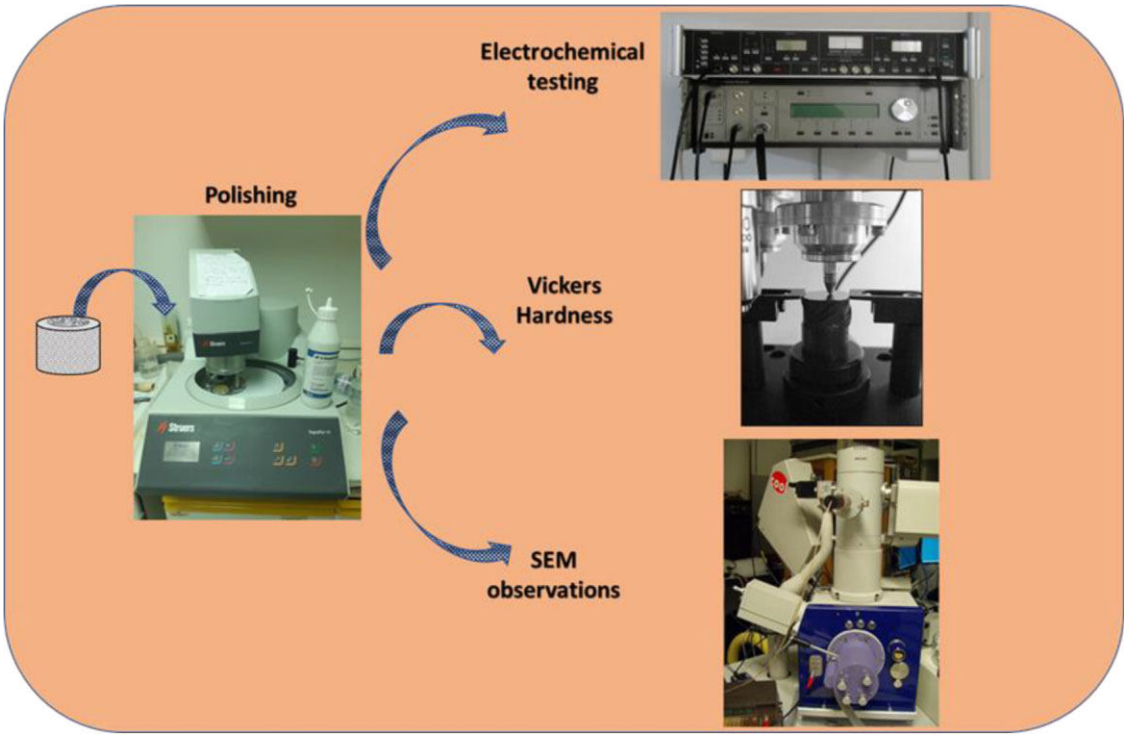

Fig. 2. Part of the experimental procedure for the samples.

Fig. 3. Preparation of the samples and three-point bending test.

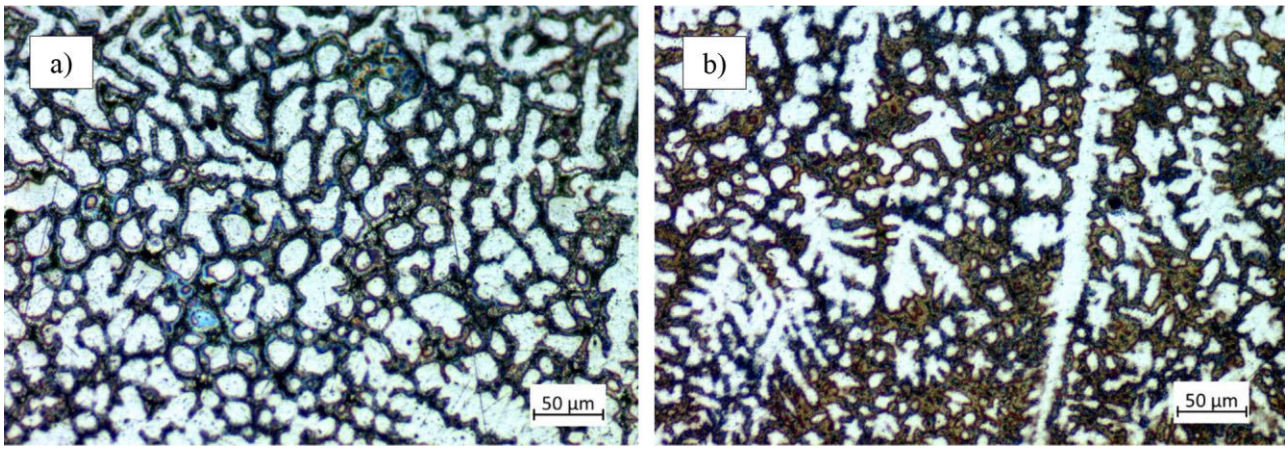

Fig. 4. Microstructure of Ti20Mo7Zr0.75Si (a) and Ti20Mo7Zr1Si (b) samples after chemical etching by optical microscopy.

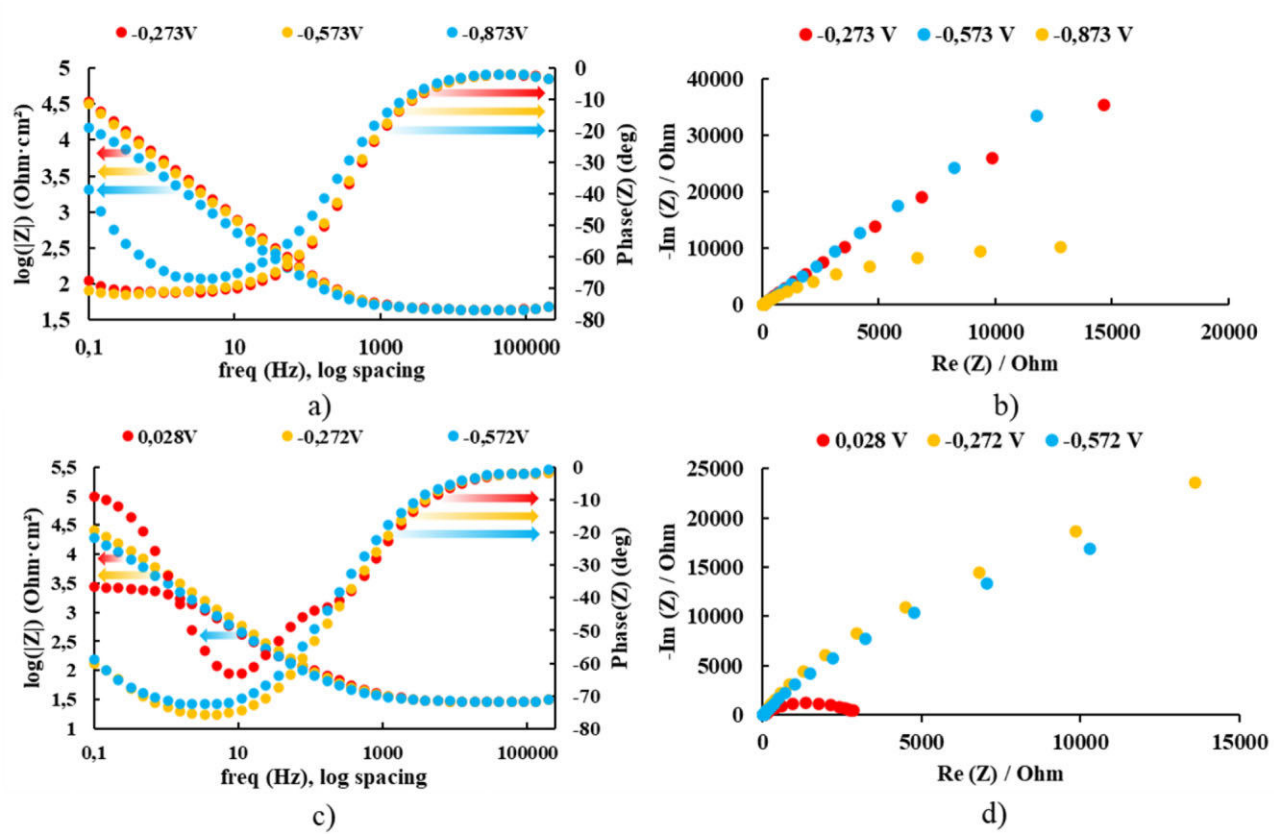

Fig. 5. Impedance diagrams for: Ti20Mo7Zr0.75Si (a and b); for Ti20Mo7Zr1Si (c and d).

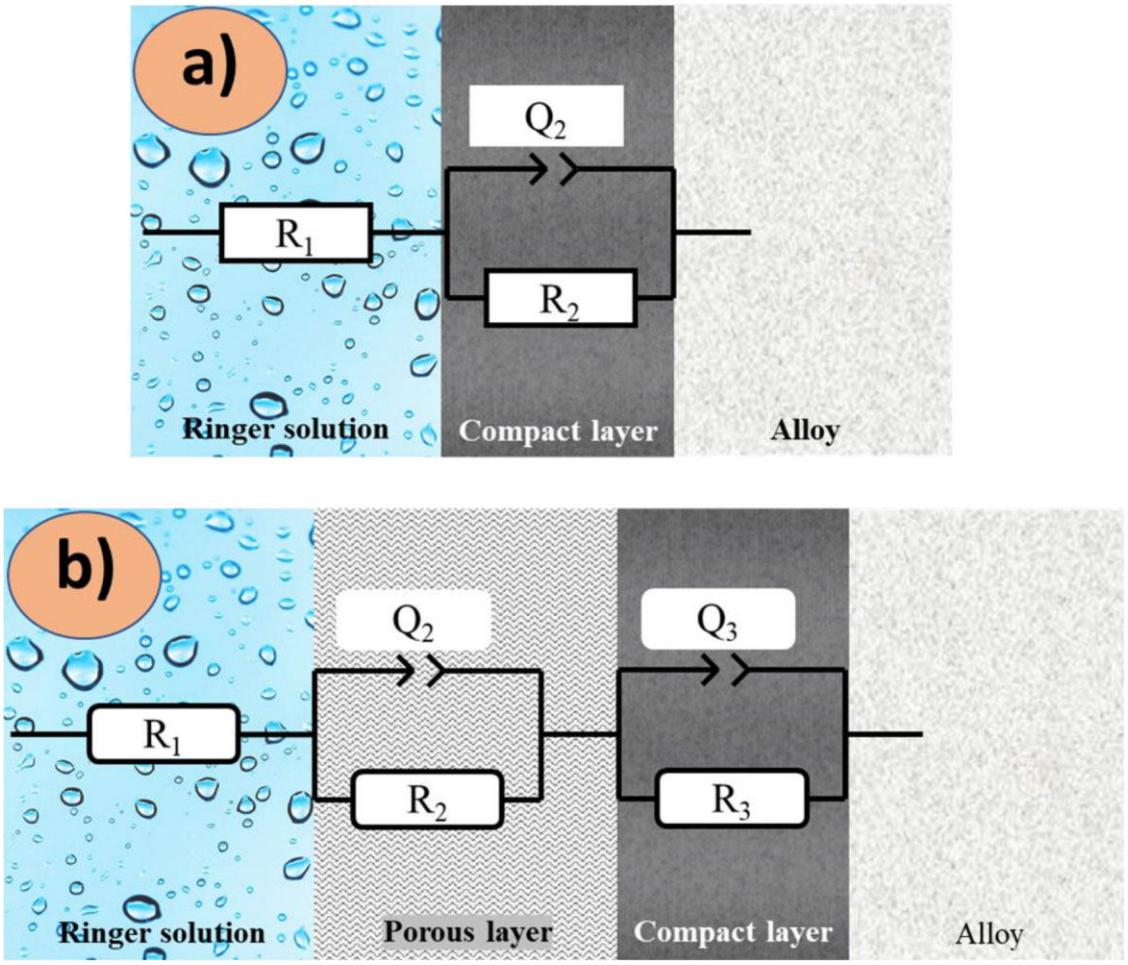

Fig. 6. Equivalent electrical circuits used for the fitting of experimental data for: a) Ti20Mo7Zr0.75Si and b) Ti20Mo7Zr1Si.

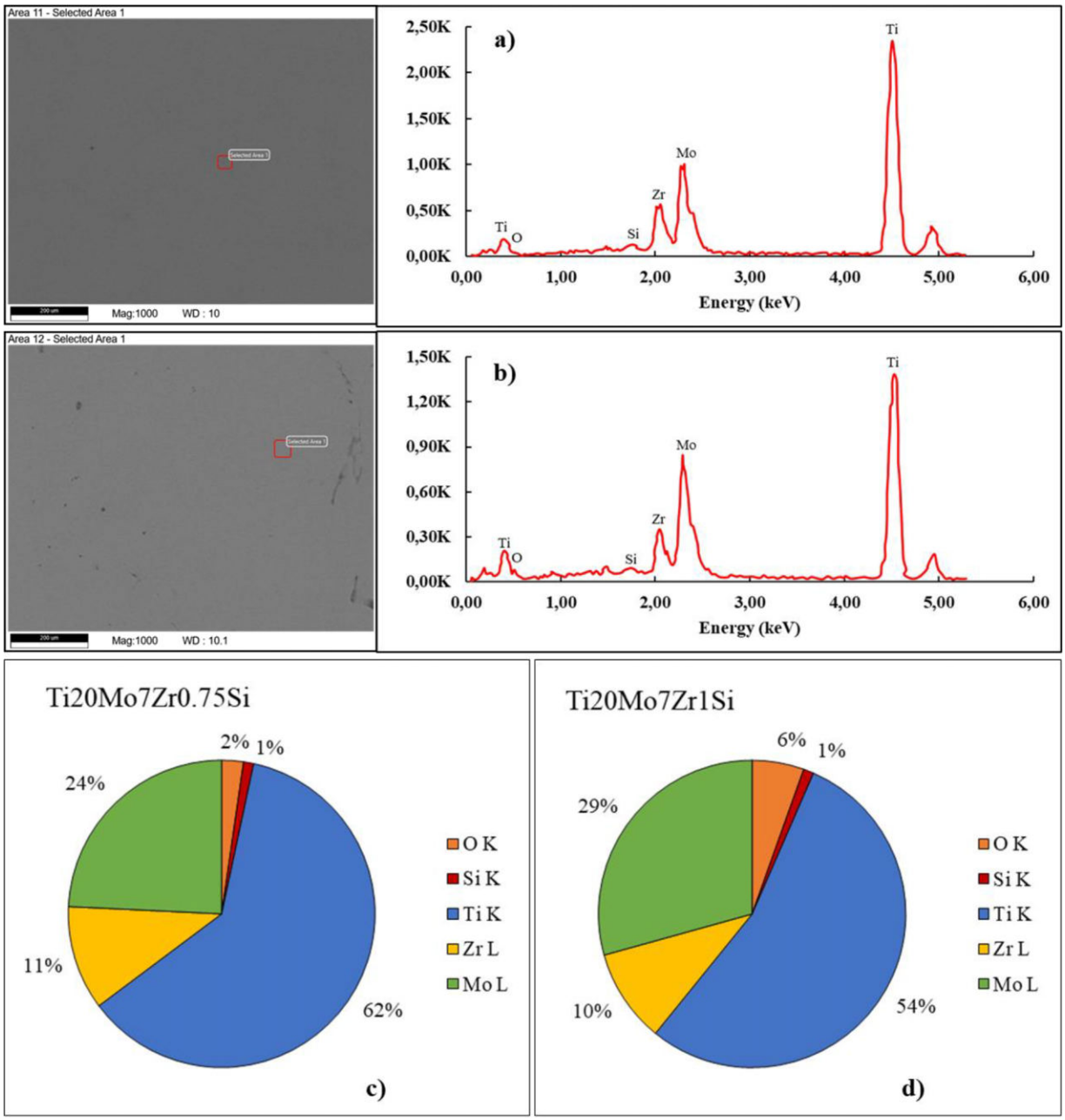

Fig. 7. EDS spectra for Ti20Mo7Zr0.75Si (a) and Ti20Mo7Zr1Si (b) samples and quantification (c, d).

Table 1. Young's modulus values obtained from Ti20Mo7Zr0.75Si and Ti20Mo7Zr1Si specimens.

Sample	Modulus of elasticity E (GPa)
Ti20Mo7Zr0.75Si	54.4 ± 6.5
Ti20Mo7Zr1Si	82.7 ± 21.5

Table 2. Microhardness values of applied loads of soft and hard phases of Ti20Mo7Zr0.75Si and Ti20Mo7Zr1Si samples.

	Ti20Mo7Zr0.75		Ti20Mo7Zr1Si	
	Microhardness (HV)		Microhardness (HV)	
Load (gf)	Soft phase	Hard phase	Soft phase	Hard phase
5	214	365	115	243
25	239	383	137	366
50	319	399	158	356

References

1. I. Hulka, N.R. Florido-Suarez, J.C. Mirza-Rosca, A. Saceleanu, Ti–Ta dental alloys and a way to improve gingival aesthethic in contact with the implant, *Mater. Chem. Phys*. **287** (2022) 126343. https://doi.org/10.1016/j.matchemphys.2022.126343.
2. A. Saceleanu, N. Florido-suarez, C. Jimenez-marco, J. Mirza-rosca, Relation Between Composition, Structure and Properties of Different Dental Alloys, **28** (2022) 684–688. https://doi.org/10.1017/S1431927622003221.
3. J.C. Florido-Suarez, Nestor, Verdu-Vazquez, Amparo, Socorro-Perdomo, Pedro, Mirza-Rosca, Past Advances and Future Perspective of Ti-Ta Alloys, *Glob. J. Eng. Sci*. **7** (2021) 20–22. https://doi.org/10.33552/gjes.2021.07.000668.
4. C. Jiménez-Marcos, M.S. Baltatu, N.R. Florido-Suárez, P.P. Socorro-Perdomo, P. Vizureanu, J.C. Mirza-Rosca, Mechanical properties and corrosion resistance of two new titanium alloys for orthopaedics applications, *Mater. Today Proc*. **72** (2022) 544–549. https://doi.org/10.1016/j.matpr.2022.09.394.
5. C. Jimenez-Marcos, J.C. Mirza-Rosca, M.S. Baltatu, P. Vizureanu, Experimental Research on New Developed Titanium Alloys for Biomedical Applications, *Bioengineering*. **9** (2022) 686. https://doi.org/10.3390/bioengineering9110686.

Artículo 4. Two novel Ti-Mo-Ta-Zr alloys for medical devices: their microstructure, corrosion resistance and microhardness characteristics

Materials Chemistry and Physics 334 (2025) 130511

Contents lists available at ScienceDirect

Materials Chemistry and Physics

journal homepage: www.elsevier.com/locate/matchemphys

Two novel Ti–Mo–Ta–Zr alloys for medical devices: Their microstructure, corrosion resistance and microhardness characteristics

Cristina Jiménez-Marcos [a], Julia Claudia Mirza-Rosca [a,b,*], Madalina Simona Baltatu [c], Petrica Vizureanu [c]

[a] Mechanical Engineering Department, Las Palmas de Gran Canaria University, Las Palmas de Gran Canaria, 35014, Spain
[b] Transilvania University of Brasov, Materials Engineering and Welding Department, Brasov, 500036, Romania
[c] Department of Technologies and Equipments for Materials Processing, Faculty of Materials Science and Engineering, Gheorghe Asachi Technical University of Iasi, Iasi, 700050, Romania

HIGHLIGHTS

- Two new titanium alloys with non-toxic elements and near β structure were analyzed.
- The passive film formed on the surface of both alloys is compact and protective.
- The increasing of Mo content significantly enhanced the corrosion resistance.

GRAPHICAL ABSTRACT

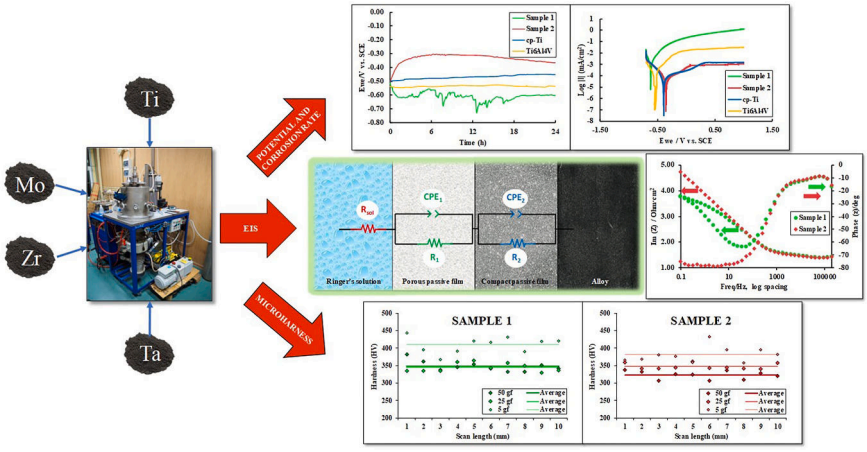

ARTICLE INFO

Keywords:
Titanium alloys
Microhardness testing
Corrosion resistance
Microstructural analysis

ABSTRACT

Titanium alloys have gained a solid reputation in the field of biomedicine due to their exceptional biocompatibility. However, it is important to note that some of these alloys do release toxic ions, which could potentially limit their application in sensitive scenarios. This study examines two new titanium alloys, TixMo15Ta7Zr (x = 15, 20 wt%) and it designed these alloys to overcome certain challenges by including helpful elements like molybdenum (Mo), tantalum (Ta) and zirconium (Zr). Advanced metallography, scanning electron microscopy, X-ray diffraction, microhardness measurements and electrochemical testing conclusively showed that the importantly elevated Mo content substantially improves corrosion resistance (with a corrosion rate value of 0.64 μm year^{-1}) by promoting the formation of an importantly more flexible passive layer, while simultaneously maintaining mechanical properties closely comparable to those of conventional titanium biomaterials possessing

* Corresponding author. Mechanical Engineering Department, Las Palmas de Gran Canaria University, Las Palmas de Gran Canaria, 35014, Spain.
E-mail addresses: julia.mirza@ulpgc.es, juliaclaudia.mirza@ulpgc.es (J.C. Mirza-Rosca).

https://doi.org/10.1016/j.matchemphys.2025.130511
Received 12 December 2024; Received in revised form 20 January 2025; Accepted 5 February 2025
Available online 6 February 2025

Vickers hardness values around 350 HV. These findings show that an important number of these alloys represent a revolutionary, promising solution for biomedical implants that are safer as well as more durable.

1. Introduction

Since its discovery by William Gregor in 1791, titanium has been recognized for its distinctive combination of strength, durability, and biocompatibility, which has made it a pivotal component in a diverse range of applications, including aerospace and modern medicine [1,2]. This metal is of particular value in the medical field, where it is utilized in orthopedic and dental implants, as well as an array of medical devices, due to its capacity to integrate with the human body without eliciting adverse reactions and it has the capacity to generate a passive film that serves as a protective barrier against external stimuli (TiO_2) [3].

However, the utilisation of commercial titanium alloys in biomedical applications is not without certain problems. Cp-Ti is recognized for its high biocompatibility, however, its mechanical and corrosion resistance in physiological environments is inadequate for numerous critical applications [4]. Additionally, the Ti–6Al–4V alloy utilized in orthopedic and dental implants has been linked to the development of allergies and other illnesses, including Alzheimer's and Parkinson's disease, due to the incorporation of aluminum (Al) and vanadium (V) [5,6]. In contrast, the Ti–6Al–7Nb alloy was developed to enhance biocompatibility and is employed in prosthetics and medical devices. However, it necessitates the presence of a robust protective coating [7,8]. Nitinol (TiNi), which is optimal for use in vascular stents and guidewires in minimally invasive surgery due to its capacity to revert to its original configuration, has the potential to release nickel, which can elicit allergic reactions and induce a range of cardiovascular and renal disorders [9].

To address these limitations, new titanium alloys composed of non-toxic elements such as Si, Ga, Zr, Ta and Mo, are under investigation. These elements have unique qualities that set them apart from commercial alloys, in addition to avoiding the dangers that come with using materials like Al, V, or Ni. One of the most important components of human biology is silicon, which is essential for the biological processes that promote the formation of new bone and connective tissues [10]. Gallium also reduces the risk of infections by exhibiting antibacterial qualities and contributing to biocompatibility [11]. Molybdenum, a β-stabilizing element with a low toxicity, has been studied for its potential to create Ti–Mo alloys, producing a stable oxide coating (MoO_3), preventing titanium corrosion, especially when present in optimized concentrations between 15 % and 20 %, improving the mechanical properties, and being thermally stable [12,13]. Tantalum is also a β-stabilizer that, at concentrations above 15 %, enhances biocompatibility, facilitating the formation of bone tissue around implants [14]. Zirconium is becoming a desired substitute for most medical applications, which contributes a combination of low elasticity and high corrosion resistance, ideal characteristics for biomedical applications [15]. The choice of these specific compositions responds to both previous findings and the need to combine biocompatibility, durability and superior mechanical properties.

When compared to previous Ti–Mo–Zr and Ti–Ta–Mo–Zr alloy systems, the TixMo15Ta7Zr alloys (where x can be 15 or 20 wt%) offer significant improvements. Even though Ti–Mo–Zr alloys showed improved resistance to corrosion, the addition of Ta to the new compositions improves biocompatibility even more, encouraging ideal integration with bone tissue and lowering the possibility of biological rejection. Furthermore, the Mo content, ranging from 15 % to 20 %, has been meticulously adjusted to ensure the formation of a more stable passive film, thereby surpassing the protective capabilities of earlier systems in simulated body fluids [16,17]. Finally, these alloys achieve an advanced balance between mechanical strength and elasticity, making them more suitable for critical applications than Ti–Ta–Mo–Zr systems, where elasticity was still limited.

The present study focuses on evaluating the corrosion behavior and mechanical properties of TixMo15Ta7Zr alloys in simulated body fluids, comparing them with reference materials such as Cp-Ti and Ti–6Al–4V, thereby completing our previous research [18]. A comparison of the new alloys with these reference materials reveals their superior corrosion resistance, enhanced biocompatibility, and their capacity to circumvent adverse reactions, such as those associated with the use of aluminum (Al) or vanadium (V). These compositions not only enhance the known properties of titanium, but also expand the possibilities for the design of more durable, safer, and more functional biomedical implants.

2. Experiment and methods

The following titanium alloys were subjected to investigation: Samples 1 and 2 were fabricated from pure elemental powders in a vacuum arc remelting (VAR) furnace. Sample 1 was composed of 63 % Ti, 15 % Mo, 7 % Zr, and 15 % Ta, while Sample 2 was composed of 58 Ti, 20 % Mo, 7 % Zr, and 15 % Ta. The purity of the elemental powders was greater than 99.90 %. A series of preliminary operations were conducted on the obtained ingots, including cutting and embedding them in epoxy resin. Then, the specimens were subjected to the polishing process at 150 rpm and 15 N of force utilizing the Struers TegraPol-11 polishing equipment (Copenhagen, Denmark). The progressive carbide abrasive papers with progressively higher grit were employed, ranging from P400 to P2500. Lastly, a 0.2 μm alumina suspension was employed on mirror-polishing cloths.

The samples were prepared for metallographic analysis in accordance with the standards set forth in ASTM E3-11(2017). The optical microscope Axio Vert.A1 MAT ZEISS (Jena, Germany) was utilized for the examination. Each sample was subjected to immersion in a solution of Kroll's reagent, which consists of 20 mL $C_2H_2O_2$, 30 mL HCl, and 10 mL HNO_3, for approximately 40 s. For elemental analysis, a Zeiss Sigma 300 VP scanning electron microscope (Carl Zeiss, Jena, Germany) was utilized in conjunction with an energy-dispersive X-ray spectrometer (EDX). For phase analysis of the materials, a Bruker D8 Advance X-ray diffraction (XRD) instrument was utilized. The research employed CuK radiation (1.5406 Å) with a step size of 0.02°, a current of 40 mA, and a power of 45 kV in the range of $2\theta = 10–80$.

Ten measurements, each lasting 15 s, were taken with the Future Tech FM-810 microhardness tester in compliance with ISO 14577–1:2015 for each load with the loads being 5, 25, and 50 gf, respectively. The observed diagonal lengths were then used by the iVicky application to automatically calculate the Vickers microhardness values.

In accordance with ISO 10271:2020, three electrodes were utilized for the electrochemical assessments: a working electrode (the specimen under examination), a counter electrode (a platinum electrode), and a reference electrode (a saturated calomel electrode). The area of each sample was determined using ImageJ software in order to conduct the experiments. The following components were quantified in mmol/L in the Ringer Grifols solution (Grifols Laboratories, Barcelona, Spain): The concentrations of the ions present in the solution were as follows: sodium (Na^+) 129.90 mmol/L; potassium (K^+) 5.40 mmol/L; chloride (Cl^-) 111.70 mmol/L; lactic acid ($C_3H_6O_3$) 27.20 mmol/L; and calcium (Ca^{2+}) 1.80 mmol/L. The corrosion behavior of the alloys was investigated employing a potentiostat-galvanostat BioLogic Essential SP-150 (Seyssinet-Pariset, France) in accordance with the following order: open circuit potential, linear polarization, and electrochemical impedance spectroscopy.

The 24-h open circuit potential of the study samples was determined

using the "E_{corr} vs. Time" method, as implemented in the EC-Lab program. In order to obtain the linear polarization curve, the surface area value and density of each sample were calculated. The potential scanning rate was 10.00 mV/min in the range from −0.70 V to 1.00 V vs. SCE. Impedance measurements were conducted using potentio electrochemical impedance spectroscopy, in accordance with ISO 16773–1:2016. The frequency range was set between 200 kHz and 100 mHz, and the data was displayed using Nyquist and Bode diagrams. Additionally, an electrochemical circuit was employed.

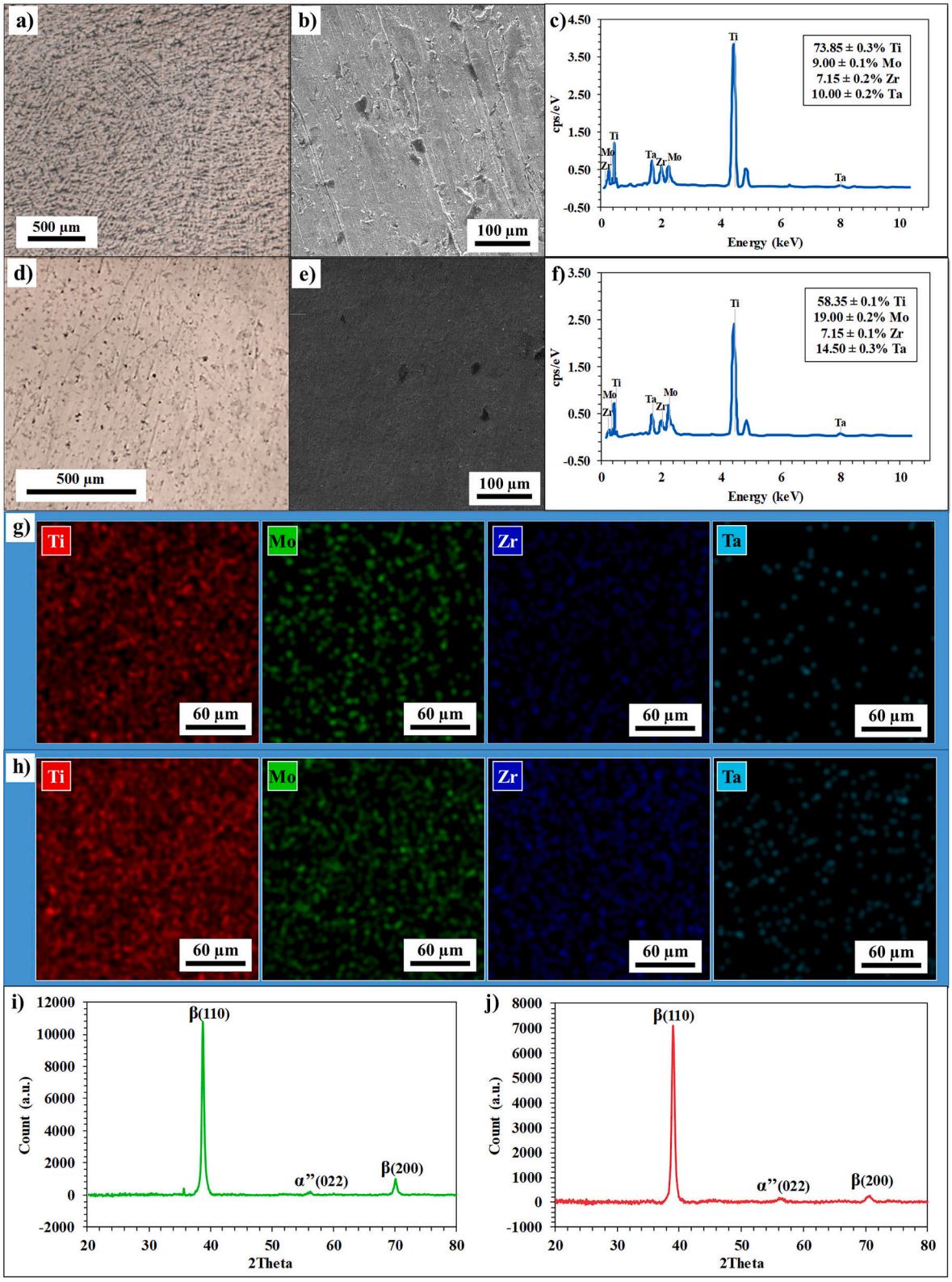

Fig. 1. Metallography (a, d), SEM image (b, e), EDX spectra and quantification (c, f), EDX elemental maps (g, h) and XRD spectra (i, j) for Sample 1 and Sample 2, respectively.

3. Results and discussion

The metallographic images of the two samples depicted in Fig. 1 illustrate a β lamellar microstructure with the presence of minor quantities of α phase, which can be attributed to the stabilizing influence of β-stabilizing elements, namely Zr and Ta. The point-specific EDX spectra and maps reveal the segregation of elements within the phases. This observation suggests that Mo also functions as an extremely effective stabilizer for the β solid solution. The stability of these features can be evaluated through the use of an Mo_{eq} equivalence assay. In accordance with the Mo equivalency formula (Mo_{eq} = Mo (wt.%) + Ta (wt.%)/4) [19], the Mo_{eq} values of the recently developed alloys demonstrate an increase as the Mo concentration rises. In particular, the Mo_{eq} values span a range of 18.75 %–23.75 %, which is considerably above the critical threshold of approximately 10 % for a stable β solid solution [20].

Fig. 2 displays the microhardness values HV0.005, HV0.025, and HV0.05 together with the mean, obtained from the 10 indentations made on each specimen. The application of 5 gf to each sample resulted in a considerable range of microhardness values, indicative of element segregation, reaching values between 380 and 410 HV (with standard deviation (SD) values of about ±22). However, at 25 or 50 gf, the indentations display greater uniformity for both samples and the values varies from 350 to 320 HV (with SD lower than ±15). These values were higher than those for Cp-Ti hardness and similar to those for Ti–6Al–4V (160–360 HV and 350–430, respectively) [21]. With increasing loading, the average depth of the footprint increased from approximately 0.9 nm–3.4 nm for both samples.

The open circuit potential curves of the studied samples, in addition to those of cp-Ti and Ti–6Al–4V, were analyzed over a 24-h testing period while the samples were submegerd in Ringer's solution (see Fig. 3a). The initial potential value of Sample 2 is −0.49 V, which is higher than that of Sample 1 due to the higher concentration of Mo (with a more anodic potential than Ti). The potential of Sample 1 exhibits oscillatory behavior during the test period, which can be attributed to the onset of localized corrosion. This process gives rise to alterations in the local environment, including changes in pH, chloride ion concentration, and oxygen availability. These fluctuations in the surrounding conditions, in turn, contribute to the observed fluctuations in the potential. It is possible that degradation and repassivation of the passive film on the alloy surface may occur in a repetitive cycle. This phenomenon could potentially lead to fluctuations in the open circuit potential, or OCP. Furthermore, the occurrence of anodic dissolution and cathodic reduction simultaneously can result in oscillatory behavior in the open circuit potential (OCP) if the system is not in a steady state. It can be observed that Sample 2 rapidly attained a stable potential of −0.27 V vs. SCE. The concentration of Mo has been demonstrated to influence the thickness, composition, and stability of the protective passive oxide film that forms on the surface of the alloy [22]. In the case of cp-Ti and Ti6Al4V, it is evident that they exhibit a tendency to stabilise their potential over the 24-h testing period.

Fig. 3b illustrates the outcomes of the linear polarization technique employed to ascertain the corrosion rate of the alloys, cp-Ti and Ti6Al4V, plotted on a semi-logarithmic scale. It can be observed that the passive range is considerable for Sample 2, indicating that the passive layer is stable and effective. The corrosion rate, V_{corr}) was found to be lower for Sample 2 (0.64 μm $year^{-1}$) in comparison to that of Sample 1 (9.95 μm $year^{-1}$) and the V_{corr} of Ti6Al4V (0.73 μm $year^{-1}$). Furthermore, the polarization resistance (R_p) of 10^6 Ohm·cm^2 was notably high for new titanium alloys, indicating that they possess considerable corrosion resistance.

The bigger capacitive arc for Sample 2 is indicative of a greater charge transfer resistance (R_{ct}), as shown in Fig. 4a. This result suggests a more effective passive film, which may be attributed to the alloy's optimal composition. Mo and Ta promote the formation of a compact inner layer, whereas Zr improves overall corrosion resistance. It has been shown that by blocking the flow of ions and electrons across the contact, this passive layer slows down the dissolution processes of the underlying metal. In biomedical applications, this enhanced durability and reduced release of hazardous metal ions are crucial characteristics that promote implant safety and reliability.

With a higher Mo concentration than Sample 1, Sample 2 demonstrated better corrosion resistance, suggesting a more effective and durable protective layer. Fig. 4b illustrates the impedance and Bode phase diagrams, which represent the logarithm of the impedance values (primary axis) and phase angles (secondary axis) as a function of frequency. The Bode impedance plot showed a higher impedance modulus value in Sample 2, reaching 56 kΩ cm^2 in the low-frequency region, indicating higher resistance to charge transfer or lower ionic conductivity through the passive film. Sample 2 also showed a higher maximum phase angle of 78.7° over a wider frequency range, indicating a more capacitive response, characteristic of a compact and stable passive layer. This higher capacitance reflects the system's ability to store electrical charge, which is related to the quality and homogeneity of the passive film formed. The presence of Mo, which promotes the creation of a thick and stable oxide film (MoO_3), and the combined effects of Ta and Zr, which increase mechanical strength and corrosion resistance, are responsible for Sample 2's passive layer's robustness. This capacitive characteristic strengthens corrosion resistance and durability, which is especially important for biological applications that need long-term stability. In order to gain a more nuanced understanding of the corrosion layer structure and characteristics, a computational model based on the equivalent electrical circuit (EEC) was employed to simulate the impedance spectra, as illustrated in Fig. 4c. The main parameters derived from the fitting using ZSimpWin software are as follows: R_{sol} represents the solution resistance, and two parallel pairs, R_1/CPE_1 and R_2/CPE_2, correspond to the porous and compact passive layer (see Fig. 4c). It was states that the inner barrier layer is created by the inward

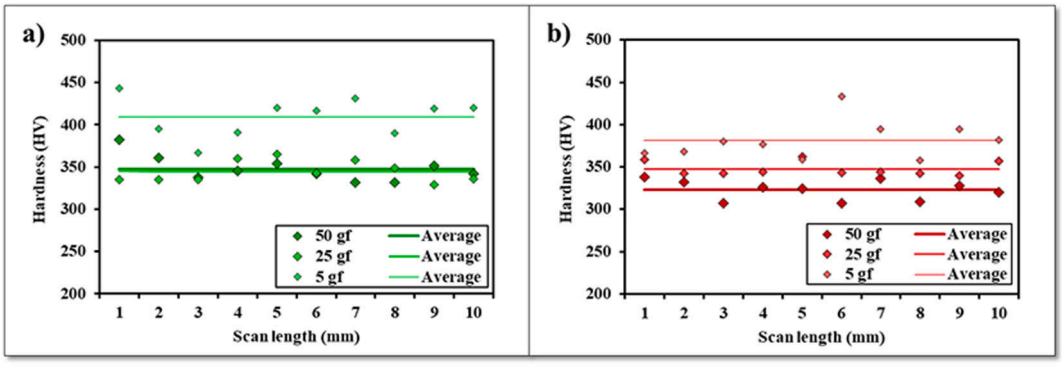

Fig. 2. Microhardness results of a) Sample 1 and Sample b).

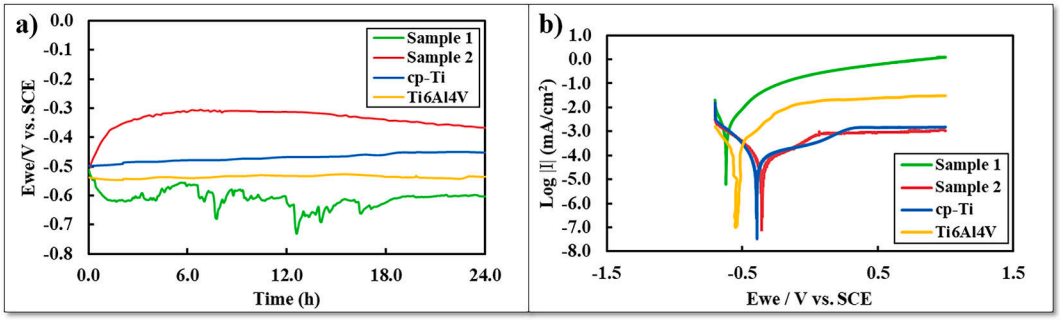

Fig. 3. a) Open circuit potential after 24 h' immersion time; b) linear polarization curves.

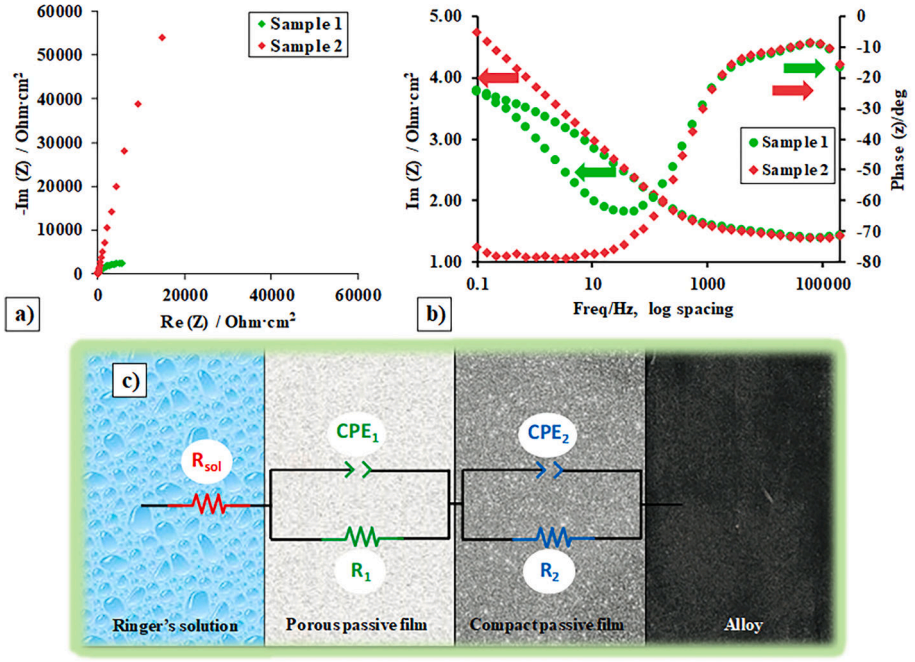

Fig. 4. a) Nyquist, b) Bode-IZI and Bode-phase diagrams at E_{corr}, c) equivalent circuit.

transition of oxygen ions and the outer porous layer is formed by the hydrolysis of cations flowing from the inner barrier layer [23,24]. The use of a constant phase element (CPE) in place of pure capacitance serves to highlight the non-ideal capacitive response, which is a consequence of the heterogeneous nature of the passive film in alloys. The electrical impedance of the CPE can be determined using the following equation [25]:

$$Z_{CPE} = Y^{-1}(jw)^{-n} \quad (1)$$

In this context, Y represents a constant with dimensions of $\Omega^{-1}\cdot s^n$, which is also known as the CPE coefficient or pseudo-capacitance. The imaginary unit, j, is defined as $j^2 = -1$, while ω denotes the angular frequency. Finally, n is the CPE exponent, with $0 \leq n \leq 1$. When $n = 1$, the CPE behaves like an ideal capacitor. Conversely, when $n = 0$, it behaves like a pure resistor.

The parameters extracted from the fitting of the experimental data are presented in Table 1. It has been demonstrated that the enhanced resistance of the inner compact passive layer (R_2 or R_{ct}) in Sample 2, which is approximately 8 times higher than in Sample 1, underscores the capacity of this alloy to establish an effective barrier against corrosion. In general, the corrosion resistance ($R_p = R_1 + R_2$) is higher for Sample 2, reaching values up to 10^5 Ohm·cm^2. This finding is particularly significant in physiological environments, where the stability of the inner passive layer is imperative to avert the release of metal ions. The higher compactness of this layer (n_2 close to 1) in Sample 2 suggests that the film is less susceptible to diffusion processes, resulting in prolonged protection. In comparison, the diffusive behavior observed in Sample 1 (n_1 close to 0.5) and its thicker outer layer (smaller Y_1) could indicate a lower overall protection efficiency. These observations, attributable to the Mo content, underscore the necessity of optimizing the chemical composition to ensure the optimal performance of these alloys in critical applications, such as biomedical implants, where corrosion resistance and structural integrity are essential. During exposure to simulated body fluid, Mo is oxidized to Mo^{+4} (MoO_2) and Mo^{+6} (MoO_3 and MoO_4^{2-}), following the reactions:

Table 1
Equivalent electric circuit parameters for fitting the experimental EIS data.

Parameters	Sample 1	Sample 2
Y_1 (Ohm·cm^2)	$3.93\cdot10^{-5}$	$1.20\cdot10^{-4}$
n_1	0.97	0.48
R_1 (Ohm·cm^2)	$1.41\cdot10^{3}$	19.48
Y_2 (S·sec^n/cm^2)	$1.03\cdot10^{-4}$	$2.28\cdot10^{-5}$
n_2	0.68	0.88
R_2 (Ohm·cm^2)	$1.03\cdot10^{4}$	$8.60\cdot10^{5}$
χ^2	$7.14\cdot10^{-3}$	$8.56\cdot10^{-4}$

$$Mo + 2H_2O \rightarrow MoO_2 + 4H^+ + 4e^- \quad (2)$$

The compound of hexavalent molybdenum is very important; is illustrated by molybdenum trioxide and by its ionic form:

$$MoO_2 + H_2O \rightarrow MoO_3 + 2H^+ + 2e^- \quad (3)$$

$$MoO_2 + 2H_2O \rightarrow MoO_4^{2-} + 4H^+ + 2e^- \quad (4)$$

The same phenomenom occurs with Ta:

$$2Ta + 5H_2O \rightarrow Ta_2O_5 + 10H^+ + 10e^- \quad (5)$$

4. Conclusions

This study examined the corrosion behavior and microstructural characteristics of two recently developed titanium alloys containing biocompatible elements (Mo, Zr, and Ta). The alloy with a higher Mo content displays enhanced corrosion resistance due to a more robust passive layer. The microhardness values of both alloys are consistent with those of commonly used Ti biomaterials, indicating uniformity and good mechanical performance. These findings substantiate the potential of these novel, presumably non-toxic titanium alloys as promising candidates for biomedical applications.

Future research should concentrate on an extensive investigation of higher Mo content, integrating alloy manufacturing, improved characterization, mechanical and electrochemical evaluations, and biocompatibility analyses. By progressively increasing Mo content and refining the alloy composition, one may methodically assess the tradeoffs and advantages, hence facilitating the advancement of superior titanium alloys for clinical applications.

CRediT authorship contribution statement

Cristina Jiménez-Marcos: Writing – original draft, Investigation, Formal analysis. **Julia Claudia Mirza-Rosca:** Writing – review & editing, Validation, Supervision. **Madalina Simona Baltatu:** Resources, Methodology, Conceptualization. **Petrica Vizureanu:** Writing – review & editing, Supervision, Resources.

Declaration of competing interest

The authors declare that they have no known competing financial interests or personal relationships that could have appeared to influence the work reported in this paper.

Acknowledgements

We hereby acknowledge the European project 2023-1-RO01-KA220-HED-000159985: Smart Healthcare Engineering and the project Cabildo22-01.

Data availability

Data will be made available on request.

References

[1] Y. Zhang, K. Chu, S. He, B. Wang, W. Zhu, F. Ren, Fabrication of high strength, antibacterial and biocompatible Ti-5Mo-5Ag alloy for medical and surgical implant applications, Mater. Sci. Eng. C. 106 (2020) 110165, https://doi.org/10.1016/J.MSEC.2019.110165.

[2] W. Abd-Elaziem, M.A. Darwish, A. Hamada, W.M. Daoush, Titanium-Based alloys and composites for orthopedic implants Applications: a comprehensive review, Mater. Des. 241 (2024) 112850, https://doi.org/10.1016/j.matdes.2024.112850.

[3] B. Wu, Y. Tang, K. Wang, X. Zhou, L. Xiang, Nanostructured titanium implant surface facilitating osseointegration from protein adsorption to osteogenesis: the example of TiO2 NTAs, Int. J. Nanomed. 17 (2022) 1865–1879, https://doi.org/10.2147/IJN.S362720.

[4] M. Najafizadeh, S. Yazdi, M. Bozorg, M. Ghasempour-Mouziraji, M. Hosseinzadeh, M. Zarrabian, P. Cavaliere, Classification and applications of titanium and its alloys: a review, J. Alloy. Compd. Commun. 3 (2024) 100019, https://doi.org/10.1016/j.jacomc.2024.100019.

[5] G. Senopati, R.A. Rahman Rashid, I. Kartika, S. Palanisamy, Recent development of low-cost β-Ti alloys for biomedical applications: a review, Metals 13 (2023), https://doi.org/10.3390/met13020194.

[6] J. Dias Corpa Tardelli, C. Bolfarini, A. Cândido dos Reis, Comparative analysis of corrosion resistance between beta titanium and Ti-6Al-4V alloys: a systematic review, J. Trace Elem. Med. Biol. 62 (2020) 126618, https://doi.org/10.1016/j.jtemb.2020.126618.

[7] M.V. Popa, D. Raducanu, E. Vasilescu, P. Drob, D. Cojocaru, C. Vasilescu, S. Ivanescu, J.C.M. Rosca, Mechanical and corrosion behaviour of a Ti-Al-Nb alloy after deformation at elevated temperatures, Mater. Corros. 59 (2008) 919–928, https://doi.org/10.1002/maco.200805003.

[8] Ş. Culfa, S.M. Toker, Interaction of Ti-6Al-7Nb alloy with simulated body fluid; a preliminary biocompatibility investigation, Front. Life Sci. Relat. Technol. 4 (2023) 111–117, https://doi.org/10.51753/flsrt.1294479.

[9] G. Genchi, A. Carocci, G. Lauria, M.S. Sinicropi, A. Catalano, Nickel: human health and environmental toxicology, Int. J. Environ. Res. Publ. Health 17 (2020) 679, https://doi.org/10.3390/ijerph17030679.

[10] A. Bordbar-Khiabani, M. Gasik, Electrochemical and biological characterization of Ti–Nb–Zr–Si alloy for orthopedic applications, Sci. Rep. 13 (2023) 2312, https://doi.org/10.1038/s41598-023-29553-5.

[11] R. McHendrie, N.H. Nguyen, M.T. Nguyen, K. Fallahnezhad, K. Vasilev, V. K. Truong, R. Hashemi, Development of novel antibacterial Ti-Nb-Ga alloys with low stiffness for medical implant applications, J. Funct. Biomater. 15 (2024) 167, https://doi.org/10.3390/jfb15060167.

[12] Q. Chen, G.A. Thouas, Metallic implant biomaterials, Mater. Sci. Eng. R Rep. 87 (2015) 1–57, https://doi.org/10.1016/j.mser.2014.10.001.

[13] A.H. Awad, M. Saood, H.A. Aly, A.W. Abdelghany, Role of Mo and Zr additions in enhancing the behavior of new Ti–Mo alloys for implant materials, Met. Mater. Int. (2024), https://doi.org/10.1007/s12540-024-01813-7.

[14] S. Bălțatu, P. Vizureanu, D. Mareci, L.C. Burtan, C. Chiruță, L.C. Trincă, Effect of Ta on the electrochemical behavior of new TiMoZrTa alloys in artificial physiological solution simulating in vitro inflammatory conditions, Mater. Corros. 67 (2016) 1314–1320, https://doi.org/10.1002/maco.201609041.

[15] C. Jimenez-Marcos, J.C. Mirza-Rosca, M.S. Baltatu, P. Vizureanu, Experimental research on new developed titanium alloys for biomedical applications, Bioengineering 9 (2022) 686, https://doi.org/10.3390/bioengineering9110686.

[16] E.-B. Lee, M.-K. Han, B.-J. Kim, H.-J. Song, Y.-J. Park, Effect of molybdenum on the microstructure, mechanical properties and corrosion behavior of Ti alloys, Int. J. Mater. Res. 105 (2014) 847–853, https://doi.org/10.3139/146.111092.

[17] K. Glowka, M. Zubko, P. Świec, K. Prusik, M. Szklarska, D. Chrobak, J.L. Lábár, D. Stróż, Influence of molybdenum on the microstructure, mechanical properties and corrosion resistance of Ti20Ta20Nb20(ZrHf)20−xMox (where: x = 0, 5, 10, 15, 20) high entropy alloys, Materials 15 (2022) 393, https://doi.org/10.3390/ma15010393.

[18] M.S. Baltatu, M.C. Spataru, L. Verestiuc, V. Balan, C. Solcan, A.V. Sandu, V. Geanta, I. Voiculescu, P. Vizureanu, Design, synthesis, and preliminary evaluation for Ti-Mo-Zr-Ta-Si alloys for potential implant applications, Materials 14 (2021) 6806, https://doi.org/10.3390/MA14226806.

[19] W. Weng, A. Biesiekierski, J. Lin, Y. Li, C. Wen, Impact of rare earth elements on nanohardness and nanowear properties of beta-type Ti-24Nb-38Zr-2Mo alloy for medical applications, Materialia 12 (2020) 100772, https://doi.org/10.1016/j.mtla.2020.100772.

[20] W. Bai, G. Xu, M. Tan, Z. Yang, L. Zeng, D. Wu, L. Liu, L. Zhang, Diffusivities and atomic mobilities in bcc Ti-Mo-Zr alloys, Materials 11 (2018) 1909, https://doi.org/10.3390/ma11101909.

[21] P.A. Lopes, A.F.P. Carreiro, R.M. Nascimento, B.R. Vahey, B. Henriques, J.C. M. Souza, Physicochemical and Microscopic Characterization of Implant – Abutment Joints, 2019, pp. 100–104, https://doi.org/10.4103/ejd.ejd.

[22] J. Zhang, C. Wang, N. Shareef, Microstructure and properties of Ti-Zr-Mo alloys fabricated by laser directed energy deposition, Materials 16 (2023) 1054, https://doi.org/10.3390/ma16031054.

[23] Y.-W. Cui, L.-Y. Chen, P. Qin, R. Li, Q. Zang, J. Peng, L. Zhang, S. Lu, L. Wang, L.-C. Zhang, Metastable pitting corrosion behavior of laser powder bed fusion produced Ti-6Al-4V in Hank's solution, Corros. Sci. 203 (2022) 110333, https://doi.org/10.1016/j.corsci.2022.110333.

[24] H. Liu, Z.-X. Wang, J. Cheng, N. Li, S.-X. Liang, L. Zhang, F. Shang, D. Oleksandr, L.-Y. Chen, Nb-content-dependent passivation behavior of Ti–Nb alloys for biomedical applications, J. Mater. Res. Technol. 27 (2023) 7882–7894, https://doi.org/10.1016/j.jmrt.2023.11.203.

[25] B.A. Boukamp, A Nonlinear Least Squares Fit procedure for analysis of immittance data of electrochemical systems, Solid State Ionics 20 (1986) 31–44, https://doi.org/10.1016/0167-2738(86)90031-7.

Artículo 5. Preliminary studies of new heat-treated titanium alloys for use in medical equipment

Results in Engineering 25 (2025) 104477

Contents lists available at ScienceDirect

Results in Engineering

journal homepage: www.sciencedirect.com/journal/results-in-engineering

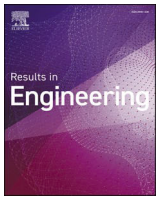

Research paper

Preliminary studies of new heat-treated titanium alloys for use in medical equipment

Cristina Jiménez-Marcos [a], Julia Claudia Mirza-Rosca [a,*], Madalina Simona Baltatu [b], Petrica Vizureanu [b]

[a] Mechanical Engineering Department, Las Palmas de Gran Canaria University, 35017, Tafira, Spain
[b] Department of Technologies and Equipments for Materials Processing, Faculty of Materials Science and Engineering, Gheorghe Asachi Technical University of Iasi, Blvd. Mangeron, No. 51, 700050 Iasi, Romania

ARTICLE INFO

Keywords:
Titanium alloys
Microhardness
Corrosion
Microstructure

ABSTRACT

Titanium alloys are essential in the biomedical field due to their exceptional corrosion resistance, mechanical strength and biocompatibility, making them ideal for producing safe medical implants and devices. Novel heat treatment techniques have been developed to optimize the microstructure, mechanical, corrosion and surface characteristics of alloys in biological environments, thereby reducing internal stresses and improving passive layer formation, thus prolonging implant service life. The analyzed samples were stress relieved titanium-molybdenum alloys (Ti-15Mo) with Si additions of 0%, 0.5%, 0.75% and 1.0%. Microstructure, microhardness and corrosion behavior were studied to evaluate the potential of these alloys for use in the human body, with a particular focus on medical devices where durability, hardness and corrosion resistance are critical factors. The addition of molybdenum as a β-phase stabilizer enhanced the formation of the advantageous lamellar microstructure of α + β phases for mechanical performance. The corrosion behavior was examined in simulated body fluid (Ringer's solution) and the higher silicon content contributed to the formation of a thicker and protective passive layer, which substantially reduced the corrosion rate. The microhardness of silicon-enriched alloys under various stress conditions was higher than that of commercially pure titanium (CpTi), demonstrating their capability for better performance in biomedical applications.

1. Introduction

The materials used for load-bearing dental and orthopedic applications must demonstrate not only excellent biocompatibility but also good mechanical properties (fatigue, tensile, compressive, elastic modulus, etc.) in conjunction with adequate ductility, hardness, and fracture toughness. Consequently, metallic implant biomaterials are more advantageous and appropriate for these applications compared to conventional ceramic and polymeric biomaterials [1]. In orthopedic and vascular surgery, classical alloys, such as Ti6Al4V, CoCrMo alloys and NiTi alloys, account for approximately 95% of orthopedic devices and 80% of implants [2].

However, special problems arise when metallic implants are used. First, the elastic modulus of metals is significantly higher than that of bone; this can lead to osteoporosis. In addition, many metallic biomaterials have some limitations in terms of biocompatibility, wear resistance, and corrosion resistance, and they release toxic ions into nearby tissues. In an attempt to solve these problems, various alloying elements that are not harmful to the body have been investigated [3,4].

Titanium and its alloys have become biomaterials that can be used for a wide range of purposes, from modern medicine to aerospace. Due to its biocompatibility [5], corrosion resistance [6], thermal stability [7], low modulus of elasticity [8], excellent fatigue resistance [9], high strength and low weight contribute to efficiency and performance in their use for biomedical applications. Titanium's exceptional corrosion resistance is attributed to its ability to build a stable oxide layer, primarily made up of titanium oxide (TiO_2) [10,11].

Nonetheless, commercial titanium alloys have distinct drawbacks when used in medical settings. The Ti-6Al-4V alloy, used to manufacture orthopedic and dental implants, may induce allergies and illnesses such as Parkinson's or Alzheimer's due to its aluminum and vanadium content [12,13]. Because it can revert to its natural form, TiNi (nitinol), which is perfect for vascular stents and guides in minimally invasive surgery, can release nickel, which can lead to both allergies as well as

* Corresponding author.
E-mail address: julia.mirza@ulpgc.es (J.C. Mirza-Rosca).

https://doi.org/10.1016/j.rineng.2025.104477
Received 20 December 2024; Received in revised form 21 February 2025; Accepted 23 February 2025
Available online 24 February 2025

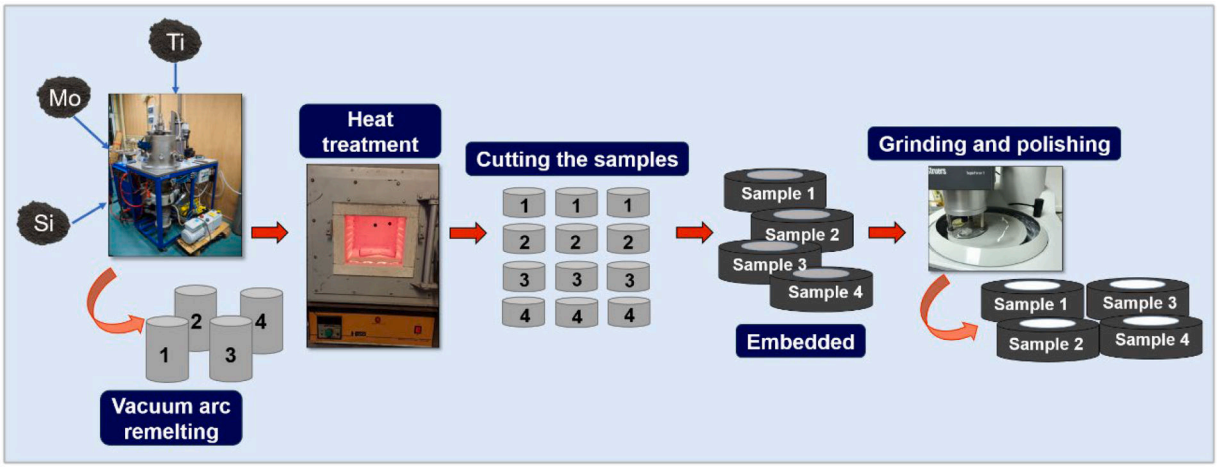

Fig. 1. Studied alloys preparation.

kidney and cardiovascular problems [14,15]. Ti-6Al-7Nb alloy, which is utilized in prostheses and medical equipment, was designed to increase biocompatibility by replacing V with Nb; nonetheless, it has a solid protective layer and presents improved mechanical properties [16,17].

The addition of highly biocompatible alloying elements such as molybdenum, helps improve the properties of titanium. Molybdenum is a low-toxicity, beta-stabilizing element that when combined with titanium, it produces a stable oxide film, shielding it from corrosion and deterioration in harsh settings [18]. Because of the high melting temperatures of the components that form the titanium-molybdenum system, the method used to obtain these alloys was vacuum arc remelting. The advantages of using this type of equipment are, in addition to the manufacture of metallic alloys with variable geometry and containing elements with very high melting temperatures, the obtaining of almost pure metallurgical environments by successive argon purging, a good homogeneity of the alloys by melting several times on each side of the ingots and the possibility of obtaining rapid water cooling [19].

In order to improve the properties, other different elements were added to Ti-Mo alloys like Zr [20–22], Nb [23], Fe [24], Cr [25], Cu [26], Au [27], Al [28], V [29], etc. The human body contains silicon, which can enhance biocompatibility and assist in controlling a material's mechanical characteristics [30,31]. Silicon (Si) can be present as a solid solution and/or silicide and even the Si content is typically restricted to below 0.5 wt%, however vacuum metallurgy demonstrates the capability to produce titanium alloys with elevated Si levels. The incorporation of silicon enhances the creep resistance, strength and oxidation resistance of titanium alloys; nevertheless, it diminishes fluidity, particularly at ambient temperature [32,33].

Heat treatment is used to minimize the residual tensions that are created during the fabrication process of titanium and titanium alloys. This process is known as stress relieving and through the use of this technique, residual stresses that are caused by the various stages of manufacturing are reduced, which helps to maintain shape stability and eliminates unfavorable situations such as the Bauschinger effect.

In this study, we focused on the effect of silicon addition on the microstructure and corrosion resistance of stress-relieved titanium alloys. The analyzed samples were titanium-molybdenum alloys with Si additions of 0%, 0.5%, 0.75% and 1.0%. The corrosion behavior was investigated to assess their performance in simulated body fluid. In addition to corrosion testing, this study aims to investigate the microstructure and microhardness behavior of these alloys. This research aims to assess the potential of these materials for use in the human body, with a particular focus on medical devices where durability, hardness and corrosion resistance are critical factors.

2. Materials and methods

2.1. Material preparation

The following alloys were produced in a vacuum arc remelting (VAR) furnace from pure alloying elements (Ti, Mo and Si): Sample 1 (85% Ti, 15% Mo), Sample 2 (84.5% Ti, 15% Mo, 0.5% Si), Sample 3 (84.25% Ti, 15% Mo, 0.75% Si), and Sample 4 (84% Ti, 15% Mo, 1% Si). In order to achieve the required homogeneity, the four alloys were subjected to a total of six remelting operations, with three repetitions on each side, under the protection of high-purity argon gas. The samples were heat treated for stress relieving at 900 °C with a heating rate of 10 °C per minute and then quenching in water.

A series of preliminary operations were conducted on the samples, including cutting with a precision saw and embedding them in epoxy resin with a catalyst mixture, followed by demolding after 24 hours. Afterward, the specimens were ground and polished at 150 rpm and 15 N of force utilizing the polishing equipment. Carbide abrasive sheets of increasing grit were used, starting with P400 grit and ending with P2500 grit [34]. Then, mirror polishing cloths containing a 0.06 μm colloidal silica polishing suspension were used (see Fig. 1). These metallographic analysis sample preparation techniques complied with ASTM E3–11 (2017) [35].

2.2. Microstructural characterization

The microstructure of the samples was examined by taking micrographs of the surfaces of each sample using an optical microscope (AxioVert.A1 MAT ZEISS) at various magnifications. For approximately 40 ss, each sample was immersed in Kroll's reagent solution, which consists of 100 ml of water, 1–3 ml of hydrofluoric acid and 2–6 ml of nitric acid. The surface that had been exposed to the reagent was then analyzed and the test was repeated three times for each sample.

An energy-dispersive X-ray spectrometer (EDX) coupled with an Apreo Field Emission scanning electron microscope was utilized for elemental analysis.

A Malvern-Panalytical diffractometer was employed for phase analysis of the samples. A CuK radiation (1.5406 Å) in the range of $2\theta = 30–70$ was used for the investigation, with a power of 45 kV, a step size of 0.02° and a current of 40 mA.

2.3. Microhardness test

In accordance with ISO 14,577–1:2015 [36], ten measurements were taken with the hardness tester Future Tech FM-810, each lasting 15 ss, for each load applied to the specimen—in this case, 5, 25 and 50 gf. As

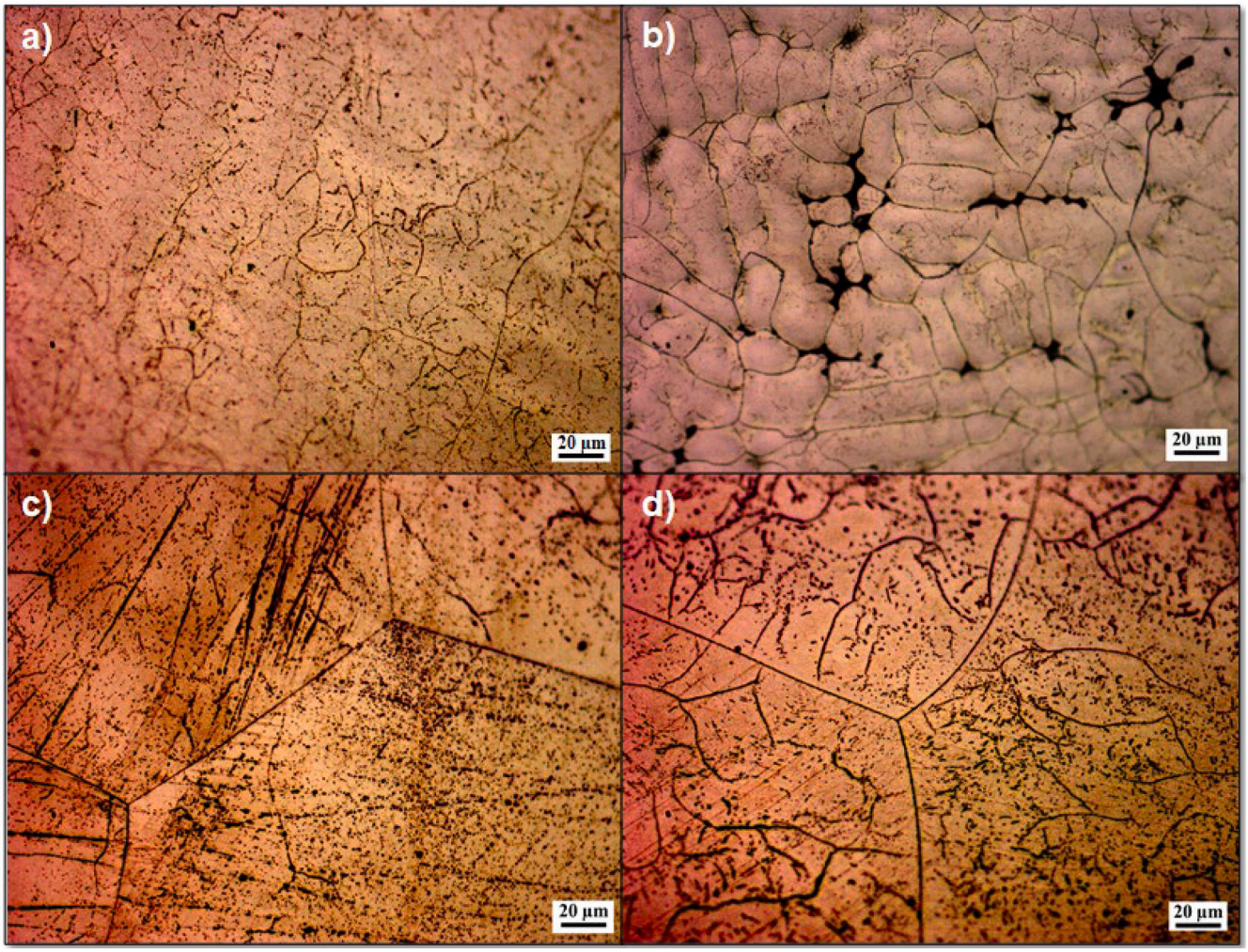

Fig. 2. Optical microstructure of: a) Sample 1, b) Sample 2, c) Sample 3 and d) Sample 4, after reagent etching.

the load increases, the impression left by the indenter can cover parts of different phases, thereby providing an approximate measure of the overall hardness of the material. The footprint can only be identified in one phase when relatively low loads are positioned, allowing the hardness of that phase to be evaluated. Subsequently, the corresponding software used the recorded diagonal lengths to automatically calculate the Vickers microhardness values. The number of indentations produced was plotted against the scan length.

2.4. Electrochemical tests

The electrochemical tests employ a three electrodes cell containing the working electrode (the material being tested), the reference electrode (saturated calomel) and the counter electrode (platinum electrode), according to ISO 10,271:2020 [37]. To conduct the tests, the area of each sample under investigation was measured. The following components were measured in mmol/L in the Ringer Grifols solution: Na^+ 129.90, Cl^- 111.70, K^+ 5.40, Ca^{2+} 1.80; and $C_3H_5O_3$ 27.20. Using the potentiostat-galvanostat SP-150 BioLOGIC, three tests were employed in the following order to study the corrosion behavior of the alloys: corrosion potential, linear polarization and electrochemical impedance spectroscopy.

2.4.1. Corrosion potential (E_{corr})

The "E_{corr} vs. Time" technique of the EC-Lab software was used to evaluate the corrosion potential of each sample after 24 hours of immersion in Ringer solution. Potential measurements were made every 300 ss or whenever the potential changed by 200 mV, conditions that, according to our previous experience [38], are sufficient to stabilize the corrosion potential as much as possible.

2.4.2. Linear polarization

To conduct these tests, the "Linear Polarization" technique was chosen, and its feasibility was confirmed by entering the sample surface area value, the 20-minute test duration and performing it three times for each sample. The used parameters were apreliminary scan rate of 0.167 mV/s, potential ranging from -1.0 to 2.0 V with respect to the reference electrode and data collected at 0.50 s intervals. Following the display of these linear polarization curves, the corrosion rate (V_{corr}) was calculated for each sample using the "Tafel Fit" approach.

2.4.3. Electrochemical impedance spectroscopy (EIS)

To characterize the oxide layer by EIS, impedance spectra were registered in the range of ±300 mV vs. E_{corr} with a step of 100 mV by continuously polarizing the sample and allowing the system to equilibrate for 600 s at each potential following ISO 16,773–1–4:2016 [39]. All the tests were normally repeated three or four times to ensure that they presented reasonable reproducibility. The data were displayed using Nyquist and Bode diagrams and an equivalent circuit (EC) was employed to fit the experimental data.

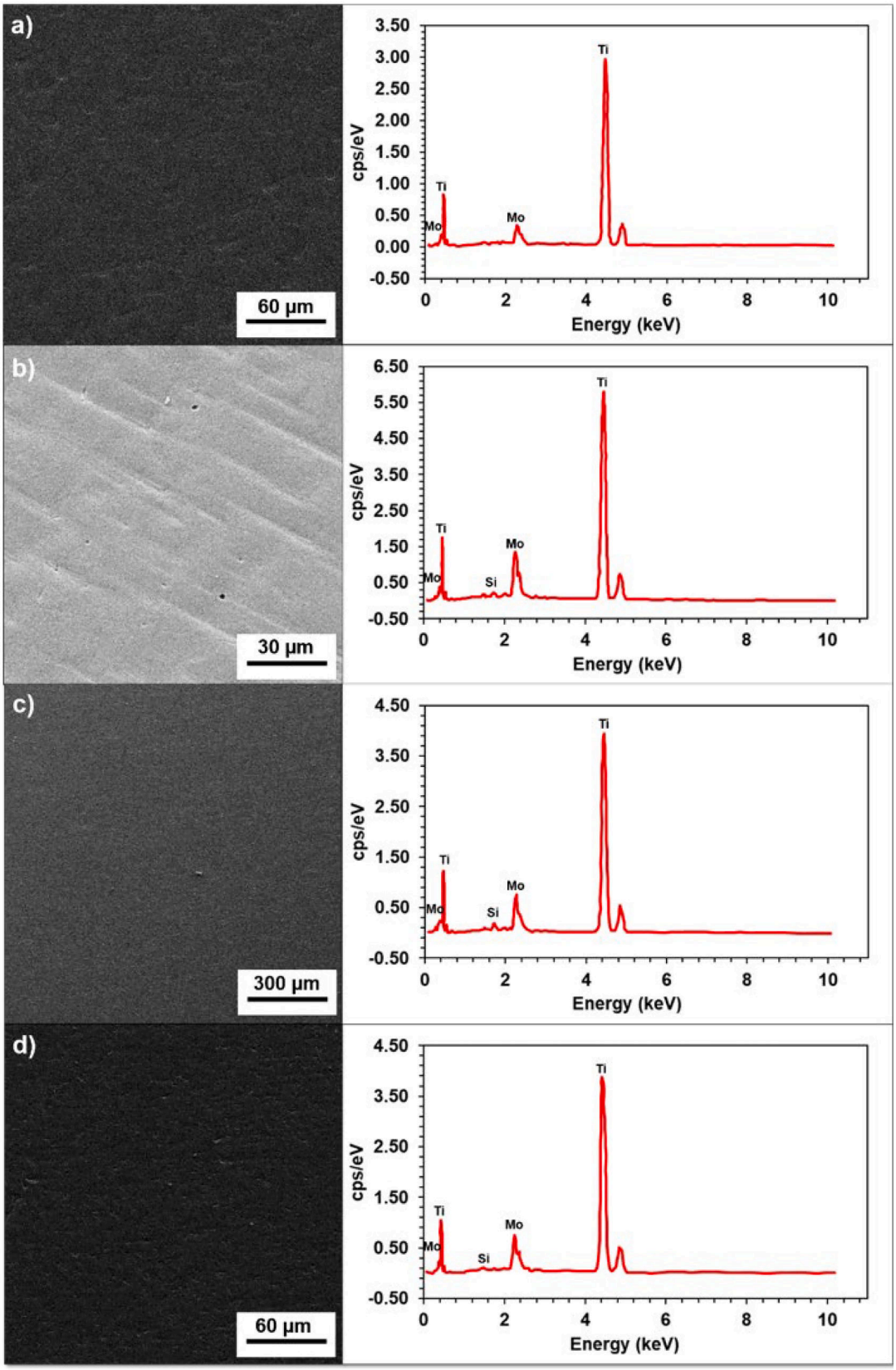

Fig. 3. SEM image and EDX spectra for: a) Sample 1, b) Sample 2, c) Sample 3 and d) Sample 4.

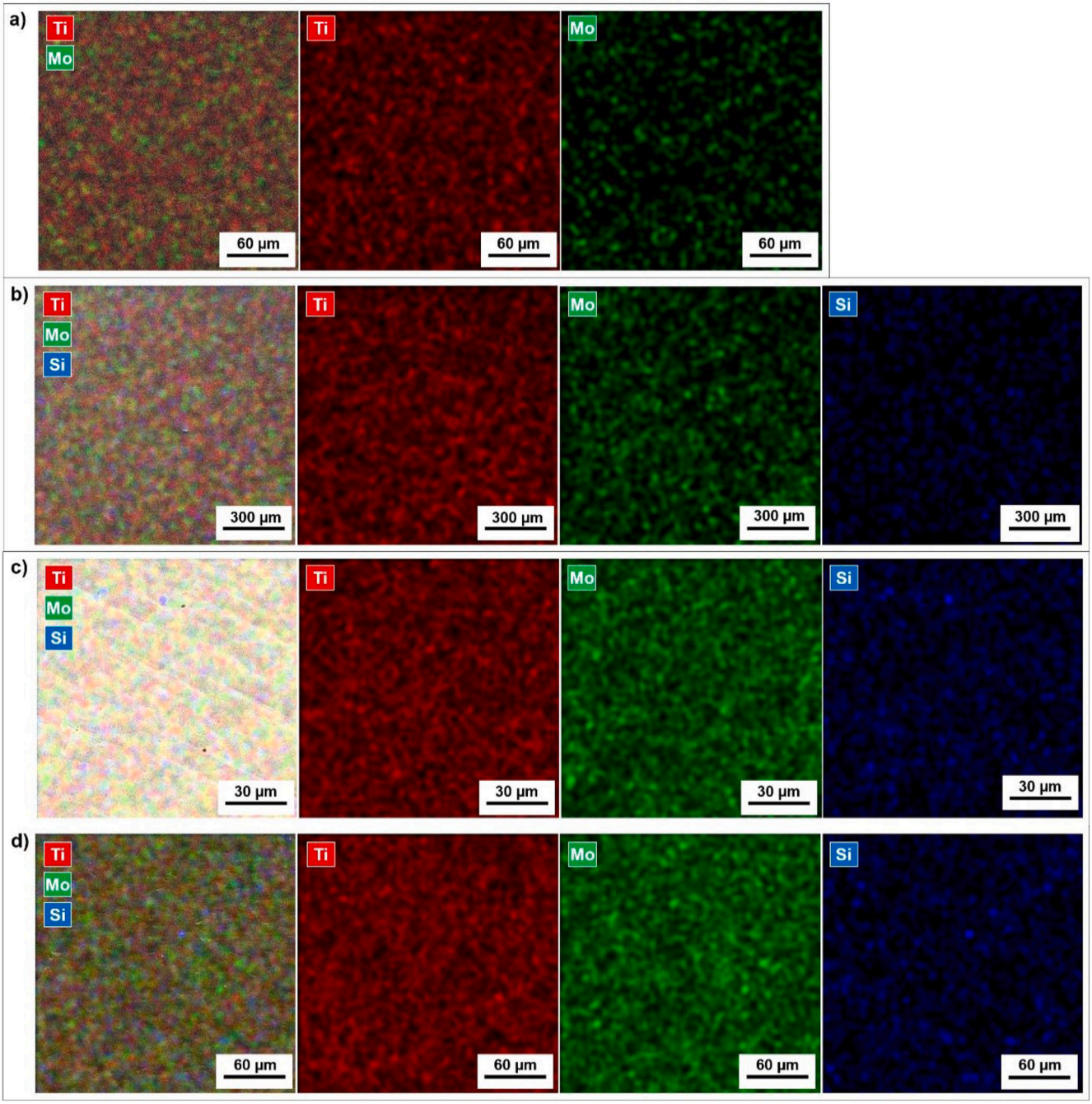

Fig. 4. EDX elemental maps of: a) Sample 1, b) Sample 2, c) Sample 3 and d) Sample 4.

3. Results and discussions

3.1. Microstructural investigation

Due to the similarity of their lattice characteristics and crystal structures, Mo and Ti can completely dissolve in one another, resulting in optimal undercooling. This facilitates the formation of the β metastable phase at elevated temperatures [40]. The β-phase (BCC structure) is achieved by including the transition components Mo and Si.

Silicon can reduce the phase transition temperature because it is an eutectoid β-stable element and typically exists as a solid solution or silicide in titanium-based alloys. The various morphological forms of silicon can be interconverted under specific conditions, which enables the variation of titanium alloy properties by silicide [32]. The silicide in this case is an intermetallic compound formed between silicon and titanium.

The optical microscope images of the four samples, as presented in Fig. 2, illustrate the microstructural changes occurring with varying silicon concentrations. At lower silicon concentrations, it can be observed that the precipitation of silicide begins near the grain boundaries of the β-phase (see Fig. 2a). As silicon concentrations increase, silicide precipitation is seen to begin within the crystal structure itself (refer to Figs. 2a and 2b). These observations align with established patterns reported in the literature [41,42], where similar behavior has been noted under comparable conditions.

Figs. 3 and 4 display SEM pictures, EDX spectra and EDX elemental maps for the examined area of each sample. In the presented SEM images (Fig. 3), different magnifications were employed not to emphasize

Table 1
EDX quantification of the samples analyzed.

Samples	Composition (in wt%)		
	Ti	Mo	Si
Sample 1	84.44 ± 2.35	15.56 ± 1.56	–
Sample 2	83.79 ± 1.80	15.93 ± 1.23	0.28 ± 0.08
Sample 3	83.84 ± 2.02	15.30 ± 0.98	0.86 ± 0.16
Sample 4	83.79 ± 2.11	15.19 ± 1.61	1.02 ± 0.34

microstructural clarity but to optimize the surface details necessary for detailed elemental analysis by EDX. These magnifications were selected based on the need to effectively capture compositional variations that could not be adequately represented at a single scale.

The quality of the SEM images, as presented in our study, differs from that of the optical microscope images (see Fig. 2) due to the specific objectives of each imaging technique. Unlike optical imaging, which focuses on microstructural clarity, the SEM images were specifically optimized for the comprehensive elemental analysis essential for our research. This optimization was targeted at enhancing the accuracy of EDX data rather than visual detail, which is critical to the goals of our study.

The EDX quantification provides a summary of the mean chemical compositions of the alloys researched (see Table 1), which demonstrates a close agreement with the theoretical concentrations of the chemical elements, with only slight differences due to local inhomogeneities or measurement uncertainty. The presence of SiO_2 has been identified by EDX, a method that is essential not only for the detection SiO_2 but also for confirming the integration of silicon in the passive films, which correlates with the varying silicon content in the different samples: Sample 1 without Si, Sample 2 with 0.5% Si, Sample 3 with 0.75% Si and Sample 4 with 1% Si.

The silicon content in these alloys plays an important role in enhancing the formation and stability of SiO_2 within the passive films. As the percentage of silicon increases from 0.5% to 1%, we observed an improvement in the compactness and stability of the film, which can be directly attributed to a higher concentration of SiO_2. This enhancement is supported by the literature [43,44] indicating that SiO_2 effectively improves the corrosion resistance and mechanical properties of protective films.

The generated atomic distribution maps (see Fig. 4) provide clear evidence of the absence of elemental segregation or the connection of impurities within the alloy matrix. By confirming the lack of inclusions and segregations, we can infer that the alloy processing methods used were effective in achieving a homogeneous material structure. This homogeneity indicates higher material integrity and predictability of clinical performance.

The diffraction diagrams of the alloys being studied are shown in Fig. 5. Only two phases—major β and minor Ti_5Si_3—were discernible in this instance. It is evident that all alloys present significant peaks that correlate with the titanium β phase. Silicon and molybdenum, two alloying elements added to titanium, are β-stabilizers, meaning they prevent other phases from precipitating [45]. Our X-ray diffractograms support the equivalent molybdenum hypothesis, according to which, at room temperature, the predominance of the β-phase requires the use of at least 10 wt% molybdenum [46].

3.2. Microhardness test

Fig. 6 and Table 2 show the microhardness results at HV 0.005, HV 0.025, and HV 0.05, together with the mean, median, standard deviation (SD), minimum, maximum and depth values for each of the ten indentations performed on each sample. As can be seen, there is little variation in the data and a mean of about 350 HV for the values applied in Samples 1, 3 and 4. Sample 3 displayed the highest values for the applied loads of 5 and 25 gf; however, Sample 4 displayed a higher value when the load of 50 gf was applied. On the other hand, Sample 3 provided the lowest hardness value for the 5 gf load, while Sample 1 provided the minimum values for the other two charges. However, it is difficult to determine whether the proportion of silicon increases or decreases, as the data shows that the surfaces of both samples are somewhat uniform. Sample 2, on the other hand, showed Vickers hardness values with a considerable variance, ranging from 290 to 530 HV and a standard deviation of 55 to 77, suggesting the existence of hard

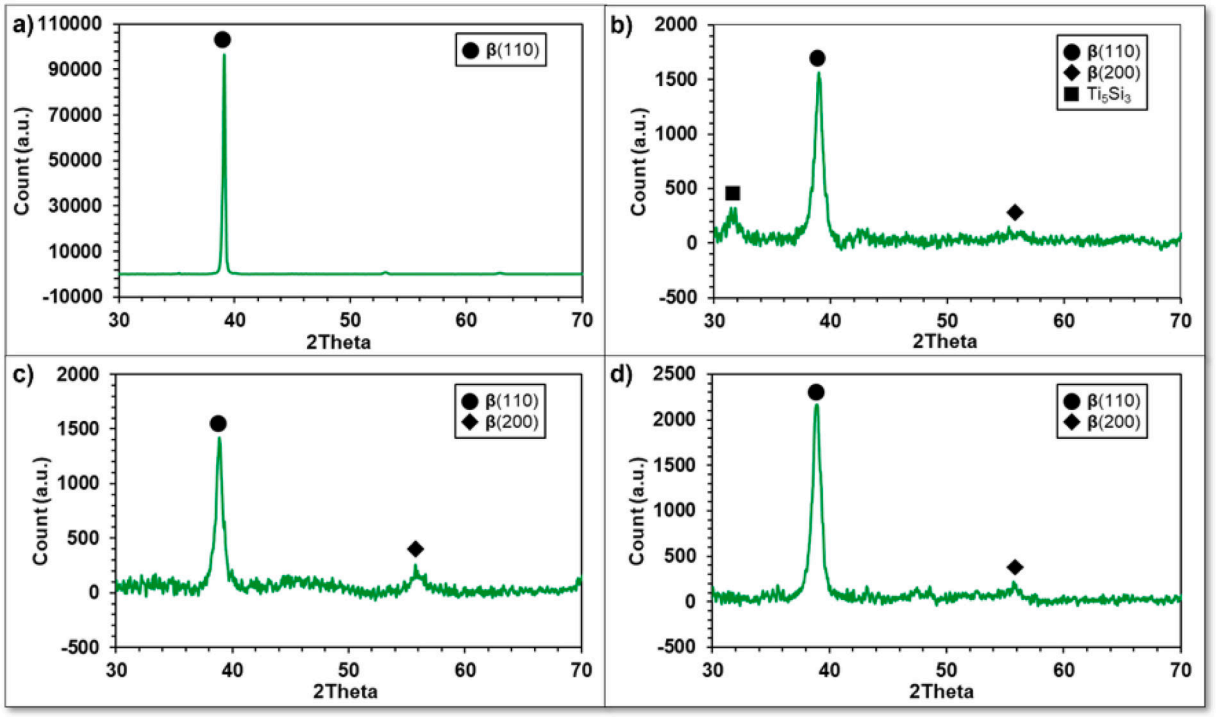

Fig. 5. X-ray diffraction (XRD) pattern of the studied alloys: a) Sample 1, b) Sample 2, c) Sample 3 and d) Sample 4.

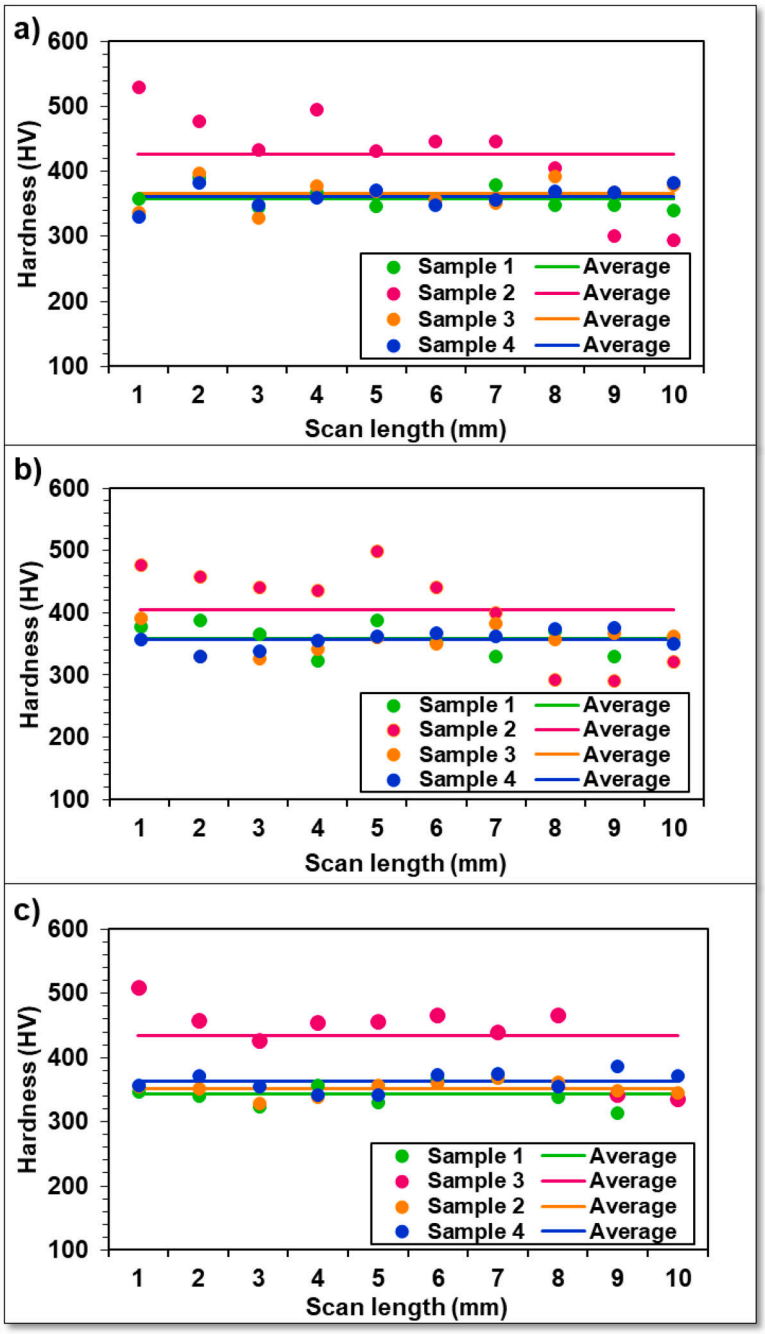

Fig. 6. Microhardness results for each indentation for the test specimens under loadings of 5 (a), 25 (b) and 50 (c) gf.

and soft zones (different phases) on its surface.

Additionally, the maximum hardness values found in this study were higher than those of cp-Ti (180 - 300 HV) [47,48] but lower than those of Ti6Al4V (330 - 540 HV) [49,50].

The SD of all specimens tends to decrease at higher loads since the higher the load, the greater the penetration into the material. This fact can be demonstrated by calculating the thickness of the footprint.

The following formula is used to calculate the depth of the indentation, where F is the applied force in kgf and HV is Vickers hardness in kgf/mm^2.

$$\delta = 0.202 \cdot \sqrt{\frac{1.8544 \cdot F}{HV}} \quad (1)$$

Because the hardness levels of the materials were equal, when a higher load was applied, the average depth of the footprint rose from 0.9 μm to 3.3 μm.

As established by the Hall-Petch relationship, the microhardness of materials can be improved by grain refinement [51]. The grain sizes of Sample 2 are significantly refined compared to those of the other samples, thereby increasing the microhardness. The precipitation of silicide at the boundary of the crystal generates a big difference between the maximum and minimum values of the microhardness, depending on the phase. For samples 2 and 3, due to their homogeneity and the uniform silicides inside the crystals, the microhardness values are kept at roughly the same levels.

3.3. Electrochemical tests

3.3.1. Corrosion potential

The corrosion potential versus time curves of the studied samples

Table 2
Microhardness values and depth of the four samples for 5, 25 and 50 gf.

Essay		Microhardness (HV)					Depth (μm)
		Mean	Median	SD	Maximum	Minimum	
Sample 1	5 gf	358	353	16	390	340	1.03
	25 gf	358	363	24	388	323	2.30
	50 gf	343	342	18	368	314	3.32
Sample 2	5 gf	426	440	76	530	294	0.94
	25 gf	405	438	77	498	290	2.16
	50 gf	435	455	55	509	335	2.95
Sample 3	5 gf	366	368	23	397	328	1.02
	25 gf	357	359	21	392	326	2.30
	50 gf	351	354	12	368	328	3.28
Sample 4	5 gf	361	363	16	382	330	1.02
	25 gf	357	360	15	376	330	2.30
	50 gf	363	364	15	386	341	3.23

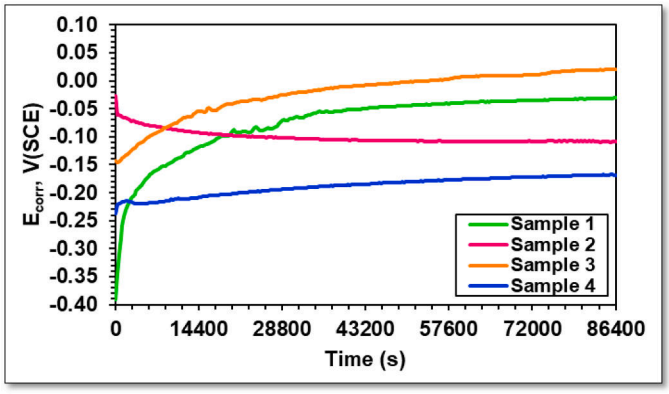

Fig. 7. Corrosion potential curves for the four samples after 24 hours' immersion time.

Table 3
Results of the corrosion potential for the investigated samples submerged in Ringer Grifols electrolyte at the beginning, 2 hours later, 12 hours later, and 24 hours later.

Potential (V)	Sample 1	Sample 2	Sample 3	Sample 4
Initial	-0.345	-0.062	-0.147	-0.221
After 2 hours	-0.159	-0.082	-0.093	-0.217
After 12 hours	-0.050	-0.106	-0.007	-0.185
After 1 day	-0.031	-0.108	0.021	-0.168

were analyzed after a 24-hour testing period during which the samples were immersed in Ringer's solution (see Fig. 7 and Table 3). Under these circumstances, the potential—known as the open circuit potential, or OCP—indicates the sample's propensity to resist corrosion.

Thus, immersing the alloys in Ringer's solution for 24 hours showed that the four samples had a high qualitative tendency to passivate.

Table 3 shows that the initial potential values of the samples tend to increase with the addition of silicon. From the data collected during the first two hours of immersion, Sample 1, Sample 3 and Sample 4 reached more positive values between -0.345 V and -0.093 V, while Sample 2 suffered a slight drop in the potential from -0.062 V to -0.082 V. Subsequently, after 12 hours, Sample 2 continues to reach more negative potential values to reach -0.106 V. Nevertheless, the potential of the rest

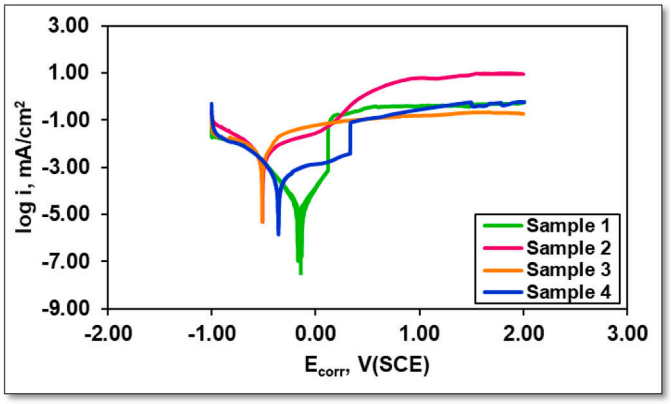

Fig. 8. Polarisation curves of the four test samples.

Table 4
Corrosion parameters obtained for all samples tested.

Parameters	Sample 1	Sample 2	Sample 3	Sample 4
E_{corr} (mV vs. Ref)	-260 ± 2	-138 ± 1	-239 ± 2	-69 ± 2
I_{corr} (μA/cm²)	$7.60 \cdot 10^{-4}$	$3.00 \cdot 10^{-1}$	$3.00 \cdot 10^{-3}$	$3.00 \cdot 10^{-3}$
β_c (mV/dec)	14.5 ± 1.3	14.9 ± 2.1	4.5 ± 1.7	4.1 ± 1.9
β_a (mV/dec)	35.3 ± 2.4	26.4 ± 2.7	32.3 ± 2.6	143.2 ± 3.5
Equivalent weight (g/eq)	23.94	23.52	23.66	23.38
Density (g/cm³)	5.36	5.34	5.35	5.34
Surface (cm²)	1.00	1.10	1.08	1.12
Corrosion rate (mpy)	$4.39 \cdot 10^{-3}$	$1.56 \cdot 10^{-1}$	$2.12 \cdot 10^{-3}$	$1.52 \cdot 10^{-3}$
R_p (MOhm·cm²)	2.84 ± 0.32	1.18 ± 0.06	1.22 ± 0.47	2.10 ± 0.24

of the samples in the study continues to increase. At the end of the test, positive behavior can be observed for all the samples, because they tend to achieve a certain stability. For the examined samples, the constant movement of the potential towards noble values suggested that the passive layer underwent modifications during the testing, becoming more protective. The Si content can influence the stability, thickness and composition of the passive oxide layer formed on the alloy surface.

3.3.2. *Linear polarization*

Fig. 8 and Table 4 illustrate the outcomes of the linear polarization technique employed to assess the corrosion rate of the alloys, presented on a semi-logarithmic scale of the actual results.

As can be observed in Table 4, Sample 4 exhibits higher anodic corrosion potential and current values (E_{corr} and I_{corr}, respectively), which indicate the extent of alloy oxidation, than the other samples examined.

To determine the Tafel slopes (β_c and β_a), the curve was examined against reference potential throughout a range of -1.0 to 2.0 V. A value of βa larger than βc indicates an alloy that is prone to passivation, whereas a value of β_a less than β_c indicates an alloy that is prone to corrosion. In this instance, the analysis revealed a propensity for all four samples to undergo passive layer formation on their surface [52].

Additionally, as illustrated in Table 4, the Tafel curve parameters and the corrosion rate (V_{corr}) of the tested samples are presented. These are determined using the corrosion current (I_{corr}), the density (d) in g/cm³, the area (A) of each sample (in cm²), the equivalent weight (EW) in g/eq and the constant (K) that determines the corrosion rate units (1.288·105 milinches/A-cm-year). The equivalent weight was calculated for each sample applying the following formula, which is from the standard ASTM G102–23 [53]:

$$EW = \frac{1}{\sum \frac{nifi}{Wi}} \quad (2)$$

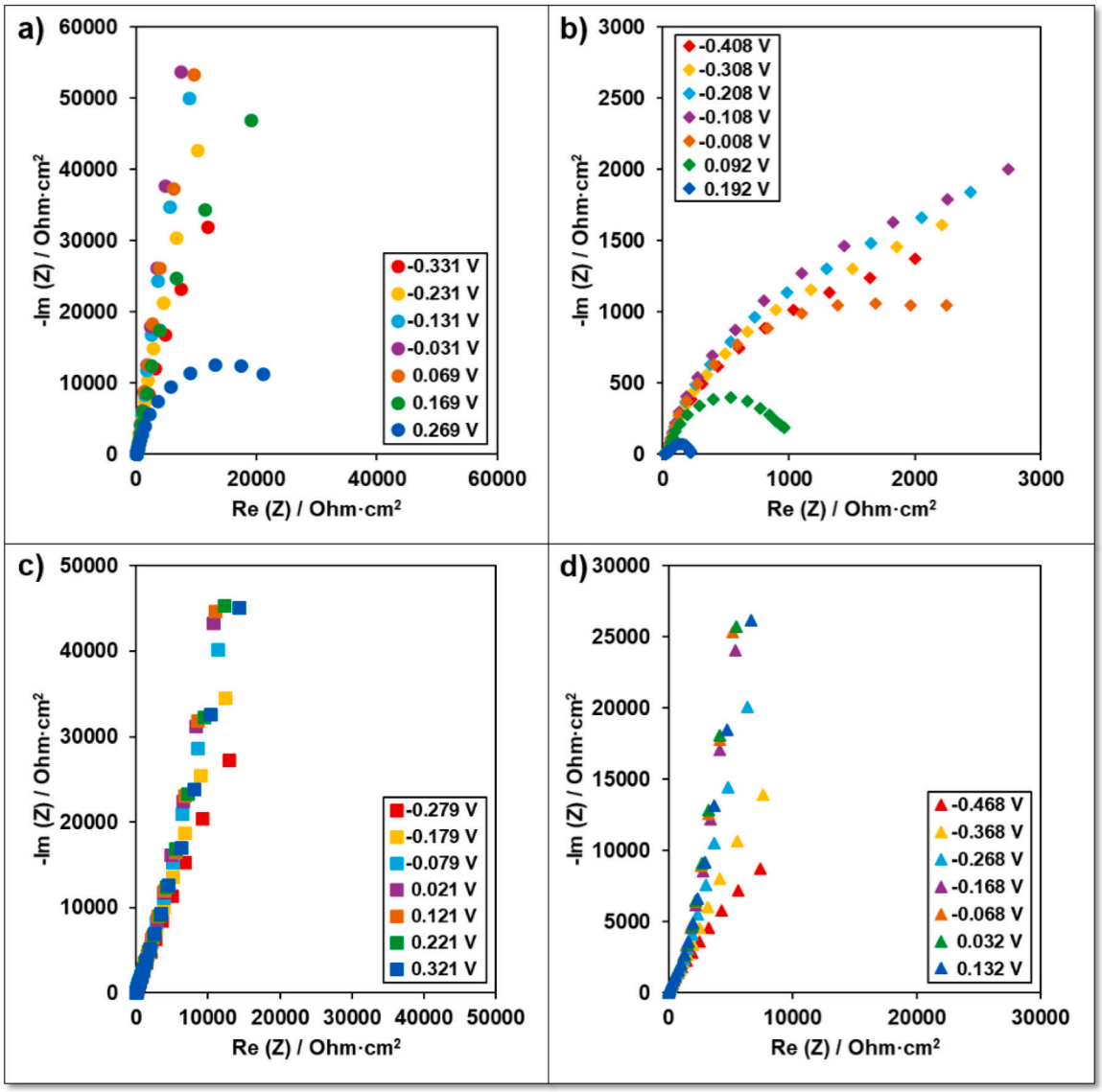

Fig. 9. Nyquist diagrams of: a) Sample 1, b) Sample 2, c) Sample 3 and d) Sample 4.

Where ***Wi*** is the atomic weight of the ith element in the alloy, ***ni*** is its valence, and ***fi*** is its mass fraction in the alloy.

In this case, a minimum V_{corr} of $1.52{\cdot}10^{-3}$ mpy was reached for Sample 4 and a maximum V_{corr} of $1.56{\cdot}10^{-1}$ mpy for Sample 2. Ti-6Al-4V and cp-Ti, under similar circumstances, showed a higher corrosion rate of about 10^{-2} mpy [50,54].

As the polarization resistance (R_p) value increases, the corrosion resistance of the alloy also improves, as shown by the results of the "R_p Fit" study. Sample 1, Sample 3 and Sample 4 exhibit an extremely high degree of corrosion resistance, with R_p values reaching as high as 10^6 $\Omega{\cdot}cm^2$ for highly corrosion-resistant materials. In this case, the R_p values achieved for these ssamples were higher than those obtained for cp-Ti (10^5 $\Omega{\cdot}cm^2$) [48], except for Sample 2, which has a R_p of 10^4 $\Omega{\cdot}cm^2$.

3.3.3. *Electrochemical impedance spectroscopy*

Figs. 9, 10 and 11 show the Nyquist and Bode impedance and Bode phase diagrams obtained for seven applied potentials (±0.3 V vs. reference electrode (E_{ref})) of each sample from high to low frequencies (200 KHz – 0.1 Hz).

Analyzing the Nyquist plot in Fig. 9, which shows the imaginary impedance versus the real impedance, Sample 1 and Sample 3 have similar impedance values for their E_{corr} (at 0.0 V vs. E_{corr}), slightly superior for Sample 1, which indicates a larger arc and is therefore more capacitive. There is also a tendency for the impedance values of Sample 3 and Sample 4 to increase at more positive potentials, while the impedance values of Sample 1 and Sample 2 exhibit a decrease in response to higher potentials (from 0.2 to 0.3 V vs E_{corr}).

In the Bode-IZI diagrams presented in Fig. 10, at high and medium frequencies, the impedance spectra exhibit similar curves. However, at a low frequency of 0.1 Hz, a flat surface impedance is observed, representing the sum of surface layer resistance, transfer resistance, and electrolyte resistance. This is associated with the inherent quality of the protective film.

In this instance, the impedance values obtained for Sample 3 and Sample 4 exhibited an increasing trend as more positive potentials were applied during the test, while Sample 1 and Sample 2 reached their maximum values at 0.0 V against E_{corr}. In this scenario, Sample 1 achieved the maximum impedance.

As demonstrated in Fig. 11 and Table 5, the Bode phase diagrams illustrate the phase transition as a function of frequency for varying potentials in comparison to the reference electrode. It is evident from the data that the maximum values of the phase angle occur when the corrosion potential is applied, with Sample 1 demonstrating higher values. Furthermore, the process occurs in two or three stages (time

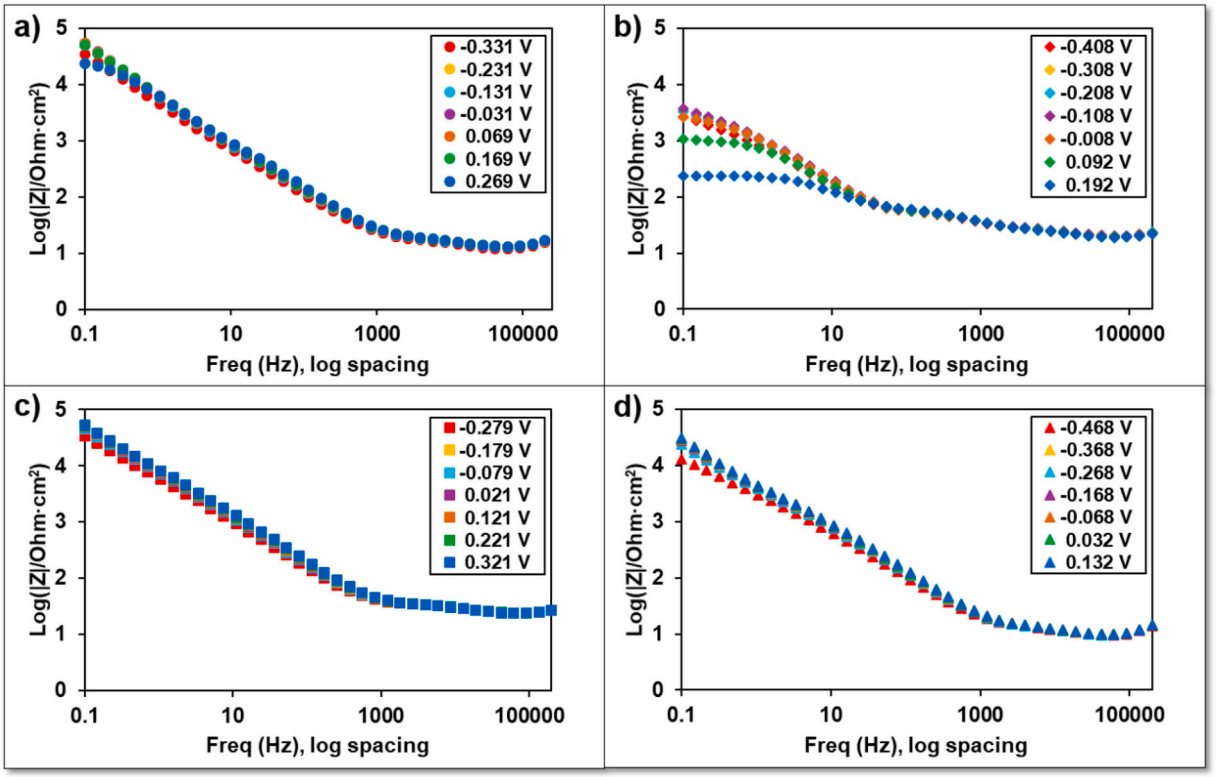

Fig. 10. Bode-impedance diagrams of: a) Sample 1, b) Sample 2, c) Sample 3 and d) Sample 4.

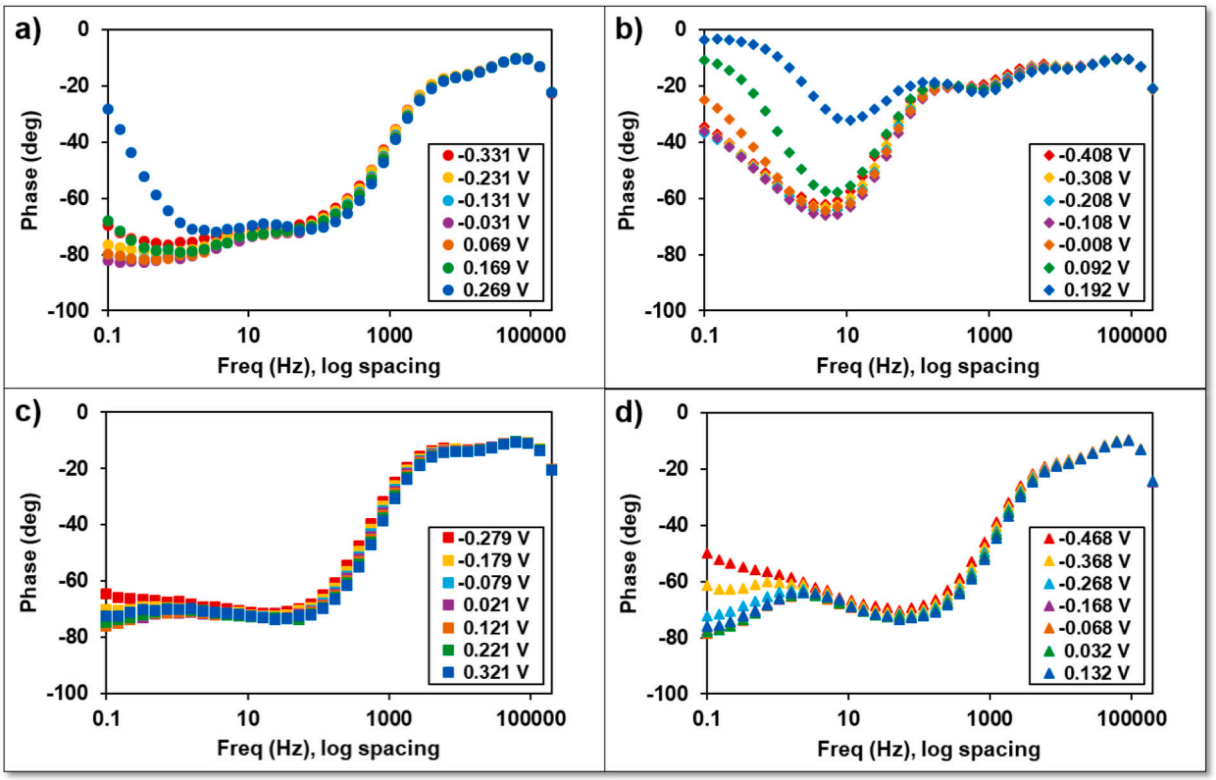

Fig. 11. Bode-phase diagrams of: a) Sample 1, b) Sample 2, c) Sample 3 and d) Sample 4.

constant) as the curve angles towards lower frequencies. The maximum phase angle is centered at approximately 10 Hz for Sample 2 and 100 Hz for Sample 1, Sample 3 and Sample 4. Furthermore, an increase in the response of the phase angle values of Samples 3 and 4 is observed at more positive potentials, indicating a transition from a capacitive to a resistive film. In contrast, the impedance values of Samples 1 and 2 show

Table 5
Results from the Bode plots of the samples studied at different potentials (±0.3 V vs. E_{corr}).

Parameters	Sample 1	Sample 2	Sample 3	Sample 4
Potential (V)	-0.331	-0.408	-0.279	-0.468
Max impedance (Ω·cm²)	34,044.51	2424.45	30,218.44	11,418.86
Max phase angle (°)	76.05	62.02	71.44	69.28
Potential (V)	-0.031	-0.108	0.021	-0.168
Max impedance (Ω·cm²)	54,279.79	3391.53	44,615.95	24,646.11
Max phase angle (°)	82.73	66.10	76.05	77.31
Potential (V)	0.269	0.192	0.321	0.132
Max impedance (Ω·cm²)	23,939.60	221.38	47,380.15	27,010.55
Max phase angle (°)	72.08	32.09	73.72	75.77

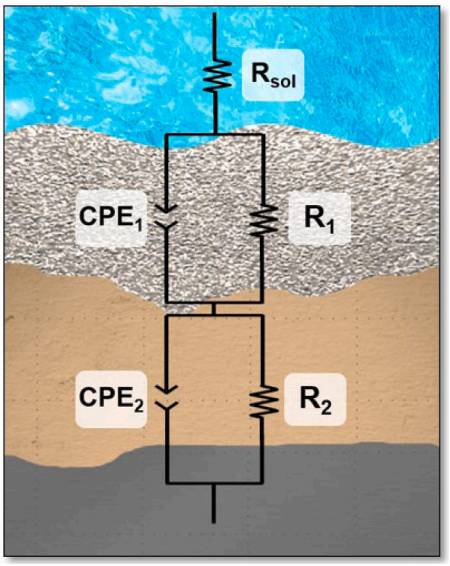

Fig. 12. Equivalent circuit $R_{sol}(CPE_1\ R_1)(CPE_2\ R_2)$ applied for the studied samples.

a decrease in response to higher potentials (0.2 to 0.3 V vs. E_{corr}).

It is evident that corrosion resistance is dependent on impedance and phase angle values, with Sample 1 demonstrating notable resistance and Sample 2 exhibiting significantly lower values.

Fig. 12 displays the analogous circuit model R(CPE R)(CPE R) applied from the results obtained, which best fits the experimental results of the research and demonstrates that the surface of the samples is resistant to dissolution along with a double passive film (porous and compact) up until the alloy is obtained.

The model and the following equations represented the electrolyte's resistance in ohms as R_{sol}, the passive film's capacitances as CPE_1 and CPE_2 and the constant phase elements and the porous and compact passive film resistances as R_1 and R_2, respectively. The constant phase element replicates the semi-infinite Warburg impedance (n = 0.5), the resistor (n = 0.0), and the capacitor (n = 1.0) as a function of the applied frequency (f) and the values of the parameters n_1 and n_2 [55].

$$Z_{series} = Z_1 + Z_2 + Z_3 \tag{3}$$

$$\frac{1}{Z_{parallel}} = \frac{1}{Z_{CPE}} + \frac{1}{Z_R} \tag{4}$$

$$Z_{parallel} = \frac{Z_R \cdot Z_{CPE}}{Z_R + Z_{CPE}} \tag{5}$$

$$Z_R = R\ Z_{CPE} = \frac{1}{Y^0(jw)^n} \tag{6}$$

$$Z_{parallel} = \frac{R}{1 + RY^0(jw)^n} \tag{7}$$

$$Z(f) = R_{sol} + \frac{R_1}{1 + R_1 Y_1^0(jw)^{n_1}} + \frac{R_2}{1 + R_2 Y_2^0(jw)^{n_2}} \tag{8}$$

The results obtained through the application of the equivalent circuit $R_{sol}(CPE_1\ R_1)(CPE_2\ R_2)$ were found to be in accordance with the experimental data. Furthermore, the chi-squared values were of the order of 10^{-3}, thereby indicating that the simulation quality was satisfactory. The spectra obtained from EIS, when interpreted through the lens of a two-time constant equivalent circuit model, point to the presence of a two-layer passive film structure.

As in the Nyquist and Bode graphs, Fig. 13 shows the evolution of the values of different resistances and constant phase elements of the porous and compact protective layers with the seven potentials applied.

In general, resistance values tend to increase up to -0.1 V for all the samples tested, being higher R_1 for Sample 4. This finding suggests that the incorporation of silicon enhances the corrosion of the outer passive layer of the sample. Sample 1 had a stronger corrosion resistance ($R_p = R_1 + R_2$), reaching values of up to 10^3 KOhm·cm², while Sample 2 had the lowest resistance results (4 KOhm·cm² max). The R_2 values are higher than the R_1 values, which is indicative of the fact that the outer porous layer exhibits a lower resistance than the inner compact film.

In addition, Sample 1 and Sample 2 have lower resistance values as the applied voltage became more positive. This decline in resistance as the applied potential increases to positive values can be attributed to two phenomena: film thinning and breakdown at higher potentials. In contrast, Sample 3 has the maximum resistance value at 0.0V and Sample 4 at -0.1 V. Except for Sample 2, the studied samples had strong corrosion resistance since their values were between 10^4 and 10^6 Ohm·cm².

The fitted values of Y_1 and Y_2 decrease as Si concentration increases, indicating that the compactness and stability of the passive protective film have improved due to SiO_2 production.

4. Conclusions

This paper has studied four heat-treated titanium alloys that contain non-toxic and biocompatible components, such as molybdenum (Mo) and silicon (Si). The main conclusions of the study are briefly summarized below:

- The results showed that the addition of silicon to the Ti-15Mo alloy affects the homogeneity and distribution of phases. The X-ray diffraction (XRD) analysis showed the predominant presence of β phase with a smaller amount of silicide.
- It was observed that during immersion in Ringer's solution, the samples retain the stability of their potential, with the sample with 0.75%Si having a higher potential that inhibits the cyclic rupture and repassivation of the passive layer that has developed on its surface. On the other hand, it has been shown that a higher concentration of silicon (more than 0.5% Si) slows down the corrosion process because it favors the development of a more compact and effective passive layer. The corrosion rate in simulated physiological medium decreases by more than 50% with the addition of 0.75% Si and this decrease reaches 75% if the Si concentration is 1%.
- All the alloys demonstrated comparable hardness values at varying loadings, higher than those of commercial pure titanium (CpTi). When the Si addition is very low (0.5%), the formation of the silicide at the edge of the crystals generates elevated dispersion of the microhardness values due to the lack of microstructural homogeneity.

These results were largely positive for the corrosion behavior of the samples, showing that, at Si additions higher than 0.5 wt%, there was

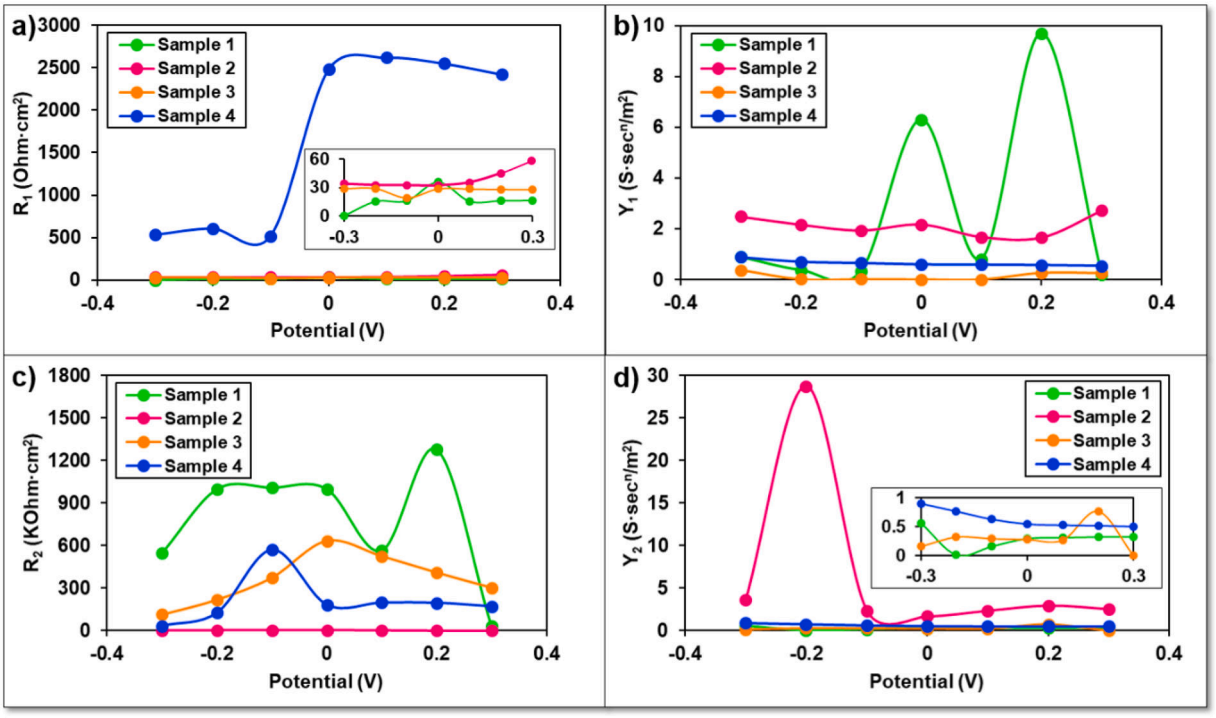

Fig. 13. Evolution of a) R_1 and b) Y_1 with the different potentials applied for the porous film, c) R_2 and d) Y_2 with the different potentials applied for the compact film of the samples studied.

very good corrosion resistance and mechanical properties similar to other commercial alloys.

CRediT authorship contribution statement

Cristina Jiménez-Marcos: Writing – original draft, Investigation, Formal analysis, Conceptualization. **Julia Claudia Mirza-Rosca:** Writing – review & editing, Methodology, Funding acquisition. **Madalina Simona Baltatu:** Resources, Investigation, Formal analysis. **Petrica Vizureanu:** Validation, Supervision, Resources, Methodology.

Declaration of competing interest

The authors declare that they have no known competing financial interests or personal relationships that could have appeared to influence the work reported in this paper.

Acknowledgements

We are grateful for the collaboration of the European project 2023–1-RO01-KA220-HED-000159985: Smart Healthcare Engineering and the Cabildo22–01 project.

Data availability

Data will be made available on request.

References

[1] D. Aggarwal, V. Kumar, S. Sharma, Drug-loaded biomaterials for orthopedic applications: A review, J. Control. Release. 344 (2022) 113–133, https://doi.org/10.1016/j.jconrel.2022.02.029.
[2] T. Hanawa, Metals and medicine, Mater. Trans. 62 (2021) 139–148, https://doi.org/10.2320/matertrans.MT-M2020268.
[3] M.K. Gouda, S.A. Salman, S. Ebied, A.M. Ashmawy, M.A.H. Gepreel, A. Chiba, Biocompatibility and corrosion resistance of low-cost Ti–14Mn–Zr alloys, J. Mater. Res. 36 (2021) 4883–4893, https://doi.org/10.1557/s43578-021-00441-w.
[4] M.K. Gouda, S.A. Salman, S. Ebied, Improvement in the microhardness and corrosion behaviour of Ti-14Mn biomedical alloy by cold working, Mater. Res. Express. 9 (2022) 015401, https://doi.org/10.1088/2053-1591/ac4b77.
[5] R.Eftekhar Ashtiani, M. Alam, S. Tavakolizadeh, K. Abbasi, The role of biomaterials and biocompatible materials in implant-supported dental prosthesis, evidence-based complement, Altern. Med. 2021 (2021) 1–9, https://doi.org/10.1155/2021/3349433.
[6] M.S. Baltatu, P. Vizureanu, A.V. Sandu, N. Florido-Suarez, M.V. Saceleanu, J. C. Mirza-Rosca, New titanium alloys, promising materials for medical devices, Materials. (Basel) 14 (2021) 5934, https://doi.org/10.3390/MA14205934.
[7] R. del Castillo, K. Chochlidakis, P. Galindo-Moreno, C. Ercoli, Titanium nitride coated implant abutments: from technical aspects and soft tissue biocompatibility to clinical applications. A literature review, J. Prosthodont. 31 (2022) 571–578, https://doi.org/10.1111/jopr.13446.
[8] Y. Fu, W. Xiao, J. Rong, L. Ren, H. Peng, Y. Wen, X. Zhao, C. Ma, Achieving large near-linear elasticity, low modulus, and high strength in a metastable β-Ti alloy by mild cold rolling, J. Mater. Sci. Technol. 189 (2024) 1–12, https://doi.org/10.1016/j.jmst.2023.11.066.
[9] E. Marin, A. Lanzutti, Biomedical applications of titanium alloys: A comprehensive review, Materials. (Basel) 17 (2023) 114, https://doi.org/10.3390/ma17010114.
[10] N. Sirdeshmukh, G. Dongre, Achieving controlled topography and wettability through laser surface texturing of Ti6Al4V for bioengineering applications, Results. Eng. 17 (2023) 100898, https://doi.org/10.1016/j.rineng.2023.100898.
[11] M.V. Popa, E. Vasilescu, P. Drob, M. Anghel, C. Vasilescu, I. Mirza-Rosca, A. S. Lopez, Anodic passivity of some titanium base alloys in aggressive environments, Mater. Corros. 53 (2002) 51–55, https://doi.org/10.1002/1521-4176(200201)53:1<51. AID−MACO51>3.0.CO;2-6.
[12] A. Azmat, S. Asrar, I.A. Channa, J. Ashfaq, I. Ali Chandio, A.D. Chandio, M. Ali Shar, M.S. AlSalhi, S. Devanesan, Comparative study of biocompatible titanium alloys containing non-toxic elements for orthopedic implants, Crystals. (Basel) 13 (2023) 467, https://doi.org/10.3390/cryst13030467.
[13] G. Khadija, A. Saleem, Z. Akhtar, Z. Naqvi, M. Gull, M. Masood, S. Mukhtar, M. Batool, N. Saleem, T. Rasheed, N. Nizam, A. Ibrahim, F. Iqbal, Short term exposure to titanium, aluminum and vanadium (Ti 6Al 4V) alloy powder drastically affects behavior and antioxidant metabolites in vital organs of male albino mice, Toxicol. Reports. 5 (2018) 765–770, https://doi.org/10.1016/J.TOXREP.2018.06.006.
[14] G. Genchi, A. Carocci, G. Lauria, M.S. Sinicropi, A. Catalano, Nickel: Human Health and Environmental Toxicology, Int. J. Environ. Res. Public Health. 17 (2020) 679, https://doi.org/10.3390/ijerph17030679.
[15] R. Patel, W. Moore, J.C. Jimenez, Severe symptomatic nickel allergy following stent graft implantation requiring excision and external iliac artery reconstruction, J. Vasc. Surg. Cases, Innov. Tech. 8 (2022) 562–564, https://doi.org/10.1016/j.jvscit.2022.08.013.
[16] I. Hulka, N.R. Florido-Suarez, J.C. Mirza-Rosca, A. Saceleanu, Mechanical properties and corrosion behavior of thermally treated Ti-6Al-7Nb dental alloy, Mater 15 (2022) 3813, https://doi.org/10.3390/MA15113813. Page1520223813.

[17] A. Silva, A.H. Plaine, Electrochemical corrosion study of biomaterials: A bibliometric study based on co-word analysis, Results. Eng. 20 (2023) 101489, https://doi.org/10.1016/j.rineng.2023.101489.
[18] W. Xu, M. Chen, X. Lu, D. wei Zhang, H. preet Singh, Y. Jian-shu, Y. Pan, X. hui Qu, C. zong Liu, Effects of Mo content on corrosion and tribocorrosion behaviours of Ti-Mo orthopaedic alloys fabricated by powder metallurgy, Corros. Sci. 168 (2020) 108557, https://doi.org/10.1016/J.CORSCI.2020.108557.
[19] C.R. Woodside, P.E. King, C. Nordlund, Arc distribution during the vacuum Arc remelting of Ti-6Al-4V, Metall. Mater. Trans. B. 44 (2013) 154–165, https://doi.org/10.1007/s11663-012-9760-1.
[20] A.H. Awad, M. Saood, H.A. Aly, A.W. Abdelghany, Role of Mo and Zr additions in enhancing the behavior of new Ti–Mo alloys for implant materials, Met. Mater. Int. (2024), https://doi.org/10.1007/s12540-024-01813-7.
[21] K. Wang, G. Cao, Y. Cai, X. Zhou, C. Xu, X. Zheng, B. Zhang, Microstructure and corrosion behavior of Ti-Mo-Zr alloy fabricated by selective laser melting in simulated oral environment, Int. J. Electrochem. Sci. 19 (2024) 100829, https://doi.org/10.1016/j.ijoes.2024.100829.
[22] A. Sotniczuk, W. Chromiński, D. Kalita, H. Garbacz, C. Xie, J. Tang, B. Dou, M. Pisarek, A. Baron-Wiecheć, Ł. Kurpaska, F. Sun, K. Ogle, Effect of Zr addition on the corrosion resistance of Ti-Mo alloy in the H2O2-containing inflammatory environment, Appl. Surf. Sci. 681 (2025) 161518, https://doi.org/10.1016/j.apsusc.2024.161518.
[23] P. Chui, R. Jing, F. Zhang, J. Li, T. Feng, Mechanical properties and corrosion behavior of β-type Ti-Zr-Nb-Mo alloys for biomedical application, J. Alloys Compd. 842 (2020) 155693, https://doi.org/10.1016/j.jallcom.2020.155693.
[24] S. Ehtemam-Haghighi, H. Attar, I.V. Okulov, M.S. Dargusch, D. Kent, Microstructural evolution and mechanical properties of bulk and porous low-cost Ti–Mo–Fe alloys produced by powder metallurgy, J. Alloys Compd. 853 (2021) 156768, https://doi.org/10.1016/j.jallcom.2020.156768.
[25] H. Zhang, F. Liu, L. Fang, J. Zhong, W. Bai, Y. Yuan, M. Rong, J. Wang, L. Zhang, L. Liu, High-throughput determination of interdiffusivity and atomic mobilities in bcc Ti–Cr–Mo alloys, J. Mater. Res. Technol. 33 (2024) 620–629, https://doi.org/10.1016/j.jmrt.2024.09.111.
[26] H. Zhang, G.-H. Zhang, Influence of Ti addition on the microstructure and comprehensive properties of Mo–Cu alloy, J. Mater. Res. Technol. 30 (2024) 2833–2847, https://doi.org/10.1016/j.jmrt.2024.04.050.
[27] N. Nohira, W.-T. Chiu, M. Tahara, H. Hosoda, Microstructural changes and mechanical property response to aging heat treatment in hypereutectoid Ti–Au–Mo biomedical alloys, Mater. Sci. Eng. A. 912 (2024) 146956, https://doi.org/10.1016/j.msea.2024.146956.
[28] W.-T. Chiu, R. Hayakawa, N. Nohira, M. Tahara, T. Inamura, H. Hosoda, Correspondence of the aging behaviors and the phase constituents of the Ti-Mo-based alloys tailored by the Al and Zr additions, J. Alloys Compd. 991 (2024) 174509, https://doi.org/10.1016/j.jallcom.2024.174509.
[29] H. Zhang, N. Gao, W. Bai, M. Rong, J. Wang, L. Zhang, L. Liu, Diffusivities and atomic mobilities in bcc Ti–V–Mo alloys, CALPHAD. 83 (2023) 102633, https://doi.org/10.1016/j.calphad.2023.102633.
[30] L. Verestiuc, M.C. Spataru, M.S. Baltatu, M. Butnaru, C. Solcan, A.V. Sandu, I. Voiculescu, V. Geanta, P. Vizureanu, New Ti–Mo–Si materials for bone prosthesis applications, J. Mech. Behav. Biomed. Mater. 113 (2021) 104198, https://doi.org/10.1016/J.JMBBM.2020.104198.
[31] A.M.G. Tavares, W.S. Ramos, J.C.G. de Blas, E.S.N. Lopes, R. Caram, W.W. Batista, S.A. Souza, Influence of Si addition on the microstructure and mechanical properties of Ti–35Nb alloy for applications in orthopedic implants, J. Mech. Behav. Biomed. Mater. 51 (2015) 74–87, https://doi.org/10.1016/j.jmbbm.2015.06.035.
[32] E. Zhao, S. Sun, Y. Zhang, Recent advances in silicon containing high temperature titanium alloys, J. Mater. Res. Technol. 14 (2021) 3029–3042, https://doi.org/10.1016/j.jmrt.2021.08.117.
[33] C. Jimenez-Marcos, J.C. Mirza-Rosca, M.S. Baltatu, P. Vizureanu, Experimental research on new developed titanium alloys for biomedical applications, Bioengineering 9 (2022) 686, https://doi.org/10.3390/bioengineering9110686.
[34] C. Jiménez-Marcos, J.C. Mirza-Rosca, M.S. Baltatu, P. Vizureanu, Evaluation of the mechanical and corrosion properties of new Ti alloys for orthopedic devices, Microsc. Microanal. 30 (2024), https://doi.org/10.1093/mam/ozae044.461.
[35] A.I.W. Conshohocken, ASTM E3-11(2017); Standard guide for preparation of metallographic specimens., (2017).
[36] International Organization for Standardization, ISO 14577-1:2015 Metallic materials — Instrumented indentation..., (2015).
[37] ISO 10271:2020 - Dentistry — Corrosion test methods for metallic materials, (2020).
[38] C. Jiménez-Marcos, J.C. Mirza-Rosca, M.S. Baltatu, P. Vizureanu, Two novel Ti–Mo–Ta–Zr alloys for medical devices: their microstructure, corrosion resistance and microhardness characteristics, Mater. Chem. Phys. 334 (2025) 130511, https://doi.org/10.1016/j.matchemphys.2025.130511.
[39] ISO 16773-1-4:2016 Electrochemical impedance spectroscopy (EIS) on coated and uncoated metallic specimens, (2016).
[40] Y. Yang, Y.A. Chang, L. Tan, Y. Du, Experimental investigation and thermodynamic descriptions of the Mo–Si–Ti system, Mater. Sci. Eng. A. 361 (2003) 281–293, https://doi.org/10.1016/S0921-5093(03)00560-4.
[41] J. Li, W. Jiang, C. Xia, Y. Deng, Y. Gao, C. Yang, Microstructural evolution and subsequent mechanical properties of Ti65 titanium alloy during long-term thermal exposure, Metals. (Basel) 14 (2024) 854, https://doi.org/10.3390/met14080854.
[42] J. Zhu, A. Kamiya, T. Yamada, A. Watazu, W. Shi, K. Naganuma, Effect of silicon addition on microstructure and mechanical properties of cast titanium alloys, Mater. Trans. 42 (2001) 336–341, https://doi.org/10.2320/matertrans.42.336.
[43] Z. Jiang, X. Dai, H. Middleton, Effect of silicon on corrosion resistance of Ti–Si alloys, Mater. Sci. Eng. B. 176 (2011) 79–86, https://doi.org/10.1016/J.MSEB.2010.09.006.
[44] C. Jimenez-Marcos, J.C. Mirza-Rosca, M.S. Baltatu, P. Vizureanu, Effect of Si contents on the properties of Ti15Mo7ZrxSi alloys, Mater 16 (2023) 4906, https://doi.org/10.3390/MA16144906. Page1620234906.
[45] R.P. Kolli, A. Devaraj, A review of metastable beta titanium alloys, Metals. (Basel) 8 (2018) 506, https://doi.org/10.3390/met8070506.
[46] P.J. Bania, Beta titanium alloys and their role in the titanium industry, JOM 46 (1994) 16–19, https://doi.org/10.1007/BF03220742.
[47] S.S. Da Rocha, G.L. Adabo, G.E.P. Henriques, M.A.D.A. Nóbilo, Vickers hardness of cast commercially pure titanium and Ti-6Al-4V alloy submitted to heat treatments, Braz. Dent. J. 17 (2006) 126–129, https://doi.org/10.1590/S0103-64402006000200008.
[48] C.N. Elias, D.J. Fernandes, C.R.S. Resende, J. Roestel, Mechanical properties, surface morphology and stability of a modified commercially pure high strength titanium alloy for dental implants, Dent. Mater. 31 (2015) e1–e13, https://doi.org/10.1016/j.dental.2014.10.002.
[49] A.V. Sandu, M.S. Baltatu, M. Nabialek, A. Savin, P. Vizureanu, Characterization and mechanical proprieties of new TiMo alloys used for medical applications, Materials. (Basel) 12 (2019) 2973, https://doi.org/10.3390/MA12182973.
[50] H. Kovacı, K. Şenel, M.T. Acar, Y.B. Bozkurt, A. Çelik, Comparative investigation of structural, morphological, mechanical, tribological and electrochemical properties of TiO2 films formed on cp-Ti, Ti6Al4V and Ti45Nb alloys, Surf. Coatings Technol. 487 (2024) 131024, https://doi.org/10.1016/j.surfcoat.2024.131024.
[51] K. Shen, W. Jiang, C. Sun, Y. Wan, W. Zhao, J. Sun, Insight into microstructure, microhardness and corrosion performance of 2205 duplex stainless steel: effect of plastic pre-strain, Corros. Sci. 210 (2023) 110847, https://doi.org/10.1016/j.corsci.2022.110847.
[52] C. Jiménez-Marcos, J.C. Mirza-Rosca, M.S. Baltatu, P. Vizureanu, Evaluation of new titanium alloys as potential materials for medical devices, Microsc. Microanal. 29 (2023) 196–201, https://doi.org/10.1093/micmic/ozad067.088.
[53] ASTM-Standards, Standard practice for calculation of corrosion rates and related information from electrochemical measurements, astm G 102 - 23. (2023) 1–3. https://doi.org/10.1520/G0102-23.
[54] F. Almeraya-Calderón, J.M. Jáquez-Muñoz, M. Lara-Banda, P. Zambrano-Robledo, J.A. Cabral-Miramontes, A. Lira-Martínez, F. Estupinán-López, C. Gaona Tiburcio, Corrosion behavior of titanium and titanium alloys in ringer's solution, Int. J. Electrochem. Sci. 17 (2022) 220751, https://doi.org/10.20964/2022.07.55.
[55] B.A. Boukamp, A nonlinear Least squares fit procedure for analysis of immittance data of electrochemical systems, Solid. State Ion. 20 (1986) 31–44, https://doi.org/10.1016/0167-2738(86)90031-7.

1 INTRODUCCIÓN

2 PUBLICACIONES

3 DOCUMENTOS DE AUTORÍA

4 PARTICIPACIONES EN CONGRESOS

5 OTRAS PUBLICACIONES

6 CONCLUSIONES FINALES

ULPGC Universidad de Las Palmas de Gran Canaria | Escuela de Doctorado

DOCUMENTO DE AUTORÍA PARA TESIS POR COMPENDIO

Los abajo firmantes, coautores del artículo titulado “Experimental Research on New Developed Titanium Alloys for Biomedical Applications”, publicado en Bioengineering a 12 de noviembre de 2022:

The undersigned, as co-authors of the published paper entitled “Experimental Research on New Developed Titanium Alloys for Biomedical Applications”, published in Bioengineering on November 12, 2022:

- Reconocemos como autor principal del artículo a Dña. Cristina Jiménez Marcos, con DNI/ID 45398413R.
  We recognize as main author to Mrs Cristina Jiménez Marcos, with ID number 45398413R.

- Renunciamos a utilizar esta publicación como núcleo principal de otras tesis doctorales, sin perjuicio de que dichas publicaciones puedan ser presentadas como méritos complementarios en las tesis doctorales que pudieran presentar los otros autores de dichas publicaciones.
  We renounce to use this publication as main nucleus of other doctoral theses, without prejudice to the fact that said publications may be presented as complementary merits in the doctoral theses that the other authors of said publications may present.

En Las Palmas de Gran Canaria a 6 de marzo de 2025

MIRZA ROSCA JULIANA CLAUDIA - 45360672A

Firmado digitalmente por MIRZA ROSCA JULIANA CLAUDIA - 45360672A
Fecha: 2025.03.07 07:49:27 Z

Julia Claudia Mirza Rosca

Madalina Simona Baltatu

Petrica Vizureanu

DOCUMENTO DE AUTORÍA PARA TESIS POR COMPENDIO

Los abajo firmantes, coautores del artículo titulado “Effect of Si Contents on the Properties of Ti15Mo7ZrxSi Alloys”, publicado en Materials a 9 de julio de 2023:

The undersigned, as co-authors of the published paper entitled “Effect of Si Contents on the Properties of Ti15Mo7ZrxSi Alloys”, published in Materials on July 9, 2023:

- Reconocemos como autor principal del artículo a Dña. Cristina Jiménez Marcos, con DNI/ID 45398413R.
  We recognize as main author to Mrs Cristina Jiménez Marcos, with ID number 45398413R.

- Renunciamos a utilizar esta publicación como núcleo principal de otras tesis doctorales, sin perjuicio de que dichas publicaciones puedan ser presentadas como méritos complementarios en las tesis doctorales que pudieran presentar los otros autores de dichas publicaciones.
  We renounce to use this publication as main nucleus of other doctoral theses, without prejudice to the fact that said publications may be presented as complementary merits in the doctoral theses that the other authors of said publications may present.

En Las Palmas de Gran Canaria a 6 de marzo de 2025

MIRZA ROSCA JULIANA CLAUDIA - 45360672A

Firmado digitalmente por MIRZA ROSCA JULIANA CLAUDIA - 45360672A
Fecha: 2025.03.07 07:47:00 Z

Julia Claudia Mirza Rosca

Madalina Simona Baltatu

Petrica Vizureanu

DOCUMENTO DE AUTORÍA PARA TESIS POR COMPENDIO

Los abajo firmantes, coautores del artículo titulado “Evaluation of New Titanium Alloys as Potential Materials for Medical Devices”, publicado en Microscopy and Microanalysis a 22 de julio de 2023:

The undersigned, as co-authors of the published paper entitled “Evaluation of New Titanium Alloys as Potential Materials for Medical Devices”, published in Microscopy and Microanalysis on July 22, 2023:

- Reconocemos como autor principal del artículo a Dña. Cristina Jiménez Marcos, con DNI/ID 45398413R.
  We recognize as main author to Mrs Cristina Jiménez Marcos, with ID number 45398413R.

- Renunciamos a utilizar esta publicación como núcleo principal de otras tesis doctorales, sin perjuicio de que dichas publicaciones puedan ser presentadas como méritos complementarios en las tesis doctorales que pudieran presentar los otros autores de dichas publicaciones.
  We renounce to use this publication as main nucleus of other doctoral theses, without prejudice to the fact that said publications may be presented as complementary merits in the doctoral theses that the other authors of said publications may present.

En Las Palmas de Gran Canaria a 6 de marzo de 2025

MIRZA ROSCA JULIANA CLAUDIA - 45360672A

Firmado digitalmente por MIRZA ROSCA JULIANA CLAUDIA - 45360672A
Fecha: 2025.03.07 07:47:29 Z

Julia Claudia Mirza Rosca

Madalina Simona Baltatu

Petrica Vizureanu

ULPGC Universidad de Las Palmas de Gran Canaria | Escuela de Doctorado

DOCUMENTO DE AUTORÍA PARA TESIS POR COMPENDIO

Los abajo firmantes, coautores del artículo titulado “Two novel Ti–Mo–Ta–Zr alloys for medical devices: Their microstructure, corrosion resistance and microhardness characteristics”, publicado en Materials Chemistry and Physics a 9 de febrero de 2025:

The undersigned, as co-authors of the published paper entitled “Two novel Ti–Mo–Ta–Zr alloys for medical devices: Their microstructure, corrosion resistance and microhardness characteristics”, published in Materials Chemistry and Physics on February 9, 2025:

- Reconocemos como autor principal del artículo a Dña. Cristina Jiménez Marcos, con DNI/ID 45398413R.
  We recognize as main author to Mrs Cristina Jiménez Marcos, with ID number 45398413R.

- Renunciamos a utilizar esta publicación como núcleo principal de otras tesis doctorales, sin perjuicio de que dichas publicaciones puedan ser presentadas como méritos complementarios en las tesis doctorales que pudieran presentar los otros autores de dichas publicaciones.
  We renounce to use this publication as main nucleus of other doctoral theses, without prejudice to the fact that said publications may be presented as complementary merits in the doctoral theses that the other authors of said publications may present.

En Las Palmas de Gran Canaria a 6 de marzo de 2025

MIRZA ROSCA JULIANA CLAUDIA - 45360672A

Firmado digitalmente por MIRZA ROSCA JULIANA CLAUDIA - 45360672A
Fecha: 2025.03.07 07:48:11 Z

Julia Claudia Mirza Rosca

Madalina Simona Baltatu

Petrica Vizureanu

ULPGC Universidad de Las Palmas de Gran Canaria | Escuela de Doctorado

DOCUMENTO DE AUTORÍA PARA TESIS POR COMPENDIO

Los abajo firmantes, coautores del artículo titulado “Preliminary studies of new heat-treated titanium alloys for use in medical equipment”, publicado en Results in Engineering a 28 de febrero de 2025:

The undersigned, as co-authors of the published paper entitled “Preliminary studies of new heat-treated titanium alloys for use in medical equipment”, published in Results in Engineering on February 28, 2025:

- Reconocemos como autor principal del artículo a Dña. Cristina Jiménez Marcos, con DNI/ID 45398413R.
  We recognize as main author to Mrs Cristina Jiménez Marcos, with ID number 45398413R.

- Renunciamos a utilizar esta publicación como núcleo principal de otras tesis doctorales, sin perjuicio de que dichas publicaciones puedan ser presentadas como méritos complementarios en las tesis doctorales que pudieran presentar los otros autores de dichas publicaciones.
  We renounce to use this publication as main nucleus of other doctoral theses, without prejudice to the fact that said publications may be presented as complementary merits in the doctoral theses that the other authors of said publications may present.

En Las Palmas de Gran Canaria a 6 de marzo de 2025

MIRZA ROSCA JULIANA CLAUDIA - 45360672A
Firmado digitalmente por MIRZA ROSCA JULIANA CLAUDIA - 45360672A
Fecha: 2025.03.07 07:48:54 Z

Julia Claudia Mirza Rosca

Madalina Simona Baltatu

Petrica Vizureanu

1 INTRODUCCIÓN

2 PUBLICACIONES

3 DOCUMENTOS DE AUTORÍA

4 PARTICIPACIONES EN CONGRESOS

5 OTRAS PUBLICACIONES

6 CONCLUSIONES FINALES

A continuación, se presentan los **congresos** en los que se ha participado durante estos tres años de realización de la tesis:

- Cristina Jiménez-Marcos; Santiago J. Brito-García; Julia C. Mirza-Rosca; Madalina S. Baltatu; Petrica Vizureanu. 9th International Conference on Materials Science and Technologies – RoMat 2022. 2022. Rumanía. Participativo - Póster.
- Cristina Jiménez-Marcos; Santiago J. Brito-García; Julia C. Mirza-Rosca; Madalina S. Baltatu; Petrica Vizureanu. Biocompatibility and mechanical characteristics of different dental alloys. 9th International Conference on Materials Science and Technologies – RoMat 2022. 2022.
- C. Jiménez-Marcos; J. C. Mirza-Rosca; A. Fratila; A. Saceleanu. Influence of Silicon Addition on the Properties of New Titanium Alloys. 28th International Symposium on Analytical and Environmental Problems. 2022. Hungría. Participativo - Póster.
- Cristina Jiménez-Marcos; Julia Claudia Mirza-Rosca; Madalina Simona Baltatu; Petrica Vizureanu. Previous Studies of New Developed Titanium Alloys for Biomedical Applications. 2nd International Congress on Scientific Advances (ICONSAD'22). 2022. Turquía. Participativo - Ponencia oral (comunicación oral).
- Cristina Jiménez-Marcos; Julia Claudia Mirza-Rosca; Madalina Simona Baltatu; Petrica Vizureanu. I Congreso Internacional Multidisciplinar de Estudiantes de Doctorado. 2023. Tenerife. Participativo - Póster.
- Cristina Jiménez-Marcos; Julia Claudia Mirza-Rosca; Madalina Simona Baltatu; Petrica Vizureanu. Evaluación de nuevas aleaciones de titanio Ti15Mo7Zr y Ti15Mo7Zr1Si como posibles materiales para dispositivos médicos. I Congreso Internacional Multidisciplinar de Estudiantes de Doctorado. 2023.

- Cristina Jiménez-Marcos; Julia Claudia Mirza-Rosca; Madalina Simona Baltatu; Petrica Vizureanu. ICIR EUROINVENT 10th Edition. Romanian Inventors Forum. 2023. Rumanía. Participativo – Póster.
- Cristina Jiménez-Marcos; Julia Claudia Mirza-Rosca; Madalina Simona Baltatu; Petrica Vizureanu. Analysis of novel Ti15Mo7ZrxSi titanium alloys experimentally developed as potential materials for medical uses. ICIR EUROINVENT 10th Edition. Romanian Inventors Forum. 2023.
- Cristina Jiménez-Marcos; Julia Claudia Mirza-Rosca; Madalina Simona Baltatu; Petrica Vizureanu. Evaluation of New Titanium Alloys as Potential Materials for Medical Devices. Microscopy and Microanalysis (M&M 2023). 2023. Estados Unidos. Participativo – Póster.
- Cristina Jiménez-Marcos; Julia Claudia Mirza-Rosca; Anca Fratila; Adriana. Influence and Comparison of the Properties of Three Cobalt-Chromium Dental Alloys. Microscopy and Microanalysis (M&M 2023). 2023. Estados Unidos. Participativo – Póster.
- Cristina Jiménez-Marcos; Julia Claudia Mirza-Rosca; Madalina Simona Baltatu; Petrica Vizureanu. Evaluation of the Mechanical and Corrosion Properties of New Ti Alloys for Orthopedic Devices. Microscopy and Microanalysis (M&M 2024). 2024. Estados Unidos. Participativo – Póster.
- Cristina Jiménez-Marcos; Julia Claudia Mirza-Rosca; Madalina Simona Baltatu; Petrica Vizureanu. Special Titanium Alloys for Biomedical Devices. The Third International Symposium on Modern Engineering Equipment and Technology. 2025. China. Participativo – Presentación (Video).

DIFFERENT COBALT CHROMIUM DENTAL ALLOYS' BIOCOMPATIBILITY AND MECHANICAL CHARACTERISTICS

ROMAT 2022
9th International Conference on Materials Science and Technologies – RoMat 2022

C. Jiménez-Marcos[1], J.C. Mirza-Rosca[1*], A. Fratila[2], A. Saceleanu[2]

[1] Mechanical Engineering Dept., University of Las Palmas de Gran Canaria, University Campus of Tafira, 35017, Las Palmas de Gran Canaria, Spain

[2] Faculty of Medicine, Lucian Blaga University of Sibiu, 550024, Sibiu, Romania

ABSTRACT

Three Co-Cr based alloys with varying concentrations, labeled Co-Cr, C, and L, which will be used as dental materials, have been examined and evaluated using metallographic, electrochemical, and three-point bending tests. Metallographic examination revealed porosities and flaws in the Co-Cr and L samples, as well as comparable dendritic structures of the dental alloys. Corrosion and pitting potential results revealed surface passivation of the samples. The corrosion resistance for sample L was also somewhat greater when using the Electrochemical Impedance Spectroscopy approach, since corrosion becomes more pronounced the more positively the applied potential is shifted, as well as the higher the impedance and phase angle values. However, alloy C, has the lowest modulus of elasticity values in the three-point bending test.

SAMPLES PREPARATION

Alloy	Composition (in wt.%)											
	Co	Cr	Mo	W	Nb	V	Si	Mn	Fe	C	N	Ni
CoCr	64.8	28.0	5.0	-	-	-	<0.1	<0.1	-	<0.1	<0.1	<0.1
L	62.5	30.5	5.0	-	-	-	1.0	0.4	-	0.3	0.3	-
C	59.4	24.5	1.0	10.0	2.0	2.0	1.0	-	0.1	-	-	-

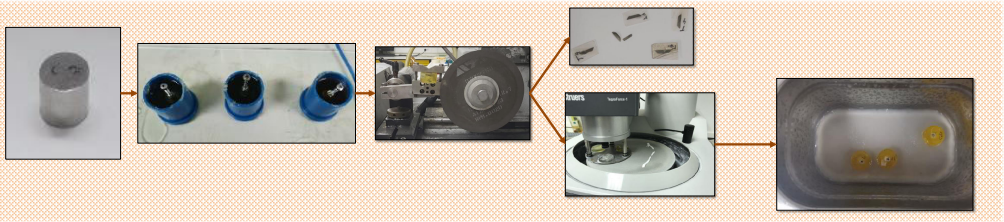

RESULTS OBTAINED

MICROSTRUCTURAL CHARACTERIZATION

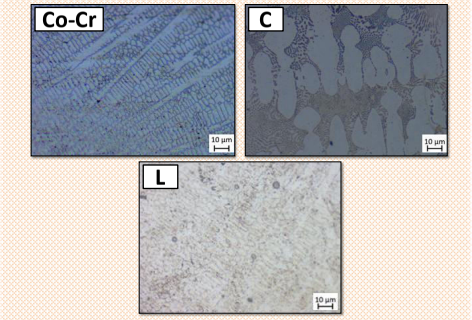

ELECTROCHEMICAL TESTS

CORROSION POTENTIAL

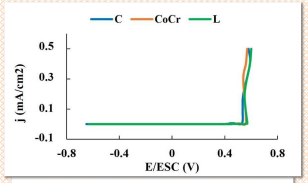

PITTING POTENTIAL

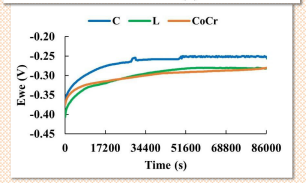

Co-Cr

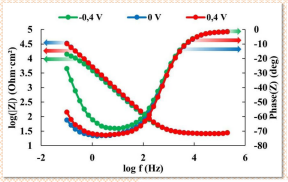

C

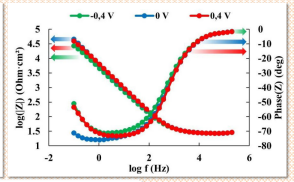

L

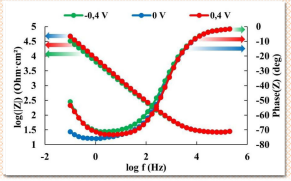

THREE-POINT BENDING TEST

Sample	E Average (GPa)
CoCr	175 ± 17
C	134 ± 13
L	148 ± 19

ROMAT 2022

9th International Conference on Materials Science and Technologies – RoMat 2022

Bucharest, Romania
November 24-25th, 2022

Biocompatibility and mechanical characteristics of different dental alloys

C. Jiménez-Marcos[1], **J. C. Mirza-Rosca[1*]**, A. Fratila[2], and A. Saceleanu[2]

1 Mechanical Engineering Department, Las Palmas de Gran Canaria University, 35017 Tafira, Spain
2 Faculty of Medicine, Lucian Blaga University of Sibiu, 550024 Sibiu, Romania

**Corresponding author: julia.mirza@ulpgc.es*

Three Cobalt-Chromium based alloys with varying concentrations, labeled Co-Cr, C, and L, which will be used as dental materials, have been examined and evaluated using metallographic, electrochemical, and three-point bending tests. The samples' surfaces were first prepared by cutting, mounting, polishing with progressive grain silicon carbide grinding papers and 0.1 micrometers of alumina suspension, and then cleaning with an ultrasonic machine. Metallographic examination revealed porosities and flaws in the Co-Cr and L samples, as well as comparable dendritic structures of the dental alloys. alloy C has the lowest modulus of elasticity values in the three-point bending test. Corrosion and pitting potential results revealed surface passivation of the samples. Moreover, the corrosion resistance for sample L was also slightly greater when using the Electrochemical Impedance Spectroscopy approach, since corrosion becomes more pronounced the more positively the applied potential is shifted, as well as the higher the impedance and phase angle values.

Keywords: Dental alloys; Cobalt-based alloys; Microstructure; Corrosion; Mechanical properties

28th International Symposium on Analytical and Environmental Problems

University of Szeged

INFLUENCE OF SILICON ADDITION ON THE PROPERTIES OF NEW TITANIUM ALLOYS

Cristina Jiménez-Marcos[1], Santiago J. Brito-García[1], Julia C. Mirza-Rosca*[1], Madalina S. Baltatu[2], Petrica Vizureanu[2]

[1] Mechanical Engineering Dept., University of Las Palmas de Gran Canaria, University Campus of Tafira, Engineering building, 35017, Las Palmas de Gran Canaria, Spain

[2] Department of Technologies and Equipments for Materials Processing, Faculty of Materials Science and Engineering, Gheorghe Asachi Technical University of Iaşi, Blvd. Mangeron, No. 51, 700050 Iasi, Romania

SAMPLES PREPARATION

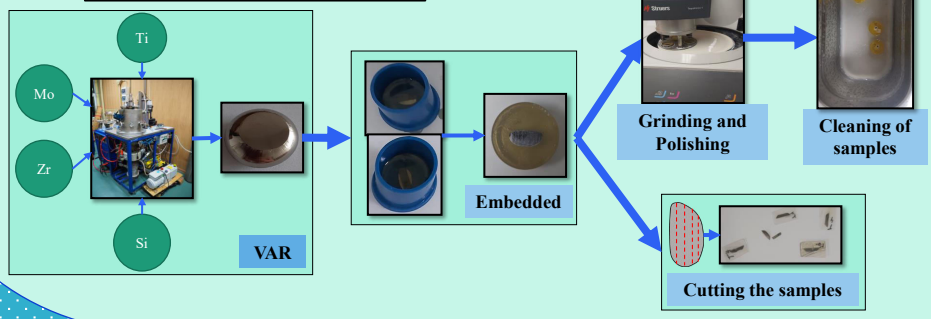

Samples	Ti (%)	Mo (%)	Zr (%)	Si (%)
TiMoZr	73.00	20.00	7.00	-
TiMoZrSi0.5	72.50	20.00	7.00	0.50
TiMoZrSi0.75	72.25	20.00	7.00	0.75
TiMoZrSi1	72.00	20.00	7.00	1.00

MICROSTRUCTURAL CHARACTERIZATION

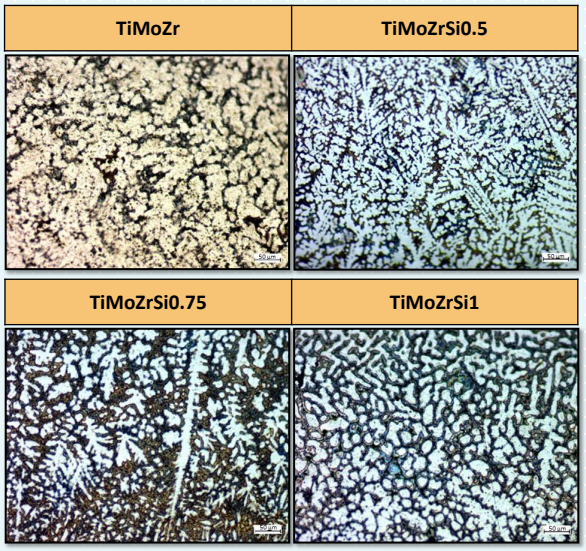

THREE-POINT BENDING TEST

Samples	Modulus of Elasticity (Gpa)
TiMoZr	87 ± 10
TiMoZrSi0.5	49 ± 12
TiMoZrSi0.75	54 ± 6
TiMoZrSi1	83 ± 22

MICROHARDNESS

TiMoZr		
Load (g)	Microhardness (HV)	
	Soft phase	Hard phase
5	174	343
25	192	386
50	318	374

TiMoZrSi0.5		
Load (g)	Microhardness (HV)	
	Soft phase	Hard phase
5	275	357
25	323	371
50	323	366

TiMoZrSi0.75		
Load (g)	Microhardness (HV)	
	Soft phase	Hard phase
5	214	365
25	239	383
50	319	399

TiMoZrSi1		
Load (g)	Microhardness (HV)	
	Soft phase	Hard phase
5	115	243
25	137	366
50	158	356

ELECTROCHEMICAL TESTS

CORROSION POTENTIAL

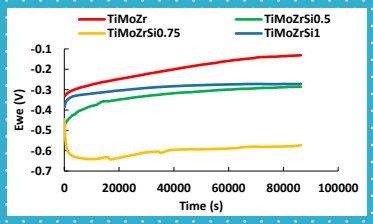

CORROSION RATE

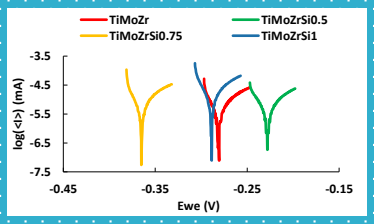

ELECTROCHEMICAL IMPEDANCE SPECTROSCOPY

TiMoZr

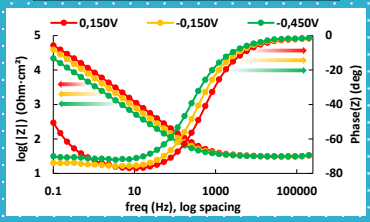

TiMoZrSi0.5

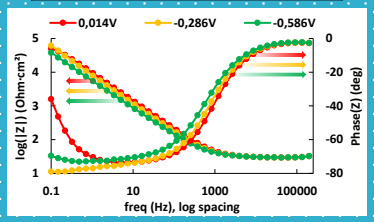

TiMoZrSi0.75

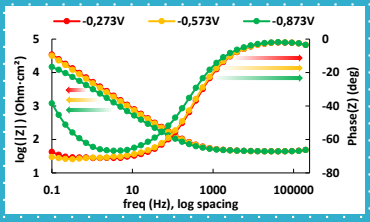

TiMoZrSi1

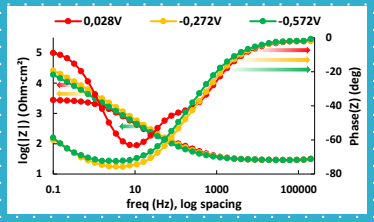

PITTING POTENTIAL

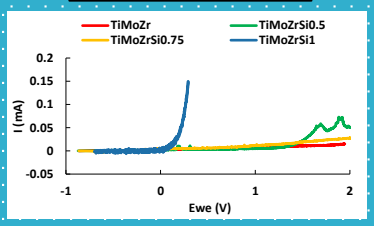

CONCLUSIONS

Metallographic analysis showed that both samples had biphasic and dendritic structures. According to electrochemical tests in body simulation fluid, the samples' corrosion resistance increases with decreasing silicon content and the samples present a double-layer passive film.

The values of modulus of elasticity are lower than those commercial alloys and nearly to the cortical human bone.

The microhardness test showed that the samples' surfaces had soft and hard phases.

ICONSAD'22

Certificate
of Participation

This is to certify that

Cristina Jiménez-Marcos

participated at the **2nd International Congress on Scientific Advances (ICONSAD'22)** held on **December 21-24, 2022** and made a presentation (oral) entitled

Previous Studies of New Developed Titanium Alloys for Biomedical Applications

Assoc. Prof. Dr. M. Nuri SEYMAN
Head of Organizing Board

The paper has been reviewed, accepted and discussed during the congress

ICONSAD'22

ULPGC Universidad de Las Palmas de Gran Canaria | Escuela de Ingenierías Industriales y Civiles

2nd International Congress on Scientific Advances

Previous Studies of New Developed Titanium Alloys for Biomedical Applications

Cristina Jiménez-Marcos

Julia Claudia Mirza-Rosca

Madalina Simona Baltatu

Petrica Vizureanu

21-24 December 2022

Congreso Internacional Multidisciplinar de Estudiantes de Doctorado (CIMED)

22-24 de Marzo de 2023

Evaluación de nuevas aleaciones de titanio Ti15Mo7Zr y Ti15Mo7Zr1Si como posibles materiales para dispositivos médicos

Cristina Jiménez Marcos[1], Julia Claudia Mirza Rosca[1*], Madalina Simona Baltatu[2], Petrica Vizureanu[2]

[1] Departamento de Ingeniería Mecánica, Universidad de Las Palmas de Gran Canaria, Las Palmas de Gran Canaria, España

[2] Departamento de Tecnologías y Equipos para el Procesado de Materiales, Universidad Técnica "Gheorghe Asachi de Iasi, Iasi, Rumanía

INTRODUCCIÓN

En los últimos años, los avances en medicina y procesamiento de materiales han permitido desarrollar nuevos biomateriales, especialmente metálicos como las aleaciones de titanio, los cuales han prevalecido sobre otros materiales convencionales debido a sus buenas propiedades mecánicas, resistencia a la corrosión y biocompatibilidad con materiales biológicos.

OBJETIVOS

Investigación de los efectos de dos concentraciones diferentes de silicio sobre las propiedades mecánicas y el comportamiento de resistencia a la corrosión de las nuevas aleaciones Ti15Mo7ZrxSi mediante pruebas metalográficas, electroquímicas, de microdureza y de flexión.

MATERIAL Y MÉTODOS

PREPARACIÓN DE LAS MUESTRAS

Composición (% de peso)

Elementos	Muestras	
	Ti15Mo7Zr	TiMo15Zr7Si
Ti	78.00	77.00
Mo	15.00	15.00
Zr	7.00	7.00
Si	-	1.00

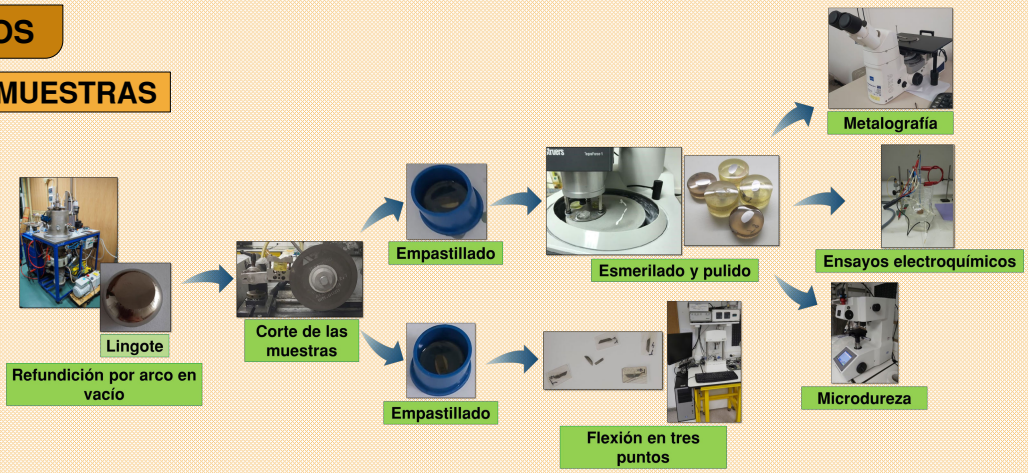

RESULTADOS

METALOGRAFÍA

TiMo15Zr7

TiMo15Zr7Si1

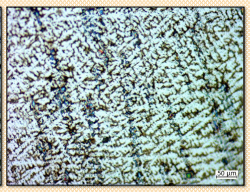

ENSAYOS ELECTROQUÍMICOS

POTENCIAL DE CORROSIÓN

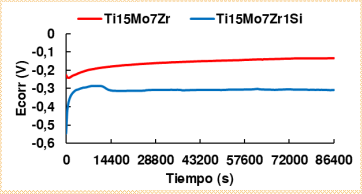

VELOCIDAD DE CORROSION

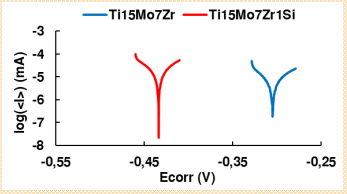

ESPECTROSCOPÍA DE IMPEDANCIA ELECTROQUÍMICA

TiMo15Zr7

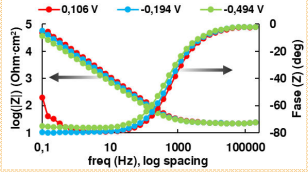

TiMo15Zr7Si1

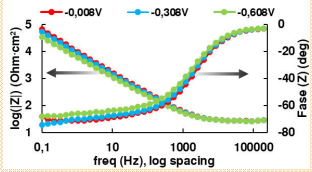

CIRCUITOS EQUIVALENTES

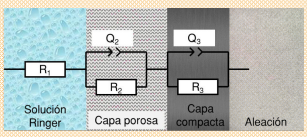

FLEXIÓN EN TRES PUNTOS

Muestra	Media del modulo de Young(GPa)
TiMo15Zr7	82.36 ± 9
TiMo15Zr7Si1	70.88 ± 8

MICRODUREZA

Carga (g)	TiMo15Zr7		TiMo15Zr7Si1	
	Microdureza (HV)		Microdureza (HV)	
	Fase blanda	Fase dura	Fase blanda	Fase dura
5	218	306	170	346
25	144	297	326	413
50	241	292	345	403

CONCLUSIONES

Se ha podido confirmar la estructura bifásica de las muestras, su tendencia a la pasivación y buen comportamiento en contacto con fluidos fisiológicos, siendo ligeramente superior la muestra sin silicio Ti15Mo7Zr. Por otra parte, el módulo de elasticidad de la muestra Ti15Mo7ZrSi ha sido menor y su dureza ha sido mayor. Por tanto, ambas muestras presentaron buenas características químicas, biológicas y mecánicas, siendo esta última mejorada mediante la adición del silicio.

CERTIFICADO

Este certificado se otorga a:

Cristina Jiménez Marcos

Por su **PARTICIPACIÓN** de forma **Virtual** en la I Edición del Congreso Internacional Multidisciplinar de Estudiantes de Doctorado (CIMED) celebrado los días 22-24 de marzo de 2023 en formato semipresencial en San Cristóbal de La Laguna (Tenerife, España).

Poster

EVALUACIÓN DE NUEVAS ALEACIONES DE TITANIO TI15MO7ZR Y TI15MO7ZR1SI COMO POSIBLES MATERIALES PARA DISPOSITIVOS MÉDICOS

Jiménez-Marcos, Cristina; Mirza-Rosca, Julia Claudia; Simona-Baltatu, Madalina; Vizureanu, Petrica

Para que así conste a los efectos oportunos, firmo en San Cristóbal de La Laguna.

Dña. Carolina González Navasa
Directora del CIMED

Dña. Olivia Marín Delgado
Coordinadora del CIMED

CERTIFICADO

Este certificado se otorga a:

Cristina Jiménez Marcos

Por ser galardonado con el premio a la mejor **Póster** en el área de conocimiento **Ingenierías y Arquitectura / Engineering and Architecture** por el trabajo de investigación:

EVALUACIÓN DE NUEVAS ALEACIONES DE TITANIO TI15MO7ZR Y TI15MO7ZR1SI COMO POSIBLES MATERIALES PARA DISPOSITIVOS MÉDICOS

Jiménez Marcos, Cristina; Mirza Rosca, Julia Claudia; Simona Baltatu, Madalina; Vizureanu, Petrica

Presentado en la I Edición del **Congreso Internacional Multidisciplinar de Estudiantes de Doctorado (CIMED)** celebrado los días 22-24 de marzo de 2023 en formato semipresencial en San Cristóbal de La Laguna (Tenerife, España).

Para que así conste a los efectos oportunos, firmo en San Cristóbal de La Laguna.

Dña. Carolina González Navasa
Directora del CIMED

Dña. Olivia Marín Delgado
Coordinadora del CIMED

Congreso Internacional Multidisciplinar de Estudiantes de Doctorado (CIMED)

Universidad de La Laguna

CIMED

EVALUACIÓN DE NUEVAS ALEACIONES DE TITANIO TI15MO7ZR Y TI15MO7ZR1SI COMO POSIBLES MATERIALES PARA DISPOSITIVOS MÉDICOS

Jiménez-Marcos, Cristina[a,b]; Mirza-Rosca, Julia Claudia[a]; Baltatu-Madalina, Simona[c]; Vizureanu, Petrica[c].

[a]Departamento de Ingeniería Mecánica, Universidad de Las Palmas de Gran Canaria, Las Palmas de Gran Canaria, España.
[b]Doctorado en Ingenierías Química, Mecánica y de Fabricación, Universidad de Las Palmas de Gran Canaria, Las Palmas de Gran Canaria, España.
[c]Departamento de Tecnologías y Equipos para el Procesado de Materiales, Universidad Técnica "Gheorghe Asachi de Iasi, Iasi, Rumanía.

Especialidad: Ingeniería Mecánica.

Palabras clave: Aleaciones de titanio, metalografía, corrosión, flexión en tres puntos, microdureza.

En los últimos años, los avances en medicina y procesamiento de materiales han permitido desarrollar nuevos biomateriales, especialmente metálicos como las aleaciones de titanio, los cuales han prevalecido sobre otros materiales convencionales debido a sus buenas propiedades mecánicas, resistencia a la corrosión y biocompatibilidad con materiales biológicos.

En este estudio, se investigaron los efectos de dos concentraciones diferentes de silicio sobre las propiedades mecánicas y el comportamiento de resistencia a la corrosión de las nuevas aleaciones Ti15Mo7ZrxSi mediante pruebas metalográficas, electroquímicas, de microdureza y de flexión.

Las aleaciones se obtuvieron aplicando el proceso de refundición por arco en vacío a partir de materias primas de gran pureza. Para realizar los ensayos, sus superficies se prepararon mediante corte, empastillado en resina epoxi, su posterior esmerilado y pulido y, finalmente, su limpieza utilizando una máquina de ultrasonidos calentada. La caracterización estructural se realizó utilizando el microscopio metalográfico Axio Vert.A1 MAT ZEISS; para determinar la dureza se empleó el microdurómetro Affri DM8 B, y para el módulo de elasticidad, la máquina Bose ElectroForce® 3100. Se efectuaron ensayos electroquímicos en corriente continua y corriente alterna con el potentiostato BioLogic Essential SP-150 y los espectros de impedancia fueron modelados con circuitos eléctricos equivalentes [1–3].

EUROINVENT
International Conference on Innovative Research
Iasi, 11th–12st of May 2023

Analysis of novel Ti15Mo7ZrxSi titanium alloys experimentally developed as potential materials for medical uses

Cristina Jiménez-Marcos[1], Julia C. Mirza-Rosca*[1], Madalina S. Baltatu[2], Petrica Vizureanu[2]

[1] Mechanical Engineering Dept., University of Las Palmas de Gran Canaria, University Campus of Tafira, Engineering building, 35017, Las Palmas de Gran Canaria, Spain

[2] Department of Technologies and Equipments for Materials Processing, Faculty of Materials Science and Engineering, Gheorghe Asachi Technical University of Iaşi, Blvd. Mangeron, No. 51, 700050 Iasi, Romania

PURPOSE

The aim of this study is to examine the biocompatibility and mechanical properties of two innovative titanium alloys, Ti15Mo7ZrxSi (x = 0, 0.5, 0.75, 1). Electrochemical, metallographic, and three-point bending tests were carried out to determine the corrosion behavior, microstructure, and Young's modulus of the samples studied.

Samples	Ti (%)	Mo (%)	Zr (%)	Si (%)
TiMoZr	78.00	15.00	7.00	-
TiMoZrSi0.5	77.50	15.00	7.00	0.50
TiMoZrSi0.75	77.25	15.00	7.00	0.75
TiMoZrSi1	77.00	15.00	7.00	1.00

MATERIALS AND METHODS

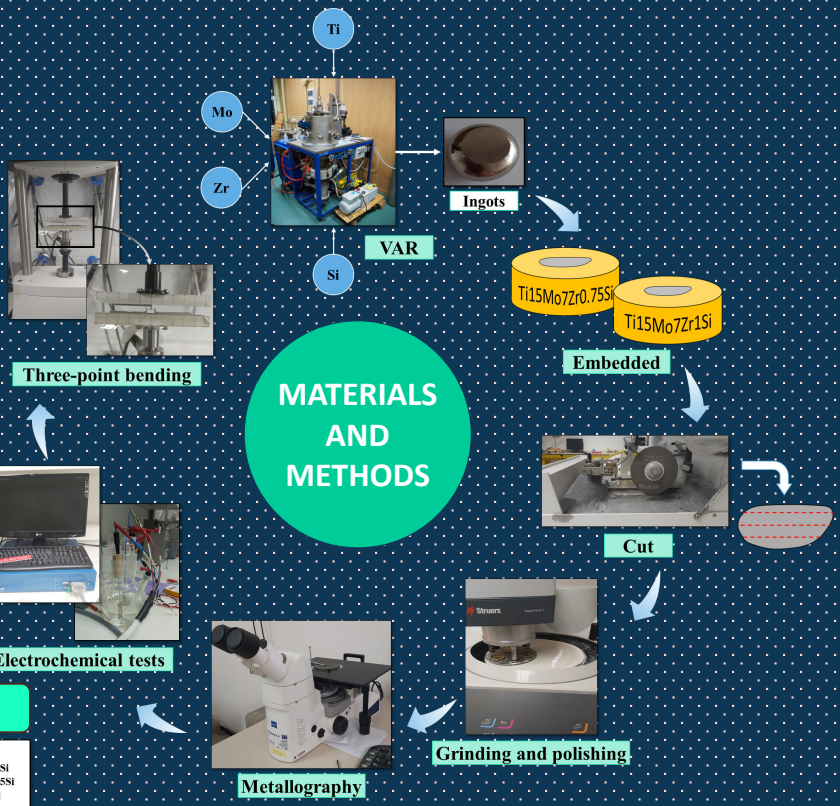

ELECTROCHEMICAL TESTS

CORROSION POTENTIAL

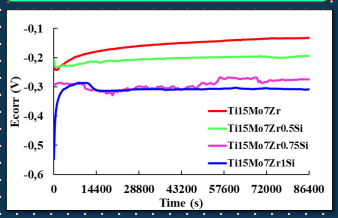

CORROSION RATE

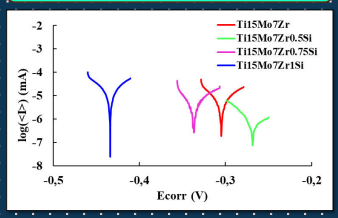

ELECTROCHEMICAL IMPEDANCE SPECTROSCOPY

Ti15Mo7Zr

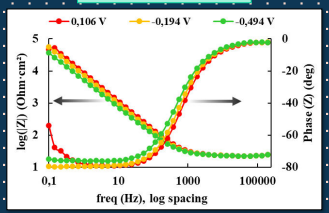

Ti15Mo7Zr0.5Si

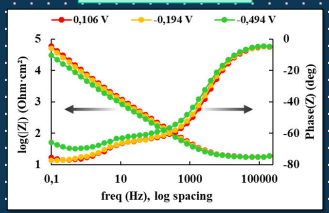

Ti15Mo7Zr0.75Si

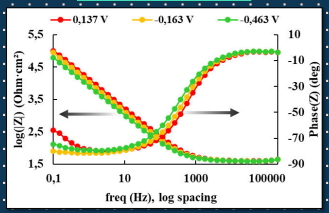

Ti15Mo7Zr1Si

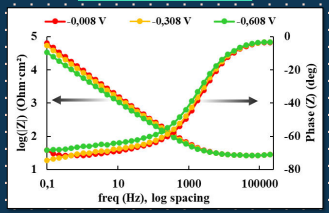

METALLOGRAPHY TEST

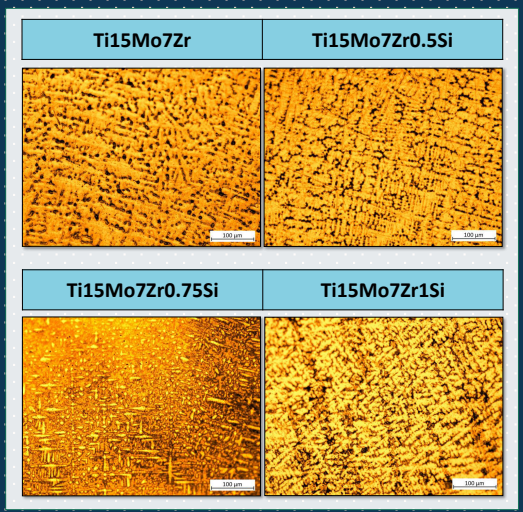

THREE-POINT BENDING TEST

Samples	TiMoZr	Ti15Mo7ZrSi0.5	Ti15Mo7ZrSi0.75	Ti15Mo7ZrSi1
Young's modulus (Gpa)	82.4 ± 9.2	61.5 ± 8.4	66.0 ± 8.0	73.4 ± 8.2

CONCLUSIONS

The study samples Ti15Mo7Zr0.5Si and Ti15Mo7Zr0.75Si have shown high corrosion potentials, lower corrosion rates and thus higher corrosion resistance, as well as modulus of elasticity values similar and closer to those of human bone. In conclusion, the evidence from this study suggests that both alloys show good corrosion behavior, high biocompatibility and modulus of elasticity values lower than those of commercial alloys used in biomedical implants.

Book of Abstracts

EUROINVENT
ICIR 2023

International Conference on Innovative Research

May 11th to 12th, 2023

Iasi – Romania

Organized by:

- **Romanian Inventors Forum**
- **Faculty of Materials Science and Engineering, The "Gheorghe Asachi" Technical University of Iasi, Romania**
- **ARHEOINVEST Platform, Alexandru Ioan Cuza University of Iasi**
- **Centre of Excellence Geopolymer and Green Technology CEGeoGTech), Universiti Malaysia Perlis (UniMAP)**
- **Department of Physics, Czestochowa University of Technology, Częstochowa, Poland**

With support of:

- **Universiti Malaysia Terengganu**
- **International Federation of Inventors' Associations - IFIA**
- **World Invention Intellectual Property Associations – WIIPA**

Editors:

Andrei Victor SANDU, Mohd Mustafa Al Bakri ABDULLAH,

Petrică VIZUREANU, Marcin NABIALEK, Che Mohd Ruzaidi GHAZALI, Ion SANDU

Analysis Of Novel Ti15Mo7ZrxSi Titanium Alloys Experimentally Developed as Potential Materials for Medical Uses

Cristina JIMÉNEZ MARCOS[1], Julia Claudia MIRZA ROSCA[1*], Madalina Simona BALTATU[2], Petrica VIZUREANU[2]

[1]Mechanical Engineering Department, University of Las Palmas de Gran Canaria, Campus Universitario Tafira, Edif. Ingenieria, 35017, Gran Canaria, Spain
[2]Department of Technologies and Equipment for Materials Processing, "Gheorghe Asachi" Technical University of Iasi, Bulevardul Profesor Dimitrie Mangeron 67, Iași 700050, Romania

[*]julia.mirza@ulpgc.es

Abstract. The aim of this study is to examine the biocompatibility and mechanical properties of two innovative titanium alloys, Ti15Mo7ZrxSi (x = 0, 0.5, 0.75, 1). These samples have been previously prepared by chipping, cutting, grinding and polishing [1]. Electrochemical, metallographic and three-point bending tests were carried out to determine the corrosion behaviour, microstructure and Young's modulus of the samples studied. The first set of analyses indicated the biphasic and dendritic structures of both samples, elastic modulus that are approximately 20 GPa away from the maximum and minimum values obtained, and positive behaviour in contact with physiological fluids at room temperature. The study samples Ti15Mo7Zr0.5Si and Ti15Mo7Zr0.75Si have shown high corrosion potentials, lower corrosion rates and thus higher corrosion resistance, as well as modulus of elasticity values similar and closer to those of human bone. In conclusion, the evidence from this study suggests that both alloys show good corrosion behaviour, high biocompatibility and modulus of elasticity values lower than those of commercial alloys used in biomedical implants.

Keywords: biomaterial, titanium alloy, biocompatibility, microstructure, corrosion resistance, modulus of elasticity.

References:

[1] C. Jimenez-Marcos, J.C. Mirza-Rosca, M.S. Baltatu, P. Vizureanu. Experimental Research on New Developed Titanium Alloys for Biomedical Applications. *Bioengineering*, 9(11), (2022), 686.

Evaluation of New Titanium Alloys as Potential Materials for Medical Devices

Cristina Jiménez-Marcos[1], Julia Claudia Mirza-Rosca[1*], Madalina Simona Baltatu[2], Petrica Vizureanu[2]

[1.] Department of Mechanical Engineering, University of Las Palmas de Gran Canaria, Las Palmas de Gran Canaria, Spain

[2.] Department of Technologies and Equipment for Materials Processing, "Gheorghe Asachi" Technical University of Iasi, Iasi, Romania

PURPOSE

Two novel Ti20Mo7ZrxSi (x = 0.75, 1) alloys were produced by vacuum arc remelting (VAR) furnace, and this study examined their microstructure, corrosion behaviour, quantitative microanalysis, Young's modulus and hardness. Metallography, scanning electron microscopy, electrochemistry, three-point bending, and microhardness testing were some of the used techniques for this study.

SAMPLES PREPARATION

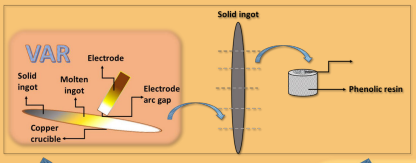

Samples	Ti (%)	Mo (%)	Zr (%)	Si (%)
Ti20Mo7Zr0.75Si	72.25	20.00	7.00	0.75
Ti20Mo7Zr1Si	72.00	20.00	7.00	1.00

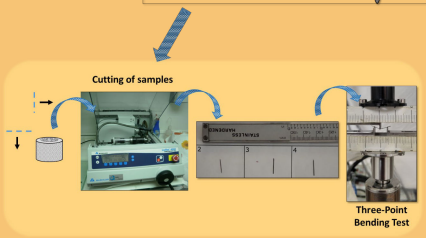

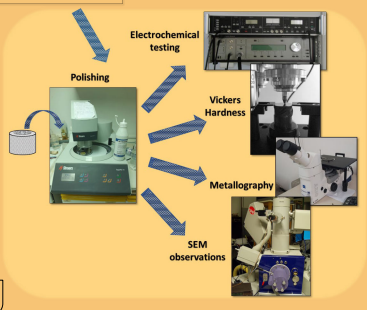

ELECTROCHEMICAL TESTS

CORROSION POTENTIAL

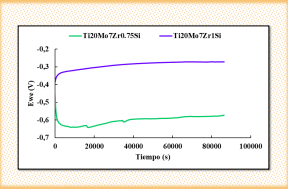

ELECTROCHEMICAL IMPEDANCE SPECTROSCOPY

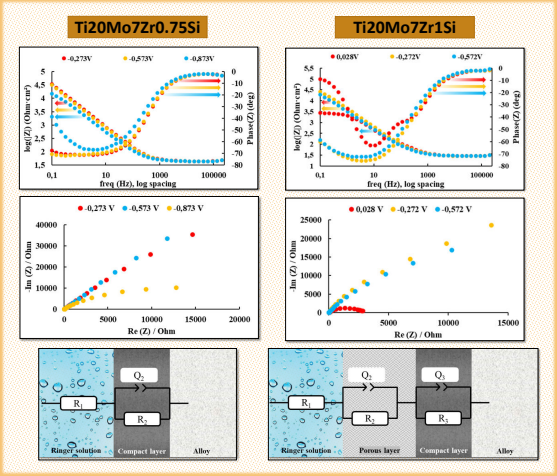

MICROSTRUCTURAL CHARACTERIZATION

METALLOGRAPHY

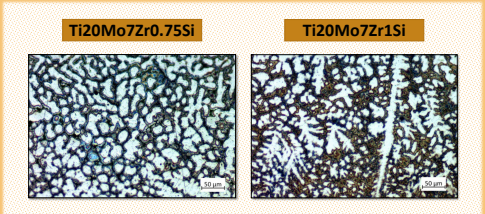

SCANNING ELECTRON MICROSCOPY

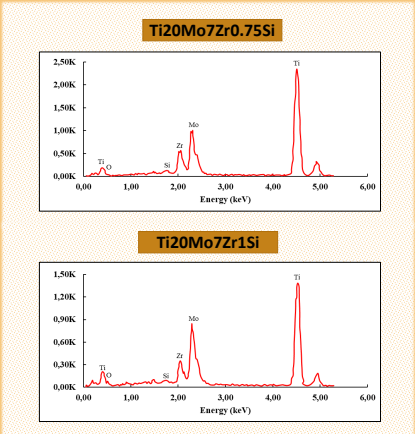

MICROHARDNESS

Load (gf)	Ti20Mo7Zr0.75		Ti20Mo7Zr1Si	
	Microhardness (HV)		Microhardness (HV)	
	Soft phase	Hard phase	Soft phase	Hard phase
5	214	365	115	243
25	239	383	137	366
50	319	399	158	356

THREE-POINT BENDING TEST

Sample	Modulus of elasticity E (GPa)
Ti20Mo7Zr0.75Si	54.4 ± 6.5
Ti20Mo7Zr1Si	82.7 ± 21.5

CONCLUSIONS

This research investigated the effect of silicon concentration on microstructure, biocompatibility, modulus of elasticity, microhardness and corrosion resistance of the TiMoZrSi alloy in a simulated body fluid. Two zones, one rich in titanium and the other in Mo, Zr, and Si, were found on the surface of the alloys. In electrochemical tests, the potential of the TiMoZrSi0.75 sample tended to corrode and showed lower corrosion resistance. The modulus of elasticity was less than that of many commercial alloys, and the Vickers hardness values increased as the silicon content increased.

Influence and Comparison of the Properties of Three Cobalt-Chromium Dental Alloys

Cristina Jiménez-Marcos[1], Julia Claudia Mirza-Rosca[1*], Anca Fratila[2], Adriana Saceleanu[2]

[1.] Department of Mechanical Engineering, University of Las Palmas de Gran Canaria, Las Palmas de Gran Canaria, Spain.

[2.] Department of Dentistry and Nursing, Faculty of Medicine, Lucian Blaga University of Sibiu, Sibiu, Romania

PURPOSE

The current study used metallography, electrochemical testing, and three-point bending tests to analyze and compare the corrosion effects and mechanical characteristics of three samples of Co-Cr alloys, called "P1", "P2" and "P3"

Composition (in wt.%)	P1	P2	P3
Co	61.00	63.00	64.00
C	31.00	28.00	28.50
Mo	5.00	0.50	5.00
W	-	3.00	-
Nb	-	4.00	-
C	0.75	-	0.50
Fe	0.75	0.50	-
Si	0.75	1.00	1.00
Mn	0.75	-	1.00

SAMPLES PREPARATION

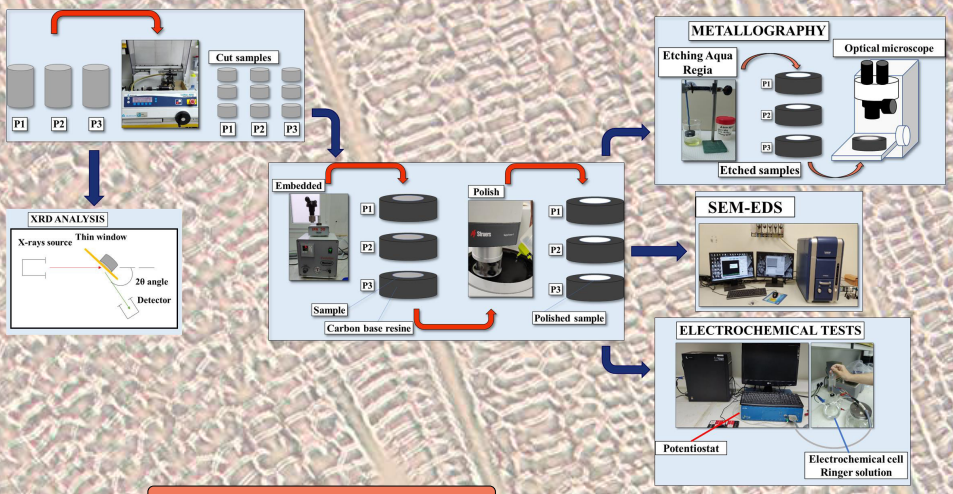

MICROSTRUCTURAL CHARACTERIZATION

METALLOGRAPHY

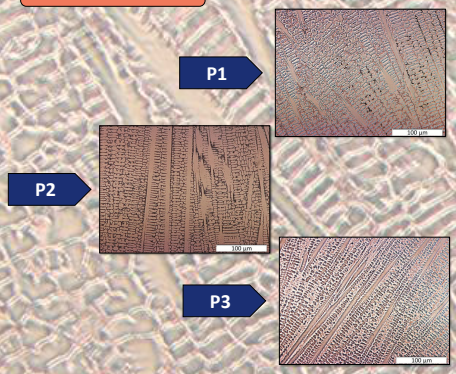

SCANNING ELECTRON MICROSCOPY

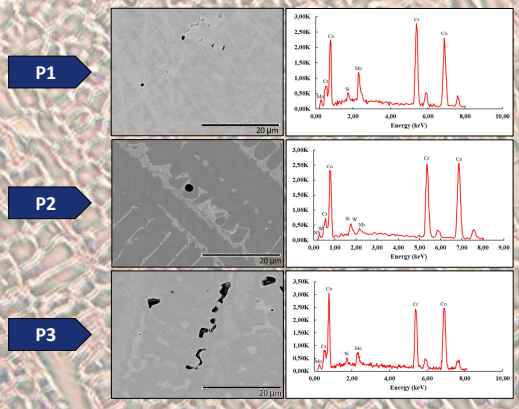

X-RAY DIFFRACTION

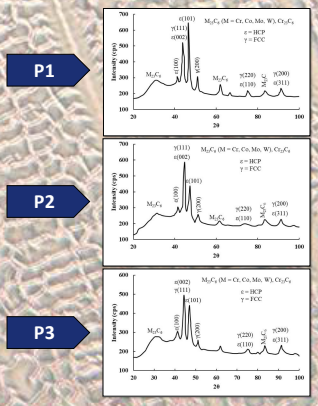

ELECTROCHEMICAL TESTS

CORROSION POTENTIAL

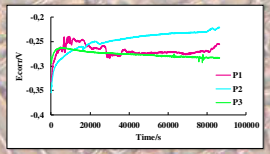

ELECTROCHEMICAL IMPEDANCE SPECTROSCOPY

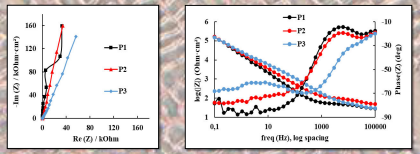

CONCLUSIONS

After analysing the results obtained, it was possible to confirm the two-phase structure of the samples and their tendency to passivation and good behaviour in contact with physiological fluids, with the sample P2 being slightly superior. Furthermore, it could be observed that the samples were mainly composed of the items listed in their respective data sheets and identified the presence of a ε phase with HCP structure, a γ phase with an FCC structure in addition to small phases of various metallic carbides. Therefore, the three samples studied presented good chemical, biological characteristics, the latter being improved by the addition of tungsten and niobium.

Evaluation of the Mechanical and Corrosion Properties of New Ti Alloys for Orthopedic Devices

Cristina Jiménez-Marcos[1], Julia Claudia Mirza-Rosca[1,2*], Madalina Simona Baltatu[3], Petrica Vizureanu[3]

[1] Mechanical Engineering Department, University of Las Palmas de Gran Canaria, Las Palmas de Gran Canaria, Spain

[2] Transilvania University of Brasov, Materials Engineering and Welding Department, Brasov, Romania

[3] Department of Technologies and Equipment for Materials Processing, Gheorghe Asachi Technical University of Iasi, Iasi, Romania

PURPOSE

The main objective of this research is to characterize and compare the mechanical and chemical properties and the degree of biocompatibility of the new titanium alloys Sample 1 (62% Ti 15% Mo, 7% Zr, 15% Ta, 1% Si) and Sample 2 (57% Ti 20% Mo, 7% Zr, 15% Ta, 1.00% Si) for possible applications in biomedical devices and thus contribute to improve the quality of life of patients and reduce the need for additional surgeries. For this purpose, metallography, electrochemical and microhardness tests were carried out.

MICROHARDNESS

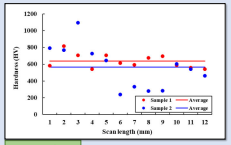

1gf

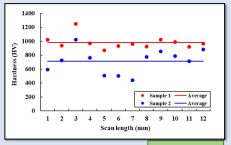

5gf

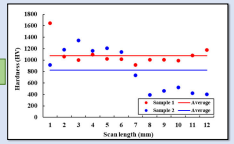

10gf

Load (gf)	Alloy	Average (HV)	Min (HV)	Max (HV)
1	Sample 1	639 ± 85	545	820
	Sample 2	567 ± 260	240	1097
5	Sample 1	980 ± 95	870	1249
	Sample 2	714 ± 174	441	1025
10	Sample 1	1085 ± 189	913	1649
	Sample 2	824 ± 372	390	1344

SAMPLES PREPARATION

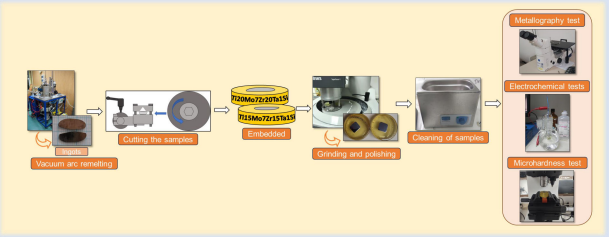

ELECTROCHEMICAL TESTS

CORROSION POTENTIAL

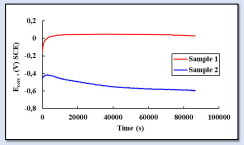

Alloy	OCP, (V) vs SCE		
	Initial	After 2 hours	After 24 hours
Sample 1	-0.16	0.03	0.03
Sample 2	-0.46	-0.44	-0.26

ELECTROCHEMICAL IMPEDANCE SPECTROSCOPY

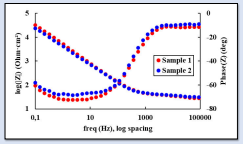

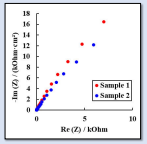

METALLOGRAPHY

Sample 1

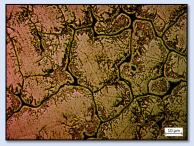

Sample 2

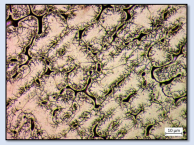

CONCLUSIONS

- In the metallographic test, the surfaces of both samples show biphasic dendritic patterns after exposure to Kroll's reagent and show showed soft and hard areas when different loads where applied.
- In the electrochemical tests, the samples showed good behavior in physiological fluids, due to their corrosion potential values and the Nyquist and Bode diagrams of the electrochemical impedance spectroscopy, with superior corrosion resistance and passivation capacity for the Sample 1 sample.

According to the results obtained, both samples would behave favorably in the human body.

The Third International Symposium on Modern Engineering Equipment and Technology

(TisMeet 2024) October 11th-13th, 2024 Shenyang, China

Certificate of Participation

THIS CERTIFICATE IS PROUDLY AWARDED TO

Cristina JIMENEZ MARCOS

from

Las Palmas de Gran Canaria University

This is to certify that **Cristina JIMENEZ MARCOS** has participated in The Third International Symposium on Modern Engineering Equipment and Technology (TisMeet 2024) as one of the oral speakers. And the title of oral speech is **Special titanium alloys for biomedical devices.**

The Committee of TisMeet 2024

October 12th, 2024

SPECIAL TITANIUM ALLOYS FOR BIOMEDICAL DEVICES

Cristina Jiménez-Marcos
Julia Claudia Mirza-Rosca
Madalina Baltatu
Petrica Vizureanu

1 INTRODUCCIÓN

2 PUBLICACIONES

3 DOCUMENTOS DE AUTORÍA

4 PARTICIPACIONES EN CONGRESOS

5 OTRAS PUBLICACIONES

6 CONCLUSIONES FINALES

A continuación, se presentan otras de las **publicaciones** enviadas y aceptadas durante estos tres años de realización de la tesis:

- **Capítulo de libro.** Cristina Jiménez-Marcos; Santiago José Brito-García; Julia Claudia Mirza-Rosca; Madalina Simona Baltatu; Petrica Vizureanu. 2022. Influence of Silicon Addition on The Properties of New Titanium Alloys. PROCEEDINGS OF THE 28th International Symposium on Analytical and Environmental Problems. pp.184-186. ISBN 978-963-306-904-2.
- **Capítulo de libro.** Cristina Jiménez-Marcos; Julia Claudia Mirza-Rosca; Madalina Simona Baltatu; Petrica Vizureanu. 2022. Previous Studies of New Developed Titanium Alloys for Biomedical Applications. PROCEEDINGS BOOK. pp.788-789. ISBN 978-605-73639-5-4.
- **Artículo científico.** Santiago Jose Brito-Garcia; Julia Claudia Mirza-Rosca; Cristina Jimenez-Marcos; Ionelia Voiculescu. 2023. Impact of Ti Doping on the Microstructure and Mechanical Properties of CoCrFeMoNi High-Entropy Alloy. Metals. MDPI. 13-5, pp.1-13. https://doi.org/10.3390/met13050854
- **Artículo científico.** Santiago Jose Brito-Garcia; Julia Claudia Mirza-Rosca; Cristina Jimenez-Marcos; Ionelia Voiculescu. 2023. EIS Study of Doped High-Entropy Alloy. Metals. MDPI. 13-5, pp.1-17. https://doi.org/10.3390/met13050883
- **Artículo científico.** Anca Fratila; Cristina Jimenez-Marcos; Julia Claudia Mirza-Rosca; Adriana Saceleanu. 2023. Mechanical properties and biocompatibility of various cobalt chromium dental alloys. Materials Chemistry and Physics. Elsevier. 304-127867, pp.1-9. https://doi.org/10.1016/j.matchemphys.2023.127867

- **Artículo científico.** Cristina Jiménez-Marcos; Julia Claudia Mirza-Rosca; Anca Fratila; Adriana Saceleanu. 2023. Influence and Comparison of the Properties of Three Cobalt-Chromium Dental Alloys. Microscopy and Microanalysis. Oxford Academic. 29-1, pp.156-160. https://doi.org/10.1093/micmic/ozad067.071
- **Artículo científico.** Santiago Brito-García; Cristina Jiménez-Marcos; Julia Mirza-Rosca; Ionelia Voiculescu. 2023. Behavior of Ti-doped CoCrFeMoNi High Entropy Alloy. Microscopy and Microanalysis. Oxford Academic. 29-1, pp.439-444. https://doi.org/10.1093/micmic/ozad067.208
- **Artículo científico.** Santiago Brito-García; Cristina Jiménez-Marcos; Julia Mirza-Rosca; Ionelia Voiculescu. 2023. An Investigation of Elastic Modulus in Zr Doped CoCrFeMoNi HEA by Three-Point Bending. Microscopy and Microanalysis. Oxford Academic. 29-1, pp.1527-1528. https://doi.org/10.1093/micmic/ozad067.786
- **Artículo científico.** Cristina Jiménez-Marcos; Julia Claudia Mirza-Rosca; Madalina Simona Baltatu; Petrica Vizureanu. 2024. Evaluation of the Mechanical and Corrosion Properties of New Ti Alloys for Orthopedic Devices. Microscopy and Microanalysis. Oxford Academic. https://doi.org/10.1093/mam/ozae044.461
- **Artículo científico aceptado.** Cristina Jiménez-Marcos; Julia Claudia Mirza-Rosca; Dinu Vermesan; Adriana Saceleanu. 2025. Evaluation of the structure, microhardness and corrosion properties of cobalt-chromium dental alloys with two different cooling media. International Journal of Metalcasting. Springer Nature.

PROCEEDINGS OF THE

28th International Symposium on Analytical and Environmental Problems

Szeged, Hungary

November 14-15, 2022

INFLUENCE OF SILICON ADDITION ON THE PROPERTIES OF NEW TITANIUM ALLOYS

Cristina Jiménez-Marcos[1], Santiago José Brito García[1], Julia Claudia Mirza-Rosca[1]*, Madalina Simona Baltatu[2], Petrica Vizureanu[2]

[1]Mechanical Engineering Department, Las Palmas de Gran Canaria University, 35017 Tafira, Spain
[2]Department of Technologies and Equipments for Materials Processing, Faculty of Materials Science and Engineering, Gheorghe Asachi Technical University of Iaşi, Blvd. Mangeron, No. 51, 700050 Iasi, Romania
e-mail: julia.mirza@ulpgc.es

Abstract
The mechanical characteristics and electrochemical behavior of the new titanium alloys TiMoZr, TiMoZrSi0.5, TiMoZrSi0.75 and TiMoZrSi1 were studied to determine their microstructure, corrosion behavior and mechanical properties. Following the use of the appropriate procedures, metallographic analysis showed that both samples had biphasic and dendritic structures. According to electrochemical tests in body simulation fluid, the samples' corrosion resistance increases with decreasing silicon content since silicon-containing samples corrode more quickly. Electrochemical Impedance Spectroscopy measurements were performed at various potentials, and the acquired spectra show a two-time constant system, due to the presence of a double-layer passive film on the samples. The three-point bending test for both samples demonstrated that the values of modulus of elasticity are lower than those commercial alloys and nearly to the cortical human bone, and the microhardness test showed that the samples' surfaces had soft and hard phases.

Introduction
Nowadays, due to the increasing use of biomaterials in various fields of medicine, they must have a number of characteristics: high biocompatibility, ductility, fatigue and wear resistance, osseointegration, absence of cytotoxicity and a combination of high strength and low Young's modulus equivalent to human cortical bone ranging between 10 and 30 Gpa [1–3].
About 70-80% of implants are made of metallic biomaterials [4], with Ti and its alloys being the most widely used, as they can modify their properties by changing the composition of the alloying elements, their biocompatibility with biological materials, high corrosion resistance, high mechanical performance, low modulus and high thermal stability [3,5–7]. The Ti6Al4V alloy is the most commonly used alloy for orthopaedic applications, although vanadium is a carcinogenic and toxic material and aluminium, in large concentrations, can cause dementia or Alzheimer's [8].
Consequently, it was decided to determine the effects of four different silicon concentrations on the microstructure, corrosion behaviour, quantitative microanalysis, modulus of elasticity and hardness of the new TiMoZrSix alloy by means of metallographic, electrochemical, scanning electron microscopy, three-point bending and microhardness tests.

Experimental
The study of four new alloys with Ti, Mo, Zr, varying the composition of Si, TiMoZr, TiMoZrSi0.5, TiMoZrSi0.75, and TiMoZrSi1, has been carried out with the aim of applying different tests to find out their properties. The production of these alloys was carried out using a Voltaic Arc Remelting (VAR) furnace in which a consumable electrode was melted in a

ICONSAD'22

2nd International Congress on Scientific Advances

2. Uluslararası Bilimsel Gelişmeler Kongresi

21-24 Aralık / December 2022

PROCEEDINGS BOOK

BİLDİRİLER KİTABI

ISBN: 978-605-73639-5-4

Previous Studies of New Developed Titanium Alloys for Biomedical Applications

Cristina Jiménez-Marcos[1], Julia Claudia Mirza-Rosca[*,1], Madalina Simona Baltatu[2], Petrica Vizureanu[2]

[*]: julia.mirza@ulpgc.es, ORCID: 0000-0003-0623-3318

[1]: *Department of Mechanical Engineering, University of Las Palmas de Gran Canaria, Las Palmas de Gran Canaria, Spain*

[2]: *Department of Technologies and Equipment for Materials Processing, "Gheorghe Asachi" Technical University of Iasi, Iasi, Romania*

ABSTRACT

The increasing demand for metallic biomaterials in various medical fields and the problems often encountered with current conventional alloys have led to the determination of the influence of four various silicon concentrations on the microstructure, corrosion behavior, modulus of elasticity and hardness of the new TiMoZrSix (x = 0, 0.5, 0.75, 1) alloy by means of metallographic, electrochemical, three-point bending and microhardness tests.

The fabrication of these alloys was performed utilizing a voltaic arc remelting (VAR) furnace, in which a consumable electrode was melted in a vacuum at a controlled rate with heat generated by the electric arc produced between the electrode and the ingot. Prior to the application of the research methodologies, the samples were embedded in epoxy resin cylinders for subsequent cutting and then, grinding and polishing with progressive grain silicon carbide abrasive papers and 0.1 micrometers alumina suspension. Finally, the samples were cleaned completely by immersing them in an ultrasonic machine for 5 minutes [1,2].

After applying the different techniques, metallographic examination revealed that the four samples exhibited biphasic and dendritic structures, with the addition of silicon reducing the size of dendrites and increasing the interdendritic zone. According to electrochemical studies performed in body simulation fluid, samples with higher silicon concentrations corrode faster, while samples with lower silicon concentrations show higher corrosion resistance. Electrochemical Impedance Spectroscopy measurements were performed at various potentials, and the obtained spectra revealed a two-time constant system, owing to the presence of a double-layer passive film on the samples. Thus, it was demonstrated that the more positive the value of the applied potential, the higher the corrosion resistance, presenting comparable impedance values. Moreover, the microhardness test suggested that the samples' surfaces had both soft and hard phases while the three-point bending test for the samples found that the values of modulus of elasticity were near to those of cortical human bone and lower than those of commercial alloys. Based on the results achieved, this samples showed good and similar chemical, mechanical and biological characteristics, with the Ti20MoZrSi0.5 sample showing slightly superior mechanical properties.

Keywords—*Biomaterial; Corrosion; Metallography; Microhardness; Three-Point Bending*

[1] Jiménez-Marcos, C., Baltatu, M. S., Florido-Suárez, N. R., Socorro-Perdomo, P. P., Vizureanu, P., y Mirza-Rosca, J. C. (2022). Mechanical properties and corrosion resistance of two new titanium alloys for orthopaedics applications. *Materials Today: Proceedings*,

metals

MDPI

Article

Impact of Ti Doping on the Microstructure and Mechanical Properties of CoCrFeMoNi High-Entropy Alloy

Santiago Jose Brito-Garcia [1], Julia Claudia Mirza-Rosca [1,2,*], Cristina Jimenez-Marcos [1] and Ionelia Voiculescu [3]

[1] Mechanical Engineering Department, University of Las Palmas de Gran Canaria, 35001 Las Palmas de Gran Canaria, Spain
[2] Materials Engineering, and Welding Department, Transilvania University of Brasov, 500036 Brasov, Romania
[3] Faculty of Industrial Engineering and Robotics, Politehnica University of Bucharest, 060042 Bucharest, Romania
* Correspondence: julia.mirza@ulpgc.es

Abstract: The design principle of high-entropy alloys is to mix many chemical elements in equal or nearly equal proportions to create new alloys with unique and special properties such as high strength, ductility and corrosion resistance. Some properties of high-entropy alloys can be adjusted via introducing new doping elements, which are selected according to working conditions. The high-entropy alloy CoCrFeMoNi was examined to determine the impact of Ti doping on its microstructure, microhardness and elastic modulus. Microstructure analysis revealed a core structure consisting of both face-centered cubic (FCC) and body-centered cubic (BCC) phases, along with the formation of a Laves phase. The addition of Ti made the alloy grains finer and reduced the Mo concentration difference between the interdendritic and dendritic regions. As a result of Ti doping, the microhardness of the alloy increased from 369 HV 0.2 to 451 HV 0.2. Ti doping produced a doubling of the breaking strength value, although no significant changes were observed in the elastic modulus of the CoCrFeMoNi alloy.

Keywords: high entropy alloys; Ti-doping; microstructure; microhardness; three-point bending

Citation: Brito-Garcia, S.J.; Mirza-Rosca, J.C.; Jimenez-Marcos, C.; Voiculescu, I. Impact of Ti Doping on the Microstructure and Mechanical Properties of CoCrFeMoNi High-Entropy Alloy. *Metals* **2023**, *13*, 854. https://doi.org/10.3390/met13050854

Academic Editors: Robert Bidulský and Jana Bidulská

Received: 30 March 2023
Revised: 22 April 2023
Accepted: 24 April 2023
Published: 27 April 2023

1. Introduction

Metallic alloys that contain at least five distinct elements in approximately equal proportions are known as high-entropy alloys (HEAs). HEAs contain numerous principal elements in high concentrations, unlike traditional alloys, which usually contain one or two main elements with minor amounts of other elements added to enhance certain properties. The high-entropy concept was introduced in 2004 by two different groups [1,2] and since then, a variety of HEAs have been developed and studied, including alloys containing elements such as nickel [3,4], aluminum [5,6], titanium [7,8] and molybdenum [9]. One of the defining characteristics of HEAs is their high configurational entropy, which is a measure of the degree of disorder in the arrangement of atoms within a material. Some potential applications of HEAs include high-temperature materials for use in jet engines or nuclear reactors [9,10], lightweight alloys for use in the aerospace or automotive industries [11,12] and corrosion-resistant coatings for use in harsh environments [13–15]. Recently, high-entropy alloys have been created for potential use in extremely effective electrochemical devices that efficiently and sustainably transform fuel energy into electricity [16]. While HEAs are a relatively new class of materials, research in this area is rapidly expanding, and there is significant interest in exploring their potential properties and applications.

The field of high-entropy alloys has found that CoCrFeMoNi possesses exceptional mechanical properties, including impressive strength and flexibility even when exposed to extremely low temperatures [17,18]. These properties, particularly its high-temperature strength and ductility, make CoCrFeMoNi a promising material for use in high-temperature structures such as gas turbines and nuclear reactors [19]. Additionally, adding Nb and

metals

MDPI

Article

EIS Study of Doped High-Entropy Alloy

Santiago Jose Brito-Garcia [1], Julia Claudia Mirza-Rosca [1,2,*], Cristina Jimenez-Marcos [1] and Ionelia Voiculescu [3]

[1] Mechanical Engineering Department, University of Las Palmas de Gran Canaria, 3500 Las Palmas de Gran Canaria, Spain
[2] Materials Engineering, and Welding Department, Transilvania University of Brasov, 500036 Brasov, Romania
[3] Faculty of Industrial Engineering and Robotics, Politehnica University of Bucharest, 060042 Bucharest, Romania
* Correspondence: julia.mirza@ulpgc.es

Abstract: The promising results obtained in the research of high-entropy alloys are increasingly encouraging new configurations of these alloys. Our research was conducted on the high-entropy CoCrFeMoNi alloy and the Ti-doped CoCrFeMoNi alloy. Electrochemical impedance spectroscopy (EIS) measurements were performed on samples with and without Ti-doped CoCrFeMoNi high-entropy alloys in order to evaluate the influence of voltage on their behavior in a simulated aggressive environment. The impedance spectra were measured between −1.0 and +0.8 V vs. SCE at various potential levels. Using an electrical equivalent circuit to match the experimental data, the impedance spectra were analyzed. The corresponding circuit that successfully fits the spectra has two time constants: the first one is for the attributes of the compact passive layer and the second one is for the features of the porous passive layer. The results show that doping CoCrFeMoNi alloy with 0.36 at.% Ti reduces the alloy's ability to resist corrosion, as the alloy can react more quickly to the surrounding environment and cause a decrease in the corrosion resistance of the alloy.

Keywords: high-entropy alloys; Ti doping; EIS; equivalent circuit; corrosion resistance

Citation: Brito-Garcia, S.J.; Mirza-Rosca, J.C.; Jimenez-Marcos, C.; Voiculescu, I. EIS Study of Doped High-Entropy Alloy. *Metals* **2023**, *13*, 883. https://doi.org/10.3390/met13050883

Academic Editor: Sundeep Mukherjee

Received: 27 March 2023
Revised: 28 April 2023
Accepted: 29 April 2023
Published: 2 May 2023

1. Introduction

High-entropy alloys (HEAs) are a new class of materials that have received a lot of attention recently due to their special qualities and promising applications in many areas [1–3]. HEAs are made up of multiple metallic elements, typically five or more, mixed together in roughly equal proportions. This results in a random atomic arrangement, which gives rise to exceptional properties, such as high strength, high ductility, excellent corrosion resistance, and high-temperature stability.

HEAs have gained widespread interest in the scientific community due to their potential to revolutionize the design of structural materials, particularly in aerospace [4], energy [5–8], and biomedical industries [9–12]. Researchers are exploring various aspects of HEAs, including synthesis, characterization, and mechanical behavior, to better understand their fundamental properties and optimize their performance.

In this field of high-entropy alloys, CoCrFeMoNi has been reported to have remarkable mechanical qualities, such as high strength and superior ductility, even at cryogenic temperatures [13]. In particular, the high-temperature strength and ductility of CoCrFeMoNi HEA make it a promising candidate for high-temperature structural applications [14], such as in gas turbines and nuclear reactors, and with Nb and different concentrations of Mo, has improved corrosion resistance of the load-bearing parts of marine equipment [15]. An ion sulfurizing technique was applied to CoCrFeMoNi HEA, and the tribological properties were improved greatly due to the fabrication of lubricant phases during sulfurization [13].

Doping refers to the intentional addition of small amounts of one element to another material in order to modify its properties [16]. When metals are used as dopants, they can have various effects on the material's properties, depending on the specific metal and the material being doped.

Materials Chemistry and Physics 304 (2023) 127867

Contents lists available at ScienceDirect

Materials Chemistry and Physics

journal homepage: www.elsevier.com/locate/matchemphys

Mechanical properties and biocompatibility of various cobalt chromium dental alloys

Anca Fratila [a], Cristina Jimenez-Marcos [b], Julia Claudia Mirza-Rosca [b,c,*], Adriana Saceleanu [a]

[a] "Lucian Blaga" University of Sibiu, Medicine Faculty, 550024, Sibiu, Romania
[b] Las Palmas de Gran Canaria University, Department of Mechanical Engineering, Tafira, 35017, Spain
[c] Transilvania University of Brasov, Materials Engineering, and Welding Department, 500036, Brasov, Romania

HIGHLIGHTS

- Dental alloys undergo spontaneous passivation due to a passive film on their surface.
- The passive potential range is large and the samples showed a good pitting corrosion resistance.
- The thickness of the passive film increases with the potential, with a capacitive response over a wide frequency range.
- Young's modulus was lowest for tungsten-rich sample with 3 points bending test.

GRAPHICAL ABSTRACT

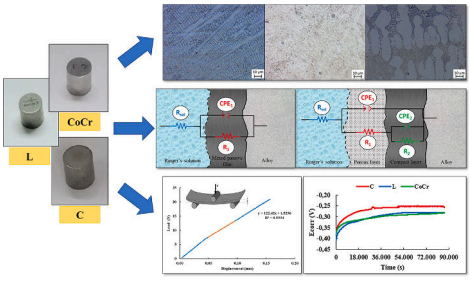

ARTICLE INFO

Keywords:
Dental alloys
Co–Cr
Microstructure
Corrosion
Three-point bending test

ABSTRACT

Cobalt-based metal alloys are often used in dentistry for prosthetic restorations because of their considerable wear and corrosion resistance. For this reason, the effect on the human body of three Co–Cr based alloys, named "Co–Cr", "C" and "L", differing in their concentrations, for subsequent use as dental materials, has been studied and compared. Metallographic observations of the microstructure, electrochemical and three-point bending tests were performed. The metallographic investigations showed similar dendritic microstructure of the Co–Cr and L dental alloys, as well similar porosities and defects. From the corrosion and pitting potential tests, it was found that the samples show surface passivation, reaching closed corrosion potential values from −0.280 V vs SCE to −0.250 V vs SCE. The Pitting Resistance Equivalent Number (PREN) values are above 38 for all the samples, which means that the studied alloys have a high resistance to pitting corrosion. Likewise, when applying the Electrochemical Impedance Spectroscopy technique, a slightly higher corrosion resistance was observed for sample L, since corrosion resistance tends to increase as the applied potential is more positive and as the impedance and phase angle values are higher. Moreover, in the three-point bending test, the alloy C presents the lowest values of the elastic modulus of 134 ± 13 GPa. The analyzed Co–Cr alloys are recommended for the efficient treatment of patients with dental prostheses that have metal frameworks, as shown by all of the obtained results.

* Corresponding author. Las Palmas de Gran Canaria University, Department of Mechanical Engineering, Tafira, 35017, Spain.
E-mail address: julia.mirza@ulpgc.es (J.C. Mirza-Rosca).

https://doi.org/10.1016/j.matchemphys.2023.127867
Received 24 January 2023; Received in revised form 21 April 2023; Accepted 30 April 2023
Available online 5 May 2023

Microscopy and Microanalysis, **29** (Suppl 1), 2023, 156–160
https://doi.org/10.1093/micmic/ozad067.071

Microscopy AND Microanalysis

Meeting-report

Influence and Comparison of the Properties of Three Cobalt-Chromium Dental Alloys

Cristina Jiménez-Marcos[1], Julia Claudia Mirza-Rosca[1,*], Anca Fratila[2], and Adriana Saceleanu[2]

[1]*Department of Mechanical Engineering, University of Las Palmas de Gran Canaria, Las Palmas de Gran Canaria, Spain*
[2]*Department of Dentistry and Nursing, Faculty of Medicine, Lucian Blaga University of Sibiu, Sibiu, Romania*
*Corresponding author: julia.mirza@ulpgc.es

Introduction

The dental materials are a reliable choice for oral rehabilitation because different properties as biocompatibility, non-toxicity, safety, stability, and mechanical qualities are necessary. The most crucial of these qualities is biocompatibility since these materials come into touch with oral tissues and can result in hypersensitivity responses or unfavourable tissue reaction [1].

High creep, corrosion, wear, temperature resistance, hardness, and non-magnetic qualities are the norm for cobalt-based alloys in order to perform their functions without having a detrimental impact on the patient [2,3]. Moreover, when present in these alloys at concentrations between 16 and 20% by weight, chromium enhances hardness, stability, resilience, and boosts corrosion resistance by causing the production of a thin passive protective film under oxidising conditions [4].

The current study used metallography, electrochemical testing, and three-point bending tests to analyze and compare the corrosion effects and mechanical characteristics of three samples of Co-Cr alloys, called "P1", "P2" and "P3" (see the composition wt% in Table 1).

Experimental

To analyze the samples' surface by XRD, the ingots were cut, and three small samples of each alloy were obtained as shown in Figure 1 and an Empyrean diffractometer Malvern-Panalytical was used.

To prepare the surfaces for the rest of the tests, the ingots were first cut, filled with epoxy resin and finally polished (see Figure 2). Optical and SEM microscopy together with electrochemical tests were performed (see Figure 3). The Olympus BX-51 microscope was used for structural characterisation after the chemical etching of the samples with Kroll reagent, together with the scanning electron microscope Hitachi TM3030. The BioLogic Essential SP-150 potentiostat and Ringer's Grifols solution, were used for electrochemical experiments in both continuous and alternate current [6].

Results and discussion

To correctly analyse the microstructure of these samples, it is first necessary to know that the finer the grain size of the samples, the higher the critical current density they will have, since the grain boundaries store internal energy that favours corrosion. Images of the three samples' surfaces after etching are illustrated in Figure 4, showing biphasic and dendritic structures, which are similar for samples P1 and P3 and slightly different for P2, possibly due to the addition of tungsten and niobium and the reduction of molybdenum´s concentration.

SEM observations and EDS results are presented in Figure 5. It could be demonstrated that samples P1 and P3 presented the elements Co, Cr, Mo and Si mainly, while P2 in its main composition showed Co, Cr, W, Nb and Si. The spectra of P1 and P3 were similar, although in the case of P3 there was a reduction in the height of the Mo and Si peaks.

Figure 6 shows the XRD spectra of the alloys examined. The analysis identified the presence of a ϵ phase with a hexagonal close-packed structure (HCP) and a γ phase with a body-centered cubic structure (FCC), which were the main phases of the samples, as well as small phases of various metallic carbides. In the case of sample P1, it showed dominant amounts of HCP ϵ-phase, while for P2 and P3 the prevalence of FCC γ-phase is evident.

For the electrochemical tests, after 24 hours, the corrosion potential (Ecorr) against time graphs for the corrosion test were analysed. Samples P1 and P2 tended to form a passive film, with a higher value of corrosion potential for sample P2, while P3 showed a slight tendency towards corrosion (see Figure 7).

The Bode and Nyquist diagrams were used to plot the curves of the logarithm of the impedance modulus and the phase angle as a function of the logarithm of the frequency for the Co-Cr samples (see Figure 8). The phase angles were higher for sample P1 and lower for sample P3, and the impedance values obtained by the three samples were comparable. The processes of the samples under study were seen to proceed in two phases. Therefore, the P2 alloy demonstrated a greater corrosion resistance.

Conclusions

After analysing the results obtained, it was possible to confirm the two-phase structure of the samples and their tendency to passivation and good behaviour in contact with physiological fluids, with the sample P2 being slightly superior. Furthermore, it could be observed that the samples were mainly composed of the items listed in their respective data sheets and identified the presence of a ϵ phase with HCP structure, a γ phase with an FCC structure in addition to small phases of various metallic carbides. Therefore,

Microscopy and Microanalysis, **29** (Suppl 1), 2023, 439–444
https://doi.org/10.1093/micmic/ozad067.208

Microscopy AND Microanalysis

Meeting-report

Behavior of Ti-doped CoCrFeMoNi High Entropy Alloy

Santiago Brito-García[1], Cristina Jiménez-Marcos[1], Julia Mirza-Rosca[1,*], and Ionelia Voiculescu[2]

[1]*NanCorr Laboratory, University of Las Palmas de Gran Canaria, Las Palmas, Spain*
[2]*Department of Materials Technology and Welding, Politehnica University of Bucharest, Romania*
*Corresponding author: julia.mirza@ulpgc.es

Introduction

High entropy alloys are an extremely diverse and interesting class of materials as they are promising materials for a wide range of industrial applications because they are very hard, heat resistant and show great variability in their magnetic behavior [1,2]. High entropy alloys or HEAs consist of five or more different metallic elements; since their macroscopic properties are highly dependent on interatomic interactions, it is of great interest to probe the local structure and structural disorder around each individual element [3,4]. In recent years, the well-known Cantor alloy (CoCrFeMnNi) has attracted considerable attention due to its excellent toughness and fracture strength but its corrosion resistance is very low because Mn interferes with the passivation process and therefore, in our study we have considered an HEA in which Mn has been replaced with Mo (CoCrFeMoNi). To further improve the properties, the alloy obtained has been microalloyed with titanium.

Experimental

The ingots of each alloy are prepared at LAMET laboratory, Romania, by Vacuum Arc Melting (VAR) in a protective argon atmosphere by using the MRF ABJ 900 VAR equipment and eight remelting operations are carried out for complete homogenization. The raw materials used to form these alloys are 99.00 % pure and the obtained alloys have the composition wt % and at % shown in Table 1. One of the samples, CoCrFeMoNi (named HEA) and that with Ti doping was named (HEATi).

The samples with and without Ti are compared: their microstructure is analyzed by optical microscopy (Olympus BX5, Japan) , SEM and EDS (HITACHI TM3030); the modulus of elasticity of the alloys was studied by a three-point bending test (Electroforce 3100 BOSE Corporation, USA) and their electrochemical responses, by linear polarization (LP) and electrochemical impedance spectroscopy (EIS) using a SP-150 potentiostat (BioLogic, France). The hardness was measured with Shimadzu HMV2T microhardness apparatus (Tokyo, Japan). The samples preparation and analysis is shown in Figure 1.

Results and discussion

a) Microstructure

The optical examination after electrochemical etching is shown a dendritic structure for both samples (See Figure 2). The microstructures were also analyzed by scanning electron microscopy and the compositions were determined by EDS.

b) Elastic modulus and hardness

The elastic modulus was determined and the hardness of both samples was calculated and the results are shown in Table 2. It can be observed that the elastic modulus is similar, but the hardness of Ti-doped sample is improved.

c) Electrochemical behavior

Figure 5 illustrates the potentiodynamic polarization curves of HEA and HEATi in 3.5 wt.% NaCl solution at 25C. The results show that both samples exhibit active dissolution starting at aprox. 0V and almost could not passivate in sodium chloride solution.

The graphs obtained from the EIS tests are presented in Figure 6 for HEA and in Figure 7 for HEATi.

As can be observed in the Nyquist plots presented in Figure 6, and Figure 7, the radius of the semicircle for HEATi is smaller than for HEA, which indicates a low polarization resistance (a low corrosion resistance) for HEATi.

Conclusions

The effects of titanium do ping on the microstructure, elastic modulus, hardness and corrosion properties of CoCrFeNiMo high entropy alloy has been investigated. Simulated corrosive solution of 3.5wt.%NaCl was used to characterize the corrosion behavior of these materials by electrochemical techniques.

- Both alloys exhibited a compact microstructure, with no cracks, porosity or other defects.
- The alloy without titanium is more resistant to corrosion, with a very low corrosion rate.
- The resistance of the passive film decreases with the addition of Ti due to the increasing of the number of defects points in the film. Without Ti the passive layer that forms on the surface of the alloy is more compact and protective [5].

Microscopy and Microanalysis, **29** (Suppl 1), 2023, 1527–1528
https://doi.org/10.1093/micmic/ozad067.786

Microscopy AND Microanalysis

Meeting-report

An Investigation of Elastic Modulus in Zr Doped CoCrFeMoNi HEA by Three-Point Bending

Santiago Brito-García[1], Cristina Jiménez-Marcos[1], Julia Mirza-Rosca[1,*], and Ionelia Voiculescu[2]

[1]*NanCorr Laboratory, University of Las Palmas de Gran Canaria, Las Palmas, Spain*
[2]*Department of Materials Technology and Welding, Politehnica University of Bucharest, Romania*
*Corresponding author: julia.mirza@ulpgc.es

In recent years there has been a great interest in high entropy alloys (HEAs) since they have good mechanical properties, high corrosion resistance and good thermal conductivity among others, which makes them interesting for various fields of research. For this reason, it is important to know their behavior in different conditions that allows us to define the possible applications of these HEA's [1–3]. The literature has been confirming the effect of doping with different elements in the improvement of the mechanical properties and corrosion resistance of HEA's [4]. One of the aspects to be considered in the mechanical properties of a HEA is the strength and fracture toughness of the alloy. These mechanical characteristics are related to the value of the modulus of elasticity (E) of the alloy, which provides information on the cohesion of the material as it is related to the binding energy of the atoms. To calculate the modulus of elasticity of the prepared alloys, a three-point bending test is performed on fibers of the material.

A non-equiatomic high entropy alloy is made with the elements: Co, Cr, Fe, Mo and Ni of chemical composition in percent by weight, wt %, of 20.67, 19.99, 19.88, 20.20 and 19.27 respectively, which we call Sample 1. From this alloy a second one, Sample 2, is obtained by doping with 0.71%wt. Zr. Two ingots are manufactured with high purity elements, 99.00%, in an arc melting furnace model MRF ABJ 900 VAR in a protective argon atmosphere. Six remelting operations are carried out on each ingot to achieve a good homogenization. To obtain an average value of the modulus of elasticity, 10 fibers obtained with a Buehler IsoMet® 4000 precision linear saw machine using 0.5 mm thick tungsten disks are made from the specimens. The fibers have a rectangular section with an average thickness of 0.45 mm and variable length. A three-point bending test is performed in an Electroforce 3100 universal testing machine providing a maximum force (F) of 22N. The fibers are placed in the bending test fixture, see Fig. 1a, and a vertical force is applied at its midpoint until the strand breaks, as in Fig. 1b, or the maximum force is reached. Finally, an analysis of the breakage zones is performed by electron fractography using a Sigma 300 VP field emission scanning electron microscope (FESEM). The observation is performed with the secondary electron detector (SE) at 15 kV at different magnifications.

With the data obtained in the three-point bending test, the force (F) displacement (w) graphs are generated (see Fig. 2). From the straight line obtained in the elastic zone, we take its slope and calculate the modulus of elasticity as $dF/dw = 48EI/L3$, where E is the modulus of elasticity, I is the moment of inertia of the rectangular section and L is the length between supports.

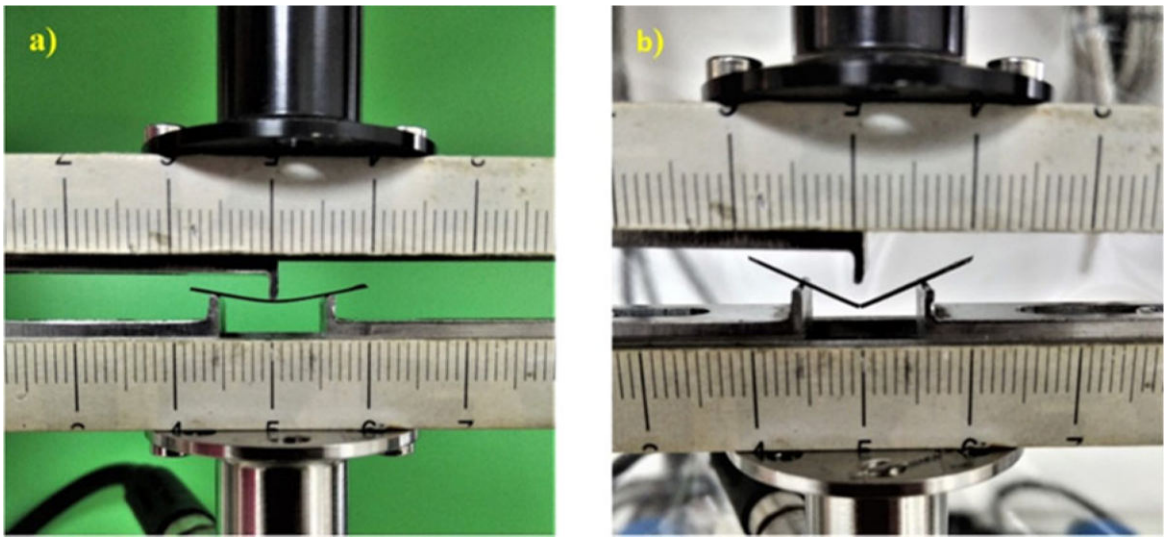

Fig. 1. a) Three-point bending test of one of the specimens and b) detail of the fracture of one of the specimens.

Microscopy and Microanalysis, **30** (Suppl 1), 2024, 936–939
https://doi.org/10.1093/mam/ozae044.461

Microscopy AND Microanalysis

Meeting-report

Evaluation of the Mechanical and Corrosion Properties of New Ti Alloys for Orthopedic Devices

Cristina Jiménez-Marcos[1], Julia Claudia Mirza-Rosca[1,2,*], Madalina Simona Baltatu[3], and Petrica Vizureanu[3]

[1]*Mechanical Engineering Department, University of Las Palmas de Gran Canaria, Las Palmas de Gran Canaria, Spain*
[2]*Transylvania University of Brasov, Materials Engineering and Welding Department, Brasov, Romania*
[3]*Department of Technologies and Equipment for Materials Processing, "Gheorghe Asachi" Technical University of Iasi, Iasi, Romania*
*Corresponding author: julia.mirza@ulpgc.es

Introduction

In the dynamic field of biomedical engineering and medicine, biomaterials play a crucial role in merging materials science with human health. These specialized materials are used to manufacture a wide range of medical devices, from prostheses to orthopedic implants, which significantly improve patients' quality of life. The choice of biomaterials not only impacts the efficacy of treatments, but also has crucial implications for safety and biocompatibility.

Although different types of biomaterials exist today, metallic implants, especially titanium (Ti) and its alloys, have emerged as a mainstay in the world of orthopedic implants, prostheses and dental devices, thanks to their exceptional biocompatibility, strength and low density [1,2]. However, some alloys, such as Ti6Al4V, release ions of aluminum, which can cause neurodegenerative diseases such as Parkinson's and Alzheimer's, and vanadium, which is a toxic and carcinogenic element, when in contact with the human body [3]. This has led to research into new titanium alloys containing elements such as molybdenum, zirconium, tantalum or silicon.

This new Ti-xMo-Zr-Ta-Si alloy is emerging as an exciting candidate for biomedical applications, incorporating molybdenum for mechanical strength, zirconium for corrosion resistance, tantalum for long-term stability and silicon for improved integration with bone tissue [4,5].

The key objectives of this research are to characterize and compare the chemical and mechanical properties and the degree of biocompatibility of the new titanium alloys TixMo7Zr15Ta1Si (x = 15 and 20) for possible applications in biomedical devices and thus contribute to improve the quality of life of patients and reduce the need for additional surgeries. For this purpose, metallography, electrochemical and microhardness tests were carried out.

Experimental

The fabrication of these alloys, which are called Sample 1 (62.00% Ti 15.00% Mo, 7.00% Zr, 15.00 % Ta, 1.00% Si) and Sample 2 (57.00% Ti 20.00% Mo, 7.00% Zr, 15.00 % Ta, 1.00% Si), was carried out at the Technical University of Gheorghe Asachi, Romania, utilizing a vacuum arc remelting (VAR) furnace model MRF ABJ 900 VAR and from this process a series of ingots were generated. The sample preparation process was started by cutting the samples using the Buehler IsoMet 4000 cutting machine (Buehler, USA) and casting them in epoxy resin. Subsequently, the specimens were roughed and polished in two stages to obtain a mirror finish using the polishing machine called StruersTegraPol-11 (Struers ApS, Denmark). Finally, the samples were cleaned using "Ultrasons-HD" from J.P. Selecta (JPS, Spain), as shown in Fig 1.

For the characterization and comparison of these samples, in the metallography test, images of their surfaces are taken with the optical microscope Axio Vert.A1 MAT by ZEISS (Zeiss, Jena, Germany), in the electrochemical tests, the corrosion potential and corrosion rate are found and electrochemical impedance spectroscopy is performed with the use of the SP-150 potentiostat (BioLogic, France). The Future Tech FM-810 hardness tester (Kawasaki, Japan) is used for Vickers microhardness testing [6].

Results and discussion

When examined metallographically, Figure 2 shows that both alloys have dendritic and biphasic structures when they are attacked by Kroll's reagent.

Table 1 shows the initial corrosion potential, or Open Circuit Potential (OCP), after two hours and one day immersed in Ringer's solution. During the 24 hours of testing, these curves tended to rise gradually until evidence of potential stabilization was detected, indicating that the passive film is thermodynamically stable under Ringer's solution conditions [7, 8].

Table 1. Variations of the corrosion potential values of Sample 1 and Sample 2 during 24 hours of testing.

	OCP, (V) vs SCE		
Alloy	Initial	After 2 h	After 24 h
Sample 1	-0.16	0.03	0.03
Sample 2	-0.46	-0.44	-0.26

1 INTRODUCCIÓN

2 PUBLICACIONES

3 DOCUMENTOS DE AUTORÍA

4 PARTICIPACIONES EN CONGRESOS

5 OTRAS PUBLICACIONES

6 CONCLUSIONES FINALES

En el presente estudio se han obtenido resultados significativos tras el análisis preliminar de las aleaciones de Ti15MoZrxSi, Ti20MoZrxSi, TixMoZrTa y TiMoxSi. Dichos resultados se presentan en los artículos correspondientes a este proyecto y contribuyen a un notable avance en el campo de los materiales de uso biomédico:

1. **Experimental Research on New Developed Titanium Alloys for Biomedical Applications**

Esta investigación evaluó y comparó el comportamiento frente a la corrosión y las propiedades mecánicas de dos novedosas aleaciones de titanio. Mediante análisis microestructural, curvas de potencial de corrosión, EIS, velocidad de corrosión, potencial de picadura, corrosimetría, SEM, ensayo de flexión en tres puntos y microdureza, se ha llegado a las siguientes conclusiones:

- Las superficies de las muestras atacadas presentan estructuras bifásicas dendríticas similares. El tamaño de las dendritas disminuye con la adición de silicio. En la superficie de las aleaciones hay una zona rica en Mo, Zr y Si y otra zona rica en Titanio. Se ha podido confirmar la presencia de una capa de óxido pasivo (TiO_2) en la superficie de cada muestra, con un aspecto poroso en contacto con el electrolito y una estructura compacta en contacto con la aleación.
- El potencial de ambas muestras aumenta durante el tiempo de inmersión sin que se produzcan caídas en los valores de potencial, lo que demuestra que la película pasiva formada en la superficie es termodinámicamente resistente en estas condiciones. La resistencia a la polarización (Rp) es muy grande por lo que ambas aleaciones son muy resistentes a la corrosión.
- Las bajas velocidades de corrosión y las bajas corrientes de corrosión atestiguan el buen rendimiento de las muestras estudiadas en el medio analizado, solución Ringer, solución salina y simulación de fiebre.
- Los valores de módulo de elasticidad y dureza obtenidos en ambos casos fueron inferiores a los de muchas aleaciones comerciales.

A la vista de los resultados obtenidos, las muestras presentaron buenas características mecánicas, químicas y biológicas, con cierta mejora en las propiedades mecánicas de la muestra Ti20MoZr0.5Si.

2. Effect of Si Contents on the Properties of Ti15Mo7ZrxSi Alloys

Después de que las muestras se expusieron al reactivo Kroll, se observaron patrones dendríticos bifásicos en sus superficies. Las dendritas se hicieron más pequeñas cuando se agregó silicio porque este es un fuerte refinador de grano en las aleaciones de titanio. Promueve la formación de granos finos que impiden la propagación de grietas, mejorando la resistencia del material a la fatiga.

Los valores de potencial de ambas muestras aumentaron durante la duración de la inmersión sin disminuir, lo que indica que la capa pasiva, que se produjo en la superficie de cada muestra, es termodinámicamente resistente en circunstancias estándar. El óxido de silicio forma una capa de óxido protectora en la superficie de la aleación, lo que reduce la tasa de oxidación y mejora la resistencia de las aleaciones a la degradación de fluidos corporales.

Como la resistencia a la polarización fue bastante grande, las bajas corrientes y tasas de corrosión mostraron el rendimiento excepcional de las muestras probadas en el entorno evaluado, la solución Ringer. R(QR)(QR) fue el circuito equivalente que se ajustó mejor a los datos de impedancia medidos y, a medida que se aplicaron potenciales positivos adicionales, el ángulo de fase y los resultados de impedancia tendieron a aumentar. La muestra 0.5 % Si tuvo la tasa de corrosión más baja porque este es el límite de solubilidad del silicio en la aleación de titanio en particular y, al exceder este contenido, la presencia de Si puede crear pares galvánicos entre las regiones que contienen Si y el resto de la aleación de titanio, lo que lleva a reacciones electroquímicas localizadas.

Al examinar la dureza a través de diferentes cargas, se identificaron dos fases diferentes, una dura y otra blanda, de la microestructura del material. Los valores de microdureza y módulo elástico para ambos casos fueron inferiores a los de varias aleaciones biomédicas convencionales.

En general, todas las muestras mostraron buenas cualidades químicas, químicas y biológicas, con resultados ligeramente mejores para la muestra Ti15Mo7Zr0.5Si.

3. Evaluation of New Titanium Alloys as Potential Materials for Medical Devices

En esta investigación se estudió el efecto de la concentración de silicio en la microestructura, la biocompatibilidad, el módulo de elasticidad, la microdureza y la

resistencia a la corrosión de la aleación TiMoZrSi en un fluido corporal simulado. y la resistencia a la corrosión de la aleación TiMoZrSi en un fluido corporal simulado, confirmando la estructura bifásica y dendrítica para ambas muestras en ensayos metalográficos. Se pueden encontrar dos zonas, una rica en titanio y otra en Mo, Zr y Si, en la superficie de las aleaciones. Se comprobó que la superficie de cada muestra formaba una capa de óxido pasiva. En las pruebas electroquímicas el potencial de la muestra TiMoZrSi0.75 tendía a corroerse y mostraba una menor resistencia a la corrosión. El módulo de elasticidad fue inferior al de muchas aleaciones comerciales. Por último, los valores de dureza Vickers aumentaron al aumentar el contenido de silicio.

Según los resultados obtenidos, la adición de un mayor porcentaje de silicio conlleva una ligera mejora de las propiedades mecánicas pero ambas aleaciones pueden utilizarse para dispositivos médicos.

4. **Two novel Ti-Mo-Ta-Zr alloys for medical devices: their microstructure, corrosion resistance and microhardness characteristics**

Este estudio examinó el comportamiento frente a la corrosión y las características microestructurales de dos aleaciones de titanio desarrolladas recientemente que contienen elementos biocompatibles (Mo, Zr y Ta). La aleación con mayor contenido en Mo muestra una mayor resistencia a la corrosión debido a una capa pasiva más robusta. Los valores de microdureza de ambas aleaciones coinciden con los de los biomateriales de Ti utilizados habitualmente, lo que indica uniformidad y buen rendimiento mecánico. Estos resultados corroboran el potencial de estas nuevas aleaciones de titanio, presumiblemente no tóxicas, como prometedoras candidatas para aplicaciones biomédicas.

La investigación futura debería concentrarse en una amplia investigación de un mayor contenido de Mo, integrando la fabricación de aleaciones, una mejor caracterización, evaluaciones mecánicas y electroquímicas, y análisis de biocompatibilidad. Aumentando progresivamente el contenido de Mo y refinando la composición de la aleación, se podrán evaluar metódicamente las ventajas y desventajas, facilitando así el avance de aleaciones de titanio superiores para aplicaciones clínicas.

5. Preliminary studies of new heat-treated titanium alloys for use in medical equipment

Los resultados mostraron que la adición de silicio a la aleación Ti-15Mo afecta a la homogeneidad y distribución de las fases. El análisis de difracción de rayos X (DRX) mostró la presencia predominante de fase β con una menor cantidad de siliciuro.

- Se ha observado que, durante la inmersión en solución de Ringer, las muestras conservan la estabilidad de su potencial, presentando la muestra con 0.75%Si un potencial más elevado que inhibe la ruptura cíclica y la repasivación de la capa pasiva que se ha desarrollado en su superficie. Por otro lado, se ha demostrado que una mayor concentración de silicio (más del 0.5% Si) ralentiza el proceso de corrosión porque favorece el desarrollo de una capa pasiva más compacta y eficaz. La velocidad de corrosión en medio fisiológico simulado disminuye en más de un 50% con la adición de 0.75% de Si y esta disminución alcanza el 75% si la concentración de Si es del 1%.
- Todas las aleaciones demostraron valores de dureza comparables con distintas cargas, superiores a los del titanio puro comercial. Cuando la adición de Si es muy baja (0.5%), la formación del siliciuro en el borde de los cristales genera una elevada dispersión de los valores de microdureza debido a la falta de homogeneidad microestructural.

Estos resultados fueron ampliamente positivos para el comportamiento frente a la corrosión de las muestras, mostrando que, con adiciones de Si superiores al 0.5% en peso, se obtenía una muy buena resistencia a la corrosión y unas propiedades mecánicas similares a las de otras aleaciones comerciales.

Mediante la caracterización preliminar de la microestructura, el comportamiento frente a la corrosión en distintos ambientes y de ciertas propiedades mecánicas como la dureza y el módulo de elasticidad de diferentes aleaciones de base Ti-Mo, se ha observado que todas las muestras ensayadas, en mayor o menor medida, han presentado unas características óptimas, para un futuro diseño y fabricación de material médico. Dichas aleaciones han demostrado un rendimiento superior al de aleaciones comerciales como CoCrMo o Ti-6Al-4V, destacando el efecto beneficioso de la adición de distintos porcentajes de silicio y de molibdeno en la mejora de sus propiedades mecánicas y electroquímicas.

En particular, el molibdeno ha contribuido a mejorar la estabilidad de la película pasiva, proporcionando una mayor resistencia a la degradación en medios fisiológicos. Estas características refuerzan la viabilidad de estas aleaciones como candidatas idóneas para implantes y dispositivos biomédicos. Asimismo, la presencia de silicio ha favorecido la formación de estructuras dendríticas más finas y homogéneas, optimizando el comportamiento frente a la corrosión gracias a la formación de una capa de óxido protectora.

La investigación futura debería concentrarse en una homogeneización de los ensayos realizados en todas las aleaciones para obtener un análisis más preciso de sus características, además de ensayar electroquímicamente las muestras en una disolución acidulada que simule las condiciones del fenómeno de "agujetas" en el cuerpo humano, lo que permitiría comprender mejor su durabilidad en escenarios clínicos exigentes.

La optimización de la composición de las aleaciones mediante la variación controlada del porcentaje de molibdeno y silicio podría potenciar aún más sus propiedades. Para ello, se requiere la fabricación de más material, permitiendo estudios a mayor escala y con ensayos complementarios que evalúen aspectos como la biocompatibilidad a largo plazo, la resistencia al desgaste y la respuesta celular. Con un enfoque integral en la caracterización y optimización de estas aleaciones, se podrá avanzar significativamente en el desarrollo de nuevos materiales para aplicaciones biomédicas de alto rendimiento.